

The Dissection of Signaling Cascades in
Neural Stem Cell Proliferation & GBM Promotion

by

Yael Kusne

A Dissertation Presented in Partial Fulfillment
of the Requirements for the Degree
Doctor of Philosophy

Approved April 2014 by the
Graduate Supervisory Committee:

Nader Sanai, Co-Chair
Janet Neisewander, Co-Chair
Nhan Tran
Ronald Hammer
Vinodh Narayanan
Joan Shapiro

ARIZONA STATE UNIVERSITY

May 2014

ABSTRACT

Cells live in complex environments and must be able to adapt to environmental changes in order to survive. The ability of a cell to survive and thrive in a changing environment depends largely on its ability to receive and respond to extracellular signals. Initiating with receptors, signal transduction cascades begin translating extracellular signals into intracellular messages. Such signaling cascades are responsible for the regulation of cellular metabolism, cell growth, cell movement, transcription, translation, proliferation and differentiation. This dissertation seeks to dissect and examine critical signaling pathways involved in the regulation of proliferation in neural stem cells (Chapter 2) and the regulation of Glioblastoma Multiforme pathogenesis (GBM; Chapter 3). In Chapter 2 of this dissertation, I hypothesize that the mTOR signaling pathway plays a significant role in the determination of neural stem cell proliferation given its control of cell growth, metabolism and survival. I describe the effect of inhibition of mTOR signaling on neural stem cell proliferation using animal models of aging. My results show that the molecular method of targeted inhibition may result in differential effects on neural stem cell proliferation as the use of rapamycin significantly reduced proliferation while the use of metformin did not. Abnormal signaling cascades resulting in unrestricted proliferation may lead to the development of brain cancer, such as GBM. In Chapter 3 of this dissertation, I hypothesize that the inhibition of the protein kinase, α PKC $_{i/\lambda}$ results in halted GBM progression (invasion and proliferation) due to its central location in multiple signaling cascades. Using *in-vitro* and *in-vivo* models, I show that α PKC $_{i/\lambda}$ functions as a critical node in GBM signaling as both cell-autonomous and non-cell-autonomous signaling converge on α PKC $_{i/\lambda}$ resulting in pathogenic downstream effects. This dissertation aims to uncover the molecular mechanisms involved in cell signaling pathways which are responsible for critical cellular effects such as proliferation, invasion and transcriptional regulation.

DEDICATION

To my parents for showing me by example that anything is possible with hard work and persistence. It is because of your unconditional love and support that I succeed.

For this I am eternally grateful.

To Jon, my best friend, my world, my rock;

I love you always and forever.

ACKNOWLEDGMENTS

First and foremost I would like to thank my mentors, Dr. Sourav Ghosh, Dr. Nader Sanai, and Dr. Zaman Mirzadeh, for all you have done for me. Thank you for your belief in me and your support through both the difficult and the exciting times. Thank you for your patience and guidance, and most of all, for your willingness to share your knowledge and expertise with me. Your unwavering support, encouragement and belief in me have provided me with a sense of security which allowed me to be adventurous, daring and confident in the lab. Each of you has shaped the scientist I have become. Without you, none of this would have been possible.

I would also like to thank my committee members, Dr. Janet Neisewander, Dr. Ron Hammer, Dr. Joan Shapiro, Dr. Nhan Tran, and Dr. Vinodh Narayanan, for your time and dedication to helping me succeed. You were there with an open door and an open mind and for that, I am grateful. *I will always aspire to be encouraging, caring, and supportive throughout my career, as you have been for me.*

A special thanks to Dr. Sanai, Dr. Mirzadeh, and Dr. Narayanan for providing me with an aspirational model of my own career as a physician-scientist. There is no one who shares your strong commitment and passion to science *and* medicine. *Your diligence, hard work, and endless effort has inspired me to work harder and to aim higher.*

Finally, I would like to thank my colleagues and students I have had the pleasure of working with throughout the years. Sabine Borwege, thank you for your camaraderie, your helpfulness, your advice, and your support. *Most of all, thank you for your laughter.*

TABLE OF CONTENTS

	Page
LIST OF TABLES	vii
LIST OF FIGURES.....	viii
LIST OF SYMBOLS / NOMENCLATURE	xi
 CHAPTER	
1 INTRODUCTION	1
Signal Transduction.....	1
Enzyme-Coupled Surface Receptor Signaling: RTKs.....	2
The PI3K/PTEN/AKT Pathway	3
The PI3K/AKT/mTOR Pathway	4
Mammalian target of rapamycin (mTOR) Function	5
The EGFR/PI3K/PTEN/AKT Pathway in in GBM	7
Atypical Protein Kinase C (aPKC)	10
TNF α , aPKC & NF- κ B signaling in GBM.....	11
Figures.....	14
2 MTOR SIGNALING IN NEURAL DEVELOPMENT AND AGING	20
Introduction to Manuscript	20
mTOR in Embryonic Neural Development & Neurodevelopmental Disorders	20
mTOR in Adult Neural Stem Cell Proliferation, Differentiation & Neurogenesis	24
Stabilization, Survival & Integration of Adult Newborn Neurons	30
Manuscript: Contrasting Effects of Chronic, Systemic Treatment with mTOR Inhibitors Rapamycin and Metformin on Adult Neural Progenitors in Mice	34
Abstract	34
Introduction	34
Materials and Methods	37

	Page
Supplementary Materials and Methods.....	43
Results.....	45
Discussion	49
Figures.....	52
Supplementary Figures	60
Acknowledgements	62
3 SIGNALING IN GLIOBLASTOMA	63
Introduction to Manuscript	63
Glioblastoma.....	63
The Heterogeneity of GBM.....	65
The GBM Tumor Stroma & Extracellular Signaling.....	67
Primary GBM Intracellular Signaling	69
Manuscript: Targeting aPKC Simultaneously Disables Cell Autonomous and Non-cell Autonomous Oncogenic Signaling in Glioblastoma	73
Abstract	73
Introduction	73
Materials and Methods	74
Results.....	84
Discussion	96
Figures.....	99
Supplementary Figures	114
Acknowledgements	129
4 DISCUSSION AND IMPLICATIONS	130
mTOR Signaling in GBM	130
aPKC and mTOR Signaling in NSC Proliferation & Differentiation	134
SVZ Niche, Polarity in NSC Proliferation & Differentiation.....	136
TNF- α and EGFR Signaling in NSC Proliferation & Differentiation.....	140

	Page
EGFR Signaling and NF- κ B	142
The Glioma Stem Cell Hypothesis	145
Inhibitors in GBM Clinical Trials	148
REFERENCES.....	151
APPENDIX	
A Curriculum Vitae	181

LIST OF TABLES

Table	Page
2.1 Neither rapamycin nor metformin significantly increase food intake or body weight.....	53
2.2 Rapamycin, but not metformin, inhibits the proliferation of neural progenitors in vitro	57
2.3 Rapamycin, but not metformin, causes G1 phase arrest in vitro	58
3.S1 List of primers	112
3.S2 List of siRNA and shRNA sequences	113

LIST OF FIGURES

Figure	Page
1.1 Receptor Tyrosine Kinase (RTK) Signaling	14
1.2 The PI3K/AKT Signaling Pathway	15
1.3 The PI3K/AKT/mTOR Signaling Pathway	16
1.4 TCGA analyses of GBM tumor mutations.....	17
1.5 atypical Protein Kinase C (aPKC)	18
1.6 TNF- α /NF- κ B Signaling.....	19
2.1 Chronic, systemic rapamycin & metformin administration in mice inhibits mTOR activity in the brain	52
2.2 Chronic rapamycin treatment, but not metformin, inhibits the proliferation of neural progenitors in the SVZ region of the adult mammalian brain.....	54
2.3 Chronic rapamycin treatment, but not metformin, inhibits the proliferation of neural progenitors in DG	55
2.4. Rapamycin, but not metformin, inhibits proliferation of neural stem cells <i>in-vitro</i>	56
2.5 Rapamycin, but not metformin, inhibits differentiation of neural stem cells <i>in-vitro</i>	59
2.S1 Chronic rapamycin, but not metformin, treatment reduces neural progenitor numbers in the SVZ region of the adult mammalian brain	60
2.S2 Chronic rapamycin treatment, but not metformin, reduces neuroblasts and/or immature neuron numbers.....	61
3.1 Clinical association and therapeutic efficacy of targeting aPKC in mouse models of GBM	99
3.2 aPKC is activated downstream of tumor-intrinsic oncogenic RTK signaling pathways.....	101

Figure		Page
3.3	Myeloid cells, paracrine TNF α and NF- κ B signature are detected in GBM and favor progression	102
3.4	Myeloid cell-derived TNF α promotes GBM proliferation, invasion and EGFR kinase inhibitor resistance and correlates with aPKC activation	103
3.5	TNF α -induced NF- κ B signaling in GBM is dependent on aPKC	105
3.6	Bimodal function of aPKC in EGF and TNF α induced signaling in GBM cells	109
3.7	Schematic illustrating aPKC-containing signaling complexes in cell autonomous RTK and non cell-autonomous TNF α /NF- κ B oncogenic signaling in GBM	111
3.S1	aPKC expression in non-tumor brain and in histologically characteristic regions of GBM	114
3.S2	Validation of aPKC knockdown efficiencies and PZ09 inhibitory effect.....	115
3.S3	EGFR isoforms expression in GBM6 and EGFR phosphorylation kinetics in GBM6 and U251/EGFR	116
3.S4	Myeloid cells, TNF α production and NF- κ B activation in mouse models of GBM	117
3.S5	TNF α is produced by myeloid cells when in contact with GBM cells.....	118
3.S6	Human myeloid cell-derived TNF α contributes to increased GBM proliferation and invasion.....	119
3.S7	Murine myeloid cell-derived TNF α contributes to increased GBM proliferation and invasion.....	120
3.S8	Phosphorylation of aPKC precedes phosphorylation of p65.....	121
3.S9	TNF α induced I κ B α degradation is not affected by aPKC silencing.....	122

Figure		Page
3.S10	Activation of aPKC and induced NF- κ B gene signature in GBM cells upon co-culture with myeloid cells	123
3.S11	Myeloid cell-induction of GBM proliferation and invasion is dependent on aPKC	124
3.S12	Erlotinib, but not aPKC inhibition, suppresses EGFR phosphorylation	125
3.S13	Induction of distinct sets of genes by EGF and TNF α signaling in GBM cells	126
3.S14	Validation of EGFR, AKT and Src inhibition in U87/EGFRVIII	127
3.S15	<i>PRKCI</i> is the predominant GBM-associated isoform of aPKC	128

LIST OF SYMBOLS / NOMENCLATURE

AKT	protein kinase B	NSC	neural stem cell
aPKC	atypical protein kinase C	OB	olfactory bulb
ATP	adenosine trisphosphate	Par-3/6	partitioning defective 3/6
BDNF	brain derived neurotrophic factor	PB1	phox/bem domain
BrdU	5-bromo-2'-deoxyuridine	PDK1	3-phosphoinositide-dependent kinase1
C1/C2	conserved region 1/2	PI3K	phosphoinositide 3 kinase
CBP	creb binding protein	PIP2	phosphatidylinositol 4,5-bisphosphate
CNS	central nervous system	PIP3	phosphatidylinositol 3,4,5-triphosphate
cPKC	conventional PKC	PTEN	phosphatase and tensin homolog
DAG	diacylglycerol	Rheb	ras homolog enriched in brain
DG	dentate gyrus	RTK	receptor tyrosine kinase
EGF	epidermal growth factor	RTS	Rubinstein Taybi syndrome
EGFR	EGF receptor	SGZ	subgranular zone
FADD	fass-associated death domain	SH2	src homology domain
GBM	glioblastoma multiforme	SVZ	subventricular zone
GSC	glioma stem cell	TCGA	The Cancer Genome Atlas
IGF	insulin growth factor	TMZ	temozolomide
IL	interleukin	TNF α	tumor necrosis factor alpha
IRS	insulin receptor substrate	TNFR	tumor necrosis factor receptor
MCP	monocyte chemoattract protein	TRADD	TNFR-associated death domain
NF1	neurofibromatosis	TSC	tuberous sclerosis complex
NF- κ B	nuclear factor kappa b	VCAM	vascular cell adhesion protein
nPKC	novel protein kinase C	VEGF	vascular endothelial growth factor

CHAPTER 1

INTRODUCTION

The work presented in this dissertation comprises two distinct topics which both involve cell signaling pathways in cells of the central nervous system (CNS). Chapter 2 describes mammalian target of rapamycin (mTOR) signaling and the use of mTOR inhibitors in the proliferation of neural stem cells in aging mice. This work is presented as a manuscript which was published in February 2013 in the journal *Age*. Chapter 3 describes an investigation of atypical protein kinase C (α PKC) signaling in Glioblastoma Multiforme (GBM). Chapter 3 is currently in revision for publication. This introductory chapter will provide an overview for both Chapter 2 and Chapter 3, focusing on topics such as oncogenetic signaling, proliferation and differentiation – which are all processes controlled by signal transduction pathways.

Signal Transduction

Cells live in a complex environment and must monitor and respond to stimuli in order to survive. They must be able to detect extracellular stimuli and transfer signals to the interior cytoplasm of the cell. Received signals are converted through a signaling pathway leading to a cellular response or change in cell behavior, such as gene transcription. There are multiple types of signaling, including endocrine signaling, paracrine signaling, and autocrine signaling. Endocrine signaling involves hormones which are secreted by an endocrine gland and travel to their effector cell where they regulate cellular changes. This type of signaling can involve hormones traveling over long distances to reach their effector cell which may lie anywhere in the body. Paracrine signaling refers to signaling which takes place between cells in close proximity, affecting cells only in the local environment. Autocrine signaling occurs when a cell produces signals that it responds to itself. For instance, cancer cells produce their own signals, such as growth factors, which stimulate their proliferation and oncogenicity in an autocrine signaling manner.

The signal transduction process initiates with a receptor on a target cell. Receptors are molecules that act as a gateway between the intracellular and extracellular space. Usually containing an extracellular and intracellular domain, receptors bind to ligands on the extracellular surface of the cell and transmit the signal through their intracellular domains downstream to effector proteins, eventually leading to an alteration in metabolism, gene expression, movement, or behavior. At any given point in time within the extracellular space, there are a multitude of extracellular signals a cell must interpret, including many proteins, peptides, amino acids, nucleotides, and other signal molecules. The specificity of receptors expressed by a target cell is the determining factor as to whether signaling occurs and/or a cellular response is initiated. Receptors bind with high affinity to their target protein, or ligand, which allows for specialized signal transduction cascades to occur.

Enzyme-Coupled Surface Receptor Signaling: Receptor tyrosine kinases (RTKs)

Enzyme-coupled receptors are receptor proteins containing a ligand binding domain on the extracellular surface of the plasma membrane and are capable of enzyme activity (either intrinsic or associated) in the intracellular cytosolic domain. Receptor tyrosine kinases (RTKs) are the most abundant class of enzyme-coupled receptors. RTKs are able to directly phosphorylate tyrosine targets on their intracellular domain as well as on other intracellular tyrosine targets. Upon ligand binding, the receptor dimerizes, which allows for the cross-phosphorylation (or transautophosphorylation) of the receptor chains (Figure 1.1). This increase in phosphorylated tyrosines creates docking sites for other signaling proteins. Signaling complexes can then be assembled at these docking sites in order to deliver the signal further downstream to other effector proteins. This signal cascade may eventually lead to the nucleus, causing a change in the transcriptional regulation of various genes. An example of such an RTK is the Epidermal Growth Factor Receptor (EGFR), which plays an important role in cell survival, proliferation, and cell growth. EGFR signaling is imperative for proper development and disruption of its signaling cascade can lead to detrimental effects, including cancer. EGFR activation,

initiated by epidermal growth factor (EGF) ligand binding to EGFR, leads to EGFR transautophosphorylation which activates downstream kinases such as phosphoinositide 3-kinase (PI3K).

The PI3K/PTEN/AKT Pathway

PI3K is a kinase containing a Src homology domain region (SH2) which mediates binding to phosphorylated tyrosines. It is a plasma-membrane-bound enzyme which can bind to the intracellular RTK chains upon their transautophosphorylation. Upon binding to intracellular phosphorylated RTK chains, PI3K is then responsible for phosphorylating the 3 position of the membrane inositol ring, which generates multiple phosphorylated lipids, or phosphoinositides, including the formation of active phosphatidylinositol 3,4,5-triphosphate (PIP3) from inactive phosphatidylinositol 4,5-biphosphate (PIP2). Phosphoinositides play an important role in signal transduction as they too act as a docking site and recruit other signaling molecules. PI3K is activated through various RTKs, including EGFR, and plays a role in the regulation of growth and cell survival signals. Mutations leading to activation of PI3K are common in cancer (including GBM; Figure 1.4) as active PI3K leads to unrestricted growth signals, proliferation, and cell survival (Figure 1.2). PI3K pathway inhibitors have the potential to improve clinical outcome in various cancers as inhibition of this oncogenic pathway could induce cell death, halt oncogenic proliferation, invasion and cell survival (Wen, Lee, Reardon, Ligon, & Alfred Yung, 2012).

Negative signal regulation also occurs in the cell. Phosphatase and tensin homolog (PTEN) is a phosphatase that dephosphorylates PIP3 to the inactive PIP2. Loss of PTEN is oncogenic and occurs in multiple cancers including GBM, breast, endometrium and colon cancer, among others (Wong, Engelman, & Cantley, 2010). Either the inactivation or the loss of PTEN and/or the activation of PI3K leads to uncontrolled downstream PI3K signaling resulting in unregulated growth signals and/or oncogenesis.

Further downstream of PI3K and PTEN is the protein kinase AKT (also known as protein kinase B). AKT is a serine/threonine protein kinase which contains a pleckstrin homology (PH)

domain, a protein-protein interaction domain that facilitates its binding to phosphoinositides on the cell membrane. In the case of EGFR signaling, EGF ligand initially binds to EGFR leading to transautophosphorylation which begins the signaling cascade. PI3K then binds to the intracellular dimerized receptor chains and catalyzes the formation of active PIP3 from inactive PIP2 at the membrane. Due to AKT's ability to associate with phosphoinositides, this phosphorylation of PIP2 into PIP3 recruits AKT to the membrane where it binds to PIP3, leading to its activation (Figure 1.2). Upon binding, AKT is phosphorylated by 3-phosphoinositide-dependent kinase (PDK1) and the mammalian target of rapamycin complex 2 (mTORC2; (J. Wang et al., 2012). This subsequently leads to phosphorylation by Akt of numerous downstream targets involved in cell survival, proliferation and cell growth (J. Wang et al., 2012).

The PI3K/AKT/mTOR Pathway

The PI3K/AKT pathway regulates cell growth through the use of another serine/threonine kinase, mTOR. In the cell, mTOR can be found in 2 protein complexes which have different upstream activators and downstream effectors, mTOR complex 1 (mTORC1) and mTOR complex 2 (mTORC2). mTORC1 associates with the protein raptor and is sensitive to the inhibitor rapamycin. mTORC2 associates with rictor and is rapamycin-insensitive. mTORC1 stimulates ribosome production and protein synthesis and thus encourages cell growth. Among other extracellular signals, various growth factors activate mTORC1 via the PI3K/AKT pathway and through a complex mechanism involving the GTPase Ras homolog enriched in brain (Rheb) and a protein heterodimer consisting of tuberous sclerosis 1 and 2 (TSC1 and TSC2; (Laplane & Sabatini, 2012). The TSC1/TSC2 heterodimer acts as a GTPase-activating protein (GAP) for Rheb, a GTPase, which directly binds mTORC1 when in its active (GTP-bound) conformation (Figure 1.3). When active GTP-bound Rheb binds to mTORC1, mTORC1 becomes activated and its kinase activity is stimulated (Laplane & Sabatini, 2012). Negative regulation of mTORC1 activity also occurs via the GAP TSC1/TSC2, as it converts Rheb into an inactive (GDP-bound) conformation causing Rheb and mTORC1 to disassociate. Interestingly, mTORC1 participates in

negative feedback inhibition of its own activator, PI3K, through the downstream effector target of mTORC1, p70 s6 kinase (S6K1; Figure 1.3). mTORC1 activation leads to phosphorylation of S6K1, which then inhibits PI3K in a negative regulation feedback manner (J. Huang & Manning, 2009; Laplante & Sabatini, 2012).

Mammalian target of rapamycin (mTOR) Function

mTORC is considered a signal integrator and is crucial for cell growth and homeostasis (Zoncu, Efeyan, & Sabatini, 2011). Cell growth depends heavily on the cells environment as increase in size or number of cells requires sufficient supply of nutrients and energy. If conditions are favorable, the cell can synthesize new proteins, nucleic acids, and lipids for growth. Through a myriad of downstream signaling processes, mTOR plays a critical role in cell growth processes, including, general protein synthesis, as well as lipid synthesis for proliferating cells, inhibition of cell degradation (autophagy), cell metabolism and ATP production. This is due to mTORs central role in coordinating growth through its environment-dependent activation. For instance, mTORC1 regulates the synthesis of ribosomal RNAs (rRNAs) by upregulating the activity of RNA Poll, the rRNA polymerase, allowing for the biogenesis of ribosomes. The synthesis of ribosomes is energetically costly to the cell, and thus occurs in times of energy and nutrient abundance. The mTORC1 GTPase Rheb has also been found to play a role in this process as a loss of Rheb inhibits mTORC1 activation during nutrient starvation (S. C. Johnson, Rabinovitch, & Kaeberlein, 2013).

mTORC1 also inhibits autophagy, which is an important process allowing for recycling of cellular components. If in an environment with low nutrient availability, the cell may participate in autophagy by way of recycling proteins and organelles in order to synthesize nutrients (Zoncu et al., 2011). During autophagy, intracellular components are isolated into autophagosomes and are later degraded by lysosomes. Interestingly, a strong correlation between autophagy and lifespan/aging has been well established in the literature (D. W. Lamming et al., 2012; Dudley W. Lamming, Ye, Sabatini, & Baur, 2013). As the aging process occurs, cellular physiology declines,

leading to the decreased function of cells and entire organs as well as a decrease in autophagy. The inactivation of genes necessary for autophagy results in a reduced lifespan in yeast, *C. elegans* and *Drosophila* while an increase in autophagy extended lifespan in *Drosophila* (Alvers et al., 2009; Hars et al., 2007; Lionaki, Markaki, & Tavernarakis, 2013), providing evidence for the prominent role of autophagy in aging and lifespan. mTOR signaling has been proven to be a regulator of this process. Inhibition of mTOR using rapamycin results in an increase in autophagy and extends lifespan in multiple organisms including mice (Cornu, Albert, & Hall, 2013). In yeast, inhibition of mTOR through rapamycin treatment increased lifespan while mTOR stimulation decreased lifespan (Alvers et al., 2009). Furthermore, the use of another mTOR inhibitor, metformin, was also shown to extend life span in mice (Vladimir N. Anisimov et al., 2008; V. N. Anisimov et al., 2011). In addition to rapamycin and/or metformin treatment, dietary restriction, resulting in amino acid deprivation for cells, has been shown to extend lifespan (Levenson & Rich, 2007). The effect of dietary restriction on lifespan extension has been attributed to inhibition of mTOR (Cornu et al., 2013) due to its environment-dependent activation.

mTOR signaling has also been shown to play a significant role in cell proliferation and cell cycle regulation in mouse and human cells (Fingar & Blenis, 2004; N. Gao et al., 2004; Ning Gao, Zhang, Jiang, & Shi, 2003; X. Gao, McDonald, Hlatky, & Enderling, 2013; Ohanna et al., 2005; Sehgal, 1998). Although a defined mechanism has yet to be elucidated, rapamycin is considered a good immunosuppressant as mammalian B and T cells, when treated with rapamycin, undergo a G1-phase cell cycle arrest with little toxicity (Fingar & Blenis, 2004). In the CNS, activation of mTOR signaling is upregulated during neural stem cell differentiation in mouse neural stem cells (Han et al., 2008). In addition, rapamycin has been shown to reduce BrdU+ cells in the dentate gyrus (DG) of rats (Zeng, Rensing, & Wong, 2009) and mice treated with rapamycin displayed reduced hippocampal neurogenesis (Raman, Kong, Gilley, & Kernie, 2011; Raman, Kong, & Kernie, 2013). This data, among others, provides evidence of the role of mTORC1 in the regulation of cell proliferation both within and outside of the CNS.

Given the critical role of mTOR in the regulation of cell growth, nutrient sensing, cell proliferation and organism lifespan extension, we asked whether mTORC1 signaling was capable of impacting the age-related decline in neural progenitor proliferation. In Chapter 2, we tested the role of mTORC1 signaling in neural progenitor proliferation of aged-mice by using inhibitors of mTORC1, rapamycin and metformin. Not surprisingly, in aged mice, we found a decrease in proliferation compared to young mice. Unexpectedly, however, in aged mice treated with rapamycin, we found an even greater decrease compared to aged mice treated with vehicle alone or mice treated with metformin. While both rapamycin and metformin inhibit mTORC1, the two inhibitors mediate inhibition via different mechanisms. Rapamycin works by inhibition of mTORC1 directly, while metformin activates adenosine monophosphate-activated protein kinase (AMPK), an inhibitor of mTOR. Given that rapamycin treatment extended lifespan in animal models, and given the prominent role of mTOR in cellular growth and proliferation, it was surprising to discover a rapamycin-mediated decrease in neural progenitor proliferation in aged mice. This examination and its findings are presented as a published manuscript in Chapter 2.

The EGFR/PI3K/PTEN/AKT pathway in Glioblastoma Multiforme (GBM)

While the EGFR/PI3K/PTEN/AKT pathway activates mTOR (Figure 1.3), it also activates other downstream effector proteins and plays a central role in cellular signaling. The EGFR/PI3K/PTEN/AKT signaling pathway is an important regulator of oncogenesis. Activation of this pathway is oncogenic promotes various cancers including GBM (Wong et al., 2010). GBM is classified by the World Health Organization (WHO) as a grade IV astrocytoma, the highest grade of glioma. It is the most common and most aggressive tumor of the CNS with tumor cells rapidly dividing and invading surrounding normal brain tissue. This devastating disease has an extremely poor prognosis with a 5-year survival rate of 5% (CBTRUS) despite receipt of the current standard of care which includes surgical resection, radiation, and chemotherapy with temozolomide (TMZ), an alkylating agent. This aggressive treatment regimen fails often due to the tumor cells ability to evade radiation and chemotherapy as well as their stealth invasion into

surrounding areas. In 2008, The Cancer Genome Atlas (TCGA) study profiled roughly 200 GBM tumor samples in an effort to describe the mutations leading to GBM formation (R. McLendon et al., 2008). The study was repeated with additional samples in 2013 by Brennan et al., (2013). The complementary results of these studies was the elucidation of several signal transduction pathways gone awry (Figure 1.4;(Brennan et al., 2013; Roger McLendon et al., 2008)).

The most frequent genetic aberrations discovered included signaling pathways which lead to proliferation and survival, key aspects to the oncogenicity of GBM (Brennan et al., 2013; Roger McLendon et al., 2008). These are displayed in Figure 1.4. For example, a homozygous deletion of *CDKN2A/CDKN2B* (P16/INK4A) is found in 61% of GBM samples. *CDKN2A* and *CDKN2B* are tumor suppressor proteins that inhibits *CDK4*, a cyclin dependent kinase found amplified in 14% of GBM samples (Brennan et al., 2013; Roger McLendon et al., 2008). *CDK4* phosphorylates retinoblastoma protein (RB), eventually allowing the cell to progress from G1 phase to S. *RB1*, which controls cell cycle progression, is found to be deleted or mutated in 7.6% of tumors (Brennan et al., 2013; R. McLendon et al., 2008). These genetic mutations contribute to the highly proliferative and highly oncogenic aspect of GBM while also making it difficult to treat successfully.

Data from the TCGA study also found that *EGFR* amplification is seen in roughly 57% of GBM patients, while RTK signaling in general is mutated in 90% of patients overall (Figure 1.4; (Brennan et al., 2013; Roger McLendon et al., 2008). The *EGFRVIII* mutation results in the deletion of exons 2-7 of *EGFR* and is frequently seen in GBM patients who already have an *EGFR* amplification mutation (Brennan et al., 2013; Roger McLendon et al., 2008). *EGFRVIII* leads to a loss of the extracellular domain of *EGFR*, leaving *EGFR* unresponsive to EGF ligand and resulting in constitutive activation of the *EGFR* signaling pathway (Brennan et al., 2013; Roger McLendon et al., 2008). However, the 2013 study elucidated other mutations which frequently occur to the *EGFR* gene. For instance, three different C-terminal mutations were discovered to alter the cytoplasmic terminals of *EGFR*, and these mutations have been shown to

be tumorigenic in mouse animal models of GBM (Brennan et al., 2013; Cho et al., 2011). In addition, deletions of exons 12-13 and exons 14-15 were found in 28% and 3% of GBM tumors, respectively (Brennan et al., 2013). Furthermore, roughly 25% of patients have a gain of function mutation in *PIK3CA* or *PIK3R1*, which encode for the PI3K subunits p110a and p85 respectively (Brennan et al., 2013; Roger McLendon et al., 2008). In addition, approximately 40% of GBM cases have a deletion of *PTEN*, the negative regulator of *PI3K*, once again, leading to its unrestricted activation (Brennan et al., 2013; Roger McLendon et al., 2008). The authors report that 89% of tumors had at least one mutation in the PI3K signaling pathway and roughly 40% had two or more mutations (Brennan et al., 2013). Interestingly, these two mutations, *PI3K* and *PTEN* mutations were found to be mutually exclusive, as over 50% of tumors had a mutation in either PI3K or PTEN (Brennan et al., 2013). Many of these genomic mutations (*EGFR* gain of function mutation, *EGFRV8*, *PI3K* gain of function mutation, *PTEN* loss of function mutation) lead to an unrestricted downstream activation of *PI3K*, a master regulator of cell growth and proliferation. Unfortunately, many GBM patients present with multiple mutations affecting this pathway, allowing the tumor cells to be extremely aggressive and making the pathway difficult to control.

Due to the strong reliance on EGFR signaling in GBM, EGFR inhibitors have been tested as therapy for GBM patients (Brandes et al., 2008; Huse, Holland, & DeAngelis, 2013; Huse & Holland, 2010; Reardon et al., 2010; Uhm et al., 2011). However, despite the multitude of clinical trials studying EGFR inhibitors, they have mostly proven to be unsuccessful in improving patient survival (Brandes et al., 2008; Huse et al., 2013; Huse & Holland, 2010; Reardon et al., 2010; Uhm et al., 2011). Chapter 3 presents a manuscript submitted for publication which describes a novel therapeutic which we found to be more effective than EGFR therapy. This therapy involved the inhibition or silencing of atypical Protein Kinase C (aPKC), a kinase found to be downstream of both EGFR and PI3K in GBM cells (Chapter 3). Inhibition and/or silencing of aPKC resulted in reduced EGFR-induced oncogenic proliferation, invasion and migration in glioma cells, as well as in animal models of GBM.

Atypical Protein Kinase C (aPKC)

The protein kinase C (PKC) family of Ser/Thr kinases comprises ~2% of the human kinome and is broadly conserved. 12 isoforms exist in mammal species and are classified into three subgroups based on regulatory and functional characteristics (Figure 1.5a): conventional PKCs (cPKC), novel PKCs (nPKC) and atypical PKCs (aPKC). All subgroups maintain a conserved carboxy-terminal catalytic domain and an N-terminal regulatory domain, which are linked by a hinge region. In addition, all subgroups possess a pseudosubstrate domain, which acts to maintain inactivation by blocking kinase activity. The cPKC subgroup consists of PKC α , PKC β , and PKC γ . cPKC members have both a conserved region 1 (C1) and a conserved region 2 (C2) domain, allowing them to be activated by diacylglycerol (DAG) and Ca²⁺, respectively. PKC δ , PKC ϵ , PKC θ comprise the nPKC subgroup. Similar to cPKCs, nPKCs contain a C1 region and are DAG responsive. However, they lack a functioning C2 domain and thus are insensitive to Ca²⁺ stimulation. Both the cPKC subgroup and the nPKC subgroup have two zinc fingers. The third subgroup of the PKC family, aPKCs, are atypical both in structure and function, having only one zinc finger and lacking a functioning C1 or C2 region. There are two members of this subfamily, aPKC ζ and aPKC λ/ι , and neither is activated by either DAG or Ca²⁺. Instead, aPKCs are activated by binding to other proteins through a Phox/Bem1 domain (PB1), which is not present in the cPKC or the nPKC subgroups. Differential PB1 domain binding may provide a means for downstream signaling specificity. For example, aPKC binding to partitioning defective 6 (Par6) through its PB1 domain forms the aPKC-Par6 complex which has been shown to play important roles for cellular polarity, while the aPKC-p62 complex has been shown to regulate nuclear factor kappa b (NF- κ B) activity (Figure 1.5b).

Importantly, while *Aplasia* and *Drosophila* have only one aPKC gene, the aPKC subgroup in vertebrates is comprised of two genes, *PRKCI* and *PRKCZ*. These genes encode for three distinct proteins. *PRKCI* encodes for aPKC λ/ι , while *PRKCZ* codes for aPKC ζ (Figure 1.5c).

PKM ζ arises from an alternative internal promoter of *PRKCZ*, which creates PKM ζ , the shortened and constitutively active form of PKC ζ which lacks the N-terminus entirely. Because aPKC ζ and aPKC λ/ι share a 72% sequence homology, evidence regarding differences in aPKC λ/ι versus aPKC ζ signaling cascades is lacking. This is likely due to a lack of specific reagents for discrimination. Nevertheless, more recent data has successfully analyzed the differential roles of the aPKC isoforms (Parker et al., 2013b). Interestingly, differential distribution of the isoforms in the CNS has been reported which revealed abundant expression of aPKC λ/ι and PKM ζ with reduced expression of aPKC ζ (Parker et al., 2013b).

aPKC has been shown to respond to EGF ligand and participate in the EGF/PI3K/AKT pathway in various cell types (Akimoto et al., 1996; Herrera-Velit, Knutson, & Reiner, 1997; Hirai & Chida, 2003; Mary L. Standaert, Bandyopadhyay, Kanoh, Sajan, & Farese, 2001; M. L. Standaert et al., 1997). In rat 3Y1 cells (Akimoto et al., 1996), adipocytes (Mary L. Standaert et al., 2001) and monocytes (Herrera-Velit et al., 1997), aPKC was found to be activated downstream of PI3K. Furthermore, aPKC has been shown to bind and phosphorylate AKT (Diaz-Meco & Moscat, 2001) and it is phosphorylated by PDK1 at Thr-410 (Le Good et al., 1998; Mary L. Standaert et al., 2001). In addition, PIP3 was found to induce dose-dependent increases in aPKC activity (Mary L. Standaert et al., 2001), thus further implicating it as a player in the EGFR/PI3K/AKT pathway. As described in Chapter 3, we found aPKC λ/ι to play a significant role in EGFR/PI3K/AKT signaling in GBM cells as it's silencing and/or inhibition lead to reduced EGFR-dependent gene transcription, migration, invasion, and proliferation. Interestingly, we found most GBM samples to have a significant over-expression of aPKC λ/ι while expressing little to no aPKC ζ (Chapter 3).

TNF- α , aPKC and NF- κ B signaling in GBM

While we found aPKC λ/ι to be activated downstream of EGFR signaling in GBM, we also found it to participate in NF- κ B signaling. Nuclear factor κ B (NF- κ B) is an important

heterodimeric transcription factor playing a critical role in the transcription of numerous genes. It consists of a heterodimer of p50 and p65 subunits, which when inactive, are found in the cytoplasm bound to I κ B, an inhibitory protein. Upon stimulation, such as tumor necrosis factor alpha (TNF- α) ligand binding to TNFR, I κ B is phosphorylated, dissociates from the NF- κ B complex, and is degraded. This exposes the nuclear localization signal on NF- κ B allowing it to translocate to the nucleus where it may bind to response elements on gene promoters and activate transcription of genes necessary for survival, inflammation, angiogenesis, invasion, apoptosis, and proliferation (Figure 1.6). NF- κ B is found to be constitutively active in most cancers (Chaturvedi, Sung, Yadav, Kannappan, & Aggarwal, 2011b) and high levels of NF- κ B are considered a hallmark of inflammation. Furthermore, several oncogenic signaling pathways involve NF- κ B activation (Chaturvedi et al., 2011b) and its inhibition has been shown to result in better patient outcomes (Drappatz, Norden, & Wen, 2009; Yamagishi & H. Takebe, 1997; Zanutto-Filho et al., 2011). Specifically in GBM, heterozygous deletions of *NFKBIA*, the gene which encodes for the NF- κ B inhibitor, I κ B α , are found in an estimated 25% of GBMs (Markus Bredel et al., 2011) and has been associated with poor patient outcome. Several factors influence activation of NF- κ B in cancers, including inflammatory cytokines and chemokines such as interleukin 1 β (IL-1 β) and TNF- α . Our comprehensive analyses found *AKC1* to be a mediating factor between TNF- α and NF- κ B signaling in GBM cells (Chapter 3).

TNF- α is a cytokine that was isolated in 1984 from macrophage-conditioned media (Aggarwal, Schwarz, Hogan, & Rando, 1996; Pennica et al., 1984). Originally considered to be anti-tumorigenic, TNF- α is now recognized as a mediator of cancer (Aggarwal et al., 1996) as its activation of NF- κ B controls oncogenic processes such as survival, proliferation, invasion, angiogenesis and metastasis (F. Balkwill, 2002). GBM cells have been shown to produce TNF- α and are also capable of responding to TNF- α through TNFRs (Aggarwal et al., 1996). However, other cells in the tumor microenvironment may also be responsible for the production of TNF- α .

As a cytokine initially found in macrophages, we examined the production of TNF- α from brain tumor associated microglia in GBM (Chapter 3). We found microglia to produce TNF- α upon their contact with GBM cells, thus indicating a paracrine signaling interaction between the two cell types. In recent years the tumor microenvironment has gained attention as providing a supportive environment for oncogenicity (Hanahan & Weinberg, 2011). For instance, inflammation is considered an enabling characteristic of cancer and is often called pro-tumorigenic (Hanahan & Weinberg, 2011). Various signaling molecules are secreted within the tumor microenvironment during the inflammatory response including growth factors, survival factors, and angiogenic factors, which may lead to an oncogenic environment. Paradoxically, we found microglia-dependent TNF- α to be a pro-tumorigenic factor secreted by the tumor microenvironment (Chapter 3).

Given that GBM cells express TNFR, we found that they were able to respond to the paracrine microglia secreted TNF- α signal by signaling through aPKC and leading to activation of NF- κ B in GBM cells. Thus, overall, we found aPKC λ/ι to be a central player in the signaling of two pathways in GBM: the EGFR/PI3K/AKT signaling pathway and the microglia secreted TNF α /NF- κ B signaling pathway. Inhibition or silencing of aPKC reduced GBM cell proliferation, invasion, and migration, thus proving aPKC λ/ι to be a better therapeutic target than the targeting of EGFR or NF- κ B alone. This data is presented in full as a manuscript in Chapter 3.

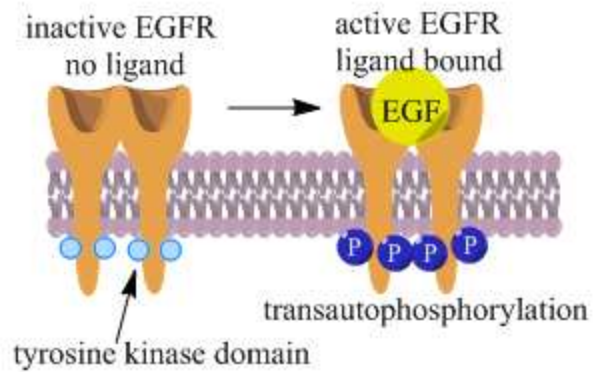


Figure 1.1. Receptor tyrosine kinase (RTK) signaling. RTKs are able to directly phosphorylate tyrosines on their intracellular domain and on other intracellular signaling proteins. Upon ligand binding, the receptor dimerizes, which allows for the cross-phosphorylation (or transautophosphorylation) of the receptor chains. Adapted from Schlessinger, J. (Schlessinger, 2000).

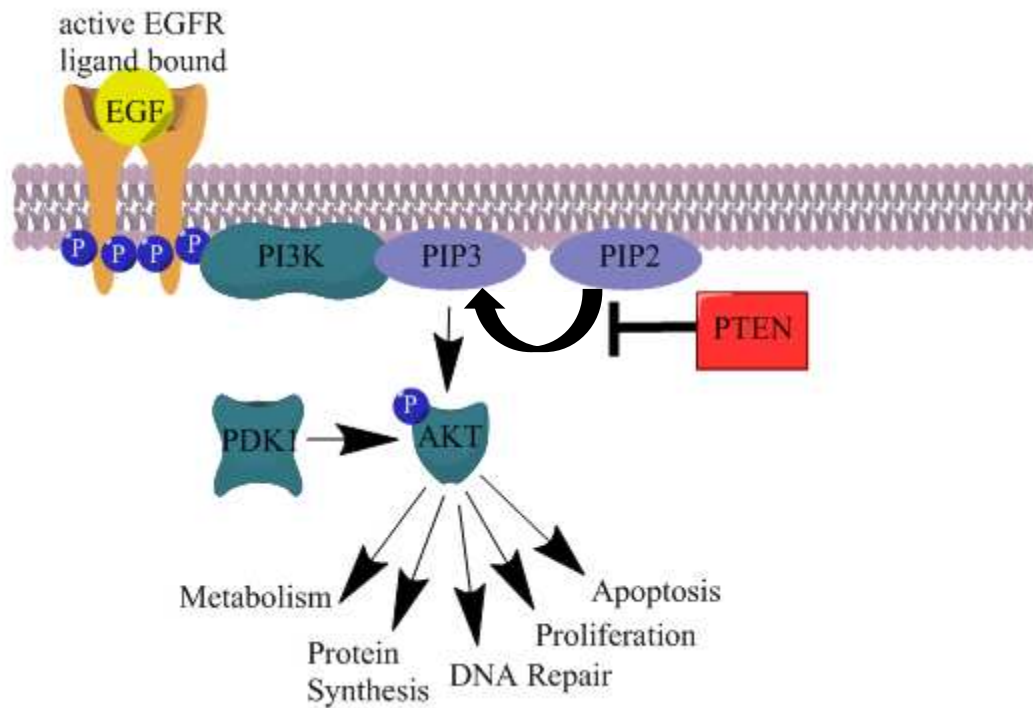


Figure 1.2. The PI3K/AKT signaling pathway. Upon ligand binding and transautophosphorylation, PI3K binds to phosphorylated tyrosine targets and converts inactive PIP2 into active PIP3. PTEN is a negative regulator of PI3k and converts active PIP3 back into inactive PIP2. AKT is recruited through an SH2 domain to bind to PIP3. Upon binding, AKT is phosphorylated by PDK1. This subsequently leads to AKT phosphorylation of numerous downstream targets involved in cell survival, proliferation, protein synthesis, cell growth, metabolism, and others. Adapted from Hennessy *et al.* (Hennessy, Smith, Ram, Lu, & Mills, 2005).

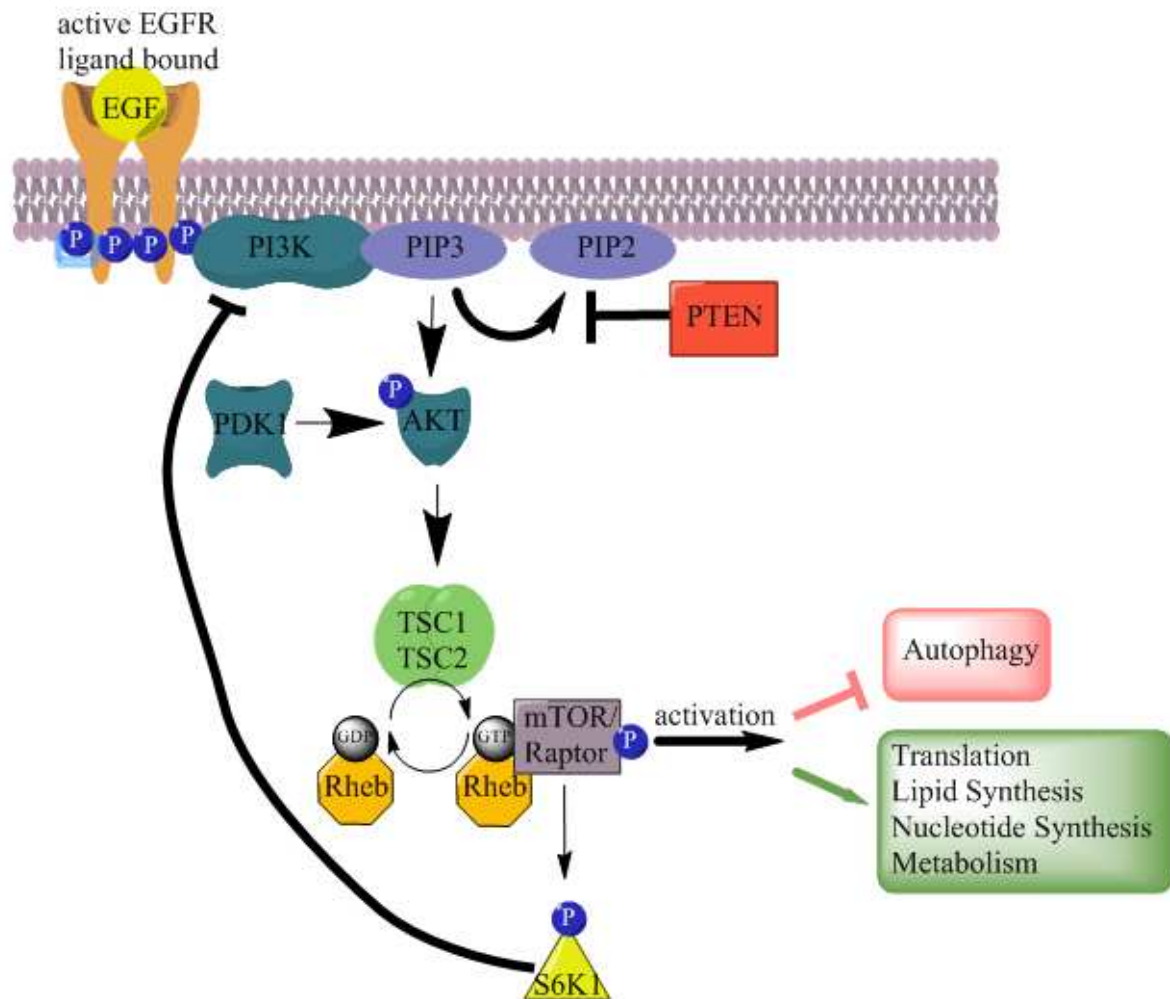


Figure 1.3. The PI3K/AKT/mTOR signaling pathway. Activation of AKT results in stimulation of the TSC1-TSC2 heterodimer complex. TSC1-TSC2 then acts as a GAP for Rheb, which binds to mTORC1 in its active GTP-bound conformation. mTORC1 kinase activity is then stimulated. Negative regulation of mTORC1 occurs via TSC1-TSC2 as it also converts Rheb into inactive GDP-bound conformation causing Rheb and mTORC1 to dissociate. mTORC1 also phosphorylates S6K1 which then inhibits PI3K in a negative feedback manner. Adapted from Laplante, M. and Sabatini, D.M. (Laplante & Sabatini, 2012).

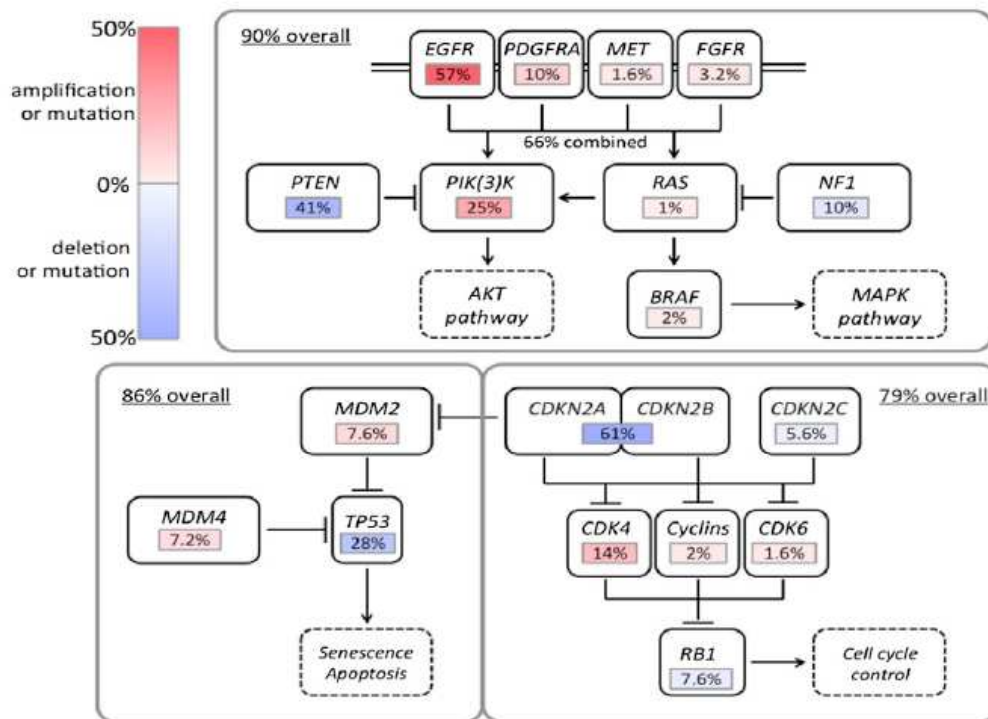


Figure 1.4. TCGA analyses of GBM tumor mutations. The 2013 TCGA study profiled ~500 cases of GBM in an effort to identify oncogenic mutations. Results showed an RTK signaling alteration in 90% of samples. An EGFR amplification or gain-of-function mutation (EGFRV8) was seen in 57%, while PI3K gain-of-function mutation was found in 25%. Homozygous loss of the PI3K negative regulator, PTEN, was found in 41% of cases. P53 signaling was altered in 86% overall, and (c) RB signaling was altered in 79% of cases studied. Adapted from Brennan et al., 2013 (Brennan et al., 2013).

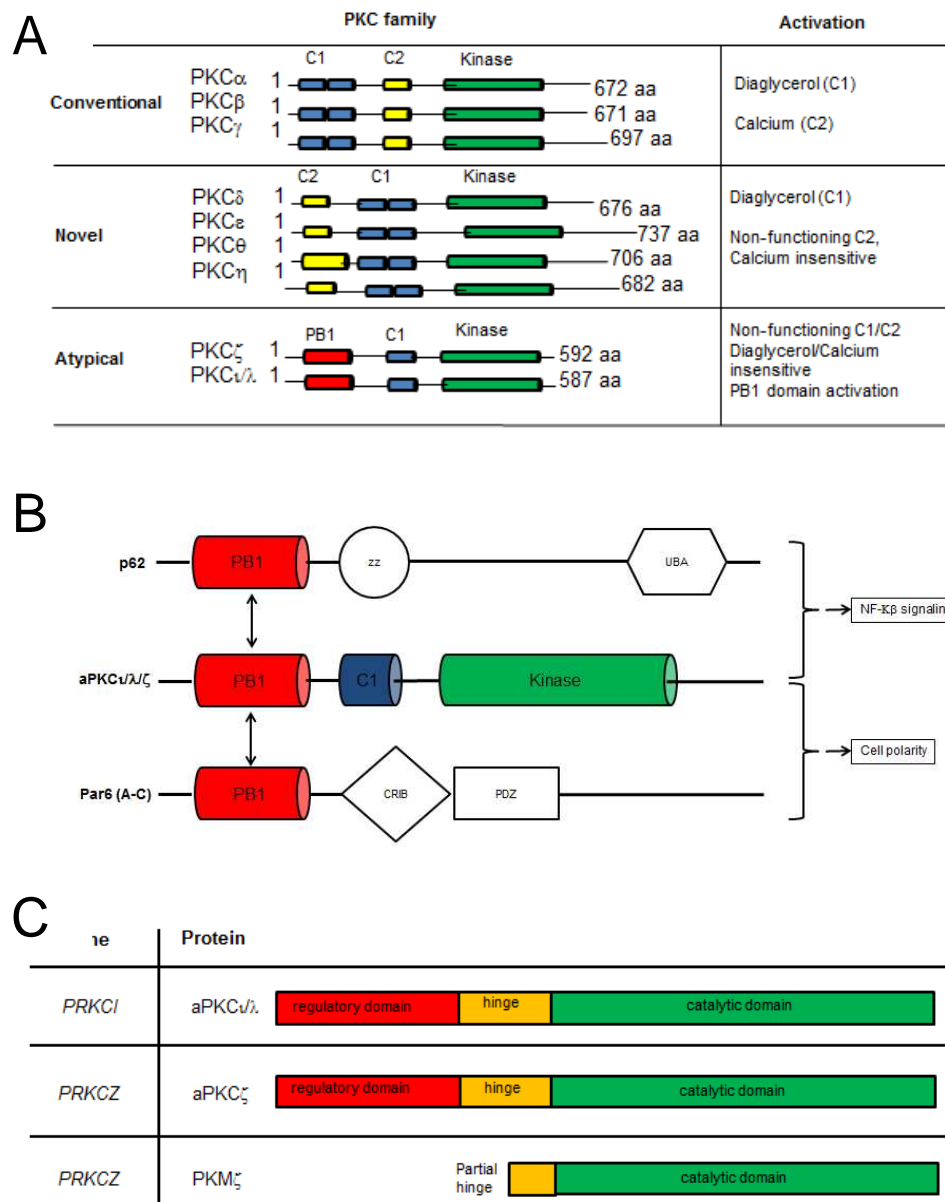


Figure 1.5. Atypical Protein Kinase C. The PKC family consists of 12 broadly conserved isoforms classified into three subgroups based on regulatory and functional characteristics (a). aPKC $\iota/\lambda/\zeta$ binds to proteins via its PB1 domain. When aPKC is associated with p62, it is usually found to participate in NF- κ B signaling whereas its association with Par6 has been shown to be important for cell polarity functioning, such as astrocyte directional migration (b). Two distinct aPKC genes encode for three proteins (c). Adapted from Moscat, J., Diaz-Meco, M., and Wooten, M. (Jorge Moscat, Diaz-Meco, & Wooten, 2007; J. Moscat, Diaz-Meco, & Wooten, 2009b) and Parker *et al.* (Parker *et al.*, 2013b)

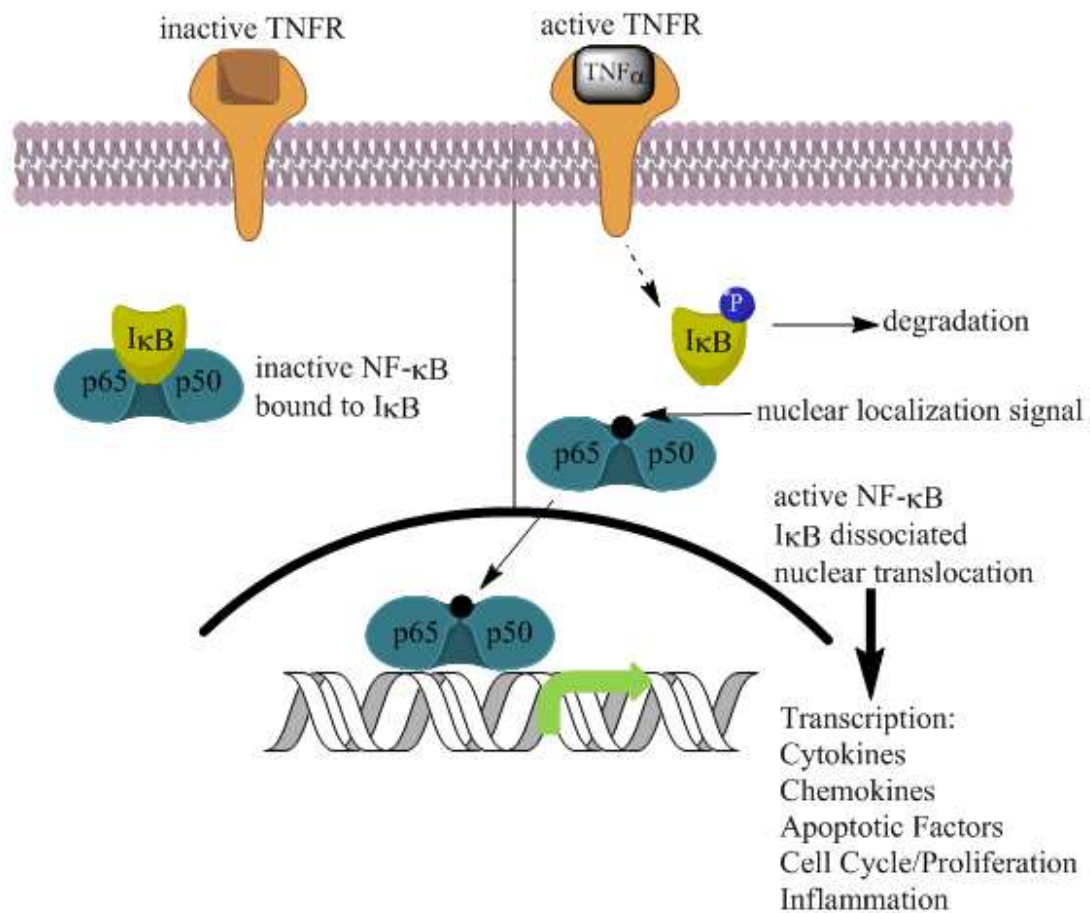


Figure 1.6. TNF- α /NF- κ B Signaling. NF- κ B is a heterodimer transcription factor found in the cytoplasm bound to I κ B, an inhibitory protein. Upon TNF- α ligand binding to TNFR, I κ B is phosphorylated, ubiquitinated and degraded, freeing NF- κ B to enter the nucleus via its nuclear localization signal. Once in the nucleus, NF- κ B binds to the DNA where it begins transcription of various genes including cytokines, chemokines, apoptotic factors, cell cycle genes, and inflammatory genes. Adapted from Hayden, M.S., and Ghosh, S. (Hayden & Ghosh, 2008).

CHAPTER 2

MTOR SIGNALING IN NEURAL DEVELOPMENT AND AGING

INTRODUCTION TO MANUSCRIPT

mTOR in Embryonic Neural Development & Neurodevelopmental Disorders

The development of the mammalian brain is a complex and highly regulated process involving numerous signaling pathways. Without appropriate signaling events and regulation, the embryo may not develop normally leading to birth defects and often death in-utero. The proper signaling cascades lead to brain development and the development of neurons, or neurogenesis. Prior to neurogenesis during embryonic development, polarized neuroepithelial cells function as neural stem cells and first undergo symmetrical cell divisions in order to expand their population. Neuroepithelial cells span from the ventricle to the basal membrane of the epithelial sheet and are polarized along their apical-basal axis. They have compartmentalized expression of transmembrane proteins, such as the apical expression of the ternary complex aPKC/Par3/Par6 and the basal expression of integrin $\alpha 6$, a receptor shown to bind to the basal lamina. As they divide, the cells undergo interkinetic nuclear migration (INM) along this polar axis, as the nucleus migrates basally for replication and back to the apical surface for mitosis.

At approximately E9-E12 in the developing mouse embryo, these neuroepithelial cells begin to divide asymmetrically and produce radial glia, a related neuronal progenitor. While radial glia retain several aspects of the neuroepithelial cells, including their apical basal polarity (i.e., apical localization of aPKC/Par3/Par6); they also begin to express various astroglial properties, including the expression of GFAP and GLAST. These cells extend a long process which contacts the basal lamina and a short process that maintains contact with the apical ventricular lumen, where aPKC/Par3/Par6 is located. Similar to neuroepithelial cells, radial glia also undergo INM. INM was first discovered in 1935 after Sauer observed and reported a differential nuclear positioning during different stages of cellular division (Sauer, 1935). During replication, the nuclei travel basally and return to the apical surface for mitosis. Cells in G1 and G2 phase are

found in between the apical and basal regions. Therefore, apical-basal polarity may be critical for interkinetic nuclear movement and neural progenitor cell division in general or specifically for asymmetric cell division and differentiation.

In addition to the regulation of division by apical-basal polarity, various signaling mechanisms have been shown to regulate the appropriate proliferation and differentiation of radial glia. For example, Notch, a protein found apically localized, has been shown to impact the process of cellular differentiation (Dorsky, Chang, Rapaport, & Harris, 1997; Gaiano & Fishell, 2002). Notch is a cell-surface receptor that upon ligand binding, undergoes cleavage of its intracellular domain which then eventually travels to the nucleus to regulate transcriptional programs. Activation of Notch has been shown to maintain the proliferative status of neural stem cells as well as radial glial cells and block their differentiation (Dorsky et al., 1997; Gaiano, Nye, & Fishell, 2000). Through its ability to enter the nucleus and participate in transcriptional regulation, Notch is able to activate genes such as *hes1* and *hes5*, which then block normal cell differentiation by neutralizing genes which promote neuronal identity (Gaiano et al., 2000; Iso, Kedes, & Hamamori, 2003). This, among other elegant studies, has shown the importance of the Notch signaling cascade in the control of neural stem cell proliferation and differentiation programs.

In addition to Notch signaling, mTOR signaling has been implicated in embryonic neural development. Using transgenic mouse technologies, Shiota, et al (2006) disrupted the normal expression of rictor, a binding partner of mTORC2 (Shiota, Woo, Lindner, Shelton, & Magnuson, 2006). At E9.5, rictor null embryos experience halted growth until death at E11.5. These embryos displayed reduced phosphorylation of AKT at Ser473, an mTORC2 phosphorylation site, indicating a significant reduction in mTORC2 signaling (Shiota et al., 2006). Furthermore, AKT-null mice displayed in a reduction of mTOR activity as evidenced by ribosomal protein S6 phosphorylation in the brain (Easton et al., 2005). These mice developed significantly smaller

brains than their wild type littermates (Easton et al., 2005), thus providing evidence towards the important role of the PI3K/AKT/mTOR pathway in proper embryonic neural development.

A striking report in 2012 by Lee, et al (2012) found that the PI3K/AKT/mTOR pathway was responsible for the development of hemimegalencephaly in postnatal children (J. H. Lee et al., 2012). This malformation, where one half of the brain becomes abnormally larger than the other, occurs during brain development and results in seizures and mental retardation. Patients with hemimegalencephaly may begin showing abnormal hemispheric growth in-utero (Sarnat, Flores-Sarnat, Crino, Hader, & Bello-Espinosa, 2012). Hemimegalencephalic brains display cortical dyslamination and abnormal immature neurons, which indicate abnormalities in neuroglial differentiation and migration (J. H. Lee et al., 2012). Using mass spectrometry and exome sequencing in samples from patients with hemimegalencephaly, Lee et al (2012) found gain of function mutations in PI3K/AKT/mTOR genes in 30% of cases. In addition, the authors reported an increase in S6 protein phosphorylation in the affected brain tissue, providing evidence of a deregulated and over-activated mTOR signaling (J. H. Lee et al., 2012).

Interestingly, the pathological abnormalities found in hemimegalencephaly patients are also seen in patients with tuberous sclerosis (TS), which results from mutations in TSC1 and TSC2 (J. Huang & Manning, 2009; Inoki, Corradetti, & Guan, 2005). In addition to the abnormal neuronal differentiation and migration seen in patients with hemimegalencephaly, patients with TSC develop hamartomas in various organs (J. Huang & Manning, 2009; Inoki et al., 2005). During embryonic development and beyond, cortical tubers may appear, which are characterized by an abnormal pathologic disorganization of the laminar cortex. These cortical tubers may later become the cause of epileptic seizures. In addition, cells may appear abnormal, including dysplastic neurons and large astrocytes. Furthermore, subependymal nodules may appear during fetal development in TSC patients (J. Huang & Manning, 2009; Inoki et al., 2005). These result from benign lesions within the ventricles of the brain, which eventually evolve into subependymal giant cell astrocytomas, a type of tumor. The mutations of TSC1 and TSC2 in

patients with TSC typically result in reduction or loss of function of the TSC complex, leading to hyperactivated mTOR signaling, as in hemimegalencephaly (J. Huang & Manning, 2009; Inoki et al., 2005). Furthermore, TSC patients often times present with symptoms of autism spectrum disorders (ASDs), including abnormal social interactions and inhibited intellectual ability. Murine models of TSC and patients with TSC have been treated with rapamycin in order to inhibit mTOR and the results have proven encouraging (Franz et al., 2006; H. Kenerson, Dundon, & Yeung, 2005; H. L. Kenerson, Aicher, True, & Yeung, 2002; Krueger et al., 2010; L. Lee et al., 2005; Meikle et al., 2008). For instance, treatment of TSC heterozygous mice with deficits in learning and memory, show significant improvement upon rapamycin treatment (Auerbach, Osterweil, & Bear, 2011) and several NIH clinical trials are currently underway to evaluate the efficacy of mTOR inhibitors for autism.

Mice which lacked TSC1 in *emx1*-expressing embryonic telencephalic neural stem cells displayed the abnormal neuropathologies associated with TSC affected patients, including ASD phenotypes (Magri et al., 2011). A loss of TSC1 in these cells resulted in hyperactivation of the mTOR pathway which resulted in a variety of clinically relevant pathological symptoms. Due to an increase in embryonic SVZ neural stem cell proliferation and abnormal premature differentiation, the brains of these mice displayed cortical lamination defects, neuropathological lesions, and epileptic seizures (Magri et al., 2011), as seen in patients with TSC. Embryonically at E16.5, the mutant mice displayed differences in brain size and cortical thickness, indicating abnormal proliferation, differentiation, and lamination (Magri et al., 2011). Using BrdU at E15.5, the authors found that the mutant mice had a significant increase in BrdU positive cells. Furthermore, the amount of Pax6+ radial glial cells, TBR2+ and PH3+ intermediate progenitor cells participating in mitosis was significantly increased, which indicates that the proper differentiation of these progenitor cells was disrupted (Magri et al., 2011). Given that patients with TSC are generally treated with rapamycin, the authors treated these transgenic mice with rapamycin from p8-p60 to inhibit mTOR signaling. This treatment resulted in the cessation of seizures in the mice, and a

normalization of cortical thickness and layering which was identical to the wild type vehicle-treated control (Magri et al., 2011).

The deletion of PTEN in mice using different brain specific cres resulted in macrocephaly, hypertrophy and seizures. PTEN lies upstream of mTORC1 and participates as a negative regulator of the AKT pathway, thus increasing mTORC activity, mimicking a loss of TSC complex. Using the neuron specific *Eno2* cre, *PTEN^{fl/fl}* mice displayed seizures, impaired learning abilities and impaired social interactions (Zhou et al., 2009). These mice develop macrocephaly progressively as well as dendritic and axonal cortical neuron hypertrophy, beginning at 4-5 weeks of age, which correlates with their behavioral phenotypes (Zhou et al., 2009). Interestingly, treatment of these PTEN mutant mice at 5-6 weeks of age inhibited the cellular abnormalities of cortical neuron hypertrophy, reduced the frequency of seizures, and improved the social ability of the mice (Zhou et al., 2009). Similar positive results were obtained when *PTEN^{fl/fl}*;GFAP-cre mice, who display comparable symptoms, were treated with CC1-779, an analog of rapamycin (Kwon, Zhu, Zhang, & Baker, 2003).

Various other neurodevelopmental diseases result from dysregulation of the mTOR signaling pathway including Neurofibromatosis type 1 (NF1), Cowden Syndrome, Proteus syndrome and Lhermitte-Duclos disease (Inoki et al., 2005). These pathologies are caused by mutations in genes which regulate or participate in mTOR signaling and result in hamartomas in multiple organs including the brain, indicating abnormal proliferation regulation of CNS cells. Thus, the mTOR pathway is a critical component of appropriate neural stem cell proliferation and differentiation in the developing brain and dysregulation of its function may lead to neurodevelopmental disorders.

mTOR in Adult Neural Stem Cell Proliferation, Differentiation, and Neurogenesis

In the adult, neurogenesis occurs in two specialized regions of the brain – the subventricular zone (SVZ) of the lateral ventricles and the subgranular zone (SGZ) of the dentate gyrus in the hippocampus. In the SVZ, adult neural stem cells, or GFAP+ type-B cells,

differentiate to give rise to GFAP- type-C Cells, or transit amplifying cells. Type-C cells then divide to produce DCX+ type-A cells, or neuroblasts. Neuroblasts then leave the SVZ and migrate up to a distance of 5mm as a neuroblast chain through the rostral migratory stream (RMS) until reaching the olfactory bulb (OB). Upon reaching the olfactory bulb, the neuroblasts mature into NeuN+ granule or periglomerular neurons. In contrast to the SVZ, SGZ neural stem cells are classified as Type 1 GFAP+ hippocampal progenitors, which have a radial process spanning the granule layer. These cells give rise to Type 2 GFAP- progenitors, which only have a short process. Type 2 transit amplifying cells then give rise to a DCX+ progenitor cell, which will mature to express mature neuronal markers, such as NeuN and Tuj1. Newborn neurons from the SGZ do not migrate nearly as far as SVZ neurons, as upon reaching the granule cell layer of the DG (from the SGZ), they stop migrating to become dentate granule cells. Both newborn neurons generated in the SVZ and SGZ become integrated into the existing circuitry and have been shown to receive functional input (Zhao, Deng, & Gage, 2008).

Methods used to study neurogenesis and adult neural stem cell proliferation or differentiation include the use of 5'-bromo-2'-deoxyuridine (BrdU), a thymidine analog that incorporates into the DNA during S-phase of dividing cells as they undergo DNA synthesis. Cells which are born of the BrdU+ cell will maintain BrdU in their DNA, as well, as it is passed on to progeny through division. Based on the time of BrdU treatment, as well as the time after treatment and before sacrifice, different cell populations may be labeled, allowing the investigator to answer various experimental questions. For example, the intraperitoneal injection of BrdU 2-4 hours prior to sacrifice will label the dividing type-B cells in the SVZ and type-1 cells in the SGZ, thus providing an idea of the cells in S-phase at the time of injection. The use of Ki67, a nuclear protein which is expressed from late G1 through cell cycle exit, as an endogenous marker of cellular proliferation is also quite popular in the neural stem cell and neurogenesis field. Furthermore, Ki67 is frequently used as a proliferation marker in cancer studies. The use of both BrdU and Ki67 provides further information regarding cellular proliferation. For example, the

injection of BrdU 24 hours prior to sacrifice and the co-immunostaining of brain tissue using anti-Ki67 antibody as well as anti-BrdU antibody will result in BrdU+Ki67⁻ cells and BrdU+Ki67⁺ cells. BrdU+Ki67⁻ cells represent cells which were undergoing mitosis at the time of injection, but have since left the cell cycle and are no longer dividing. Cells which are BrdU+Ki67⁺ represent cells which were dividing at the time of injection and still active through the cell cycle at the time of sacrifice. BrdU can also be injected and then “chased” with an interval of time at which point no more BrdU is given. An example of this experimental paradigm includes the consecutive injection of BrdU⁺ for 3 days, followed by 2 weeks sans BrdU prior to sacrifice. After fixation and immunostaining with anti-BrdU antibody, BrdU⁺ cells may be found in the SVZ, along the RMS, and within the OB. This is because the cells which were dividing at the time of injection may have since differentiated into type-C cells, progressed into type-A cells, and migrated through the RMS and made their way into the OB while still expressing BrdU. Thus the use of this experimental paradigm allows an overall snapshot of all of these processes, however does not provide the answer to specific questions such as the effect of an agent to the proliferation of type-B neural stem cells, or the effect of an agent on the migration of type-A neuroblasts. Other markers of proliferation include phosphor-histone H3, which is expressed during M-phase, proliferating cell nuclear antigen (PCNA), which is expressed most significantly during S-phase and MCM2, a protein required for initiation of S-phase and is expressed throughout the cell cycle. Tools such as these have allowed for the discovery of adult neurogenesis in both the mouse and the human.

Studies examining the regulation of adult neurogenesis and the factors which promote it are extremely abundant. Evidence suggests that both intrinsic and extrinsic factors may control neurogenesis of neural stem cells (NSCs) in the adult brain (Lledo, Alonso, & Grubb, 2006). Extrinsic factors for SVZ neurogenesis include neurotransmitters such as serotonin (5-HT) and acetylcholinesterase (ACh), hormones such as thyroid hormone and prolactin, and growth factors such as brain derived neurotrophic factor (BDNF) and epidermal growth factor (EGF). Similar extrinsic factors regulate neurogenesis in the DG; however, in addition DG neurogenesis is also

regulated by environmental conditions, such as running, environmental enrichment, and stress (J. Brown et al., 2003). Kato-Semba, et al. (2002) showed that stimulation of BDNF enhances DG neurogenesis and this BDNF-induced increased neurogenesis can be blocked by using antibodies specific to BDNF (Kato-Semba et al., 2002). Early studies looked at the effect of BDNF for SVZ neurogenesis in-vitro (Ahmed, Reynolds, & Weiss, 1995; Kirschenbaum & Goldman, 1995). These studies found that BDNF supports the survival of newborn neurons in-vitro, and therefore increases neurogenesis in the adult. Zigova, et al. (1998) confirmed that ventricular infusion of BDNF led to an in-vivo increase in BrdU+ cells in the OB (Zigova, Pencea, Wiegand, & Luskin, 1998). Using a knock-in mouse with a variant form of BDNF which impairs its activity dependent secretion and a BDNF haploinsufficient mouse (BDNF+/-), Chen, et al., (2008) found no change in the proliferation of B cells in the SVZ (Z. Y. Chen, Bath, McEwen, Hempstead, & Lee, 2008). However, they did find a significant decrease in the number of BrdU+ A cells in the OB in both strains. The authors explored the mechanism of this effect and determined that BDNF, though TrkB receptors are critical for A cell survival and migration (Z. Y. Chen et al., 2008). An interesting study by Doetsch, et al., (2002) found that infusion of EGF into the ventricle of adult mice led to an increase in the number of B and C cells, and an increase in their mitotic index (dividing versus non-dividing cells) (F. Doetsch, Petreanu, Caille, Garcia-Verdugo, & Alvarez-Buylla, 2002). They reported, however, no increase in neuroblasts, and therefore suggest that EGF infusion led to an increase in self-renewing divisions of the B cells and C cells, at the expense of new neuron production. Therefore, EGF is acting to regulate the self-renewal of B cells and C cells in the SVZ, but not their differentiation into A cells. However, it is interesting to note that EGF had no proliferative effect on hippocampal precursor cells (Kuhn, Winkler, Kempermann, Thal, & Gage, 1997). Recently, another study described the importance of Insulin-like growth factor 2 (IGF2) in DG neurogenesis (Bracko et al., 2012). Using transcriptome analyses, the authors compared differences in gene expression between adult NSCs and immature neurons. They found significantly higher levels of IGF2 in DG NSCs compared to

immature neurons and knocked out IGF2 in-vivo to confirm a reduction in adult DG NSC proliferation (Bracko et al., 2012). Interestingly, another report found that IGF2 is secreted in the CSF by the choroid plexus and stimulates the proliferation of adult NSCs in the SVZ (Lehtinen et al., 2011).

Given the importance of growth factor signaling regulation of adult neural stem cell proliferation, differentiation and neurogenesis, it is not surprising to learn that mTOR has been shown to play a role as well. BDNF, for example, can activate mTOR (Schratt, Nigh, Chen, Hu, & Greenberg, 2004; Slipczuk et al., 2009; Takei et al., 2004; Yang, Hu, Zhou, Zhang, & Yang, 2013), and BDNF has been implicated in various psychiatric disorders, including depression. Successful treatment of depression using selective serotonin reuptake inhibitors (SSRIs) has been shown to require neurogenesis (David et al., 2009; Santarelli et al., 2003). In addition, the infusion of BDNF into the hippocampus resulted in increased neurogenesis (Scharfman et al., 2005) and reduced depression symptoms (Shirayama, Chen, Nakagawa, Russell, & Duman, 2002). Although these studies did not directly examine the effect of BDNF on mTOR signaling, it can be hypothesized that mTOR activity was increased due to its strong activation downstream of BDNF (Schratt et al., 2004; Slipczuk et al., 2009; Takei et al., 2004; Yang et al., 2013).

Perhaps more direct evidence of the role of mTOR in adult neurogenesis comes from a study by Paliouras et al (2012). These authors found mTOR activation to be increased in embryonic neurogenesis and maintained in the adult SVZ niche. Interestingly, within the SVZ, they found that approximately 95% of phosphorylated S6 positive cells were positive for Ki67, a proliferation marker. Their results also found that approximately 80% of the phosphorylated S6 positive cells were also positive for Mash1, a neuronal progenitor cell marker. The authors infused rapamycin into the mouse ventricles and found a reduction in Ki67+ Mash1+ progenitors. No changes were found in caspase-3 staining, indicating that the effect of rapamycin on the neuronal progenitors in the SVZ was an effect of proliferation, rather than apoptosis (Paliouras et al., 2012). Furthermore, in-vitro treatment of neural progenitors grown as neurospheres with EGF

resulted in an increase in phosphorylated S6 and phosphorylated mTOR, indicating mTOR activation downstream of EGF stimulation in these cells. When these cells were treated with rapamycin or KU0063794, which inhibits both mTORC1 and mTORC2, the result was a reduction in the number and size of the neurospheres, indicating a deficit in progenitor cell proliferation caused by mTOR inhibition. In addition, the authors found that while mTOR was activated in neural progenitors expressing proliferative markers, it was reduced during differentiation (EGF-withdrawal) of these cells (Paliouras et al., 2012).

Given that neural stem cell proliferation and neurogenesis declines with age, the authors conducted immunohistochemistry for phosphorylated S6 and Ki67 in the SVZ of aging mice (Paliouras et al., 2012). Their results showed a reduction in both of these markers, providing a correlation between decreased mTOR activation and reduced SVZ neural stem cell proliferation. Interestingly, upon infusion of EGF into the ventricles of aged mice, the authors found re-activation of mTOR activity and increased proliferation of neural stem cells in the SVZ. However, mice that received a co-infusion of EGF with rapamycin did not display the same effects. Instead, these mice failed to show an increase in proliferation or mTOR activation in SVZ neural progenitors (Paliouras et al., 2012).

Kim, et al (2009) studied the function of Disrupted-in-schizophrenia 1 (DISC1) in adult hippocampal newborn neurons (Ju Young Kim et al., 2009). A DISC1 genetic alteration was discovered to correlate with schizophrenia, bipolar disorder and depression from studies examining a Scottish family (Blackwood et al., 2001; Ju Young Kim et al., 2009; Millar et al., 2000). It is now well recognized that DISC1 is a risk factor for many psychiatric illnesses, including schizophrenia, bipolar disorder, and depression. In 2009, Kim, et al. found that suppression of DISC1 in newborn dentate granule cells of the hippocampus led to increased activation of AKT (J. Y. Kim et al., 2009). The authors note increased phosphorylation of S6 ribosomal protein, indicating increased mTOR activation. These increased signaling changes resulted in defects in both the growth and morphogenesis of the adult newborn neurons and their

positioning in the dentate gyrus of the adult hippocampus. The newborn cells also displayed limited dendritic growth and reduced synapse formation. Furthermore, the treatment of these mice with rapamycin to inhibit AKT and mTOR activation was successful in rescuing the abnormal defects (Ju Young Kim et al., 2009). Given these results and the association of DISC1 with psychiatric disorders, some researchers have postulated that abnormal adult neurogenesis may play a significant role in the development of adult onset psychiatric disorders (Kimberly Christian, 2010; Ming & Song, 2011). This study, among others, and those described above in relation to embryonic neural stem cell proliferation and differentiation, provide evidence regarding the importance of mTOR signaling for these biological processes.

Stabilization, Survival and Integration of Adult Newborn Neurons

Initial proliferation and differentiation of NSCs is not the only important factor in neurogenesis, stabilization and survival of newborn neurons is also an important regulatory process. Evidence has shown that only ~50% of SVZ & DG-newborn neurons will survive longer than a month (Dayer, Ford, Cleaver, Yassaee, & Cameron, 2003; Petreanu & Alvarez-Buylla, 2002). After young OB neurons are matured and have made stable synaptic connections, their survival is dependent on the level of activity they receive (Petreanu & Alvarez-Buylla, 2002). Similar conclusions can be drawn regarding the survival of newborn neurons in the DG. The full integration and synaptic connectivity of these newborn cells is important for their survival.

Data regarding the functional integration of adult-born young neurons came from studies using viral vectors. In 2002, Carlen, et al. injected a GFP-expressing virus into the brain which selectively infects and replicates in neurons (Carlen et al., 2002). The virus is transported along axons and dendrites to infect other neurons in a functioning circuit. In order to investigate the integration of SVZ-born OB neurons, mice were given BrdU for 4 weeks, followed by a 3 week chase period. This chase allows for the subsequent detection of integrated newborn neurons. Newborn neurons are mostly periglomerular, and these neurons extend axons only locally. However, these new cells do receive inputs from other neurons in the OB which project axons to

the piriform cortex (projection neurons). Therefore, the investigators injected the GFP virus into the piriform cortex and upon analyses, found GFP expression in BrdU+ periglomerular neurons of the OB (Carlen et al., 2002). Because this virus requires synaptic transmission, this experiment indicates that the new neurons were connected into a functional circuit. They conducted a similar experiment to evaluate functional connectivity of SGZ-born neurons and found GFP expression in BrdU+ neurons of DG neurons. This initial report was one of the first to show successful synaptic connections on adult-newborn neurons (Carlen et al., 2002).

More recent evidence using patch clamp techniques and immunohistochemistry has shown that within 24hrs of reaching the OB, SVZ-newborn neurons receive GABAergic and glutamatergic input synapses (Panzanelli et al., 2009). Three days later, cells take on a mature morphology and extend dendrites with clearly defined spines into the external plexiform layer (Panzanelli et al., 2009). Interestingly, OB neurons can generate either granule cells or periglomerular cells. The different fate acquired occurs at the maturation stage. In periglomerular cells, voltage-dependent sodium current precedes synaptic contacts. However, granule cells first establish synaptic connections and then develop the sodium current (Belluzzi, Benedusi, Ackman, & LoTurco, 2003; Carleton, Petreanu, Lansford, Alvarez-Buylla, & Lledo, 2003). Although correlative, other evidence of fully functioning newborn neurons comes from decreased olfactory discrimination and odor memory upon genetic manipulation to reduce newborn cells in the OB (Breton-Provencher, Lemasson, Peralta, & Saghatelian, 2009; Z. Y. Chen et al., 2008; Enwere et al., 2004; Gheusi et al., 2000).

Similar to the OB, in the DG, newborn neurons also make connections almost immediately after the immature neurons exit the cell cycle. Around 10 days after birth, mossy fibers are detected and will extend until reaching the CA3 region before mature spines are formed (Zhao et al., 2008). Recent evidence indicates that the newborn cells receive afferent projections from the entorhinal cortex between 14-21 days after birth (Zhao et al., 2008). At this age they do have glutamate receptors, however, most synaptic currents are GABA-mediated (Overstreet

Wadiche, Bromberg, Bensen, & Westbrook, 2005). In addition, electron microscopy studies showed that by 30 days of age, newborn neurons receive synaptic inputs from axosomatic and axodendritic connections, closely resembling their already matured DG neuron neighbors (Lledo et al., 2006). Various electrophysiological studies have showed that newborn neuron synaptic integration follows the sequence that embryonic neurons undergo -- including initial excitatory GABAergic inputs which later convert to inhibitory inputs (Ben-Ari, 2002). Interestingly, while the newborn neurons seem to function as their mature neighbors, they do display enhanced synaptic plasticity (Schmidt-Hieber, Jonas, & Bischofberger, 2004). It has been suggested that this may facilitate long-term changes in the network, as the neuron is hyperactive and thus has an advantage over the mature neurons for stabilization of its synaptic connections (Tashiro, Sandler, Toni, Zhao, & Gage, 2006; Toni et al., 2008). Using confocal microscopy, Ramirez-Amaya, et al., (2006) examined the expression of the immediate early gene Arc (Ramirez-Amaya, Marrone, Gage, Worley, & Barnes, 2006). Arc mRNA and its protein have been reported to be induced by spatial exploration in the same cells which are electrophysiologically activated in the hippocampus. By the evaluation of Arc expression after giving mice BrdU and subjecting them to a behavioral paradigm, the investigators were able to identify BrdU+ cells that respond to behavioral exploration. They found that matured (5 month old) newborn granule cells do express Arc after behavioral exploration, and that that a larger amount of BrdU+ cells expressed Arc as opposed to BrdU- cells (Ramirez-Amaya et al., 2006). This data adds to the convincing evidence in the field that newborn neurons participate in preexisting hippocampal networks. Upon maturation and full integration, these newborn neurons become a permanent part of the functioning circuit, as BrdU-labeled neurons were found to be stable at least 11 months after their neurogeneration (Kempermann, Gast, Kronenberg, Yamaguchi, & Gage, 2003; Leuner et al., 2004).

mTOR signaling has been implicated in the survival and integration of newborn neurons. For instance, rapamycin treatment reduced dendritic complexity, or arborization, of growing neurons, and transfection of constitutively active PI3K and AKT results in increased dendritic

arborization and an increase in phosphorylated S6, or mTOR activation (Kumar, Zhang, Swank, Kunz, & Wu, 2005). mTOR activation has been shown to regulate local protein synthesis at the synapse, regulating synapse formation, which is required for newborn neurons to live (Jacinto & Hall, 2003). Interestingly, mTOR activation is induced upon ketamine administration, a drug shown to result in anti-depressant effects (N. Li et al., 2010). In accordance with the hypothesis that a potential mechanism for anti-depressant efficacy requires increased synaptic connectivity, ketamine treatment in mice results in increased synaptic protein synthesis and increased synaptic spines as well as increased synaptic strength (N. Li et al., 2010). The infusion of rapamycin prior to ketamine administration completely blocks the synaptic effects of ketamine in addition to blocking the anti-depressive effects (N. Li et al., 2010), suggesting a role for mTOR in synaptic stabilization.

In conclusion, the study of adult neurogenesis is of extreme interest to the scientific field. Uncovering the signaling mechanisms regulating neurogenesis and the division of neural stem cells harbors enormous potential for the treatment of neurodegenerative diseases. Data over the past 20 years has elucidated the strong role of growth factors and signaling cascades on this process and this has implications for potential therapies. Furthermore, advances in electrophysiological techniques, viral labeling techniques and transgenic mouse production has led to the confirmation of the long-held hypothesis that newborn neurons are indeed fully functioning and integrated into existing circuits. Data has shown that the newborn cells are capable of receiving and inducing signals, as well as releasing neurotransmitters. In addition, the newborn neurons are hyperactive, therefore giving them an advantage for survival and integration, as they can respond faster to stimuli. Although many advances have been made in this field, a further more detailed look at the role of these new neurons in learning and memory is warranted. In addition, very little knowledge of neurogenic regulation has been gleaned from higher species or humans. The future of this field should attempt to enter more into human studies, as learning how to regulate this process for human application will prove invaluable.

MANUSCRIPT: CONTRASTING EFFECTS OF CHRONIC, SYSTEMIC TREATMENT WITH
MTOR INHIBITORS RAPAMYCIN AND METFORMIN ON ADULT NEURAL PROGENITORS IN
MICE

ABSTRACT

The chronic and systemic administration of rapamycin extends lifespan in mammals. Rapamycin is a pharmacological inhibition of mTOR. Metformin also inhibits mTOR signaling, but by activating the upstream kinase AMPK. Here we report the effects of chronic and systemic administration of the two mTOR inhibitors, rapamycin and metformin, on adult neural stem cells of the subventricular region and the dentate gyrus of the hippocampus in mouse. While rapamycin decreased the number of adult neural stem cells, metformin-mediated inhibition of mTOR had no such effect. Adult-born neurons are considered important for cognitive and behavioral health, and may contribute to improved health span. Our results demonstrate that distinct approaches of inhibiting mTOR signaling can have significantly different effects on organ function and underscore the importance of screening individual mTOR inhibitors on different organs and physiological processes for potential adverse effects that may compromise health span.

INTRODUCTION

The mTOR signaling pathway has a conserved role in the regulation of replicative and chronological life span in yeast and organismal life span in *Caenorhabditis elegans*, *Drosophila*, and mammals (S. C. Johnson et al., 2013). The inhibition of mTOR signaling with chronic, systemic 2.24-mg/kg (14 ppm) administration of rapamycin, a product of the soil bacteria *Streptomyces hygroscopicus*, extends life span in mice, even when introduced late in life (Harrison et al., 2009). Rapamycin 4.7, 14, and 42 ppm in food also slows age-dependent pathology of the liver, heart, and tendons (Wilkinson et al., 2012). A recent study demonstrated that chronic 2.24-mg/kg rapamycin inhibits age-associated cognitive decline (Halloran et al., 2012). Furthermore, rapamycin treatment was associated with anxiolytic and anti-depressive effects (Halloran et al., 2012).

While neurogenesis occurs primarily during embryonic and early postnatal mammalian development, the adult mammalian brain does retain the ability to produce new neurons. Cognitive functions, learning and memory, and behavioral health can be improved by increased adult neurogenesis (Deng, Aimone, & Gage, 2010; Lazarov, Mattson, Peterson, Pimplikar, & van Praag, 2010; Ramirez-Amaya et al., 2006). Additionally, antidepressants function by stimulating adult neurogenesis (Yun Li et al., 2008; Malberg, Eisch, Nestler, & Duman, 2000). Neurogenesis in an adult mammal occurs in specialized regions of the brain such as the subventricular zone (SVZ) and the subgranular zone of the dentate gyrus (DG) (Kriegstein & Alvarez-Buylla, 2009). In these regions, slowly cycling B cells (GFAP+), the self-renewing adult neural stem cell population, give rise to transient amplifying C cells (EGFR+), which in turn produce neuroblasts marked by the expression of doublecortin (DCX+). Adult-born neurons integrate into functional circuits (Yan Li, Mu, & Gage, 2009). Adult neurogenesis decreases with aging and the loss of neurogenesis can be correlated with cognitive and behavioral decline (Kuhn, Dickinson-Anson, & Gage, 1996; Lazarov et al., 2010). Conversely, caloric restriction, which extends life span, increases adult neurogenesis (Lazarov et al., 2010; Levenson & Rich, 2007).

From *Drosophila* to mice, multiple steps during neurogenesis—neural progenitor proliferation, survival, and differentiation into neurons—have been reported to engage the mTOR signaling pathway (Fishwick, Li, Halley, Deng, & Storey, 2010; Han et al., 2008; Ju Young Kim et al., 2009; L. Li et al., 2010; McNeill, Craig, & Bateman, 2008; Palazuelos, Ortega, Diaz-Alonso, Guzman, & Galve-Roperh, 2012; Paliouras et al., 2012; Raman et al., 2011). For example, the loss of activators of mTOR signaling, IgfR1, in neural precursors, results in reduced proliferation in the SVZ and microcephaly (Kappeler et al., 2008; Lehtinen et al., 2011; W. Liu, Ye, O'Kusky, & D'Ercole, 2009). Conversely, increased Igf activity resulted in increased proliferation in the SVZ and macrocephaly (Lehtinen et al., 2011). Two independent mTOR complexes—mTORC1 and mTORC2—are found in mammalian cells (Laplane & Sabatini, 2012). Rapamycin is a well-characterized mTORC1 inhibitor (Guertin & Sabatini, 2009). This macrolide first binds to the

cyclophilin FKBP12 in mammalian cells, and the complex subsequently interacts with mTOR and inhibits its function. Paliouras *et al.* (Paliouras et al., 2012) demonstrated that rapamycin infusion (0.5 mM) into the left ventricle of mice for 7 days results in a 48 % reduction of proliferating neural stem cell numbers (Paliouras et al., 2012). Furthermore, rapamycin reduces neural stem cell proliferation in vitro; both the size and number of neural stem cells grown as neurospheres were reduced following rapamycin treatment (Paliouras et al., 2012). Additionally, neural stem cells fail to differentiate normally in the presence of this drug (Paliouras et al., 2012). Four weeks of rapamycin treatment (10 mg/kg) significantly decreased social interaction time in mice (Zhou et al., 2009). In contrast, 1 and 4 weeks of rapamycin treatment (20 and 10 mg/kg, respectively) have been reported not to affect gross morphology of the important neurogenic niche, DG, or normal, newborn neurons and the performance of mice in open field behavioral tests (Ju Young Kim et al., 2009).

Metformin represents an additional pharmacological approach to inhibit mTORC1 signaling (Mihaylova & Shaw, 2011). This anti-diabetic biguanide acts by increasing AMP activated protein kinase (AMPK) activity (Shaw et al., 2005). When activated, AMPK negatively regulates mTOR activation (Laplante & Sabatini, 2012). AMPK activation slows aging in *C. elegans* (Apfeld, O'Connor, McDonagh, DiStefano, & Curtis, 2004; Mair et al., 2011) and is being considered as a calorie restriction mimetic (Ingram et al., 2006). Therefore, metformin has been used for life extension in mammals and, in some studies although not all, has demonstrated gerosuppressive effects (Vladimir N. Anisimov et al., 2008; V. N. Anisimov et al., 2011; Berstein, 2012). Interestingly, 12 days of treatment with metformin has been shown to increase adult neurogenesis and spatial memory (J. Wang et al., 2012). However, the effect of longer term treatment remains unknown.

We directly investigated the effects of a chronic, systemic rapamycin or metformin treatment on proliferating neural progenitor cells of the SVZ and DG in mice. Here we report that a 9-week chronic administration of rapamycin, but not metformin, reduces the number of

proliferating neural progenitors in the mammalian neurogenic niches in adult mice. Additionally, a similar decrease in proliferation and in neuronal differentiation was observed in murine adult neural stem cells cultured in vitro upon rapamycin treatment. In contrast, metformin treatment did not significantly reduce neural stem cell proliferation or differentiation. Our studies indicate that two distinct methods of inhibiting mTOR activity differentially affect mammalian adult neural stem cells.

MATERIAL AND METHODS

Mice

Adult male (12 weeks) C57BL/6J mice were purchased from the Jackson Laboratory (Bar Harbor, ME). All mice were housed under specific pathogen-free conditions at the University of Arizona, maintained under a strict 12-h light cycle and given a regular chow diet. Upon arrival, the mice were rested for 1 week prior to manipulation. The mice were kept in individual metabolic cages for an initial 24-h adaptation period followed by a 24-h period during which food intake was measured. Baseline, 4- and 8-week measurements were performed. The mice were given free access to food and water for the entire study period. The mice were weighed before and after being placed into the metabolic cages. All experimental procedures were conducted with approval from the University of Arizona Institutional Animal Care and Use Committee. Rapamycin (LC Labs) and metformin (Sigma) were administered by daily i.p. injection during the treatment period. Rapamycin was administered in a high (2.5 mg/kg) or low (75 µg/kg) dose. Metformin was administered at a dose of 200 mg/kg. Control mice received daily PBS i.p. injections. BrdU (50 mg/kg, Sigma) was given by i.p. injection every 12 h, beginning 48 h prior to harvest.

Antibodies

For immunoblotting, rabbit phospho-S6 ribosomal protein (Ser240/244, #5364) and mouse S6 ribosomal protein (#2317) antibodies were purchased from Cell Signaling and were used at a concentration of 1:1,000. For immunocytochemistry, mouse Tuj1 (MAB1637) and rabbit Nestin (MAB5922) antibodies were purchased from Millipore and used at a concentration of 1:250

and 1:500, respectively. For immunohistochemistry, rabbit DCX (ab18723), rat BrdU (ab6326), and rabbit Ki67 (ab16667) antibodies were purchased from Abcam and used at a concentration of 1:100. Rabbit Phospho-S6 ribosomal protein (Ser235/236) conjugated to Alexa Fluor 647 was purchased from Cell Signaling (4851) and used at 1:100. Species-specific Alexa Fluor conjugated secondary antibodies were purchased from Invitrogen and used at 1:500. HRP-conjugated species-specific secondary antibodies were purchased from Promega and used at 1:2,000.

Measurement of rapamycin and metformin

Method was adapted from Streit *et al* (Streit, Armstrong, & Oellerich, 2002).

Measurement of rapamycin and metformin in mouse blood were performed using a TSQ Quantum liquid HPLC-electrospray ionization-tandem mass spectrometry system (Thermo Finnigan, San Jose). Serial dilutions of a known amount of rapamycin or metformin spiked into blank EDTA mouse blood were used as internal standards for quantitation of the drugs in the blood. The scan for rapamycin was performed at 931.5 (M+NH₄) \rightarrow 864.7 at a collision energy of 20 eV. Metformin was detected by selective reaction monitoring; parent mass/charge ratio for metformin is 130.1 and the fragment monitored is 71.1. The collision energy was 33 eV.

Chemicals

Rapamycin white powder was stored at -20 °C, Clarithromycin (internal standard; Sigma catalog # A3487) white powder stored at 4 °C, Methanol Optima LC/MS grade (Thermo Fisher Scientific), Zinc Sulfate (as heptahydrate) (Fisher Chemical), Water collected from an in-lab Barnstead water purification system. Metformin white crystalline powder was stored at room temperature, Methanol Optima LC/MS grade (Thermo Fisher Scientific), Zinc Sulfate (as heptahydrate) (Fisher Chemical), Water collected from an in-lab Barnstead water purification system.

Immunohistochemistry

Mice were euthanized and perfused with 30 mL PBS before the brains were quickly removed and flash frozen in isopentane. Specimens were then stored at -80°C . The brains were mounted using OCT and sectioned at $14\text{ }\mu\text{m}$. For BrdU staining, slides were first fixed in 4 % PFA for 15 min and subsequently washed 3x in PBS for 10 min each. Slides were denatured in 2 N HCl for 15 min at 37°C , and then for another 15 min in 2 N HCl at room temperature (RT). Slides were rinsed in boric acid buffer (0.2 M orthoboric acid, pH 8.4) and incubated for further 10 min at RT. They were then washed 3x in PBS, blocked in 5 % donkey serum with 0.1 % Triton X- 100 for 2 h at RT. Sections were incubated in primary antibody in blocking buffer at 1:100 overnight at 4°C . Slides were washed 3x in PBS with 0.1 % Triton X- 100 (PBST) for 10 min each and subsequently incubated with secondary antibodies for 2 h at RT. Slides were washed in 3x in PBS for 10 min, and fixed again in 4 % PFA. Slides were subsequently washed and denatured again prior to blocking and incubation in the second primary antibody (DCX) overnight at 4°C . After overnight incubation, the slides were washed 3x in PBS and incubated for 10 min in 100 ng/mL DAPI before being mounted in Prolong Gold Antifade Reagent (Invitrogen), cover-slipped and imaged using a Leica SP5 confocal microscope. For immunohistochemistry using p-S6 ribosomal protein antibodies, sections were fixed in 4 % PFA, washed 3x in PBS and then blocked in 10 % donkey serum in PBST for 2 h at RT. Sections were incubated with primary antibody at 1:100 in blocking buffer overnight at 4°C . Sections were washed 3x with PBS and incubated for 10 min in 100 ng/mL DAPI before being cover-slipped and imaged on a Leica SP5 confocal microscope.

Quantification of BrdU+ Cells

Fourteen-micrometer sections were collected beginning at the olfactory bulbs and ending at the cerebellum. Series of every 15th section through each sample were processed for BrdU immunohistochemistry as described above and every adjacent section was stained with H&E. The SVZ was defined as beginning at the bregma 1.41 mm until -0.11 mm . Only cells existing

within 0.1 mm lateral to the ependymal lining were counted. No cells on the medial SVZ were considered. The total number of sections in which the SVZ appeared were ~85-100 (roughly 1.2 mm rostral-caudal). The DG was defined as beginning at the bregma -1.077 mm until the bregma -3.39 mm. The total number of sections in which the DG appeared were ~130-170 (roughly 2 mm rostral-caudal). The areas of the SVZ and DG were measured using ImageJ (NIH). For cell counting, the investigator was blinded to the experimental condition. BrdU-labeled cells were exhaustively counted on every 15th section through the entire DG or SVZ.

Neural Stem Cell Isolation

For both neurosphere and adherent neural stem cell culture, postnatal day 30 (p30) C57BL/6 mice were used. Briefly, the brains were removed and placed in ice-cold Leibovitz's L15 media (Invitrogen) for dissection. Using a microsurgery knife, a 1-mm coronal section was obtained corresponding to the region of the SVZ. Cuts were made vertically following the ventricle ventrally and horizontally following the ventricle dorsally. A small piece of SVZ was then dissected and placed into a 1.5-mL microcentrifuge tube containing 300 μ L of 0.25 % Trypsin-EDTA in PBS and incubated at 37 °C for 20 min. Seven hundred microliter of complete media (see Supplementary Information) was added, and the tissue was gently triturated until single cell suspension was obtained. Cells were then plated either in complete media (for neurospheres) or N5 media (for adherent neural stem cell culture). The composition of N5 media is provided in the Supplementary Information. Overnight treatment with different concentrations of rapamycin and metformin were tested on neural stem cells and the concentrations showing maximal inhibition of mTOR (assayed by inhibition of rS6 phosphorylation) without significant cell death were used in the study (200 nM rapamycin and 500 μ M metformin).

Immunoblotting

For immunoblotting, neurospheres were grown in the presence or absence of rapamycin or metformin for 3 h prior to lysing. For lysis, ice-cold 1 % NP-40 buffer (20 mM Tris-HCl at pH 8, 137 mM NaCl, 10 % glycerol, 1 % NP-40) supplemented with phosphatase and protease

inhibitors (Halt protease and phosphatase inhibitor cocktail, Thermo Scientific) was used. Briefly, cells were washed 3x with ice-cold PBS and then resuspended in cold NP-40 buffer. Lysates were kept cold and sonicated ten times, 1 s each, and then centrifuged at 12,000xg for 5 min at 4 °C. LDS sample loading buffer (Invitrogen) with DTT was added, and the immunoprecipitates were boiled for 5 min prior to loading onto precast SDS-PAGE gels (Invitrogen). Gels were transferred onto methanol pre-soaked PVDF membranes and subsequently blocked with 5 % BSA in TBS for 2 h. The blot was incubated in phospho-S6 ribosomal protein antibody (Cell Signaling, #5364, 1:1,000) overnight at 4 °C, after which blots were washed 3x with TBST (TBS+0.1 % Tween) for 15 min each, followed by incubation with secondary antibodies (1:2,000) for 1 h at RT. Blots were then washed 3x for 30 min each in TBST, with a final wash in TBS alone. Blots were stripped and reprobed using total S6 ribosomal protein antibody (Cell Signaling, #2317, 1:1,000) overnight at 4 °C prior to secondary incubation and developing. All blots were developed using Super Signal West Dura (Thermo Scientific) on the UVP Imager.

Neural Stem Cell Proliferation and Apoptosis

Neurospheres and adherent neural stem cell cultures were treated overnight with 200 nM rapamycin and 500 µM metformin. For proliferation assays, cells were grown overnight in the presence of 10 µM BrdU. BrdU was detected using a BrdU-APC (BD Pharmingen #552598) kit according to manufacturer's instructions. For cell cycle analysis, cells were washed 3x with PBS and resuspended in 1 mL of ice-cold PBS in polypropylene tubes. For fixation, cells were gently vortexed while adding 3 mL of ice-cold absolute ethanol dropwise and then fixed overnight at 4 °C. For staining, cells were washed with ice-cold PBS and resuspended in 300 µL of propidium iodide solution (200 ng/mL RNase A, 20 mg/mL propidium iodide, 0.1 % Triton X-100 in PBS) for 15 min at 37 °C. Data were collected using an Accuri C6 (BD Biosciences) and was analyzed using FlowJo (Tree Star). In vitro apoptosis experiments were performed on dissociated adherent neural stem cells using the ApoDetect Annexin V-FITC kit (Invitrogen #33-1200) according to the manufacturers' instruction.

Neural stem cell culture and differentiation

Neurospheres were maintained in complete media. For differentiation, neurospheres were dissociated using TrypLE (Invitrogen) following manufacturer's instructions and seeded onto acid-etched coverslips (70 % EtOH, 1 % HCL in PBS, 5 min followed by extensive PBS wash) in differentiation media #1 or without rapamycin or metformin for 2 days. The media was then changed to differentiation media #2 for 5 days with or without drug.

For in vitro proliferation and differentiation experiments, rapamycin was used at 200 nM, metformin was used at 500 μ M. Differentiation Media #1 was composed of 49.9 mL Control Media, 100 μ L heparin solution, and 0.5 μ g bFGF2. Differentiation Media #2 consisted of 49 mL control media and 1 mL of FBS.

Immunocytochemistry

Following differentiation, coverslips were fixed with 4 % PFA for 15 min at RT, then washed 3x with PBS and permeabilized with PBST for 15 min at RT. Cells were blocked for 2 h with 2 % normal horse serum (Invitrogen) in PBS at RT. Primary antibodies were diluted in 2 % normal horse serum and cells were incubated overnight at 4 °C. Subsequently, coverslips were washed 3x with PBS and secondary antibodies (Alexa-Fluor-488 and 594) diluted in 2%normal horse serum were added for 2 h at RT. Following the secondary antibody incubation, cells were stained with 100 ng/mL DAPI for 10 min at RT. Finally, coverslips were washed 3x with PBS and mounted onto slides using ProLong Gold antifade reagent (Invitrogen) and sealed with nail polish. Images were obtained using a Leica SP5 confocal microscope.

Statistical analysis

Differences between the means of experimental groups were analyzed with a two-tailed t test (Prism GraphPad Software, Inc.). P values ≤ 0.05 were considered significant. A minimum of five mice per category (control, rapamycin 75 μ g/kg, rapamycin 2.5 mg/kg and metformin-treated groups) were tested for all in vivo experiments described. In vitro experiments were performed in triplicates.

SUPPLEMENTARY MATERIAL AND METHODS

Neural stem cell culture

Complete Media was prepared as follows: 49.7 mL of Control Media, 200 mg BSA, 100 μ L heparin solution, 1 μ g EGF, and 0.5 μ g bFGF2. Control Media consisted of 415 mL DMEM/F12, 10 mL 30% glucose, 7.5 mL 7.5% NaHCO₃, 2.5 mL 1M HEPES, 5 mL of 200 mM L-glutamine, 50 mL hormone mix and 1% penicillin/streptomycin. 10X Hormone mix consisted of 400 mL DMEM/F12, 8 mL 30% glucose, 6 mL 7.5% NaHCO₃, 2 mL 1M HEPES, 400 mg Apo-transferrin, 40 mL insulin solution, 40 mL putrescine solution, 40 μ L 200 μ M Progesterone and 40 μ L 3mM sodium selenite. The solution was sterilized by filtering through a 0.2 μ m filter. N5 media consisted of DMEM/F12, 5% FCS, 35 μ g/mL bovine pituitary extract, 20 ng/mL EGF, and 20 ng/mL FGF2.

Neural stem cell differentiation

Differentiation Media #1 was composed of 49.9 mL Control Media, 100 μ L heparin solution, and 0.5 μ g bFGF2. Differentiation Media #2 consisted of 49 mL control media and 1 mL of FBS.

Chemicals

Rapamycin white powder was stored at -20 °C, Clarithromycin (internal standard; Sigma catalog # A3487) white powder stored at 4°C, Methanol Optima LC/MS grade (Thermo Fisher Scientific), Zinc Sulfate (as heptahydrate) (Fisher Chemical), Water collected from an in-lab Barnstead water purification system.

Analytical System

Analysis was performed on a TSQ Quantum system (ThermoFinnigan, San Jose, CA) consisting of a Surveyor MS Pump, Surveyor autosampler and TSQ Quantum Ultra triple quadrupole mass spectrometer. Analysis was done in MS/MS mode. The scan for rapamycin was 931.5 (M+NH₄)⁺ 864.7 at a collision energy of 20 eV. The scan for clarithromycin was 747.9 (M+H)⁺ 590.6 at a collision energy of 37 eV. Analytes were ionized using electrospray ionization

with spray voltage of 5000 V, sheath gas (nitrogen) and auxiliary gas at respective flow rates of 49 and 24 arbitrary units (au) and a capillary temperature of 311°C. Argon was used as collision gas at a constant pressure of 0.8 mTorr. Chromatographic separation was achieved on a Luna C-18(2) HPLC column 50 mm X 2.0mm, 5 with 4mm X 2.0 mm guard cartridge. Mobile phase consisted of 30 mM ammonium acetate (A) and methanol (B). The flow rate was 300 µl/min with initial solvent proportion of 20% B until 1 minute increasing to 97% B from 1 minute to 2 minutes, holding at 97% B from 2 minutes to 5 minutes with re-equilibration at 20% B from 5.1 minutes to 8 minutes. Injection volume was 10 µl and total analysis time was 8 minutes.

Preparation and Extraction of Standards and Samples

25 µl of standard and 25 µl of clarithromycin internal standard were added and subsequently evaporated to dryness in a speed-vac. For unknown samples, only internal standard was added. 25 µl of whole blood was then added and vortexed. 150 µl of 70:30(v/v) Methanol:0.3 M ZnSO₄ was added and vortexed to mix. Samples were then centrifuged at 12000 rcf for 10 minutes at 4°C. 100 µl of supernatant was transferred to autosampler vials for analysis.

Chemicals

Metformin white crystalline powder stored at room temperature, Methanol Optima LC/MS grade (Thermo Fisher Scientific), Zinc Sulfate (as heptahydrate) (Fisher Chemical), Water collected from an in-lab Barnstead water purification system.

Analytical System

Analysis was performed on a TSQ Quantum Ultra triple-quadrupole mass spectrometer in conjunction with a Finnigan Surveyor Autosampler and Finnigan Surveyor quaternary HPLC pump (Thermo Finnigan, San Jose, CA). The mass spectrometer was operated in the positive ionization mode utilizing atmospheric pressure chemical ionization (APCI). Spray voltage was 3500 V, sheath gas (nitrogen) flow was 21 (arbitrary units), auxiliary gas (nitrogen) flow was 5, vaporizer temperature was 395°C, capillary temperature was 200°C and argon was used as the collision gas at a pressure of 0.8 mTorr. Detection utilized selective reaction monitoring (SRM);

parent mass/charge ratio for metformin was 130.1 and the fragment monitored was 71.1. The collision energy was 33 eV. HPLC separation was achieved using a 3 BDS Hypersil Cyano 50 X 4.6 mm column (Thermo Scientific, Bellefonte, PA). Mobile phase was 60:20:20 10 mM ammonium acetate:acetonitrile:methanol (v/v) Flow rate was 650 µl/minute.

Injection volume was 20 µl. The autosampler needle was washed with 200 µl of 50% acetonitrile followed by 200 µl of 100% acetonitrile following each injection. During the first minute of analysis time, eluent was diverted to waste. Total analysis time was 5 minutes. Metformin eluted at ~2.6 minutes.

Preparation and Extraction of Standards and Samples

12.5 µl of standards (12.5 µl of methanol for blank) were added to 25 µl of mouse serum and mixed by vortexing. Unknown samples were stored at -80°C and thawed before analyses. 12.5 µl of methanol were added to the unknown samples and mixed by vortexing. 300 µl of cold acetonitrile was added and mixed by vortexing before centrifuging for 5 minutes at 12000 g at 4°C. 100 µl of supernatant was transferred to autosampler vials for analysis.

RESULTS

Chronic and systemic administration of rapamycin, but not metformin, decreases BrdU incorporation in SVZ and DG neurogenic niches

We used an ~9-week regimen of daily intraperitoneal (i.p.) injection of rapamycin at 75 µg/kg (low dose) or 2.5 mg/kg (high dose), or metformin at 200 mg/kg daily in adult C57BL/6J mice (Fig. 2.1a). The low-dose rapamycin was selected to match previously reported dosage that enhanced CD8 memory T cell generation (Araki et al., 2009). The high rapamycin dosage was selected to match the concentration reported to extend life span (Miller et al., 2011). The animals were 3 months old at the beginning of the treatment. Age-matched controls received daily PBS injections. The mice did not show any increase in food intake or body weight during this study; mice on high-dose rapamycin showed weight loss (Table 2.1). Sixteen hours following the last injection, the mice were harvested, and rapamycin concentration in the blood and metformin

concentration in the plasma were quantitated (Fig. 2.1b). The inhibition of mTOR activity in the brain following the pharmacological treatments was confirmed by fluorescent immunohistochemical analyses of phosphoribosomal S6 (rS6~P) on brain sections. Our results demonstrate that both concentrations of rapamycin used in this study, as well as metformin, effectively reduced rS6~P-specific immunostaining, indicating that mTOR signaling is inhibited in the brain following rapamycin and metformin treatment (Fig. 2.1c). To quantitate adult neural stem cell numbers, the mice were injected with BrdU 2 days prior to sacrifice (Fig. 2.1a). BrdU is incorporated in the DNA during S-phase and has been utilized to detect slowly cycling B cells and the proliferating C cells in adult neurogenic niches (Kee, Sivalingam, Boonstra, & Wojtowicz, 2002). First, BrdU incorporation in SVZ (Fig. 2.2a) was measured by analyses of serial sections encompassing the entire SVZ of adult mice. This experiment revealed that the number of BrdU+ cells was significantly decreased in both low and high-dose rapamycin-treated mice (Fig. 2.2b and c). Interestingly, metformin treatment did not significantly alter the number of BrdU+ cells (Fig. 2.2b and c). Next, the number of BrdU+ cells was quantified as described in the “Experimental procedures” section, and statistical analyses revealed a significant difference in BrdU incorporation between control and rapamycin-treated, but not in metformin-treated, mice (Fig. 2.2d). To independently confirm the reduction in neural progenitor numbers, SVZ sections were stained with Ki67. While BrdU can be incorporated in apoptotic cells, Ki67 is a cell cycle marker. Consistent with the effect of the drug treatment on BrdU incorporation, a decreased number of Ki67+ cells were detected following rapamycin, but not metformin treatment (Supplementary Fig. 2.S1). We also measured BrdU incorporation in the DG, an additional neurogenic niche (Fig. 2.3a). Sections corresponding to DG were stained with anti-BrdU antibody, and the number of BrdU+ cells were counted and compared between control, rapamycin-treated and metformin-treated mice. We observed fewer BrdU+ cells in the DG of the rapamycin-treated mice, in comparison to control or metformin-treated mice (Fig. 2.3b and c). Taken together, our

results demonstrate that chronic, systemic rapamycin, but not metformin, significantly reduced the number of cycling mammalian adult neural stem cells.

Neural progenitor proliferation in vitro is reduced by rapamycin but remains unaffected by metformin

To directly test the effects of rapamycin and metformin on neural progenitor proliferation, apoptosis and/or differentiation, we measured the effects of these drugs on primary, adult neural stem cells isolated from the SVZ of postnatal day 30 (p30) C57BL/6 mice and cultured in vitro. Neural stem cells were grown under two independent culture conditions, either as neurospheres or as an adherent monolayer. In vitro cultures were treated with 200 nM rapamycin or 500 nM metformin overnight, and the inhibition of mTOR was confirmed by rS6~P immunoblotting. Under these conditions, both rapamycin and metformin treatment inhibited mTOR activity in these neural stem cells (Fig. 2.4a).

Next, proliferation of the neural stem cells was measured by BrdU incorporation. Cells were incubated overnight with BrdU in the presence of rapamycin or metformin. Rapamycin treatment significantly inhibited the rate of proliferation as indicated by decreased proportion of BrdU+ cells (Fig. 2.4b; Table 2.2). Unlike rapamycin, metformin treatment did not reduce the proliferation of neural stem cells in vitro. Finally, we performed cell cycle analyses of control, rapamycin, and metformin-treated adult neural stem cells. Neural stem cells were grown under adherent conditions in the presence of rapamycin or metformin, and cell cycle analyses were performed by propidium iodide (PI) labeling and FACS. Similar to previous reports (Bez et al., 2003; Merlo et al., 2007), we found that under control conditions 78.73 ± 1.59 % of neural stem cells was in G1 phase, 9.0 ± 0.85 % in the S phase, and 11.40 ± 0.35 % in the G2/M phase (Table 2.3). Metformin treatment did not significantly alter this profile (Fig. 2.4c; Table 2.3). In contrast, rapamycin treatment increased the percentage of cells in the G1 phase and resulted in a consequent decrease in S and G2/M-phases (Fig. 2.4c; Table 2.3). Rapamycin is known to cause G1 arrest in differentiated cells (S. Huang, Bjornsti, & Houghton, 2003), and reduced S phase in

the presence of rapamycin may account for reduced BrdU incorporation observed in vivo. Neither rapamycin nor metformin induced significant apoptosis (Fig. 2.4d). Taken together, these results are consistent with our in vivo BrdU incorporation studies and suggest that rapamycin inhibits the proliferation of neural progenitors.

Rapamycin, but not metformin, reduces neuronal differentiation

We directly tested the effects of rapamycin and metformin on neuronal differentiation in vitro by using isolated neural stem cells. Following neurosphere cultures, differentiation was induced as described in the “Experimental procedures” section. Undifferentiated neural progenitors were identified as Nestin+, while differentiated neurons in culture were identified by Tuj1+ staining. Both control, as well as metformin treated cells lost their Nestin-expression, and some cells became Tuj1+ upon neuronal differentiation (Fig. 2.5). Treatment with rapamycin inhibited this differentiation in vitro. Rapamycin-treated cells failed to express Tuj1 and retained Nestin expression (Fig. 2.5). These results are also consistent with the longer G1 observed in rapamycin-treated neural stem cells in vitro. Alterations in the precise length of G1 phase in stem cells have been correlated with defects in differentiation (Lange, Huttner, & Calegari, 2009; V. C. Li, Ballabeni, & Kirschner, 2012). In summary, our in vitro results indicate that rapamycin inhibits neural progenitor proliferation and differentiation.

Since the SVZ and DG neural progenitors are the source of adult born neurons, we hypothesized that neuronal differentiation may decrease following chronic, systemic rapamycin treatment. Consistent with this hypothesis, we observed that the number of DCX+ cells in the SVZ was reduced upon chronic, systemic rapamycin treatment in comparison to control brain (Supplementary Fig. 2.S2). DCX is a widely used marker for identifying neuroblasts and immature neurons in vivo (Mina J. Bissell & William C. Hines, 2011). However, metformin treatment did not alter the number of DCX+ cells (Supplementary Fig. 2.S2). Therefore, the reduced proliferation of neural progenitors observed in vivo and in vitro in this study, along with the inhibition of in vitro

differentiation, indicate that chronic, systemic rapamycin treatment results in reduced adult-born neurons.

DISCUSSION

Our experiments demonstrate that ~9-week systemic administration of the mTOR inhibitor rapamycin reduced the number of neural progenitor cells in the adult mammalian brain. In contrast, a different pharmacological strategy of inhibiting mTOR indirectly through AMPK activation, did not significantly affect proliferation in the neurogenic niche. The molecular mechanisms accounting for the observed differences between the mTOR inhibitor rapamycin and metformin remain unclear at this point and will be the subject of future analyses. Differential effects of rapamycin and metformin could be ascribed to the unique effects of these drugs on mTORC1 versus mTORC2 complex, differential inhibition of downstream signaling components or alternative engagement of feedback regulatory pathways. The first possibility is the reported effect of rapamycin on the mTORC2 complex. Prolonged rapamycin treatment has been reported to inhibit mTORC2 (Sarbasov et al., 2006). Similarly, rapamycin-induced insulin resistance results from the disruption of the mTORC2 complex (D. W. Lamming et al., 2012). It is possible that the inhibition of adult neurogenesis by rapamycin may result from similar undesirable effects on mTORC2. Metformin-dependent AMPK signaling is likely to be restricted to the regulation of the mTORC1 complex. Secondly, differential effects on mTORC1 substrates can also account for the observed differences. For example, 4E-BP1 is the major effector for the cell cycle effects of rapamycin (Dudkin et al., 2001). Additionally, unique targets of AMPK such as Acetyl CoA carboxylase (Mihaylova & Shaw, 2011), may offset the negative effects of rapamycin through unknown mechanisms. It will be interesting to perform an unbiased, comparative assessment of differential downstream target engagement in neural stem cells following chronic rapamycin and metformin treatment. Finally, differences in the response of the IRS/Akt or Grb10 feedback loops (Hsu et al., 2011; J. Huang & Manning, 2009) following rapamycin versus metformin treatment in neural progenitors may account for the observed effects. Metformin and rapamycin have been

reported to have opposing effects on Akt activation (Zakikhani, Blouin, Piura, & Pollak, 2010). Additionally, AMPK activation in sensory neurons inhibits incision-induced acute and chronic pain and neuropathic pain by the simultaneous attenuation of both mTOR and ERK signaling (Melemedjian et al., 2011). In contrast, we observe that both pharmacological and genetic inhibition of mTORC1 evokes spontaneous pain, mechanical hypersensitivity, and increased sensory neuron excitability (Melemedjian et al., 2011). Rapamycin releases the feedback inhibition of Grb10, which is an upstream regulator of MAPK pathway (Hsu et al., 2011) and has previously been shown to increase ERK activation in TSC2^{-/-} murine embryonic fibroblasts (Ghosh et al., 2006).

Adult neural progenitor cells and adult neurogenesis are generally considered positive characteristics that may improve or preserve cognitive function and behavioral health in aging. In our study, rapamycin reduces neural progenitor numbers. Additionally, rapamycin, or the inhibition of the mTORC1 and mTORC2 complexes, have been reported to inhibit dendritic arborization of hippocampal neurons (Urbanska, Gozdz, Swiech, & Jaworski, 2012). Therefore, chronic rapamycin treatment may have a paradoxical, negative effect on health span. It remains to be seen if metformin treatment, which lacked the adverse effects associated with rapamycin in our studies, would be suitable for extending both life span and health span across mammalian species. However, we cannot formally rule out the possibility that abnormal integration of adult-born neurons into pre-existing circuits contributes to aging and the inhibition of adult neurogenesis may be beneficial to health span. It is interesting to note that at least in the nematode *C. elegans*, the loss of certain neurons has been correlated with extended life span (Alcedo & Kenyon, 2004). Careful assessment of a causal link between rapamycin effects on adult neurogenesis and learning, memory, and behavior in mammalian models of aging will be required for a comprehensive understanding of the impact of long term rapamycin treatment in cognitive health span.

In summary, our study reveals that distinct approaches of inhibiting the mTOR pathway, especially in the context of long-term, systemic treatment consistent with life span extension, can have significantly different outcomes in terms of physiological or pathological responses. The effects of mTOR inhibitors on cellular correlates of health span must therefore be carefully and comprehensively analyzed in individual organs and systems. While here we examine the effects of two distinct pharmacological approaches for mTOR inhibition only on adult neural progenitor cells, immune function, for example, will constitute another important physiological parameter for the assessment of improved health span. Rapamycin being an immunosuppressant, a thorough assessment of its effect on innate and adaptive immune function in old mice is merited.

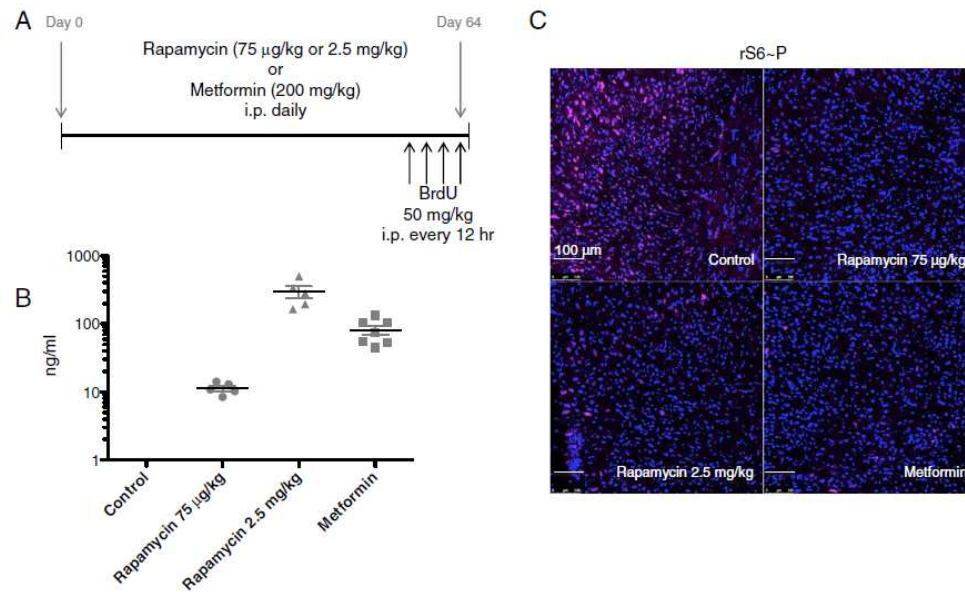


Figure 2.1. Chronic, systemic rapamycin and metformin administration in mice inhibits mTOR activity in the brain. A) Schematic representation of chronic rapamycin and metformin treatment regimens and BrdU administration prior to tissue collection. Intraperitoneal (*i.p.*). B) Rapamycin and metformin concentration in the blood and plasma, respectively, collected from mice before tissue collection. The last dose of rapamycin and metformin were given 16 h before sacrificing the mice. C) Ribosomal S6 phosphorylation (*rS6~P*) as detected by immunofluorescence, in sections from the cortex of control mice or mice treated with the indicated doses of rapamycin or metformin. Scale bar=100 μ m. Data are presented as representative of >5 mice per group

Table 2.1

Neither rapamycin nor metformin significantly increase food intake or body weight

	Average (g)	SEM
A		
Control	3.5	0.6
Rapamycin 75 mg/kg	3.5	0.2
Rapamycin 2.5 mg/kg	4.1	0.6
Metformin	5.0	0.9
B		
Control	28.8	4.5
Rapamycin 75 mg/kg	29.1	0.5
Rapamycin 2.5 mg/kg	24.8	0.8
Metformin	28.7	0.8

Average food intake (per mouse per gram) during the study (A) and average body weight (per mouse) at the end of study (B) with standard error of the mean (SEM)

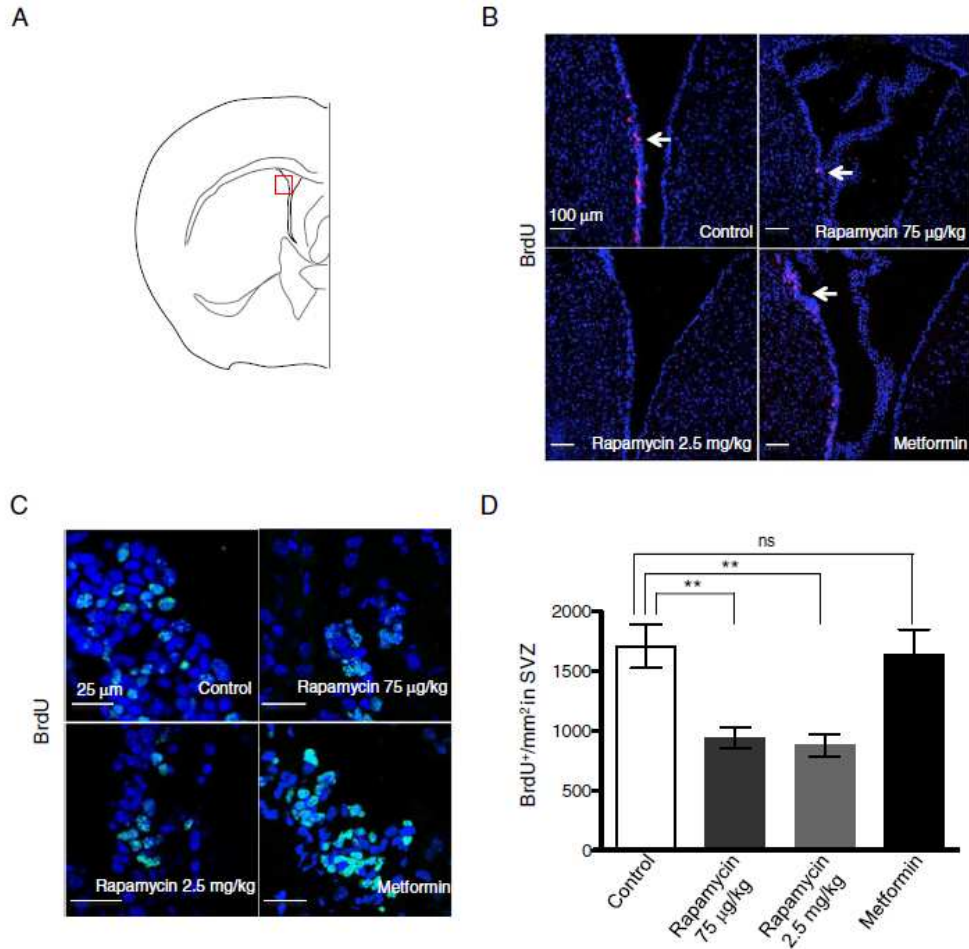


Figure 2.2. Chronic rapamycin treatment, but not metformin, inhibits the proliferation of neural progenitors in the SVZ region of the adult mammalian brain. A) Schematic indication a region of interest (*boxed area*) in SVZ. B) BrdU (*red*) incorporation as detected by immunofluorescence in the SVZ of control and treated mice. DAPI-stained nuclei are shown in *blue*. Scale bar=100µm. *Arrows* point to BrdU⁺ cells. C) BrdU (*green*) and DAPI (*blue*) in the SVZ of control and treated mice. Scale bar=25µm. D) Quantification of BrdU⁺ cells per square millimeter in the SVZ in control and treated mice. Data are presented as representative individual images or as mean± SEM from >5 mice per group. **p<0.01, *ns* is nonsignificant

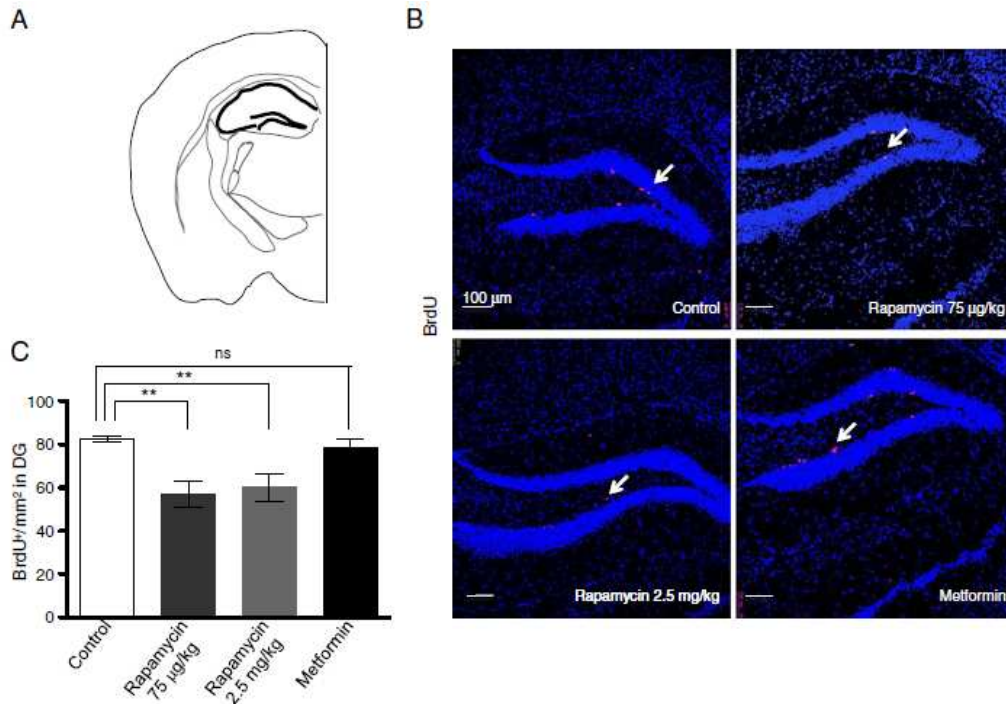


Figure 2.3. Chronic rapamycin treatment, but not metformin, inhibits the proliferation of neural progenitors in DG. A) Schematic outlining DG. B) BrdU incorporation (*red*) and DAPI (*blue*), as detected by immunofluorescence, in DG of control and treated mice. Scale bar=100µm. Arrow points to BrdU⁺ cells. C) Quantification of BrdU⁺ cells per square millimeter in the DG in control and treated mice. Data are presented as representative individual images or as mean +/- SEM from >5 mice per group. ** $p < 0.01$, ns is nonsignificant

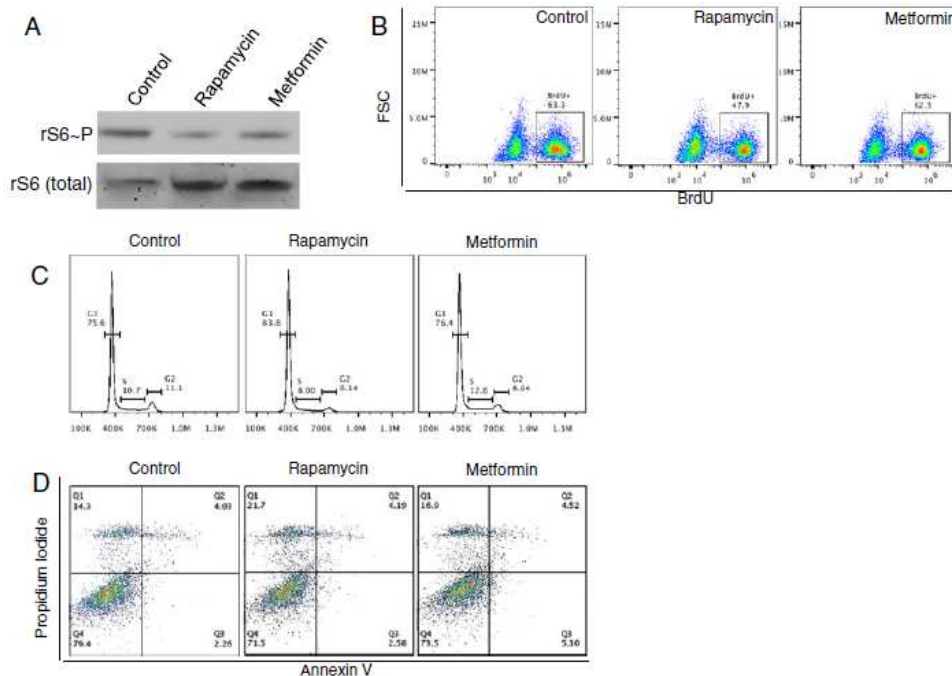


Figure 2.4. Rapamycin, but not metformin, inhibits proliferation of neural stem cells in vitro. A) Ribosomal S6 phosphorylation (rS6~P) and total ribosomal S6 in neural stem cells cultured in vitro, as detected by immunoblotting after overnight rapamycin or metformin treatment. B) Representative FACS plots of BrdU incorporation in adult neural stem cells after rapamycin or metformin treatment. C) Representative FACS cell cycle analysis of neural stem cells after rapamycin and metformin treatment. D) Representative FACS analysis of annexin V/PI staining in neural stem cells after rapamycin or metformin treatment. Data are presented as representative of three independent experiments

Table 2.2

Rapamycin, but not metformin, inhibits the proliferation of neural progenitors in vitro

Treatment	Neurosphere % Inhibition	Adherent NSC % Inhibition
Rapamycin	23.68±3.09	22.57±4.99
Metformin	-0.30±4.3	3.23±3.5

Percentage inhibition of BrdU incorporation in neural stem cells isolated from p30 SVZ and grown in vitro as neurospheres or as an adherent monolayer. Data are presented as mean +/- SEM of greater than or equal to three independent experimental repeats

Table 2.3

Rapamycin, but not metformin, causes G1 phase arrest in vitro

Treatment	G1 phase	S phase	G2 phase
Control	78.73±1.59 %	9.0±0.85 %	11.40±0.35 %
Rapamycin	85.67±0.96 %	6.63±0.68 %	7.01±0.51 %
Metformin	78.90±1.31 %	10.10±1.30 %	10.25±0.80 %

Percentage of neural stem cells at different stages of the cell cycle following in vitro rapamycin and metformin treatment, as determined by PI staining and FACS analyses. Data are presented as mean +/- SEM of greater than or equal to three independent experimental repeats

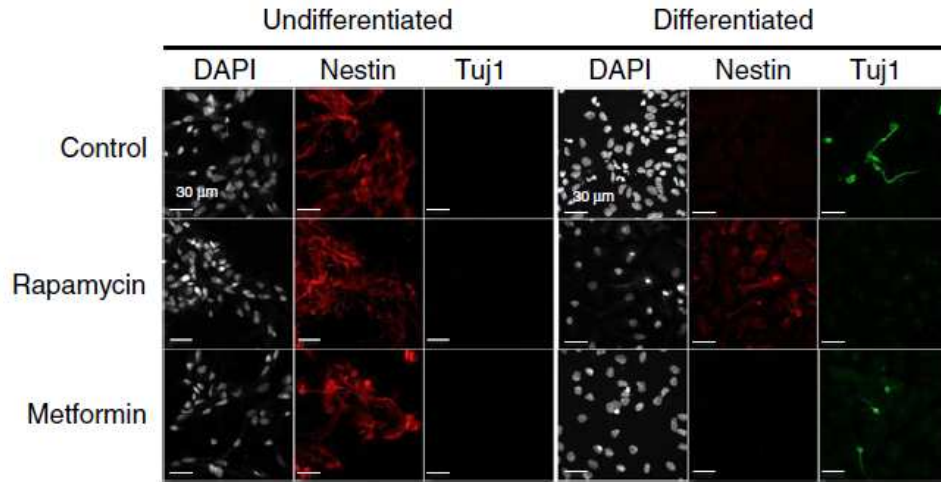


Figure 2.5. Rapamycin, but not metformin, inhibits differentiation of neural stem cells in vitro. Representative images of undifferentiated or differentiated p30 neural stem cells after rapamycin or metformin treatment. Scale bar=30 μ m. Data are representative of three independent experiments

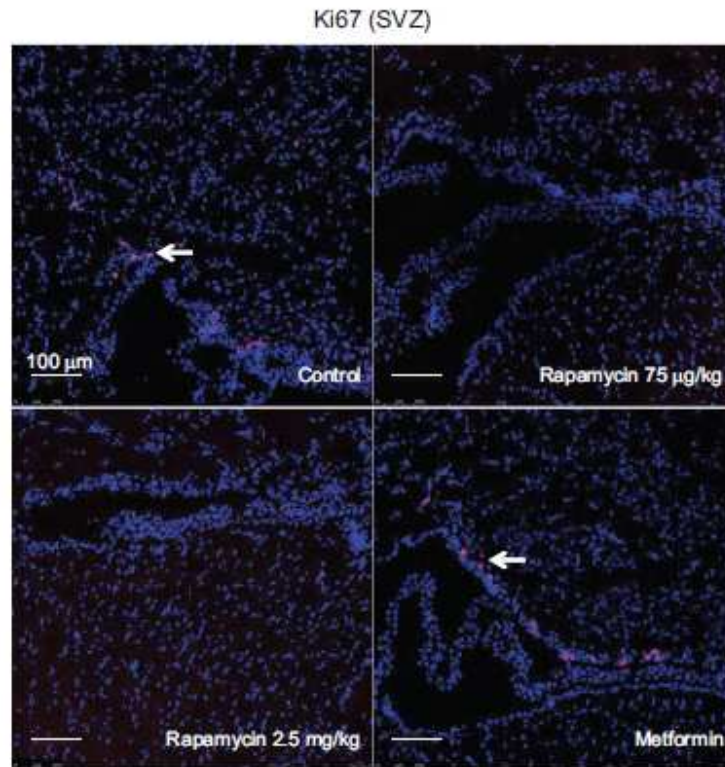


Figure 2.S1. Chronic rapamycin, but not metformin, treatment reduces neural progenitor numbers in the SVZ region of the adult mammalian brain. Ki67 staining in the SVZ of control and treated mice. Scale bar = 100µm. Arrow points to Ki67⁺ cells. Data are presented as representative images. >5 mice were included per group.

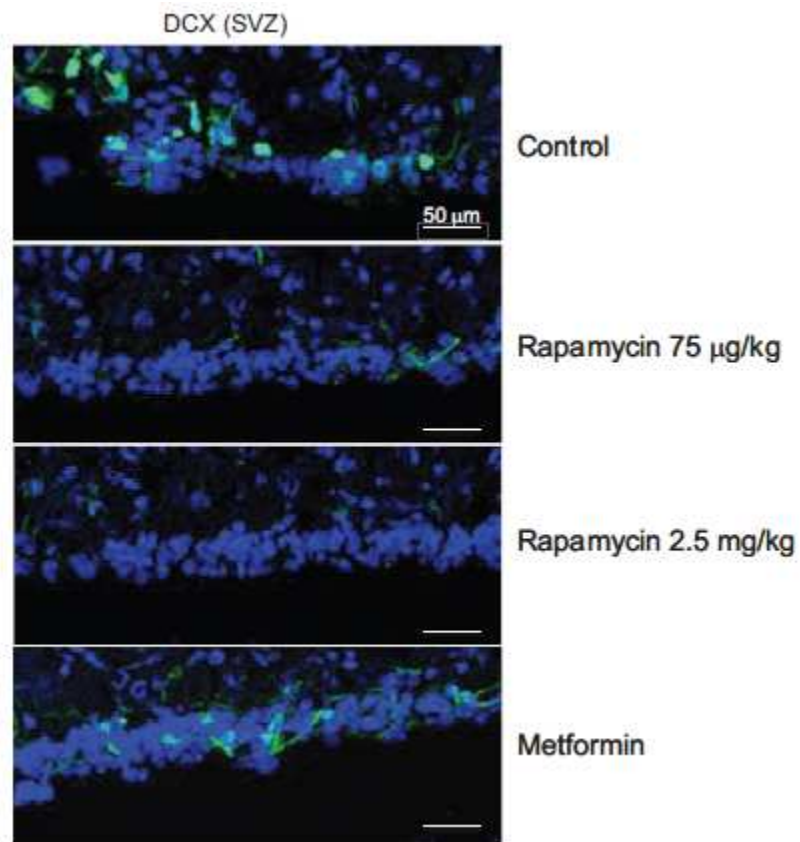


Figure 2.S2. Chronic rapamycin treatment, but not metformin, reduces neuroblasts and/or immature neuron numbers. DCX (*green*) and DAPI (*blue*), as detected by immunofluorescence, in the SVZ of control, rapamycin and metformin-treated mice. Scale bar =50µm. Data are presented as representative images. >5 mice were included per group.

ACKNOWLEDGEMENTS

This research was supported by NIAID contract HHSN 272201100017C (NIH/NIAID N01-AI-00017) to J.N.-Z. and grants from the National Institutes of Health NIH/ NCI CA95060 (S.G.), NIH/NINDS R01 NS065926 (T.J.P.), The American Pain Society (T.J.P.), The Rita Allen Foundation (T.J.P.), Pilot Biology of Aging Research Initiative from the Arizona Center on Aging (J.N.-Z.), NIH/NIDCR RC1 DE020335 (K.H.L.), NIH/NIDDK R01 DK073611 (H.L.B.), and the Arizona Cancer Center Core Support Grant (NCI 5P30CA23074). We thank Carla V. Rothlin and Eugenio A. Carrera Silva for technical expertise and for the critical evaluation of the manuscript and helpful suggestions and discussions.

CHAPTER 3
SIGNALING IN GLIOBLASTOMA
INTRODUCTION TO MANUSCRIPT

Glioblastoma Multiforme

Glioblastoma (GBM) is defined by the World Health Organization (WHO) as a grade IV diffuse glioma, a tumor arising from the astrocytic cells of the brain (Scherer, 1940). First identified by Rudolf Virchow in 1863 as a glial tumor (Virchow, 1863), GBM was originally referred to as a spongioblastoma multiforme until two physicians in 1926 renamed it by its current name, GBM (Bailey, 1926). It is the most common and most malignant of the variant glioma classifications (Kleihues, 2000). Prognosis for GBM patients is dismal due to the highly invasive and extreme heterogeneity of the cells comprising the GBM tumor. Interestingly, in 1928, a neurosurgeon named Walter Dandy removed the entire hemisphere of two GBM patients (Dandy, 1928). Unfortunately, both patients invariably died from GBM despite this aggressive surgery, providing evidence towards the highly invasive nature of GBM cells (Agnihotri, 2013; Dandy, 1928). Standard of care therapy includes surgical resection, radiation and chemotherapy with temozolomide. Nevertheless, despite the aggressive tactics taken by clinicians at targeting GBM, the median survival remains roughly 15 months (Huse et al., 2013). This is likely due to the aggressive invasion of the cells and their ability to evade chemotherapy. In addition, the dysregulation of signaling pathways in these cells promoted by aggressive genetic mutations renders potential successful therapies obsolete.

GBM tumors can be classified into either primary or secondary GBM, with primary GBM comprising more than 90% of surgically removed cases (Roger McLendon et al., 2008). Primary GBM arises *de novo*, without any previous history of disease, while secondary GBM arises from previously diagnosed low-grade glioma, such as low grade astrocytoma (WHO grade II) or anaplastic astrocytoma (WHO grade III). Interestingly, these two classifications develop through different genetic mutations, maintain different dysregulation of signaling mechanisms, and have

differential responses to treatment (Ohgaki & Kleihues, 2007). Furthermore, the age of onset differs quite significantly between those with primary and those with secondary GBM. The mean age of primary GBM patients is 62 years, while the mean age for secondary GBM patients is 35 years (Ohgaki & Kleihues, 2007). Genetically, *EGFR* and/or *PTEN* mutations tend to occur more often in primary GBM patients. While *TP53* mutations do occur in primary GBM patients, secondary GBM tumors more frequently experience this mutation. However, a loss of heterozygosity (LOH) in 10q occurs in both primary and secondary GBM with nonsignificant differences, while LOH in 10p or complete loss of chromosome 10 presents more frequently in primary GBM (Ohgaki & Kleihues, 2007).

Transcriptionally, distinct profiles comprise these two subgroups. Using microarray technologies, Tso et al., (2006) investigated the differences in glioblastoma-associated genes (GAG) within GBM tumors compared to low-grade astrocytomas (Tso et al., 2006). In comparison to low-grade astrocytomas, both primary and secondary GBMs shared 15 GAGs in common which included genes such as *MET*, a proto-oncogene (Boccaccio & Comoglio, 2006), and *VEGF*, an angiogenic factor (Ferrara & Henzel, 1989; Tso et al., 2006). Other common genes were shared between the primary and secondary GBM subgroups which the low-grade astrocytomas did not express including *CDC2*, *ADM*, and *FCGBP*, among others. Interestingly, however, these genes had quantitative differences between the primary and secondary subgroup. For instance, the expression of *CDC2*, a cell cycle regulation gene, was expressed higher in the secondary subgroup while the expression of *ADM* and *FCGBP*, extracellular response associated genes, were expressed higher in primary GBM samples. When compared to low grade astrocytomas, secondary GBM samples expressed genes such as *GAS1* (growth arrest-specific 1), *CDKN2* (cyclin-dependent kinase inhibitor 3), *CCNB1* (cyclin B1), and *PRC1* (protein regulator of cytokinesis; (Tso et al., 2006) – which are genes associated with an intracellular cell cycle or mitotic response. In contrast, primary GBM tumors, when compared to low grade astrocytomas, expressed GAGs which were indicative of a tumor stromal response. *VEGF* was more highly

expressed in primary GBM, as was *COL5A1*, *COL6A2* and *MMP-9*. *COL5A1* and *COL6A2* genes produce the proteins collagen type V α 1 and VI α 2, which, along with *MMP-9*, are extracellular matrix remodeling factors. *MMP-9* is a matrix metalloprotease which contributes to the invasiveness of GBM cells (Kessenbrock, Plaks, & Werb, 2010; Lakka et al., 2004). Other genes Tso et al., (2006) found to be expressed higher in primary GBM compared to low-grade included angiogenic factors such as *IL-8*, *CA1* and *CA2*, as well as inflammation, coagulation, immune response genes such as *SERPINA1/SERPINA3*, *SERPINE1*, *PTX3*, *TIMP1*, among others (Tso et al., 2006). Overall, the authors concluded that the pattern of enriched GAGs associated with secondary GBM were linked with a more intracellular mitotic cell cycle regulation response and genes expressed in primary GBM were more associated with a stromal response, indicating a more extracellular signaling environment (Tso et al., 2006).

The Heterogeneity of GBM

The name “multiforme” arises from early characterizations of GBM histology which identified many different cell types within a single tumor section (Rudy Bonavia, Cavenee, & Furnari, 2011). It was also found that these different subpopulations within the same tumor display different karyotypes as well as different growth characteristics (Shapiro, Yung, & Shapiro, 1981). Even within a single GBM passaged cell line, early reports found differential antigen expressivity as well as significant differences in cellular karyotypes (Wikstrand, Bigner, & Bigner, 1983). In addition, studies have shown that different regions of GBM tumors will express different protein abnormalities (R. Bonavia, Inda, Cavenee, & Furnari, 2011). For example, the various popular genetic mutations identified by the TCGA have been shown to be mutually exclusive. Subpopulations of EGFR amplified cells exist and subpopulations of PDGFRA amplified cells exist within the same tumor sample (Szerlip et al., 2012). The proliferative marker, Ki67, was shown to be heterogeneously expressed within GBM tumors, and usually expressed significantly within clusters of cells (Coons & JOHNSON, 1993). By studying multiple sections from the same tumor, Sottoriva et al (2012) found that different subtypes of GBM can be classified within the

same patient tumor (Sottoriva et al., 2013). In fact, 6 out of 10 patients expressed different molecular subtype transcriptomes belonging in the proneural, neural, classical and mesenchymal subgroups (discussed below) (Sottoriva et al., 2013).

In addition, EGFRVIII⁺ cells were found to be diffusely located within GBM tumors, and only 1/20 can be classified as displaying homogenous staining (Nishikawa et al., 2004). Inda et al (2010) hypothesized that this EGFRVIII⁺ subpopulation, although a minority within the tumor, is responsible for increased tumorigenicity as well as the maintenance of heterogeneity (Inda et al., 2010). Using non-tumorigenic primary EGFR wild-type over-expressing astrocytes from *Ink4a/Arf*^{-/-} mice which have been previously shown unable to form a tumor in intracranial xenografts, the authors showed that co-injection with astrocytes overexpressing EGFRVIII in a 9:1 ratio resulted in increased tumor volumes (Inda et al., 2010). Furthermore, *in-vitro*, using the conditioned media from EGFRVIII cells to grow EGFR wild-type cells resulted in increased soft-agar colony formation while the reverse experiment did not (Inda et al., 2010). Both *in-vitro* and *in-vivo*, the authors found that a minority population of EGFRVIII⁺ cells was able to increase the proliferation and survivability of EGFR wild-type cells (Inda et al., 2010). Mechanistically, it was discovered that EGFRVIII⁺ cells up-regulate cytokines, such as IL-6, which can lead to tumor growth enhancement of the surrounding cells (Inda et al., 2010). Thus, the authors concluded that a minor population of EGFRVIII cells mixed with EGFR wild-type expressing cells results in a more aggressive tumor.

Reasons for this differential expression of proteins within a single tumor may occur via multiple mechanisms. It is possible that each tumor represents various different cellular origins. That is, the tumor originated from multiple cells with varying oncogenic mutations, as opposed to one singular cell, giving rise to multiple different cell types. Furthermore, it is also possible that a single cell mutated and as it continued to pathologically proliferate, new mutations were gained based on the location of the cell. There are various tumor microenvironments within the GBM tumor itself. Within a single GBM tumor specimen, there are areas of necrosis, hypoxia,

angiogenesis and immune cell infiltration. Therefore, a cell incurring beneficial oncogenic mutations to adapt to its environment may lead to the development of a heterogeneous tumor. Furthermore, various cell types make up the tumor, including microglia, macrophages, astrocytes, oligodendrocytes, neurons, glial progenitors, and endothelial cells and this may lead to differential signaling between specific cells. This extreme heterogeneity in cell type, subtype, and micro-environment within a single GBM tumor likely contributes to the lack of a breakthrough therapeutic.

The GBM Tumor Stroma & Extracellular Signaling

Multiple cell types make up the GBM tumor microenvironment which can contribute to extracellular GBM signaling. These cells may include vascular cells, microglia, and peripheral immune cells, which may secrete signaling factors to which the GBM cells are capable of responding. It has been reported that microglia, the resident macrophages of the brain, may contribute up to 30% of the brain tumor mass. While the origin of GBM microglia has not yet been fully elucidated (Nikki A. Charles, Eric C. Holland, Richard Gilbertson, Rainer Glass, & Helmut Kettenmann, 2011), it has been shown that normal brain microglia are derived from blood monocytes which migrate into the brain tissue during embryonic fetal development (Davis, Foster, & Thomas, 1994). Furthermore, it is accepted that the microglia comprise a significant portion of the tumor and contribute to GBM cell signaling (Hoelzinger, Demuth, & Berens, 2007).

Activated microglia within the GBM tumor may secrete various interleukins such as IL-12, IL-14, IL-1 and IL-1 β (Watters, Schartner, & Badie, 2005). Interestingly, the quantity of microglia within the brain tumor has been correlated with grade (Roggendorf, Strupp, & Paulus, 1996b), suggesting a pro-tumorigenic contribution. Furthermore, many of these cytokines have been found to increase glioma cell proliferation or invasion. For instance, IL-1 β has been correlated with invasion and angiogenesis and its expression has been associated with an increase in TGF- β (Naganuma et al., 1996) in glioma cells. TGF- β is a protumorigenic factor

which has been shown to increase angiogenesis, proliferation and invasion of glioma cells (Watters et al., 2005). Interestingly, microglia have even been found to secrete EGF upon activation which leads to proliferation of the microglia themselves, in addition to the proliferative effect on the glioma cells (Briers, Desmaretz, & Vanmechelen, 1994; Nolte, Kirchhoff, & Kettenmann, 1997). Microglia are capable of secreting VEGF, a strong angiogenic factor and are also capable of responding to it, inducing their proliferation and migration (Forstreuter, Lucius, & Mentlein, 2002) as well as providing a pro-angiogenic environment for GBM.

In addition to microglia, other cell types have been shown to be present in GBM, as well. An increase in leukocytes was found by Farmer et al., (1989) and correlated with GBM grade (Farmer et al., 1989). T lymphocytes were identified to be present in GBM tissue in 1971 by Ridley and Cavanagh who found them in a third of the GBM tissues they examined (RIDLEY & Cavanagh, 1971). T lymphocytes are white blood cells able to secrete different cytokines, including IL-10 and adenosine, during an immune response. These signaling factors are not benign, as IL-10 and IL-6 have been reported to promote glioma cell proliferation (Goswami, Gupta, & Sharma, 1998; Huettnner, Czub, Kerkau, Roggendorf, & Tonn, 1996) and increase *in-vitro* glioma cell migration (Huettnner et al., 1996). Regulatory T-cells (Tregs) are also found in GBM (Nikki A. Charles et al., 2011). They are thought to be attracted via the chemokines MCP-1 secreted by glioma cells (Jordan & (C. E. Brown et al., 2007) and a positive correlation has been reported between Tregs and tumor grade (El Andaloussi & Lesniak, 2006, 2007). Given that Tregs express the surface antigen CD25, El Andaloussi and Lesniak (2006) treated a mouse model of GBM with anti-CD25 antibodies and found treated mice to live significantly longer than nontreated GBM mice (Andaloussi, Han, & Lesniak, 2006), therefore providing evidence of a possible direct protumorigenic effect of Tregs on GBM growth.

The GBM tumor is highly vascularized and many vascular cells are present within the tumor, including endothelial cells, pericytes, and astrocytes (Nikki A. Charles et al., 2011). De Palma et al (2005) found that Tie2 receptor expressing monocytes (Tie2+CD11b+CD45+; termed

TEMs), a hematopoietic cell type, are recruited to the site of a mouse model of GBM and are proangiogenic (De Palma et al., 2005). Furthermore, they found that mice which were depleted of TEMs had on average smaller tumors than untreated mice. The TEM depleted tumors were mostly comprised of nonviable, necrotic tissue, unlike the non-treated control tumors (De Palma et al., 2005), indicating a strong reliance of tumor cells on TEMs and angiogenesis for proliferation and growth.

Interestingly, glial cells, the support system for the brain, have been reported to play an important protumorigenic role in glioma cell signaling as well (Hoelzinger et al., 2007). Astrocytes may secrete various neurotrophic factors such as GDNF, CXCL12 and TGF- α (Nikki A. Charles et al., 2011; Hoelzinger et al., 2007), and GBM cells have been shown to over-express the receptors necessary to respond to these factors (Wiesenhofer et al., 2000). Treating rat glioma cells with GDNF resulted in increased glioma cell migration (Song & Moon, 2006). In addition, co-culture of glioma cells with astrocytes led to enhanced invasive capacities of glioma cells due to the astrocytic production of proMMP, a precursor matrix metalloprotease (Le et al., 2003). Thus, the astrocyte-glioma interaction provides protumorigenic signaling factors to the glioma cells, causing them to be more aggressive.

Given the infiltration of these various cell types within the GBM tumor stroma and given the ability for the glioma cells to respond to signaling factors secreted by these cell types, studying their contribution to GBM signaling may yield new therapeutic advances. For instance, a closer look at the ability to target TEMs within GBM patients is warranted, given the significant effects reported by De Palma et al., (2005). Furthermore, the ablation of Tregs led to increased survival in a GBM mouse model (Andaloussi et al., 2006).

Primary GBM Intracellular Signaling

Glioma cells are able to respond to the ligands, chemokines and cytokines that they themselves produce in an autocrine signaling manner. For example, glioma cells are capable of

producing their own growth factors such as EGF which stimulates motility, invasion and proliferation. In addition, glioma cells secrete factors such as G-CSF and MCP-1 which recruit microglia to the site of the tumor. While microglia are able to respond to these factors among others (Nikki A. Charles et al., 2011), glioma cells themselves have been shown to express receptors for both of these chemoattractants (Mueller et al., 1999; Platten et al., 2003) and thus may induce a protumorigenic signaling cascade autonomously. Signals such as MCP-1 and G-CSF led to increased proliferation and increased migration in glioma cells upon exposure (Mueller et al., 1999; Platten et al., 2003).

Other signaling aberrations occur in glioma cells as a consequence of their numerous oncogenic mutations. In 2008, The Cancer Genome Atlas (TCGA) profiled 206 GBM tumors using high-throughput genomic microarray technology in an effort to identify molecular targets for therapeutic discovery (Roger McLendon et al., 2008). This study was updated and expanded in 2013 to 543 samples (Brennan et al., 2013). Using only tumor samples which had 80% glioma cells (so to exclude collecting data from cells within the environment), the researchers collected specimens from newly diagnosed GBM patients representing predominantly primary GBM. The results showed a strikingly significant amount of GBM specimens with mutations found in *PTEN*, *EGFR*, *PIK3CA*, *PIK3R1* (Figure 1.5). 57% of tumors have an amplification or gain of function mutation in *EGFR* and 41% of tumors have a deletion or loss of function mutation in *PTEN*, the negative regulator of this over-activated RTK pathway (Brennan et al., 2013; R. McLendon et al., 2008). Furthermore, 25% have an amplification or gain of function mutation in *PIK3K*, a downstream signaling kinase responsible for numerous oncogenic signaling events (reviewed in chapter 1) (Brennan et al., 2013; R. McLendon et al., 2008). A striking 61% of tumors have a deletion or loss of function mutation in *CDKN2A/CDKN2B*. *CDKN2A* and *CDKN2B* are genes involved in cell cycle control, and their deletions and/or mutations results in highly proliferative cells. Nearly 80% of all tumors have a dysregulation of cell cycle control due to a genetic aberration (Brennan et al., 2013; R. McLendon et al., 2008). These mutations produce a

compounding signaling effect resulting in extremely virulent oncogenic cells which are highly invasive, proliferative, and unresponsive to treatment.

An analysis of the transcriptional data was conducted in order to delineate distinct subclasses within the analyzed GBM samples. Results revealed four subclasses of GBM – proneural, neural, classical and mesenchymal (Phillips et al., 2006; Verhaak et al., 2010). These subgroups displayed differential associations between patients. For instance, younger patients were significantly more likely to present with the proneural subtype. However, the proneural subtype patients failed to respond to aggressive therapy (Phillips et al., 2006; Verhaak et al., 2010). This is contrast to patients with classical or mesenchymal, who showed a significant beneficial response to aggressive therapy. Survival data was correlated with subtype, as the median survival of the proneural subtype was significantly longer when compared to the proliferative or mesenchymal subtypes (Verhaak et al., 2010). Interestingly, while it was previously thought that MGMT methylation was a predictor of therapy response (Hegi et al., 2005), the authors did not find any correlation or association of MGMT methylation between subtypes (Phillips et al., 2006). However, the authors did find a significant correlation with PTEN loss and poor survival (Phillips et al., 2006).

The authors also discovered that the molecular signatures of these subtypes were altered upon recurrence, and tended to shift towards the mesenchymal subtype (Phillips et al., 2006). Genes which are upregulated in the mesenchymal subtype included *CD44*, *STAT3*, *VIM*, and *YKL40*, all of which have shown to be protumorigenic signaling factors. *YKL40* is a secreted protein shown to be upregulated in glioma, as well as other cancers, and is reported to be associated with overall shorter survival in addition to being a predictor of radio resistance (Pellowski et al., 2005).

The possibility exists that these subtypes arise from different cells of origin in the brain and thus the study of their differences may prove imperative to reaching clinical success. Furthermore, it is important to consider the strong effects of the tumor microenvironment on GBM

signaling and its progression. Thus studying glioma cells *in-vitro* only may yield misleading results. It is now well accepted that mutations may arise from passaging cells *in-vitro* and can therefore change the signaling of the original specimen (Ajay Pandita, Kenneth D. Aldape, Gelareh Zadeh, Abhijit Guha, & C. David James, 2004). Therefore, the study of these tumors within their natural environment is a necessity to finding better, more successful therapeutics and impacting the prognosis for GBM patients.

MANUSCRIPT: TARGETING APKC DISABLES CELL AUTONOMOUS AND NON-CELL
AUTONOMOUS ONCOGENIC SIGNALING IN GLIOBLASTOMA

ABSTRACT

EGFR kinase inhibitors have failed to improve survival in Grade IV Glioblastoma (GBM). Here we show that the activation of protein kinase aPKC (atypical Protein Kinase C) by TNF- α in the GBM microenvironment provides a molecular rationale for EGFR kinase inhibitor resistance. Additionally, we identify a bimodal signaling role of aPKC in both paracrine TNF α -dependent NF- κ B activation, as well as in tumor cell-intrinsic receptor tyrosine kinase signaling. Inhibiting tumor cell autonomous and non-tumor cell autonomous oncogenic signaling by targeting aPKC is an effective pharmacological approach in mouse models of GBM, including in EGFR kinase inhibitor resistant GBM. Finally, aPKC expression and activity is significantly increased in human GBM tumor cells and high aPKC expression correlates with poor prognosis.

INTRODUCTION

WHO Grade IV glioblastoma or GBM is a frequently occurring brain tumor with poor prognosis (Furnari et al., 2007). The relative survival estimate for GBM indicates that only 4.46% of patients diagnosed between 1995-2006 survived five years post diagnosis (CBTRUS). While strategies to improve the currently dismal survival in GBM primarily involve identifying and targeting oncogenic signaling pathways (Furnari et al., 2007; Gilbert, 2011; Kesari, 2011; I. K. Mellinghoff, Schultz, Mischel, & Cloughesy, 2011; Ingo K. Mellinghoff, Schultz, Mischel, & Cloughesy, 2012), the therapeutic success of EGFR kinase inhibitors *in vivo* has been limited (I. K. Mellinghoff et al., 2005). The activation of additional receptor tyrosine kinases (RTK) and/or downstream tumor intrinsic mutations can provide oncogenic stimuli to GBM tumor cells and account for EGFR kinase inhibitor resistance (Ingo K. Mellinghoff et al., 2012; I. K. Mellinghoff et al., 2005). Identifying and targeting such pathways can provide improved therapeutic efficacy, despite the fact that such efforts may require simultaneously disabling multiple, parallel oncogenic

signals. The serine-threonine kinase atypical protein kinase C (aPKC) is activated downstream of multiple RTK (Akimoto et al., 1996; Victoria Aranda et al., 2006; Berra et al., 1993). We had demonstrated that aPKC regulates neural progenitor cell proliferation and migration during the embryonic development of the spinal cord (Ghosh et al., 2008a, 2008b). Abnormal activation and altered intracellular localization of aPKC resulted in increased proliferation, abnormal migration and rosette-like structures reminiscent of brain tumors (Ghosh et al., 2008a). Therefore, we hypothesized that the abnormal or unscheduled activation of the developmentally important aPKC signaling pathway may be associated with GBM progression and that aPKC inhibition may provide an improved avenue for molecular therapeutics in GBM.

MATERIAL AND METHODS

Animals

Female 6- to 8-wk-old NOD-SCID mice were acquired from Charles River. $TNF\alpha^{-/-}$ (B6.129S6- Tnf^{tm1Gkl}/J , stock 5540) and control C57BL/6J (stock 664) were acquired from the Jackson laboratory. All animal procedures conformed to protocols approved by the University of Arizona Institutional Animal Care and Use Committee.

Antibodies and Reagents

Rabbit anti-aPKC (sc-216) and rabbit anti-p65-NF- κ B phosphoSer311 (sc-101748) were purchased from Santa Cruz. Rabbit anti-aPKC phosphoThr410/403 (#9378), rabbit anti-p65-NF- κ B phosphoSer536 (#3033), rabbit anti-Akt phosphoSer473 (#9271), mouse anti-Akt (#2920), rabbit anti-Src phosphoTyr516 (#6943), rabbit anti-Src (#2123), rabbit anti-MAPK p44/42 (#4695), rabbit anti-p65 (#4764) and rabbit anti-I κ B α (#9242) were obtained from Cell Signaling. Rabbit anti-PAR6 (ab49776), rabbit anti-aPKC phosphoThr560 (ab62372) and mouse anti-p62 (ab56416) were purchased from Abcam. Rabbit anti-EGFR phosphoTyr1086 (44790) and mouse anti-EGFR (44796) were purchased from Invitrogen. Mouse anti- β -tubulin (T-2046) and mouse

anti-MAPK p44/42 phosphoThr183phosphoTyr185 (M-8159) were purchased from Sigma. Mouse anti-human CD68 antibody (#M0814) was purchased from Dako. Mouse anti-human TNF α neutralizing antibodies from Novus Biologicals (# NB120-10204) or from R&D (MAB2101) were used at a concentration of 100 ng/mL. Mouse IgG1 isotype control (MAB002) or (NBP1-97005) were purchased from Novus Biologicals and R & D Systems and used at identical concentrations as the TNF α neutralizing antibodies. Rat anti-mouse Cd11b-PE (#12-0112-85), mouse anti-human TNF α -APC (#17-7349-82) and Mouse IgG1 isotype control (#17-4714-81) antibodies were acquired from eBioscience. PE-mouse anti-human TNF α (#502908), PE-mouse IgG1k isotype control (#400139), anti-human CD11b-PB (#101235), anti-human-CD64-AF647 (#305012), anti-human CD23-APCCy7 (#338520), anti-human CD14-PECy7 (#325617), anti-human CD80-FITC (#305205) and anti-human CD163 (#333608) antibodies used for FACS were obtained from Biolegend. Species-specific secondary antibodies for IHC/IF conjugated to Alexa 488 or 594 were obtained from Life Technologies. Secondary antibodies for Western (anti-mouse-HRP, anti-rabbit-HRP) were obtained from Promega. Erlotinib was purchased from Selleck Chemicals (S1023) and was used at a concentration of 10 μ M. All other inhibitors were purchased from Calbiochem. AG1478 (#658548) was used at 10 μ M, PI3K inhibitors LY294002 (#44024) at 20 μ M, Wortmannin (#681675) at 100 nM, MEK inhibitor U0126 (#662005) at 10 μ M, and Src kinase inhibitor, SU6656 (#572636) was used at 10 μ M. NF- κ B-Reporter:GFP lentivirus was obtained from SA Biosciences (CLS-013G). The I κ B α M adenovirus was purchased from Imgenex (IMG-2500). Lentiviruses expressing GFP or aPKC shRNA constructs were produced at Viral Vector Core, The Salk Institute according to methods described in Tiscornia *et al* (Tiscornia, Singer, & Verma, 2006). VSVg pseudotyped constitutively active IKK (S177, 181E) retrovirus was generated as described in Ghosh *et al* (Ghosh et al., 2006) with minor modifications. pCLXSN-IKK Ser177,181E was transiently transfected into HEK293T cells using linear 25 Kd

polyethyleneimine (Polysciences Inc. PA, USA) with an N/P ratio of 10 (1 mg/ml in DPBS, pH 4.5). Cells were co-transfected with pCL-CMV-GAG-POL and pMD2.G. Virus containing medium was harvested at 48 h and 72 h post transfection, treated with DNase1 (1 µg/ml, Sigma) and filtered through a 0.22 µm filter (Durapore, Millipore USA) before aliquoting and storage at -80 °C. Infectious viral titers were determined by RT-qPCR of genomic DNA extracted from HEK293T cells 48 h post infection with a 10-fold dilution series of retroviral vector. PZ09 was synthesized in house following the procedure described in Trujillo *et al* (Trujillo et al., 2009) with some modifications and the inhibitor was validated by mass spectrometry and *in vitro* kinase assays. PZ09 was used at 10 µM.

Cell lines and cell culture

U87/EGFRvIII and U251/EGFR human GBM cell lines were a gift from Dr. Zhimin Lu, MD Anderson. GL261, a murine glioma cell line, was acquired from NCI. The primary GBM line 6 (GBM6) was established directly from a patient surgical sample and maintained as a subcutaneous flank xenograft through serial passaging in immune deficient mice. GBM6 flank tumor xenografts were harvested, mechanically disaggregated, and grown in short-term culture (5–7 d) in DMEM containing 2.5 % fetal bovine serum, 1 % nonessential amino acids, 2 mmol/L glutamine, 100 units/mL penicillin, and 10 µg/mL streptomycin for lentiviral transduction (Giannini et al., 2005b). Primary glioma cells were dissociated from fresh patient tumors using Miltenyi Biotec brain tumor dissociation kit (#130-095-939) and the Miltenyi Gentle Macs Dissociator. For isolation of glioma cells, the protocol published by Pistollato *et al* (Pistollato, Persano, Puppa, Rampazzo, & Basso, 2011) was used with no modification. Samples were taken from patients diagnosed with GBM and the use of the patient tissues received prior Barrow Neurological Institute/St. Joseph's Hospital Institutional Review Board authorization. Unless indicated otherwise, all cell types were grown in DMEM supplemented with 10 % FBS and 1 %

penicillin/streptomycin (p/s) (Invitrogen) at 37 °C, 5 % CO₂. THP1 cells were maintained in DMEM supplemented with 10 % FBS, 1 % penicillin and streptomycin and 0.05 mM 2-mercaptoethanol. THP1 cells were differentiated with 50 ng/mL PMA (Cell Signaling) overnight, and were subsequently washed 3 times with PBS. Media was then replaced and the cells were cultured for an additional 24 h prior to experiments. Transfection of siRNA and shRNA were done using Lipofectamine (Life Technologies) or Effectene (Qiagen), respectively. siRNAs were purchased from Life Technologies. Transfection was performed according to established protocols from the manufacturers. Cells were analyzed 48 h post-transfection. Average knockdown efficiency for *PRKCZ*, *PRKCI*, *PAR6A*, *PAR6B* and *P62* relative to control (luciferase) siRNA is shown in Supplementary Fig. 1. U87/EGFRvIII cells were transduced with lentivirus GFP or with lentivirus aPKC-shRNA to generate stable lines (U87VIII-GFP and U87VIII-aPKC-shRNA). Glioma cells were incubated with 1:5,000 dilution of virus in serum-free media overnight. Subsequently the cells were washed 3 times with PBS and cultured according to standard protocols. The cells were cultured for additional 48 h post-infection before conducting experiments. For EGF and TNF α treatments, cells were serum starved for 24 h, and then treated with 100 ng/mL EGF (Millipore) or 10 ng/ml TNF α (Calbiochem) for various time points. PZ09 was used at 10 μ M. For other inhibitors, cells were serum starved overnight and pre-incubated with inhibitor for 30 m. For NF- κ B Reporter activity, U251/EGFR or U251/EGFR-aPKC-siRNA cells were incubated with 1:1,000 dilution of Lenti NF- κ B-Reporter:GFP in serum-free media overnight. Subsequently the cells were washed 3 times with PBS and cultured for 72 h prior to overnight serum starvation. After serum starvation cells were treated for 30 min with 10 ng/mL TNF α in serum free media in the presence or absence of 10 μ M PZ09 or monoclonal anti-human TNF α antibody. Changes in GFP fluorescence was detected and quantified using a Tecan Infinite F500 microplate reader. Results

were normalized to NF- κ B reporter transduced cells which were serum starved and not treated with TNF α .

Human Monocyte isolation and monocyte-derived macrophages

Peripheral blood mononuclear cells (PBMCs) were obtained from 50 mL of buffy coats (New York Blood Center) by Ficoll gradient centrifugation. Human monocytes were isolated by CD14 positive selection (STEMCELL) from PBMCs. CD14⁺ monocytes were co-cultured with GBM6 at 1:1 ratio for *in-vitro* proliferation or invasive assay. 300,000 to 500,000 CD14⁺ monocytes per mL were plated in RPMI 1640 plus 10 % of FBS and in vitro differentiated to macrophages by adding 25 ng/mL of M-CSF. IFN- γ (50 ng/mL), IL4 (40 ng/mL) or IL10 (50 ng/mL) polarizing cytokines were added on day 3 and M0, M1, M2a and M2c monocytes-derived macrophages were harvested on day 7. Macrophage polarized phenotype was confirmed using anti human CD11b, CD64, CD23, CD80, CD163 and CD14 (Biolegend). Recombinant cytokines were purchased from R&D.

Co-culture and ELISA

For transwell co-culture experiments, 1×10^6 glioma cells were plated into a 6-well plate. Cell culture inserts (Millicell, 0.4 μ m micropore polycarbonate filter) were placed in the wells. GBM6 cells were serum starved for 24 h before adding 1×10^5 GBM6 cells alone, plus 1×10^5 THP1 cells or primary monocytes (CD14⁺) to the insert. After specified time points, cell culture inserts were removed and RNA was isolated from the GBM6 cells alone. In addition, media supernatants were collected, snap frozen with liquid nitrogen, and stored at -80 °C. The media from co-culture of macrophages and tumor cell lines were collected after 24 and 48 h and detection of TNF α in the supernatants was performed using an anti-TNF α ELISA kit (eBioscience). For proliferation assays, starved 1×10^5 GBM6 were co-cultured with 1×10^5 CD14⁺ monocytes in 6 well plate and EdU incorporation was assessed following manufacturer's instruction (Click-iT® EdU Flow

Cytometry Assay Kit, Life Technologies). CD11b staining was included to discriminate monocytes.

RNA isolation and RT-qPCR

For acutely isolated *in-vivo* mouse brain mRNA analyses, whole mouse brain was homogenized in Trizol using a glass homogenizer. Samples were centrifuged and 0.2 mL chloroform per 1 mL of Trizol was added to the supernatant. Samples were vigorously shaken for 15 seconds, incubated at RT for 3 min, and centrifuged for 15 min at 10,000 x g at 4 °C. Addition of chloroform and centrifugation was repeated. After second centrifugation, the aqueous phase containing RNA was precipitated by mixing with isopropyl alcohol for 20 min at -20 °C. RNA precipitants were washed 3 times with 75 % ethanol and spun at 7500 xg for 5 min at 4 °C. RNA was air dried, resuspended in RNase-free water and stored at -80 °C. For cellular mRNA analyses, total cellular RNA was isolated with RNeasy kit (QIAGEN). mRNA was reverse transcribed into cDNA using the Superscript III Kit (Life Technologies). Real-time PCR was performed on a 7900HT cyclor with SYBR-Green Mastermix (Applied Biosystems), and primers (IDT) summarized in Supplementary Table. For NF- κ B target gene profiling, cDNA was obtained as described and plated onto a custom TaqMan 96-well Gene Expression Signature Plate according to manufacturer's instructions. Real-time PCR was performed on a 7900HT cyclor with TaqMan Universal PCR Master Mix (Life Technologies). Primer sequences are provided in Supplementary Table.

Immunofluorescence

Glioma cells were seeded onto acid-etched coverslips (70 % EtOH, 1 % HCL in PBS, 5 min) in a 24-well plate overnight. Upon confluency, media was removed and the cells were washed 3 times with PBS. The cells were fixed with 4 % PFA for 15 min at room temperature (RT), then washed 3 times with PBS and permeabilized with 0.1 % Triton-X-PBS for 15 min at

RT. Cells were blocked for 2 h with 2 % normal horse serum (Life Technologies) in PBS at RT. Primary antibodies were diluted in 2 % normal horse serum and cells were incubated overnight at 4 °C. Subsequently, coverslips were washed 3 times with PBS and secondary antibodies (Alexa-Fluor-488 and 594) diluted in 2 % normal horse serum were added for 2 h at RT. Following the secondary antibody incubation, cells were stained with DAPI (diluted at 1:5,000 in PBS) for 10 min at RT. Finally, coverslips were washed 3 times with PBS and mounted onto slides using Prolong Gold Antifade Reagent (Life Technologies) and sealed with nail polish. Images were obtained using a Zeiss 710 confocal using a 63x objective lens.

Flow Cytometry analysis

Glioma cell lines, undifferentiated or PMA-differentiated THP1 cells, and CD14+ primary monocytes were cultured alone and together in complete DMEM medium at a 1:1 ratio. 6 h prior to harvesting, Brefeldin A was added to cells at a final concentration of 3 µg/ml. CD11b surface staining was included to discriminate primary monocytes from glioma cells. Cells were fixed with 1 % PFA and permeabilized with 0.5 % saponin. Anti-TNF α antibody or isotype control was added to cells and incubated on ice for at least 30 min. Cells were then washed with Dulbecco-PBS and suspended in 1 % BSA solution. For Ser536 phospho- NF- κ B p65 (Cell Signaling Technology) staining, GBM6 were treated with 100 ng/mL of TNF α (Calbiochem) for 1 h. After harvesting, cells were immediately fixed with 1 % PFA for 15 min, washed 2 times with PBS and then permeabilized with cold methanol for 30 min on ice. Cells were washed 3 times, blocked with PBS + 5 % human AB serum for 15 min and then incubated with anti phospho-NF- κ B p65 PE antibody for 30 min at 4 °C. Cells were finally washed and re-suspended in PBS for FACS analysis. For BrdU incorporation experiments, 1×10^6 U87/EGFRvIII or GBM6 cells were plated in a 6-well plate. Cell culture inserts (Millicell, 0.4 µm micropore polycarbonate filter) were placed in the wells. Glioma cells were serum starved for 24 h before adding 1×10^5 U87/EGFRvIII or GBM6

cells and 1×10^5 THP1 to the insert. $10 \mu\text{M}$ BrdU (BD Pharmingen, 552598) was added to the media for 24 h. Cell culture inserts were removed, and glioma cells were fixed, permeabilized and stained for BrdU using an APC BrdU Flow Kit (BD Pharmingen, 552598) according to manufacturer's instructions. For EdU incorporation, starved 1×10^5 GBM6 were co-cultured with 1×10^5 CD14⁺ monocytes isolated from PBMC in 6 well plate for 24 h. EdU was added into the culture at the last two hours. After harvesting, cells were immediately fixed with the fixative buffer, supplied with the kit (Click-iT® EdU Flow Cytometry Assay Kit, Life Technologies). Staining was performed following manufacturer's instruction. CD11b staining was included to discriminate monocytes. For *in-vivo* phenotypic analyses of tumor infiltrating macrophages within human GBM tumors, 3 patient samples were dissociated using Miltenyi Biotec brain tumor dissociation kit and Gentle Macs dissociator. Dissociated cells were blocked using 3% FBS in PBS for 30 min on ice and subsequently stained with a cocktail of anti-human CD23, anti-human CD64 and anti-human CD11b in 3% FBS/PBS for 30 min on ice. Cells were washed 3 times with PBS and fixed in 1% PFA for 30 min on ice. FACS calibur, FACS Aria or LSRII (BD) were used to analyze samples and WinMiDi software (freeware from The Scripps institute) or FlowJo were used to analyze and plot the data.

Immunoblotting and immunoprecipitation

Ice-cold 1 % NP-40 buffer (20 mM Tris-HCl at pH 8, 137 mM NaCl, 10 % glycerol, 1 % NP-40) supplemented with phosphatase and protease inhibitor (Halt Protease and Phosphatase Inhibitor Cocktail, Thermo Scientific) was used for protein isolation and immunoprecipitation. Briefly, cells were washed 3 times with ice-cold PBS and scraped in NP-40 buffer. Lysates were kept cold and sonicated 10 times, 1 sec each, and then centrifuged at $12,000 \times g$ for 5 min at 4 °C. For immunoprecipitation, the supernatant was pre-cleared using protein-A beads for 30 min at RT. The supernatant was subsequently added to protein-A beads pre-bound to aPKC antibody

(Santa Cruz, sc-216), and incubated overnight on a shaker at 4 °C. Immunoprecipitates were then washed 2 times with ice-cold NP-40 buffer, and a final wash with PBS. Sample loading buffer with DTT was added, and the immunoprecipitates were boiled for 5 min prior to loading onto precast SDS-PAGE gels (Life Technologies). Gels were transferred onto methanol pre-soaked PVDF membranes and subsequently blocked with 5 % BSA in PBS for 2 h. Primary antibodies were incubated overnight at 4 °C, after which blots were washed 3 times with TBST (TBS + 0.1 % Tween) for 15 min each, followed by incubation with secondary antibodies (1:2000) for 2 h at RT. Blots were then washed 3 times for 30 min each in TBST, with a final wash in TBS alone. Blots were developed using Super Signal West Dura (Thermo Scientific) on the UVP Imager.

Immunohistochemistry for Tissue microarrays

Tissue microarrays were prepared from archival blocks of WHO grade IV glioblastoma formalin fixed paraffin embedded specimens. All tumor cases were histologically reviewed and representative tumor areas marked on the corresponding donor paraffin blocks. Blocks were cut at 4 µm thickness for routine hematoxylin and eosin (H&E) staining and immunohistochemistry. Sources for TMAs include TGen (Phoenix, AZ), Armed Forces Institute of Pathology (Bethesda, MD) and Barrow Neurological Institute (Phoenix, AZ). Immunohistochemistry was performed using Ventana automated Discovery XT or Benchmark XT system (VMSI - Ventana Medical Systems, a Member of the Roche Group, Tucson, Arizona). All steps were performed on this instrument using VMSI validated reagents, including deparaffinization, cell conditioning (mild CC1 for CD68 and standard CC1 for aPKC, phospho-aPKC and TNF α), primary antibody staining, detection and amplification using a biotinylated-streptavidin-HRP and ultraview Universal DAB (Diaminobenzidine) detection system and hematoxylin counterstaining. Primary antibodies were incubated for 30 min (CD68, TNF α) or 1 h (aPKC, phospho-aPKC) at 37 °C. Appropriate positive

and negative (secondary antibody only) controls were stained in parallel for each round of immunohistochemistry. Following staining on the instrument, slides were dehydrated through graded alcohols to xylene and coverslipped with mounting medium.

***Ex vivo* Invasion assay**

Ex-vivo orthotopic invasion assays were performed as described by Valster *et al* (Aline Valster et al., 2005) with some modifications. Brains were obtained from 4-week-old rats and placed in ice-cold aCSF (126 mM NaCl, 3 mM KCl, 1.5 mM MgCl₂, 24 mM CaCl₂, 1.2 mM NaH₂PO₄, 11 mM glucose and 26 mM NaHCO₃). Brains were sectioned into 400 µm slices on a vibratome in ice-cold aCSF. Slices were placed on a cell culture insert (Millicell, 0.4 µm micropore polycarbonate filter) in a 6-well plate with 1.5 mL DMEM with 10 % FBS and 1 % p/s 500 µL of media was added to the insert that was placed inside the wells of a 6-well plate. The brain slices were kept in the incubator under standard culture conditions (37 °C, 5 % CO₂). GFP⁺ GBM6 and/or U87/EGFRvIII cells were resuspended in serum-free DMEM at 2x10⁸ cells/ml. Prior to the addition of cells, media was removed from the upper chamber of the 6-well plate so the slice was semidry before implantation. 10⁵ GFP⁺ GBM6 and/or U87/EGFRvIII cells were placed on the putamen in 0.5 µL volumes, and after 45 min, 500 µL of serum-free media was added back to the upper chamber. The plates were kept in the incubator for 4-5 days and subsequently fixed overnight in 4% PFA at 4 °C. The polycarbonate membrane was carefully removed and the brains were placed on a slide for imaging on a confocal microscope. Imaging and quantification was performed as described by Valster *et al* (A. Valster et al., 2005). Fluorescence at various depths into the tissue was calculated after confocal imaging. Intensity at each layer was normalized to total intensity across all depths and linear regression analysis was performed to determine the slope of invasion for each replicate. R² (coefficient of determination) for each slope was calculated and was greater than 0.88 with an average value of 0.96. Average inverse slope was

used to calculate the invasion index. Error bars represent the standard deviation of at least three repeats.

Orthotopic xenografts

Female 6- to 8-wk-old NOD-SCID, TNF α ^{-/-} and control mice were anesthetized by i.p. injection of 1.25 % avertin (200 mg/kg). Cells (U87EGFRvIII-GFP, U87/EGFRvIII-aPKC-shRNA, or GL261) were resuspended in standard media (DMEM with 10 % FBS, 1 % p/s) at a concentration of 1.25×10^5 cells/ μ L and kept on ice until injection. Intracranial injections were performed using a Hamilton syringe (Hamilton Company, Reno, Nev.). Briefly, the animal was secured onto the small animal stereotaxic apparatus (Kopf Instruments) and a midline incision was made to expose the skull. Subsequently, a burr hole was drilled 1 mm lateral and 2 mm anterior to bregma. Cells were injected at a rate of 1 μ L/min (total 4 μ L 5×10^5 cells) to a depth of 3 mm below the skull, which corresponds to the area of the caudate nucleus. Following intracranial injection, mice were observed daily for changes in weight or modified gait, and were euthanized upon moribund symptoms. Brains were then removed and processed for histopathology.

Statistical Analysis

Data are expressed as mean \pm SEM. Differences between the means of experimental groups were analyzed with either two-tailed Student's t-test or ANOVA (Prism GraphPad software, Inc.). Survival was calculated using Kaplan-Meier analysis (Prism GraphPad software, Inc.). P values ≤ 0.05 were considered significant.

RESULTS

aPKC expression inversely correlates with GBM survival and targeting aPKC reduces tumor progression in a mouse model of GBM resistant to EGFR kinase inhibitors

We examined the expression of aPKC in human non-tumor brain and GBM tissue. Immunohistochemical staining of non-tumor brain tissue sections revealed very little aPKC

staining in the brain parenchyma (Fig. 3.1A). Some cytoplasmic staining was observed in neurons (fig. 3.S1A) and trace staining was occasionally detected in oligodendrocytes. In contrast, strong aPKC staining was observed in GBM tumor cells (Fig. 3.1B,C). The distribution of staining was consistent across variable histologic patterns that define GBM such as, pseudopalisading necrosis (Fig. 3.1C and fig. 3.S1B), areas of microvascular proliferation (fig. 3.S1C), infiltrative single cells, clusters and confluent cell sheets. Next, we stained tissue microarrays (TMA) consisting of 330 GBM cases. The aPKC staining was validated using both negative and positive staining on control cores of non-neoplastic cortical grey matter, white matter, cerebellum, placenta, testis, lung, liver, kidney, and tonsil within each TMA. Within most, but not all GBM cores, tumor cells showed increased aPKC staining relative to non-tumor cells. aPKC staining within tumor cells was compared to adjacent non-tumor cells within each core and the core was assigned a numerical score of 0, 1, 2 or 3 representing negative, weak positive, intermediate positive or bright staining. Interestingly, a subset of GBM tumors was aPKC bright (100/330), and other subsets had intermediate (73/330) or weak (107/330) positive levels. A smaller fraction of GBMs were aPKC negative (50/330). This indicates that GBM tumors overall tend to express higher levels of aPKC, however the expression level of aPKC between individual GBM tumors varies and GBM tumors can be stratified based on aPKC intensity (Fig. 3.1D). Furthermore, staining a smaller set of GBM TMA (44 cases) with the aPKC activation specific, phosphoThr 410/403 antibody revealed that not only total protein level, but also aPKC activity is commonly high in GBM (Fig. 3.1E,F). The range of staining intensity for phosphorylated aPKC, compared to total aPKC, was somewhat reduced. This may be due to the reduced affinity of phosphorylation-specific antibodies relative to total aPKC antibody.

To further examine the clinical relevance of aPKC staining in GBM, we compared the association between aPKC immunoreactivity and survival. In a TMA annotated for survival data of

patients, 7 cases had no detectable aPKC staining, 17 cases were weak positive, and 20 cases showed bright aPKC staining. Statistical analyses demonstrated that there was a significant difference in overall survival between the bright aPKC staining and aPKC negative or weak positive cases (Log-rank [Mantel-Cox] test $p=0.0145$). The decrease in survival was restricted to the aPKC bright group; statistically significant difference in survival between the lower categories of aPKC intensity was not detected. While the median survival of aPKC bright staining cases was 176.5 days, aPKC weak positive had a median survival of 413 days and aPKC negative cases 532 days (Fig. 3.1G). Survival was not found to correlate with gender and age in the sampled population. All together, these results demonstrate that increased aPKC expression is detected in GBM and that there is a strong negative correlation between aPKC protein expression and survival.

To directly test the function of aPKC in GBM progression *in vivo*, we performed orthotopic xenograft experiments in NOD/SCID mice using U87/EGFRvIII and U87/EGFRvIII in which aPKC expression was silenced by shRNA. We used a viral vector encoding shRNA targeting both isoforms *PRKCZ* and *PRKCI* and obtained ~70-80% knockdown efficiencies (fig. 3.S2A). 0.5×10^6 cells were stereotactically injected into the caudate nucleus and mice were euthanized upon detection of neurological symptoms as approved by IACUC. Tumor growth was confirmed by histopathological analyses. Silencing aPKC in U87/EGFRvIII cells resulted in a significant increase in median survival following orthotopic xenografts (Log rank [Mantel Cox] test $p=0.0005$). Mice bearing U87/EGFRvIII aPKC shRNA showed a median survival of 35 days, in comparison to the median survival of 11 days in WT U87/EGFRvIII (Fig. 3.1H). Histopathological examination 6 days post implantation revealed that tumors derived from U87/EGFRvIII aPKC shRNA were significantly smaller in size, in comparison to tumors derived from WT U87/EGFRvIII (Fig. 3.1I). Subsequently, we tested the efficacy of a small molecule, benzoimidazole ATP-

competitive aPKC inhibitor PZ09 (Trujillo et al., 2009) in inhibiting tumor growth *in vivo*. 3 days post implantation, 10 μ M PZ09 was delivered by ALZET osmotic minipumps directly at the site of U87/EGFRvIII tumors, similar to convection-enhanced delivery of molecules to the brain, for 7 days. Mice were euthanized and tumor size was measured by sectioning the entire brain, staining with hematoxylin-eosin (H&E) and tumor volume was calculated using ImageJ. These experiments reveal that inhibition of aPKC reduced tumor volume by 64.68 ± 9.23 % after 7 days of treatment (Fig. 3.1J).

Next, we tested the efficacy of aPKC inhibition in patient-derived, EGFR kinase insensitive, orthotopic xenografts. GBM6 patient-derived xenograft cells retain the clinically relevant biochemical characteristics of clinical GBM, including EGFR amplification and EGFRvIII mutation (Giannini et al., 2005a; A. Pandita, K. D. Aldape, G. Zadeh, A. Guha, & C. D. James, 2004). Furthermore, GBM6 xenografts are insensitive to the EGFR kinase inhibitor erlotinib (Sarkaria et al., 2007). The acute inhibition of aPKC by PZ09 significantly reduced tumor volume in orthotopic xenografts. 2×10^6 GBM6 cells were implanted in the caudate nucleus and 10 μ M PZ09 was delivered by ALZET minipumps, 3 days after implantation and for a treatment period of 14 days. At 10 μ M, PZ09 effectively decreased aPKC activity in GBM6 cells in culture (Fig. 3.S2D). 10 μ M PZ09 *in vivo* resulted in 84.06 ± 6.27 % decrease of tumor volume after 14 day treatment (Fig. 3.1K).

aPKC functions downstream of receptor tyrosine kinases in GBM

Both wild type (WT) EGFR and EGFRvIII are frequently co-expressed in GBM (Q. W. Fan et al., 2013) and both populations were detected in GBM6, albeit EGFRvIII was the predominant population (Fig. 3.S3A). Serum starved GBM6 showed an activation of aPKC following EGF stimulation (Fig. 3.2A). Similarly, U251 stably expressing EGFR (U251/EGFR) showed aPKC activation (Fig. 3.2B). The kinetics of phosphorylation of EGFR in GBM6 and U251/EGFR (Fig.

3.S3B,C) are faster than that of aPKC, suggesting that aPKC is an indirect downstream target of EGFR. Importantly, EGF-induced expression of *CD44*, *MMP9* and *VCAM* were inhibited by PZ09 treatment in GBM6 (Fig. 3.2C). Similarly, aPKC silencing with siRNA in U251/EGFR reduced the mRNA levels of EGF-induced genes (Fig. 3.2D). Therefore, aPKC mediates EGFR signaling in GBM. Our findings are consistent with the reported function of this kinase downstream of EGFR family in tumor progression in breast cancer and squamous cell carcinomas of head and neck (V. Aranda et al., 2006; Cohen et al., 2006). Why is inhibition of aPKC effective in EGFR-insensitive GBM? aPKC was also activated downstream of activated Ras, PI3-K and Src (Fig. 3.2E). EGFR kinase inhibitor resistance is often associated with *PTEN* mutations (I. K. Mellinghoff et al., 2005). Furthermore, multiple RTKs are simultaneously activated in GBM (Stommel et al., 2007) or compensatory pathways, such as the transcriptional upregulation of Met in EGFR kinase inhibitor-resistant glioblastoma mouse models (Jun et al., 2011) render EGFR kinase inhibitors ineffective. Being a kinase which functions further downstream of *PTEN* and which participates in signaling downstream of Ras and Src, aPKC may function downstream of multiple RTKs and therefore has intrinsic advantages over EGFR as a target in GBM.

TNF α functions as a paracrine oncogenic signal in GBM

Another possibility why EGFR kinase inhibitor fails *in vivo*, whereas aPKC inhibition is effective, is the existence of paracrine factors and the induction of EGFR-independent, parallel oncogenic signals through non-cell autonomous mechanisms. For example, the tumor microenvironment is recognized to play a significant role in influencing tumor progression (M. J. Bissell & W. C. Hines, 2011; Bissell & Labarge, 2005; Coussens & Werb, 2002; Liotta & Kohn, 2001; Lukashev & Werb, 1998). We detected significant CD68⁺ cell infiltration within the tumor area in GBM tissue (Fig. 3.3A), in contrast to non-tumor brain, in 37 of the 44 (~84 %) cases examined. Interestingly, the orthotopic GBM model using GBM6 implanted in NOD/SCID mice

also showed increased Iba1⁺ cells in the tumor microenvironment (fig. 3.S4A) in contrast to contralateral control regions (fig. 3.S4B). Furthermore, we characterized the phenotype of GBM infiltrating myeloid cells in three independent GBM cases. Freshly resected GBM samples were dissociated and GBM-associated macrophages were characterized by FACS analyses. While the predominant population was of the M2 macrophage subtype (CD23⁺), a smaller but significant population of M1 subtype (CD64⁺) macrophages was consistently observed upon FACS characterization of the tumor-associated CD11b⁺ myeloid cells (Fig. 3.3B). Pro-inflammatory cytokines such as TNF α are produced by tumor-associated myeloid cells and have been shown to promote tumor initiation and progression (F. R. Balkwill & Mantovani, 2012; Wynn, Chawla, & Pollard, 2013). *In vitro* differentiated M1 macrophages, as well as M2 macrophages, when activated, secreted TNF α (Fig. 3.S4C). Consistent with this observation, we detected TNF α expression in all GBM tissues (44 cases) examined, while TNF α was undetectable in non-tumor brain (Fig. 3.3C).

Activation of the NF- κ B pathway is a strong oncogenic signal in many tumors, including GBM (Atkinson, Nozell, & Benveniste, 2010; Ben-Neriah & Karin, 2011; Chaturvedi, Sung, Yadav, Kannappan, & Aggarwal, 2011a; Karin, 2009; Laver, Nozell, & Benveniste, 2009; Naugler & Karin, 2008; Staudt, 2010; H. Wang, Zhang, Huang, Liao, & Fuller, 2004). The deletion of *NFKBIA*, which encodes the NF- κ B inhibitor I κ B α , is seen in about 20 % of GBM cases (M. Bredel et al., 2011) and the activation of NF- κ B predicts identical prognosis as EGFR gain-of-function in GBM (M. Bredel et al., 2011). Nonetheless, the loss of I κ B α overlaps with EGFR amplification in only 5 % GBM cases suggesting that these two independent tumor-intrinsic mutations do not occur simultaneously (M. Bredel et al., 2011). Loss of I κ B α driving NF- κ B activation is in fact rare in cancers; rather an inflammatory tumor microenvironment such as, paracrine TNF α more commonly drives NF- κ B activation in cancers such as colon cancer

(Grivennikov & Karin, 2010; Karin, 2009; Mantovani, Allavena, Sica, & Balkwill, 2008). α PKC is a well-established regulator of NF- κ B (Diaz-Meco et al., 1994; Duran, Diaz-Meco, & Moscat, 2003; Leitges et al., 2001). We hypothesized that α PKC regulates paracrine TNF α driven NF- κ B activation in GBM and therefore targeting α PKC confers improved efficacy in GBM by dually inhibiting RTK and NF- κ B pathways. First, we tested if NF- κ B signaling is more active in GBM harboring EGFR gain-of-mutation but without I κ B α loss of function. Freshly resected GBM tumor tissues were dissociated and tumor cells were confirmed to contain EGFR amplification and/or EGFRVIII mutation. Comparison of I κ B α mRNA expression levels between GBM and normal human astrocytes revealed that I κ B expression was unaffected. Furthermore, sequencing showed that the locus did not contain non-synonymous mutations in these samples (data not shown). Subsequently, these tumor cells were subjected to NF- κ B-target gene profiling by RT-qPCR. These GBM tumors had upregulated NF- κ B target gene expression in comparison to normal human astrocytes (Fig. 3.3D). We also extended our analyses to orthotopic murine models of GBM described above. Acutely isolated tissue from the side of NOD/SCID mouse brain bearing GBM6 tumors showed NF- κ B activation in comparison to contralateral, non-tumor bearing brain (Fig. 3.3E). Similarly, C57BL6 brains with GL261-derived tumors showed increased NF- κ B-target gene expression in comparison to contralateral, non-tumor bearing brain (Fig. 3.34D). To validate the function of microenvironment-derived TNF α in GBM tumor progression *in vivo*, C57BL6-derived GL261 mouse glioma cells were stereotactically injected into the caudate nucleus in either WT control or mice lacking the TNF α gene ($TNF\alpha^{-/-}$). The genetic ablation of $TNF\alpha$ resulted in a significant increase in survival after orthotopic xenograft of GL261 (Log rank [Mantel-Cox] test $p = <0.0001$). While WT mice bearing GL261 orthotopic xenografts had a median survival of 16.5 days, $TNF\alpha^{-/-}$ mice showed a median survival of 23 days (Figure 3.3E). These results demonstrate that NF- κ B signaling is active in GBM, and is likely driven by paracrine

TNF α . This TNF α / NF- κ B axis promotes GBM progression and acts as an EGFR-independent oncogenic signal.

Paracrine TNF α -induces aPKC activation and EGFR kinase inhibitor resistance in GBM

To directly test the role of myeloid cells and myeloid-cell derived factors, such as TNF α , on GBM proliferation and invasion, we isolated primary human monocytes from peripheral blood and co-cultured these cells with GBM6 *in vitro*. Co-culture of monocytes with GBM6 led to the production of TNF α by the monocytes (Fig. 3.4A, Fig. 3.S5A and B). We also detected high TNF α levels in the culture media when GBM6 cells were co-cultured with *in vitro* differentiated monocytic THP1 cells (Tsuchiya et al., 1982) (Fig. 3.S5C). Differentiated, but not undifferentiated THP1 cells were the source of TNF α production (Fig. 3.S5D). Co-culture of GBM6 with monocytes led to a significant increase in proliferation of GBM6 cells as assayed by EdU incorporation (Fig. 3.4B,C). This increased proliferation was blocked when an anti-human-TNF α antibody was included in the culture media to neutralize TNF α (Figure 3.4B,C and Fig. 3.S5E).

Rapid invasion of GBM cells into the surrounding parenchyma is a defining characteristic of this disease and is believed to be an important contributor to the failure of surgery and directed radiotherapy. Therefore, we compared GBM6 invasion in the absence or presence of monocytes in a modified organotypic invasion assay (A. Valster et al., 2005). GBM6 cells were transduced with GFP lentivirus and were subsequently placed on an organotypic culture of rat brain slice and allowed to invade into the tissue for 4 days. The intensity of GFP fluorescence was calculated at 10 μ m increments from the top of the slice and the fluorescence intensity at each point was divided by the total intensity. The rate of invasion was defined as the inverse of the slope obtained by linear regression analysis of the normalized fluorescence at various depths. These experiments showed that GBM6 retained the ability to invade into the brain parenchyma. GBM6 invasion was enhanced when implanted onto rat brain slices *ex vivo* together with monocytes,

while anti-human-TNF α antibody blocked this enhanced invasion (Fig. 3.4D). Similar results were obtained when GBM6 and differentiated THP1 cells were co-cultured. Differentiated THP1 increased GBM6 proliferation (Fig. 3.S6A) and invasion (Fig. 3.S6B) and the effect of THP1 was inhibited by anti-human-TNF α antibody (Fig. 3.S6A,B). The effect of myeloid cells on GBM proliferation and invasion is independent of *PTEN* status of the GBM cells as similar increase in proliferation and invasion were observed in U87/EGFRvIII co-cultured with differentiated THP1 (Fig. 3.S6C,D). Our results are consistent with the well-known role of tumor-associated macrophages in facilitating tumor-associated inflammation in cancers such as breast and colon cancer (Grivennikov & Karin, 2011; Mantovani & Sica, 2010; Ruffell, Affara, & Coussens, 2012; Terzic, Grivennikov, Karin, & Karin, 2010). Interestingly, aPKC phosphorylation status associated with monocyte-stimulated GBM proliferation and invasion. aPKC phosphorylation was enhanced in GBM6-monocyte co-cultures and was reduced when TNF α was neutralized under co-culture conditions (Fig. 3.4E,F). We also co-cultured B6-derived GL261 mouse glioma cells with mouse bone marrow-derived macrophages as an independent model of GBM-myeloid cell interaction. Analogous to GBM6-monocyte co-cultures, mouse primary macrophages also produced TNF α in the presence of GL261 (Fig. 3.S7A). Tumor cell proliferation (Fig. 3.S7B) and invasion (Fig. 3.S7C) were increased in the presence of macrophages.

Finally, we directly tested whether paracrine TNF α can indeed reduce the efficacy of EGFR kinase inhibitors in GBM. Treatment of GBM6 cells with the EGFR inhibitor erlotinib *in vitro* resulted in a significant inhibition of proliferation (Fig. 3.4G,H) and invasion (Fig. 3.4I). The addition of TNF α to GBM6 treated with erlotinib essentially obliterated these inhibitory effects (Fig. 3.4G,H,I). aPKC phosphorylation, but not EGFR phosphorylation, correlated with GBM6 proliferation and invasion. Erlotinib reduced both aPKC and EGFR phosphorylation in GBM6, but addition of TNF α that led to increased GBM6 proliferation and invasion in the presence of

erlotinib, correlated with enhanced aPKC phosphorylation but failed to affect EGFR phosphorylation (Fig. 3.4J). Our results are consistent with myeloid cells increasing GBM cell proliferation, invasion and contributing to the reduced efficacy of EGFR kinase inhibitor through the production of $\text{TNF}\alpha$ in the tumor microenvironment.

Oncogenic $\text{TNF}\alpha$ /NF- κ B signaling in GBM is dependent on aPKC activation

Next, we directly tested if aPKC activity was increased in GBM6 cells in response to $\text{TNF}\alpha$. Phosphorylation of both aPKC and the p65 subunit of NF- κ B (p65-NF- κ B) were significantly increased in GBM6 following the addition of $\text{TNF}\alpha$ (Fig. 3.5A). Additionally, PZ09 treatment resulted in a significant reduction of NF- κ B targets induced by $\text{TNF}\alpha$ (Fig. 3.5B). Analyses of Ser536 phosphorylation on p65-NF- κ B in GBM6 by FACS indicated that PZ09 treatment inhibited the $\text{TNF}\alpha$ -dependent increase at this phosphorylation site (Fig. 3.5C). Similarly, aPKC (Fig. 3.5D) and p65-NF- κ B (Fig. 3.5A) was activated upon $\text{TNF}\alpha$ stimulation in the glioma cell line U251. Silencing aPKC in U251 cells using siRNA sequences targeting both *PRKCI* and *PRKCZ* inhibited $\text{TNF}\alpha$ induced NF- κ B targets (Fig. 3.5E). Silencing aPKC in U251 prevented the $\text{TNF}\alpha$ -dependent phosphorylation of Ser311 on p65-NF- κ B (Fig. 3.5F). However, $\text{TNF}\alpha$ -induced I κ B α degradation was not inhibited (Fig. 3.5G). These results are consistent with a previous report demonstrating that aPKC regulates IKK activity and/or p65-NF- κ B phosphorylation in the NF- κ B pathway in a cell type specific manner (Leitges et al., 2001). Finally, we tested the effect of PZ09 and aPKC siRNA on NF- κ B:GFP reporter activity in U251 following $\text{TNF}\alpha$ stimulation. Both PZ09, as well as aPKC siRNA, reduced $\text{TNF}\alpha$ -dependent NF- κ B:GFP reporter activity to levels comparable with neutralization of $\text{TNF}\alpha$ using an anti-human- $\text{TNF}\alpha$ antibody (Fig. 3.5G).

We also tested the effects of inhibiting aPKC under GBM6-myeloid cell co-culture conditions. Co-culture of GBM6 and monocytes results in the phosphorylation of both aPKC and

p65 in GBM6 approximately 1 h following mixing of these cell types (Fig. 3.S8B). To assay monocyte induced NF- κ B gene expression in GBM6 by qRT-PCR, we utilized a transwell culture system. GBM6 alone or GBM6 plus monocytes were grown in the top chamber of a transwell system, while GBM6, uncontaminated by monocytes, yet exposed to the co-culture media, were grown in the bottom chamber separated by a 0.4 μ m filter. GBM6 from the bottom chamber of the transwell system described above were harvested and processed for RT-qPCR profiling. GBM6 exposed to the co-culture media showed increased mRNA levels of a number of inflammatory cytokine genes and other NF- κ B targets, such as *COX2*, *IL-1 β* , *IL6*, *IL8*, *MCP-1*, *MMP9*, *TNF α* and *VEGF*, in comparison to GBM6 grown in as monoculture (Fig. 3.5H). Similar results were obtained when the human pre-monocytic cell line THP1 was differentiated *in vitro* (Tsuchiya et al., 1982) and co-cultured with GBM6. Under these conditions we observed aPKC phosphorylation in GBM6 in the lower chamber approximately 1 h following plating (Fig. 3.S10A). NF- κ B gene expression in GBM6 (Fig. 3.S9B) or U87/EGFRvIII (Fig. 3.S9C) were enhanced under co-culture conditions with differentiated THP1. Importantly, treatment with PZ09 inhibited the induction of NF- κ B target genes observed in GBM6-monocyte co-culture conditions (Fig. 3.5H). These results demonstrate that tumor-associated myeloid cells activated aPKC-dependent NF- κ B signaling. This aPKC-dependence is also observed in *PTEN* deficient U87/EGFRvIII cells indicating that aPKC functions downstream of PTEN.

Consistent with our hypothesis that aPKC-dependent NF- κ B signaling induced by myeloid cells contributes to GBM proliferation, PZ09 was also effective in inhibiting monocyte-induced increase in GBM6 proliferation (Fig. 3.5I,J). Additionally, PZ09 was effective in inhibiting the monocyte-induced increase in invasion (Fig. 3.5K). PZ09 dependent inhibition of proliferation and invasion also correlated with inhibition of aPKC and p65-NF- κ B phosphorylation (Fig. 3.5L,M). In comparison to untreated GBM6-differentiated THP1 co-cultures, PZ09 treatment of

co-cultured GBM6 with differentiated THP1 similarly reduced proliferation (Fig. 3.S11A) and invasion (Fig. 3.S11B). We silenced aPKC expression in *PTEN* deficient U87 cells stably expressing EGFRvIII (U87/EGFRvIII) by using shRNA. In comparison to U87/EGFRvIII-differentiated THP1 co-cultures, U87/EGFRvIII aPKCshRNA cells co-cultured with differentiated THP1 showed reduced proliferation (Fig. 3.S11C) and invasion (Fig. 3.S11D). Neither, PZ09 or aPKC siRNA affected the levels of EGFR or EGFR phosphorylation in GBM6 or U251/EGFR (Fig. 3.S12A,B).

Distinct aPKC-containing signaling complexes mediate oncogenic TNF α and RTK signaling

Does GBM cell autonomous EGFR and paracrine TNF α signals converge on a unique aPKC-containing signal module in GBM cells? While both EGF and TNF α signaling in GBM resulted in aPKC activation and were critically dependent on aPKC, these pathways resulted in largely distinct transcriptional outputs at early time points. For example, EGF-induces CD44, MMP9, VCAM and uPAR in U251/EGFR at 6 h (Fig. 3.S13A), while TNF α treatment for 1 h led to the expression of a different set of genes including IL-1 β , IL-8, MCP-1 and TNF α (Fig. 3.S13B). This discrete expression profile is not apparent after overnight treatment since long term TNF α treatment leads to increase in EGF. Furthermore, the ERK-inhibitor U0126 treatment indicated that MAPK signaling downstream of aPKC was mostly relevant to EGF-specific gene expression and not TNF α -dependent gene expression (Fig. 3.S13C,D). In contrast, I κ B α M inhibited only TNF α -dependent gene expression, and not EGF-dependent gene expression with the exception of MMP9 indicating that aPKC-dependent NF- κ B signaling was specifically required for the expression of the TNF α -dependent genes (Fig. 3.S13E,F). These results indicate that while aPKC participates in both signaling pathways, these pathways do not merely converge on aPKC.

To further investigate aPKC signaling downstream $\text{TNF}\alpha$ and EGF, we investigated the PB1-domain scaffolds necessary for aPKC activation in the context of these specific signals. EGF induced/stabilized an aPKC-Par6 complex (Fig. 3.6A). EGFR kinase inhibitor, PI3-K inhibitors or Src-inhibitor that effectively inhibited their targets (Fig. 3.S14), reduced aPKC activation and also reduced aPKC-Par6 co-immunoprecipitation in U87/EGFRvIII (Fig. 3.6B). The effect of aPKC silencing was phenocopied by Par6 silencing, but not p62 silencing, for EGF-induced genes (Fig. 3.6C). In contrast, the NF- κ B signaling was dependent on the adaptor p62. Silencing p62 phenocopied aPKC silencing in the inhibition of NF- κ B signaling (Fig. 3.6D). Furthermore, Par6 and p62 had distinct intracellular localization profiles. Immunofluorescence experiments demonstrated that the majority of cellular Par6 localized with actin at the leading edge of EGF-treated U251/EGFR cells. In contrast, p62 was detected in an intracellular compartment, away from the leading edge, in $\text{TNF}\alpha$ treated U251/EGFR cells (Fig. 3.6E). Therefore, $\text{TNF}\alpha$ and EGF signaling pathways, despite sharing the important downstream kinase aPKC, use alternative PB1-domain scaffold proteins – p62 versus Par6. *In vitro* structural studies indicate that the PB1 scaffolds Par6 and p62 compete for aPKC binding (Hirano et al., 2004; Noda et al., 2003; Wilson, Gill, Perisic, Quinn, & Williams, 2003) and this may explain the specificity of $\text{TNF}\alpha$ and EGF signaling. Interestingly, the constitutively active myr-aPKC ζ indiscriminately activated CD44, MMP9, VCAM, uPAR, IL-1 β , IL-8, MCP-1 and $\text{TNF}\alpha$ (Fig. 3.6F). Taken together, our results show that activation of aPKC is not only indispensable, but also sufficient for the induction of both EGF and $\text{TNF}\alpha$ dependent genes, and that the specificity of these pathways is determined by the differential use of adaptors Par6 and p62.

DISCUSSION

The success of single agent anti-tumor therapy can be limited by downstream mutations or the induction of parallel oncogenic pathways in tumor cells. EGFR gain-of-function accounts for

~45 % of GBM, while the homozygous deletion of *PTEN* leading to downstream PI3-K activation is seen in ~36 % cases and overall PI3-K activation (due to other RTK pathway activation) is seen in ~88 % of GBM (R. McLendon et al., 2008). Cancer cells with mutant EGFR are particularly sensitive to inhibition of NF- κ B, and NF- κ B activation through deletion of I κ B α rescues EGFR-mutant cancer cells from the cytotoxic effects of the EGFR kinase inhibitor erlotinib (Bivona et al., 2011). Our results indicate that a pro-inflammatory microenvironment also increases the therapeutic challenge of targeting GBM tumor intrinsic mutations by providing parallel oncogenic signals (Fig. 3.7). Infiltration of innate immune cells within the GBM tumor mass has been described previously (Badie & Schartner, 2000; N. A. Charles, E. C. Holland, R. Gilbertson, R. Glass, & H. Kettenmann, 2011; Hussain et al., 2006; Parney, Waldron, & Parsa, 2009; Roggendorf, Strupp, & Paulus, 1996a). However, traditionally, GBM is not considered an inflammation-driven tumor and macrophages/activated microglia in GBM have often been described as anti-tumorigenic (Galarneau, Villeneuve, Gowing, Julien, & Vallieres, 2007; Zhang et al., 2009). Here we demonstrate that the interaction of GBM tumor cells with tumor infiltrating myeloid cells leads to paracrine production of TNF α that contributes to tumor growth and spread, and renders EGFR kinase inhibitors less effective. These results are consistent with reports that macrophage/microglia enhance glioma invasion and growth. Microglia, but not oligodendroglia or endothelial cells, has been reported to increase GL261 glioma cell migration *in vitro* (Bettinger, Thanos, & Paulus, 2002; Zhai, Heppner, & Tsirka, 2011). Depletion of macrophage/microglia by treatment with clodronate liposomes in an *ex vivo* organotypic brain slice culture assay also reduced GL261 invasion (Markovic, Glass, Synowitz, Rooijen, & Kettenmann, 2005). *In vivo* deletion of macrophages/microglia in the brain or the inhibition of CSF-1R significantly reduced glioma growth (Coniglio et al., 2012; Markovic et al., 2009; Pyonteck et al., 2013). Additionally, higher grade gliomas, such as GBM and WHO Grade III anaplastic astrocytomas, show the

largest increase in macrophage infiltration, in contrast to lower grade gliomas (Roggendorf et al., 1996a). A recent report has ascribed radio resistance in GBM to $\text{TNF}\alpha/\text{NF-}\kappa\text{B}$ signaling and conversion to a more aggressive, mesenchymal-subtype (Bhat et al., 2013). Thus, targeting the tumor microenvironment can provide unique therapeutic opportunities (Coussens, Zitvogel, & Palucka, 2013; Shiao, Ganesan, Rugo, & Coussens, 2011).

Intriguingly, αPKC has critical roles in distinct, but concurrent oncogenic signaling pathways. It functions downstream of EGFR and RTK signaling in GBM cells. It is also essential for tumor microenvironment-induced $\text{TNF}\alpha/\text{NF-}\kappa\text{B}$ oncogenic signaling in GBM. Altered expression of the kinase αPKC has been reported to be associated with cancer, including GBM (do Carmo, Balca-Silva, Matias, & Lopes, 2013). However, the identity of the αPKC isoforms involved and the mechanism of αPKC function have heretofore remained unclear with frequently contrasting reports. For example, one isoform of αPKC , $\alpha\text{PKC}\zeta$, has been reported to be both upregulated and down regulated in cancer, including specifically in GBM (do Carmo et al., 2013; J. Moscat, Diaz-Meco, & Wooten, 2009a). $\alpha\text{PKC}\iota$, and not $\alpha\text{PKC}\zeta$, is the αPKC isoform detected in most brain regions, except for cerebellum (Parker et al., 2013a). Our analyses reveal that most GBM tumor cell lines, as well as patient-derived xenografts show increased expression of $\alpha\text{PKC}\iota$ protein (fig. S15A,B). Interestingly, αPKC mRNA levels in GBM were not increased in comparison to normal human astrocytes, suggesting that αPKC expression in GBM is regulated through post-translational mechanisms (fig. S15D,E). Targeting the bi-modal activity of αPKC in tumor cell autonomous and non-tumor cell autonomous signaling may provide a paradigm that affords simultaneously disabling of tumor intrinsic, as well as microenvironment-induced oncogenic signals in GBM.

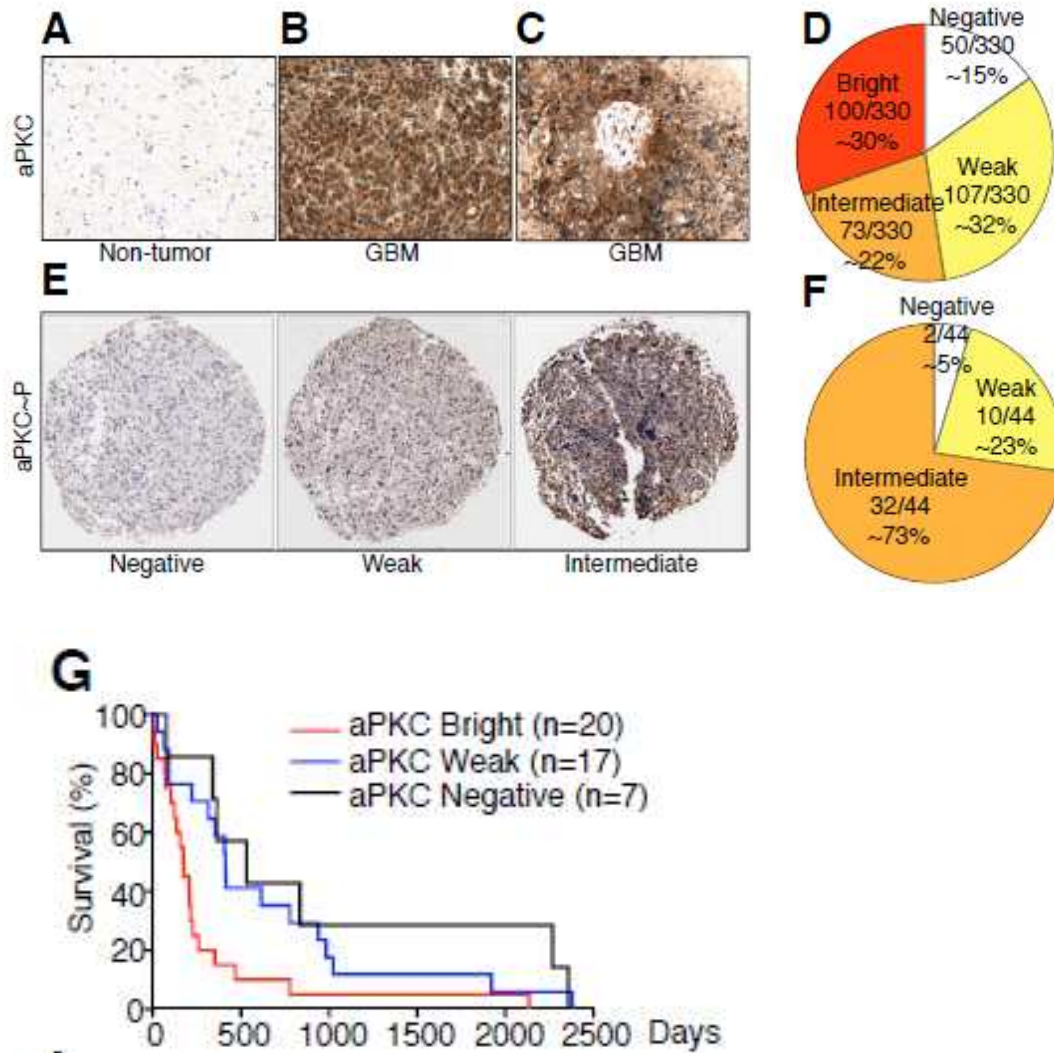


Figure 3.1. Clinical association and therapeutic efficacy of targeting aPKC in mouse models of GBM. (A) Representative example of non-tumor brain parenchyma shows low aPKC staining, while (B,C) aPKC staining is increased in GBM. (D) Stratification of 330 GBM cases according to immunohistochemical scores of aPKC. (E) Representative examples of aPKC phosphoThr410/403 staining in GBM tissue microarray. (F) Stratification of 44 GBM cases according to immunohistochemical scores of aPKC phosphoThr410/403 staining. (G) Kaplan-Meier survival curve of 44 GBM cases showing correlation of bright aPKC staining with poor survival in human patients ($p=0.0145$).

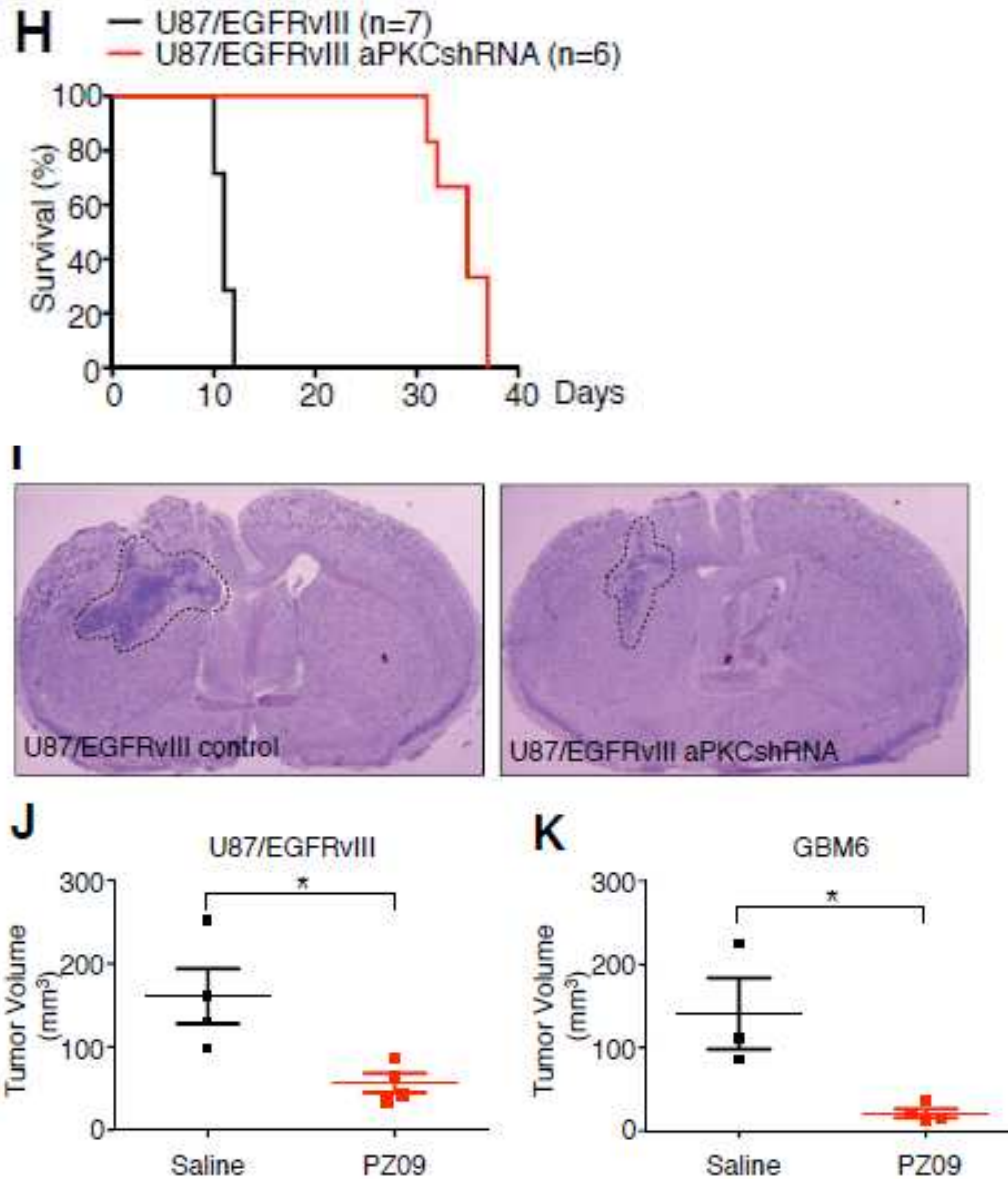


Figure 3.1, cont. (H) Kaplan-Meier survival curves of mice bearing U87/EGFRvIII intracranial xenografts stably transfected with control or aPKCshRNA ($p=0.0005$). (I) Representative images of transplanted U87/EGFRvIII control and U87/EGFRvIII aPKCshRNA tumors after 6 days post-implantation. Dashed lines circumscribe the tumor areas. Tumor volume quantification from U87/EGFRvIII (J) or EGFR kinase inhibitor-insensitive GBM6 (K) intracranial xenografts infused with 10 μ M PZ09 through an Alzet osmotic minipump for 7 and 14 days respectively, beginning 3 days post tumor implantation. Data are presented as representative individual samples or as mean \pm SEM of at least 3 independent samples per group. * $p < 0.05$.

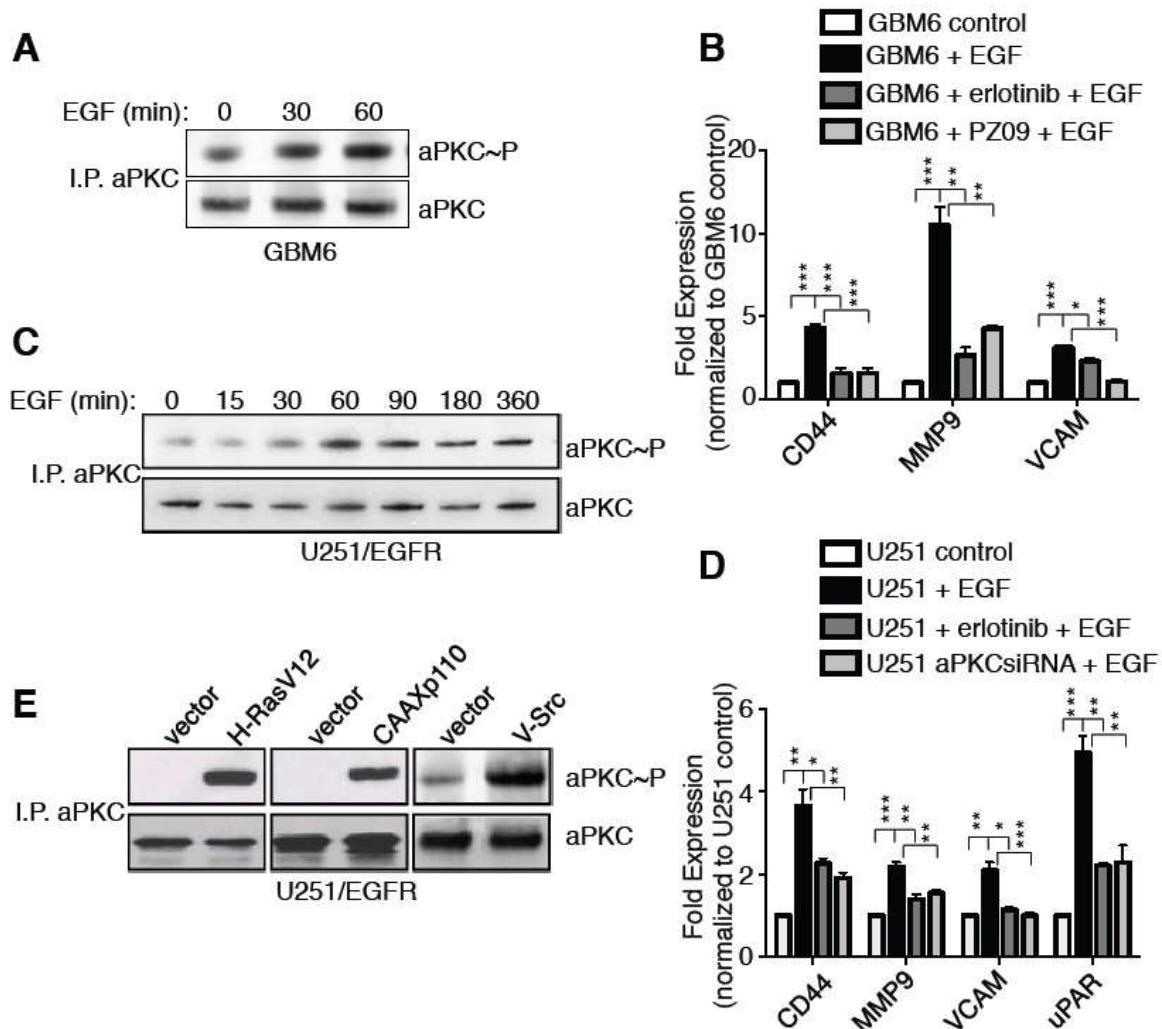


Figure 3.2. aPKC is activated downstream of tumor-intrinsic oncogenic RTK signaling pathways. (A) Activation of aPKC in GBM6 cells after 100 ng/mL EGF treatment for the indicated times. Active aPKC was detected after aPKC immunoprecipitation followed by aPKC phosphoThr410/403 immunoblotting. Total aPKC is shown as loading control. (B) Expression of indicated genes in GBM6 cells upon treatment with 100 ng/mL EGF treatment alone or in the presence of 10 μ M of PZ09 or 10 μ M of erlotinib (30 min pretreatment) for 6 h, as detected by RT-qPCR and normalized to GBM6 control. (C) Activation of aPKC in U251/EGFR cells after 100 ng/mL EGF treatment for the indicated times. Total aPKC is shown as loading control. (D) Expression of indicated genes in U251/EGFR cells, U251/EGFR cells treated with 10 μ M of erlotinib (30 min pretreatment) or in U251/EGFR cells treated with aPKC siRNA, upon treatment with 100 ng/mL EGF treatment for 6 h, as detected by RT-qPCR and normalized to U251/EGFR control. (E) Activation of aPKC in U251/EGFR cells after 48 h of transfection with vector alone or active Ras (H-RasV12), active PI3K (CAAXp110), or active Src (v-Src). Total aPKC is shown as loading control. Data are presented as representative images or as mean \pm SEM of at least 3 independent experiments. * p < 0.05, ** p < 0.01, *** p < 0.001.

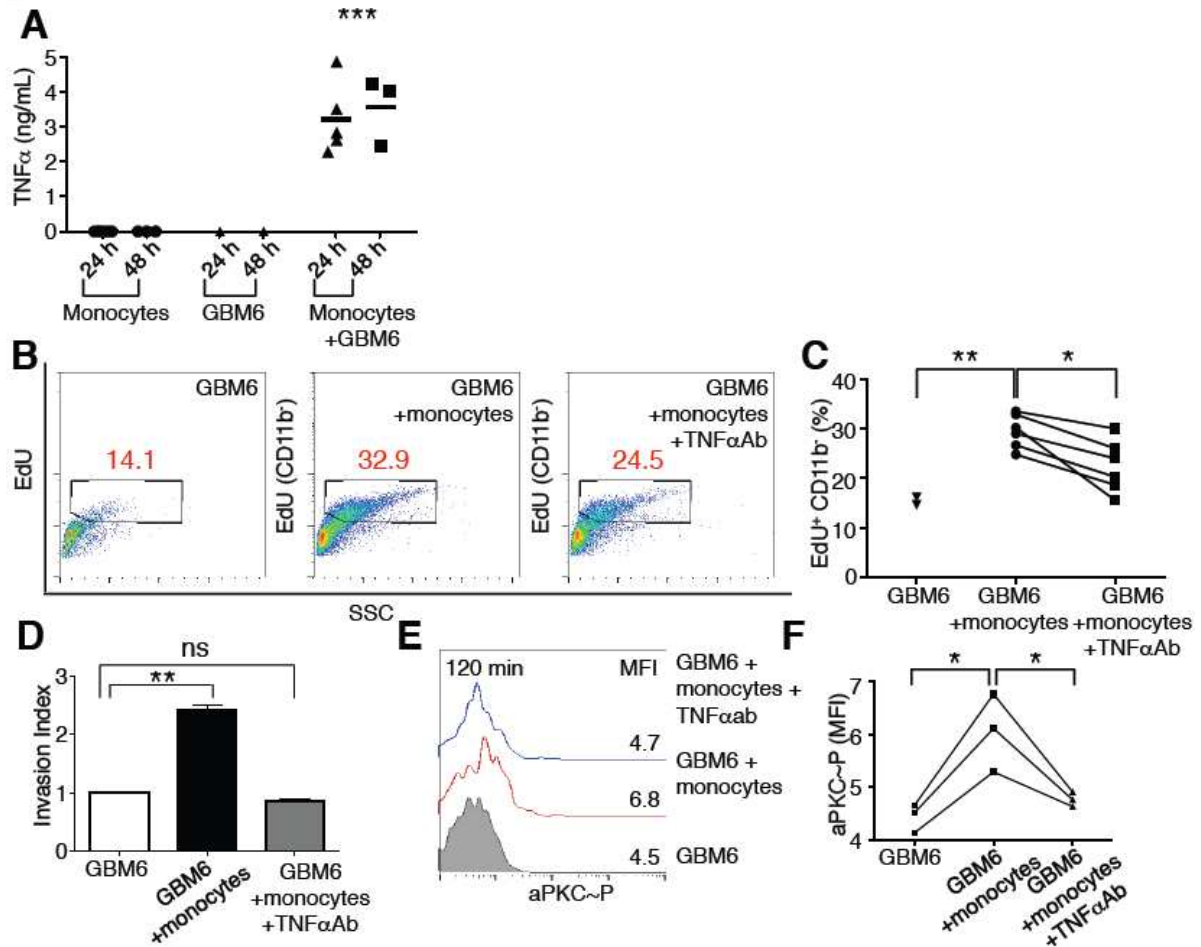


Figure 3.4. Myeloid cell-derived TNF α promotes GBM proliferation, invasion and EGFR kinase inhibitor resistance and correlates with aPKC activation. (A) Concentration of TNF α in conditioned media from monocytes, GBM6 cells, or GBM6 cells co-cultured with monocytes, as detected by ELISA. (B) Representative FACS analysis and (C) percentage (%) of EdU incorporation in GBM6 cells alone, GBM6 co-culture with monocytes in the presence of 100 ng/mL monoclonal anti-human-TNF α antibody or an isotype control at 24 h. (D) Invasion Indices of GBM6 plus monocytes in the presence of 100 ng/mL monoclonal anti-human-TNF α antibody or isotype control. (E) Representative FACS histograms and (F) mean fluorescence intensity (MFI) of aPKC Thr560 phosphorylation in GBM6 cells alone, upon co-culture with monocytes in the presence of an isotype control antibody or upon co-culture with monocytes in the presence of monoclonal anti-human-TNF α antibody.

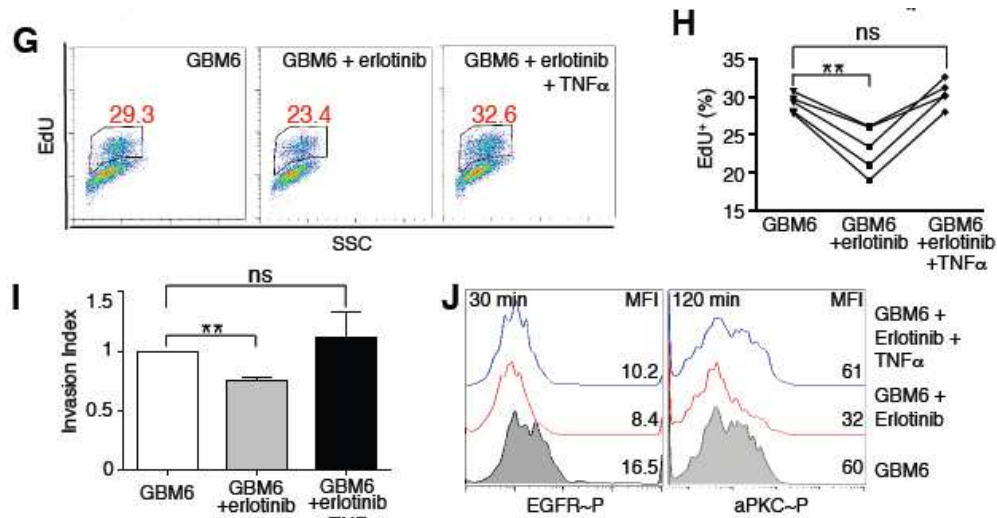


Figure 3.4, cont. (G) Representative FACS analysis and (H) percentage (%) of EdU incorporation in GBM6 cells alone, or in the presence of 10 μ M erlotinib alone or together with 10 ng/mL TNF α at 24 h. (I) Invasion indices of GBM6 alone, plus 10 μ M erlotinib and plus 10 μ M erlotinib and 10 ng/mL TNF α . (J) Representative FACS histograms of EGFR Tyr1086 phosphorylation (left) and aPKC Thr560 phosphorylation (right) in GBM6 cells alone, or in the presence of 10 μ M erlotinib alone or together with 10 ng/mL TNF α . Data are presented as representative individual samples or as mean \pm SEM of at least 3 independent samples per group. *p < 0.05, **p < 0.01, ***p < 0.001.

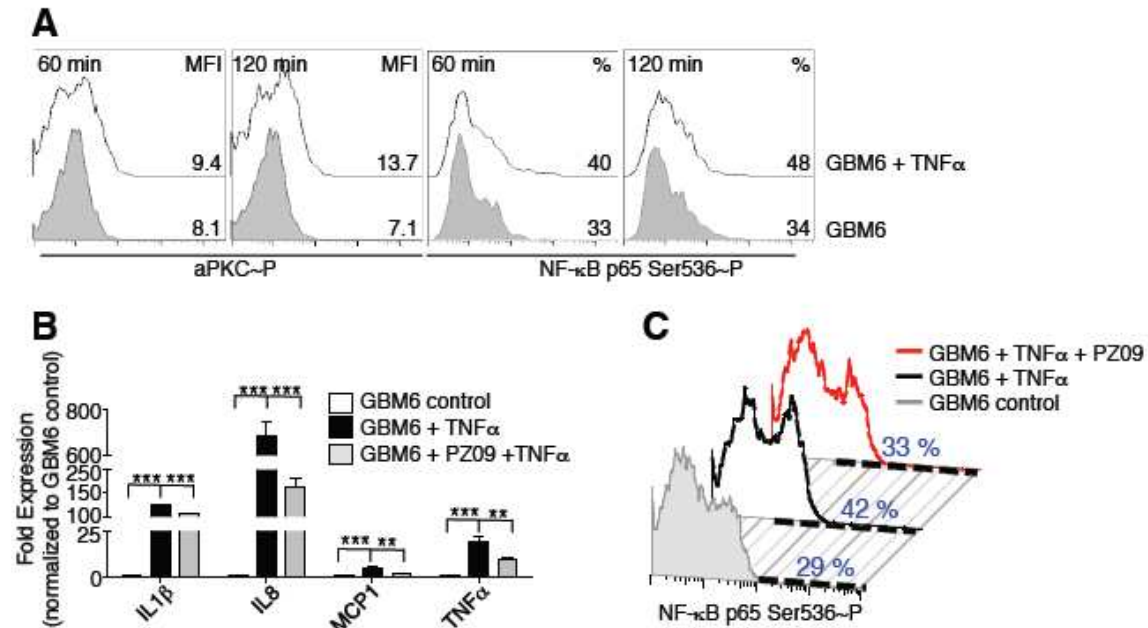


Figure 3.5. TNFα-induced NF-κB signaling in GBM is dependent on aPKC. (A) Representative FACS histograms of aPKC Thr560 phosphorylation (left) and NF-κB p65 Ser536 phosphorylation (right) at the indicated times in GBM6 cells or GBM6 cells treated with 10 ng/mL TNFα. (B) Expression of NF-κB target genes in GBM6 cells upon treatment with 10 ng/mL TNFα alone or in the presence of 10 μM of PZ09 for 1 h, as detected by RT-qPCR. mRNA levels were normalized to GBM6 control. (C) FACS analysis of phosphoSer536 p65 in GBM6 cells left untreated or treated with 10 ng/mL TNFα for 1 h in the presence or absence of 10 μM PZ09.

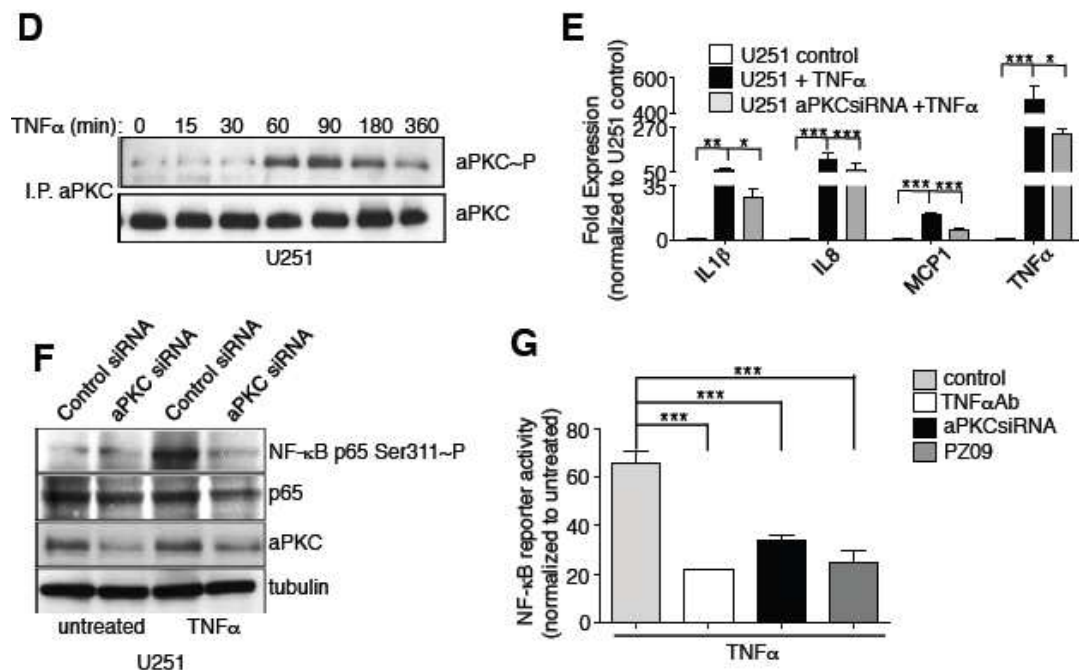


Figure 3.5, cont. (D) Activation of aPKC in U251/EGFR cells treated with 10 ng/mL TNF α for the indicated times. (E) Expression of NF- κ B target genes in U251/EGFR cells or U251/EGFR cells treated with aPKC siRNA, upon treatment with 10 ng/mL TNF α for 1 h, as detected by RT-qPCR. mRNA levels were normalized to U251/EGFR control. (F) phosphoSer311 p65 immunoblots from U251/EGFR control or aPKC siRNA transfected cells after 10 ng/mL TNF α treatment for 1 h. Total p65 and β -tubulin immunoblots were used as loading controls and aPKC antibodies show the extent of aPKC silencing. (G) NF- κ B fluorescent reporter activity following 30 min of incubation with 10 ng/mL TNF α in U251/EGFR cells alone or in the presence of 100 ng/mL anti-human TNF α antibody, U251/EGFR transfected with aPKC siRNA or U251/EGFR in the presence of 10 μ M PZ09.

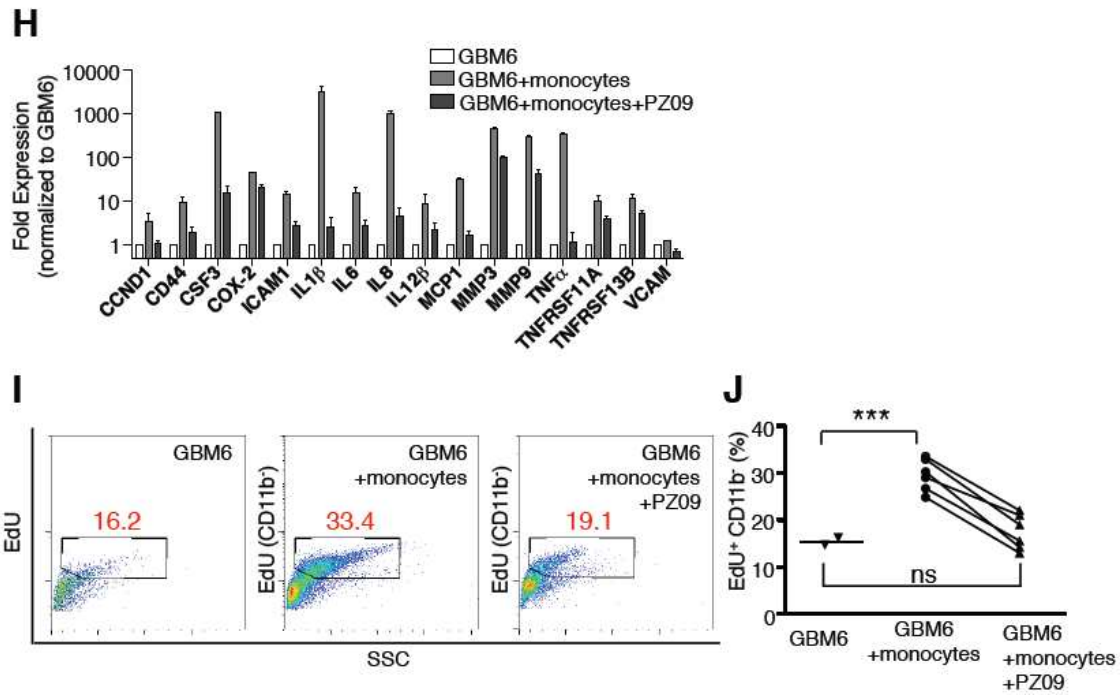


Figure 3.5, cont. (H) Expression of NF- κ B target genes in GBM6 alone, GBM6 exposed to monocyte co-culture media and exposed to co-culture media in the presence of 10 μ M PZ09, as detected by RT-qPCR and normalized to GBM6 alone samples. (I) Representative FACS analysis and (J) percentage (%) of EdU incorporation in GBM6 cells alone or when co-cultured with monocytes for 24 h, with or without 10 μ M PZ09.

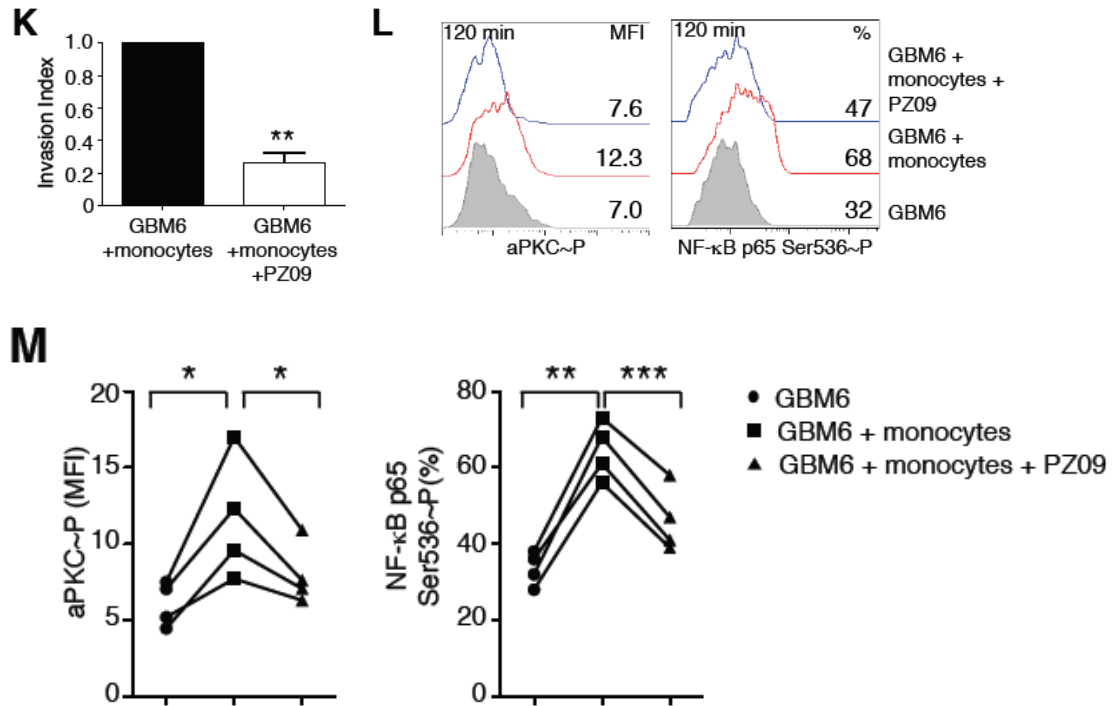


Figure 3.5, cont. (K) Invasion indices of GBM6 cells alone or when co-cultured with monocytes with or without 10 μ M PZ09. (L) Representative FACS histograms and (M) mean fluorescence intensity (MFI) of aPKC Thr560 phosphorylation (left) and NF- κ B p65 Ser536 phosphorylation in GBM6 cells alone or when co-cultured with monocytes with or without 10 μ M PZ09. Data are presented as representative images or as mean \pm SEM of at least 3 independent samples per group. * p < 0.05, ** p < 0.01, *** p < 0.001.

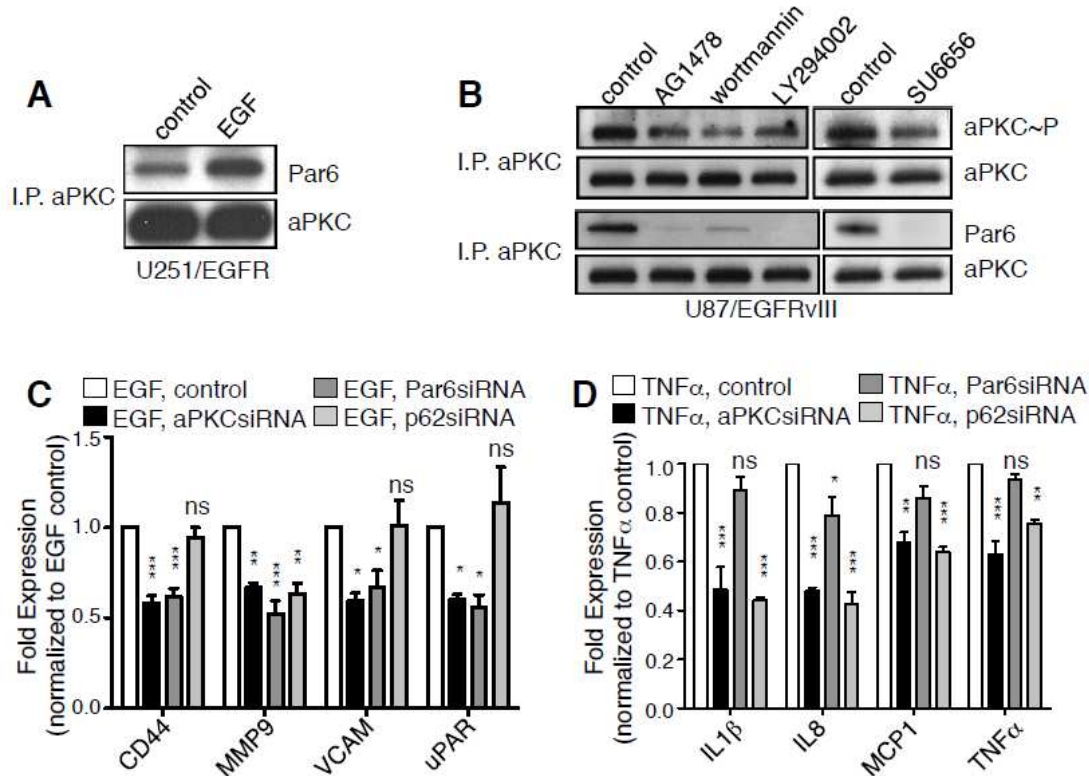


Figure 3.6. Bimodal function of aPKC in EGF and TNF α induced-signaling in GBM cells. (A) Co-immunoprecipitation of Par6 with aPKC in serum-starved U251/EGFR cells after treatment with 100 ng/mL EGF for 6 h. aPKC was immunoprecipitated and immunoblots were sequentially probed with Par6 and aPKC antibodies. Total aPKC is shown as loading control. (B) Activation of aPKC (top panel) and co-immunoprecipitation of Par6 (bottom panel) in U87/EGFRvIII cells grown in serum after incubation with 10 μ M AG1478, 100 nM wortmannin, 20 μ M LY294002 or 10 μ M SU6656 for 30 min. Total aPKC is shown as loading control. aPKC was immunoprecipitated and immunoblots were sequentially probed with phospho-aPKC Thr410/403 and aPKC or Par6 and aPKC antibodies. (C) Expression of indicated genes after treatment with 100 ng/mL EGF for 6 h in U251/EGFR control cells or transfected with aPKC, Par6 or p62 siRNA, as determined by RT-qPCR. Expression was normalized to EGF treated U251/EGFR control samples. (D) Expression of indicated genes after treatment with 10 ng/mL TNF α for 1 h in U251/EGFR control cells or transfected with aPKC, Par6 or p62 siRNA, as determined by RT-qPCR. Expression was normalized to TNF α treated U251/EGFR control samples.

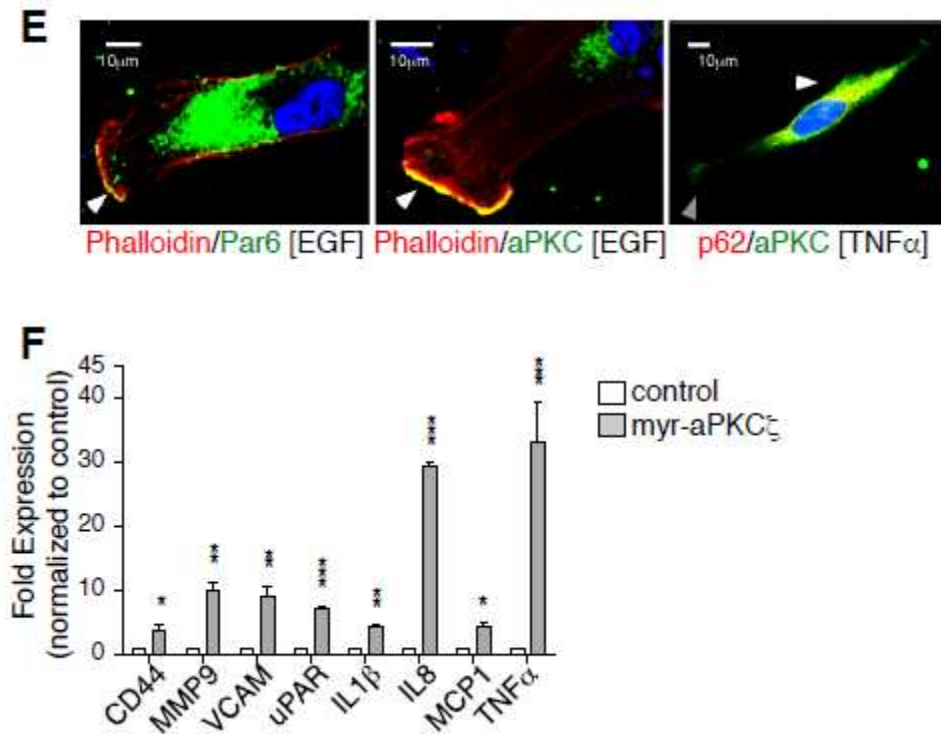


Figure 3.6, cont. (E) Representative images showing the co-localization of aPKC and Par6 with phalloidin at the lamellipodia after EGF stimulation for 6 h in U251/EGFR cells (white arrows, left and middle panels), and co-localization of aPKC and p62 in the intracellular compartment after TNF α treatment for 1 h (white arrows, right panel). Some aPKC was detectable at the lamellipodia of the cells (grey arrow). (F) Expression of indicated genes in U251/EGFR cells 48 h after myr-aPKC ζ transfection, as determined by RT-qPCR. Expression was normalized to mRNA level in U251/EGFR. Data are presented as representative images or as mean \pm SEM of at least 3 independent experiments. * $p < 0.05$, ** $p < 0.01$, *** $p < 0.001$, ns is non-significant.

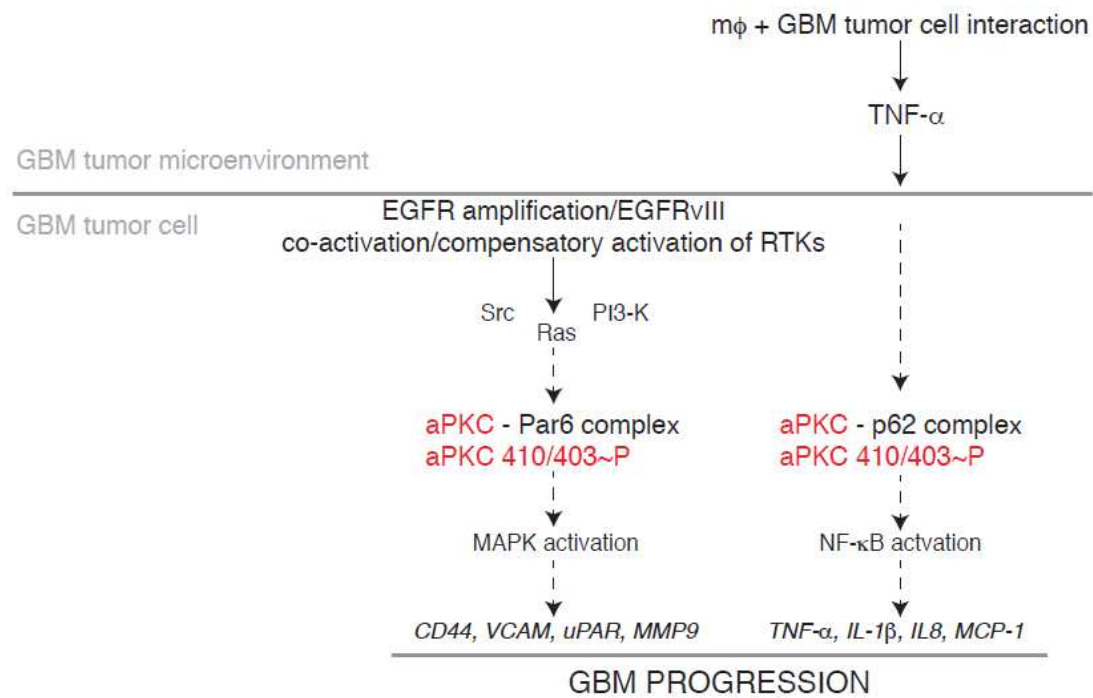


Figure 3.7. Schematic illustrating aPKC-containing signaling complexes in cell autonomous RTK and non cell-autonomous TNF α /NF- κ B oncogenic signaling in GBM.

Table 3.S1.

List of primers

Primer (RT-qPCR)	Forward	Reverse
<i>PRKCI</i>	CACTCCAGATGACGATGACATTG	TGCAGACATCAAAAGAGGATTGA
<i>PRKCZ</i>	CGCTCCCCGTTTCGACAT	CCAGGATCAGGAAAAGGT
<i>ACTB</i>	TCCCTGGAGAAGAGCTACG	GTAGTTTCGTGGATGCCACA
<i>CD44</i>	CCCATCCCAGACGAAGACAG	ACCATGAAAACCAATCCCAGG
<i>COX2</i>	TTAATGAGTACCGCAAACGC	ACCAGAAGGGCAGGATACAG
<i>GAPDH</i>	TGCACCACCAACTGCTTAGC	GGCATGGACTGTGGTCATGAG
<i>IL1β</i>	TTCTGCTTGAGAGGTGCTGA	CTGTCCTGCGTGTTGAAAGA
<i>IL6</i>	TGAACTCCTTCTCCACAAGCG	TCTGAAGAGGTGAGTGGCTGTC
<i>IL8</i>	TTTTGCCAAGGAGTGCTAAAG	AACCCTCTGCACCCAGTTTTTC
<i>MCP1</i>	GCTCGCTCAGCCAGATGCA	GGACACTTACTGCTGGTGATT
<i>MMP9</i>	CATTCGACGATGACGAGTTG	CGGGTGTAGAGTCTCTCGC
<i>PARD6A</i>	AGCATCGTCGAGGTGAAGAG	GTATAGCCAAGTAGCACGTCC
<i>PARD6B</i>	GTTGACGTTTTGGTAGGCTATGC	AGTGGATTGGCCGTTGAAACA
<i>P62/SQSTM1</i>	AAGCCGGGTGGGAATGTTG	CCTGAACAGTTATCCGACTCCAT
<i>TNFα</i>	ATGAGCACTGAAAGCATGATC	GAGGGCTGATTAGAGAGAGGT
<i>PLAUR</i>	ACCCATGGTCTTCCATTTGA	GTTGCACCAGTGAATGTTGG
<i>VCAM</i>	TCCACGCTGACCCTGAGCCC	GCTCCCATTCACGAGGCCACC
<i>EGFRvIII-1</i>	GAGCTCTTCGGGGAGCAG	GTGATCTGTCACCACATAATTACCTT TCT
<i>EGFRvIII-2</i>	GGCTCTGGAGGAAAAGAAAGGT AAT	TCCTCCATCTCATAGCTGTCTG
<i>EGFR</i> total	TTGCCGCAAAGTGTGTAACG	GTCACCCCTAAATGCCACCG
Primer (sequencing)		
<i>NFKBIA-1</i>	CTCCGAGACTTTTCGAGGAAATAC	GCCATTGTAGTTGGTAGCCTTCA
<i>NFKBIA-2</i>	GCGCCCCAGCGAGGAAGCA	CAATAAATATAAAATGTGGTCCTTCC
Primer (RT-PCR)		
<i>EGFR</i>	CTTCGGGGAGCAGCGATGCGAC	ACCAATACCTATTCCGTTACAC

Table 3.S2.

List of siRNA and shRNA Sequences

siRNA	Source	siRNA ID	Sequence
Stealth siRNA <i>Prkcz</i> D1	Invitrogen	VHS41530	5'-GCUGGUGCAUGAUGACGAGGAUAAU-3' 5'-AAUAUCCUCGUCAUCAUGCACCAGC-3'
Stealth siRNA <i>Prkcz</i> D2	Invitrogen	VHS41533	5'-GGGUACAGACAGAGAAGCACGUGUU-3' 5'-AACACGUGCUUCUCUGUCUGUACCC-3'
Stealth siRNA <i>Pard6A</i>	Invitrogen	HSS147208	5'-AGGUCUUCGCGGCUACUUCUAAUGCC-3' 5'-GGCAUUGAAGUAGCCGGGAAGACCU-3'
Stealth siRNA <i>Pard6B</i>	Invitrogen	HSS150023	5'-AUCAUUAACAGCUAAUAGUCCUGUA-3' 5'-UACAGGACUAAUAGCUGUAAUGAU-3'
Stealth siRNA <i>p62/SQSTM1</i>	Invitrogen	HSS113116	5'-AGAAGUGGACCCGUCUACAGGUGAA-3' 5'-UUCACCUAGUAGACGGGUCCACUUCU-3'
Stealth siRNA <i>p62/SQSTM1</i>	Invitrogen	HSS113117	5'-CAGGCUCCUGCAGACCAAGAACUAU-3' 5'-AUAGUUCUUGGUCUGCAGGAGCCUG-3'
GIPZ Human <i>Prkcz</i> shRNA	Open Biosystems	V3LHS_635000	5'-ACAGCTTCCTCCATCTTCT-3' sense 5'-AGAAGATGGAGGAAGCTGT-3' antisense

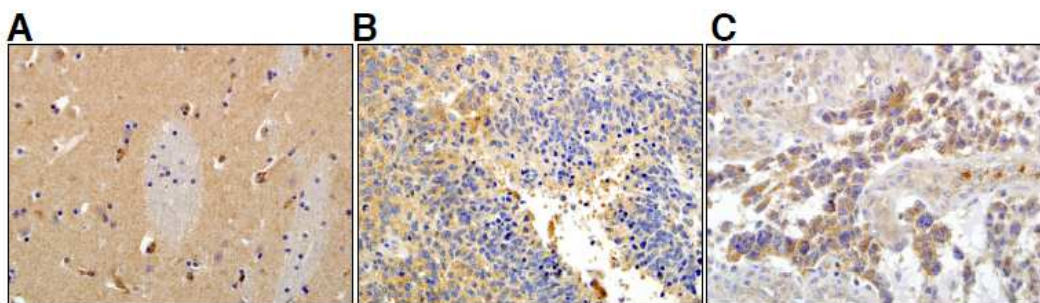


Figure 3.S1. aPKC expression in non-tumor brain and in histologically characteristic regions of GBM. Representative images of aPKC staining in (A) normal basal ganglia, (B) regions of pseudopalisading necrosis in GBM and (C) microvascular proliferation in GBM.

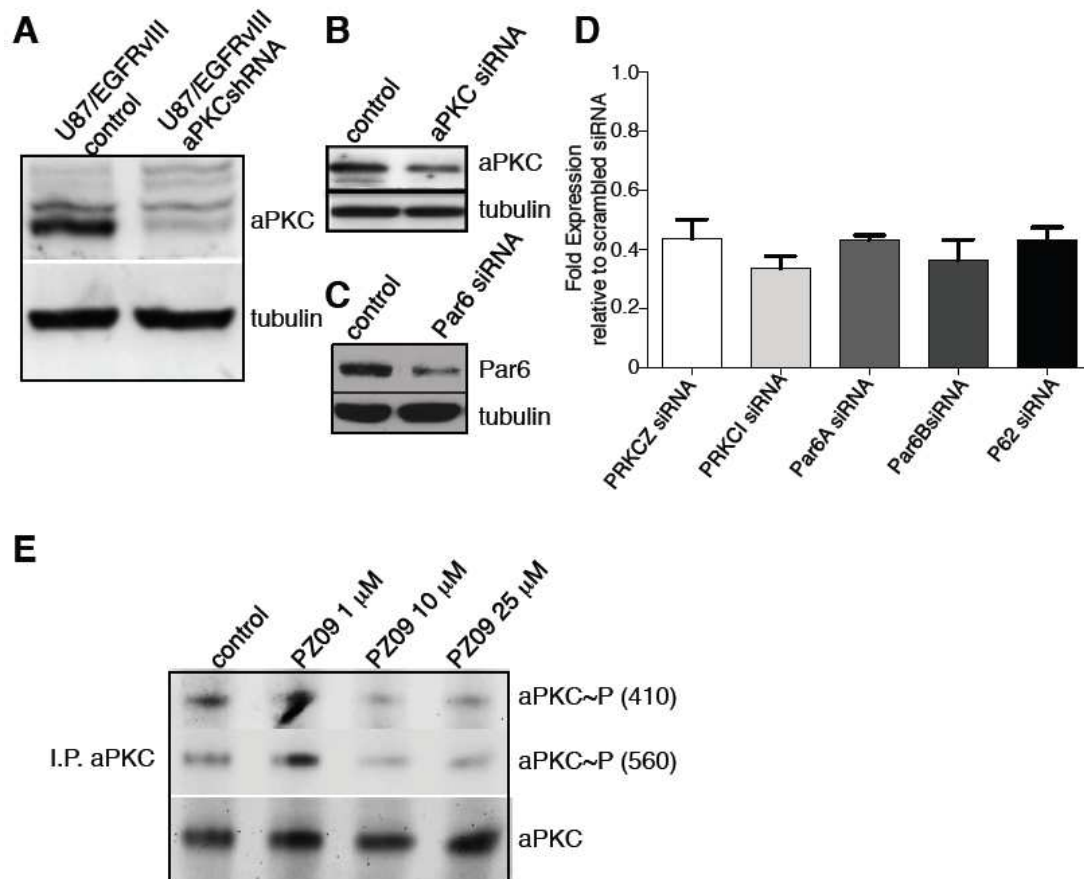


Figure 3.S2. Validation of aPKC knockdown efficiencies and PZ09 inhibitory effect. (A) Immunoblots of aPKC expression in U87/EGFRvIII control cells and U87/EGFRvIIIaPKCshRNA cells used for *in vivo* intracranial orthotopic xenograft experiments. (B) Immunoblots of aPKC expression in U251/EGFR cells transfected with luciferase or aPKC siRNA. (C) Immunoblot of Par6 expression in U251/EGFR cells transfected with luciferase or Par6 siRNA. (D) Graphical representation of knockdown efficiencies in U251/EGFR cells for each indicated genes, normalized to control (luciferase) siRNA, as measured by RT-qPCR. (E) Inhibition of aPKC activation in GBM6 with increasing concentration of PZ09 detected after aPKC immunoprecipitation followed by aPKC phosphoThr410/403 or phosphoThr560 immunoblotting. Blots were stripped and reprobed with aPKC antibodies for loading control. Data are presented as representative images or as mean \pm SEM of at least 3 independent experiments.

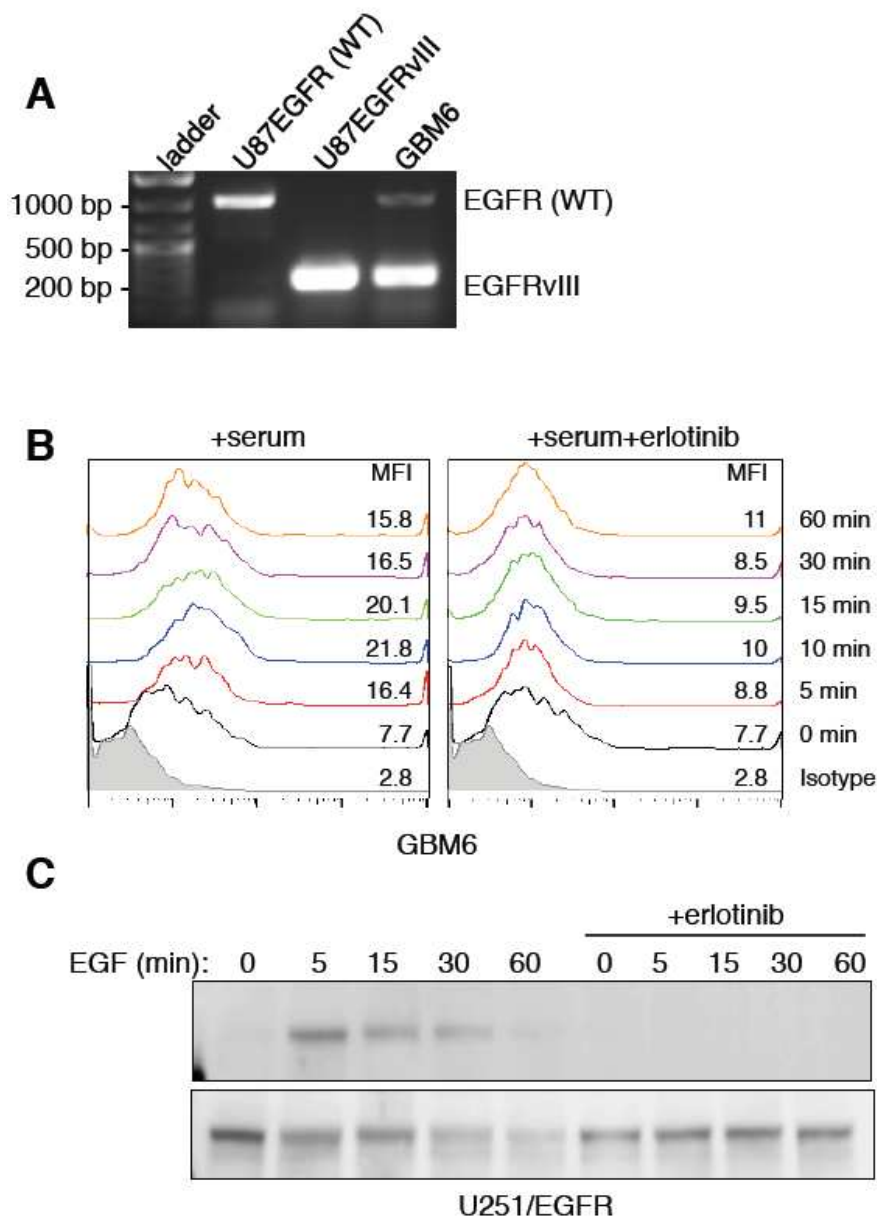


Figure 3.S3. EGFR isoforms expression in GBM6 and EGFR phosphorylation kinetics in GBM6 and U251/EGFR. (A) Expression of EGFR WT and EGFRvIII in GBM6 as detected by RT-PCR. U87EGFR (WT) and U87EGFRvIII were included as positive controls. (B) Representative FACS histograms of EGFR phosphorylation (p-Y1086) kinetics in GBM6. Serum was used to stimulate serum-starved GBM6 cells or serum-starved GBM6 cells pretreated for 30 min with 10 μ M erlotinib. (C) Representative immunoblots for EGFR phosphorylation (p-Y1086) in serum-starved U251/EGFR cells at various time points as indicated after stimulation with 100 ng EGF alone or 100 ng EGF after 30 min pre-treatment with 10 μ M erlotinib. Data are presented as representative images of at least 3 independent experiments.

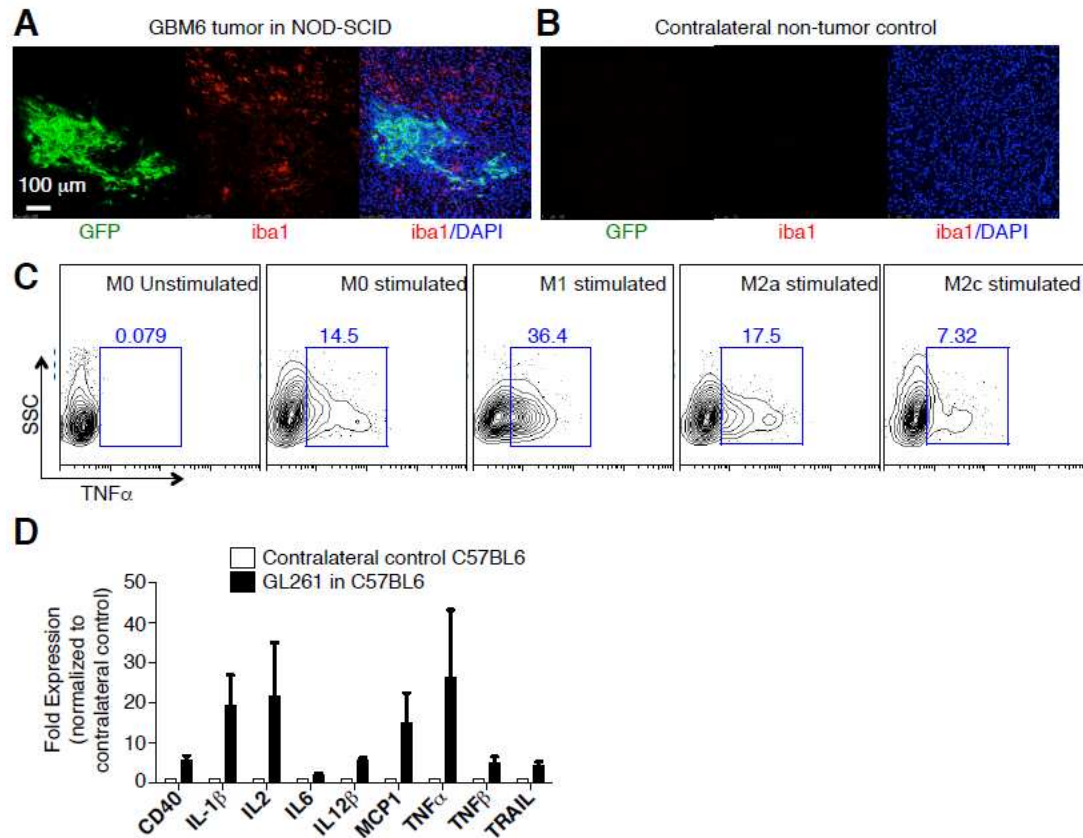


Figure S3.4. Myeloid cells, TNF α production and NF- κ B activation in mouse models of GBM. (A) Representative images of Iba1 staining of NOD/SCID mouse brain bearing GFP+ U87vIII/EGFR tumors in comparison to (B) contralateral, non-tumor bearing brain. (C) Representative FACS analysis of TNF α production by unstimulated human monocyte-derived macrophages (M0) and M0, M1, M2a or M2c stimulated with Ionomycin/PMA. (D) Expression of NF- κ B target genes in acutely isolated tissue from the side of C57BL/6 mouse brain bearing GL261 tumors in comparison to contralateral, non-tumor bearing brain as detected by RT-qPCR. Data are presented as representative images or as mean \pm SEM of at least 3 independent experiments.

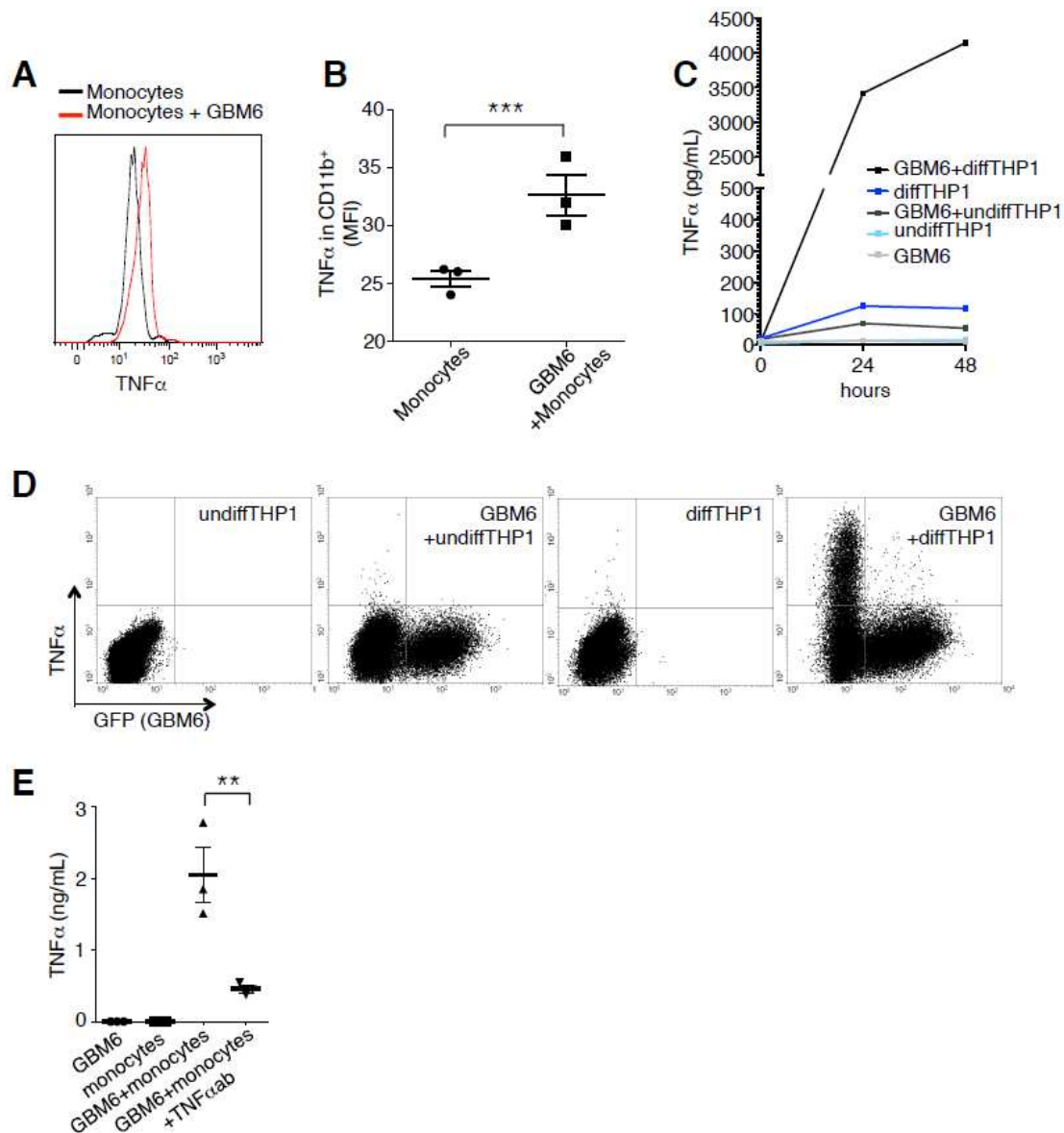


Figure 3.S5. TNFα is produced by myeloid cells when in contact with GBM cells. (A) Representative FACS analysis and (B) mean fluorescence intensity (MFI) of TNFα expression in CD11b⁺ human monocytes upon culture with GBM6 cells. (C) TNFα concentration as measured by ELISA in conditioned media from GBM6 cells alone, THP1 cells alone, or indicated cells upon co-culture. (D) Representative FACS analysis of TNFα from undifferentiated or differentiated THP1 cells upon culture with or without GBM6 cells expressing GFP. (E) TNFα concentration as measured by ELISA in conditioned media from GBM6 cells, monocytes, GBM6 co-cultured with monocytes alone or in the presence of 100 ng/mL of TNFα neutralizing antibody. Data are presented as representative plots or as mean ± SEM of at least 3 independent experiments. *p < 0.01, ***p < 0.001.

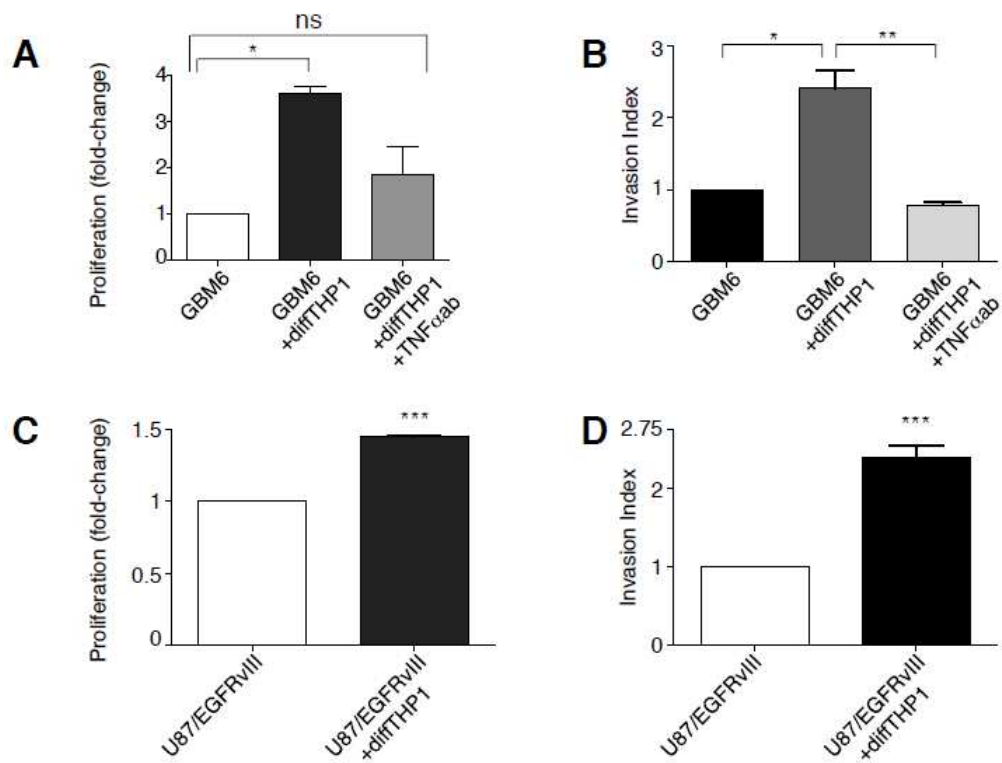


Figure 3.S6. Human myeloid cell-derived TNF α contributes to increased GBM proliferation and invasion. (A) Proliferation of GBM6 cells upon culture with differentiated THP1 cells in the presence of isotype control or neutralizing monoclonal anti-TNF α antibody and normalized to the proliferation of GBM6 alone. (B) Invasion indices of GBM6 cells upon culture with differentiated THP1 cells in the presence of isotype control or neutralizing monoclonal anti-TNF α antibody and normalized to invasion index of GBM6 cells alone. (C) Proliferation of U87/EGFRvIII cells upon culture with differentiated THP1 cells and normalized to control. (D) Invasion indices of U87/EGFRvIII cells upon culture with differentiated THP1 cells and normalized to control. Data are presented as mean \pm SEM of at least 3 independent experiments. *p < 0.05, **p < 0.01, ***p < 0.001, ns is non-significant.

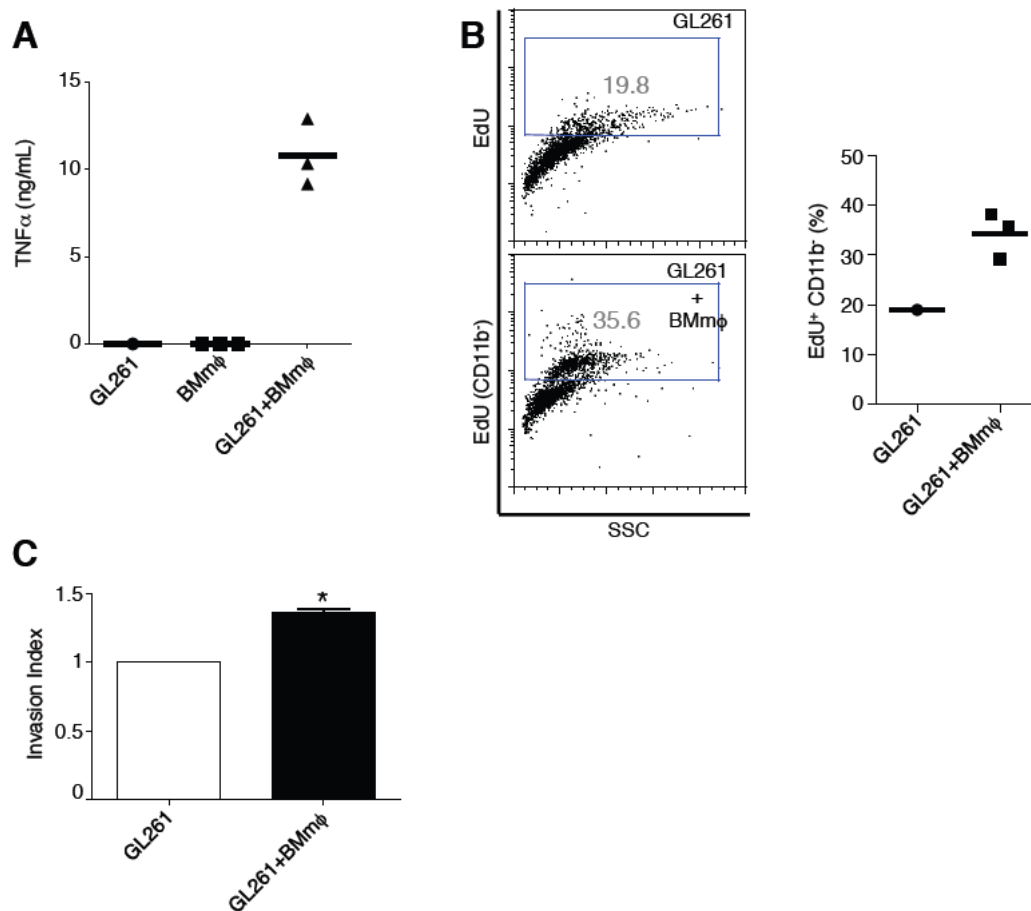


Figure 3.S7. Murine myeloid cell-derived TNF α contributes to increased GBM proliferation and invasion. (A) TNF α concentration as measured by ELISA in culture media of GL261 cells alone, primary mouse macrophages alone, or GL261 cells upon culture with primary mouse macrophages. (B) Representative FACS analysis (left panel) and percentage (%; right panel) of EdU incorporation in GL261 cells upon culture with primary mouse macrophages. (C) Invasion index of GL261 cells upon culture with primary mouse macrophages. *p < 0.05.

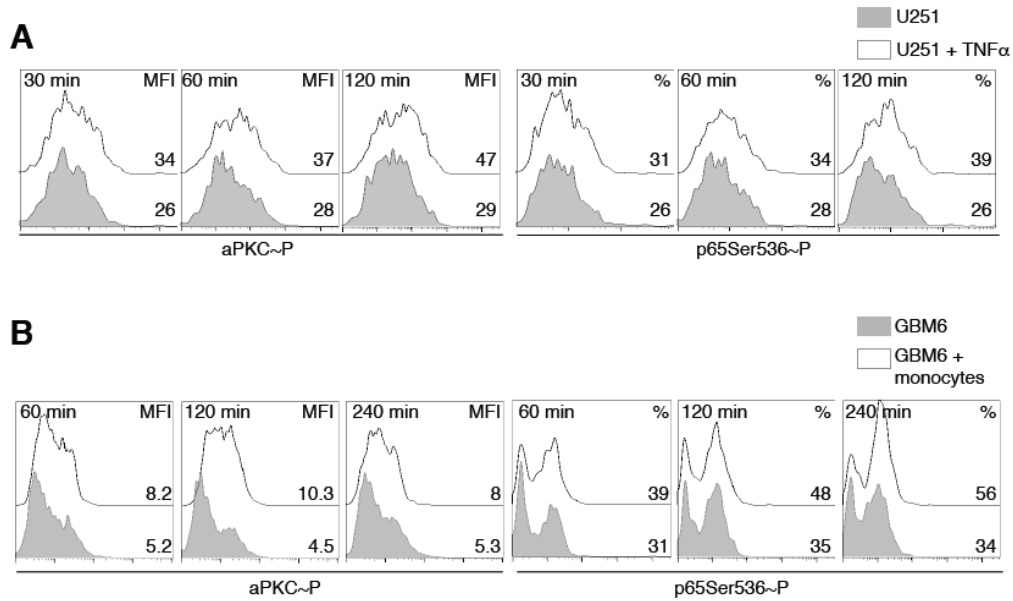


Figure 3.S8. Phosphorylation of aPKC precedes phosphorylation of p65. (A) Representative FACS histograms of aPKC Thr560 (left) and NF- κ B p65 Ser536 (right) phosphorylation at the indicated times in U251 cells alone and upon stimulation with 10 ng/mL TNF α . (B) Representative FACS histograms of aPKC Thr560 (left) and NF- κ B p65 Ser536 (right) phosphorylation in GBM6 cells alone and upon coculture with monocytes at the indicated time points. Data are presented as representative histograms of at least 3 independent experiments.

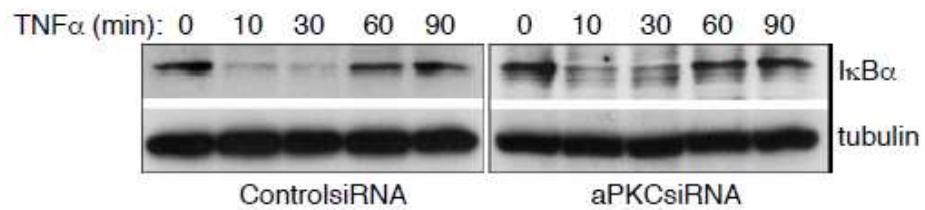


Figure 3.S9. TNF α induced I κ B α degradation is not affected by aPKC silencing. Immunoblot of I κ B α in control U251/EGFR (controlsRNA) cells or U251/EGFR cells in which aPKC expression has been silenced (aPKCsiRNA) after 10 ng/mL TNF α treatment for the indicated times. β -tubulin blotting was used for loading control.

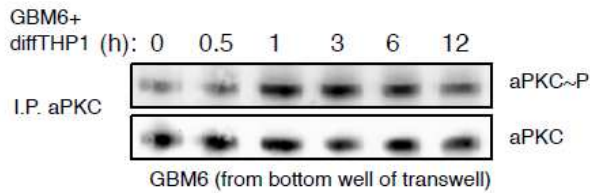
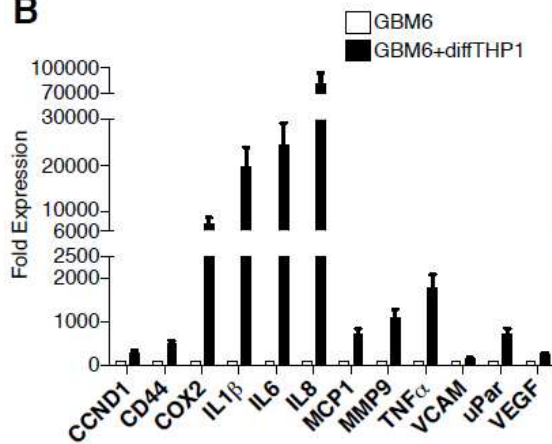
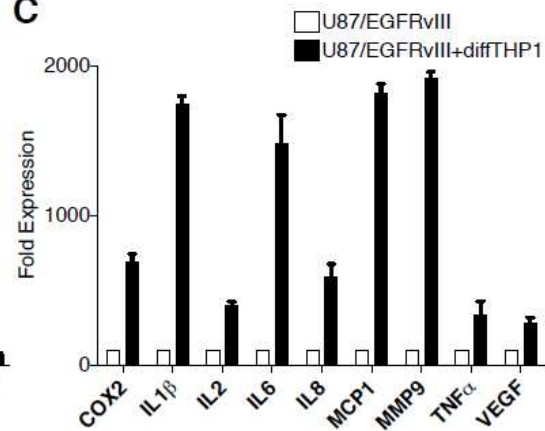
A**B****C**

Figure 3.S10. Activation of aPKC and induced NF- κ B gene signature in GBM cells upon coculture with myeloid cells. (A) GBM6 cells were grown on the bottom compartment of a transwell culture system and GBM6 together with differentiated THP1 cells were co-cultured on the top for the indicated times. Active aPKC in GBM6 from the bottom compartment at the indicated times was detected after aPKC immunoprecipitation followed by aPKC phosphoThr410/403 immunoblotting. Total aPKC is shown as loading control. (B) Expression of indicated genes in GBM6 cells and (C) U87/EGFRvIII cells upon culture with differentiated THP1 cells for 24 h as measured by RT-qPCR. GBM6 cells or U87/EGFRvIII cells were grown on the bottom compartment of a transwell culture system and GBM6 or U87/EGFRvIII cells together with differentiated THP1 cells were co-cultured on the top for the indicated times. Data are presented as representative images or as mean \pm SEM of at least 3 independent experiments.

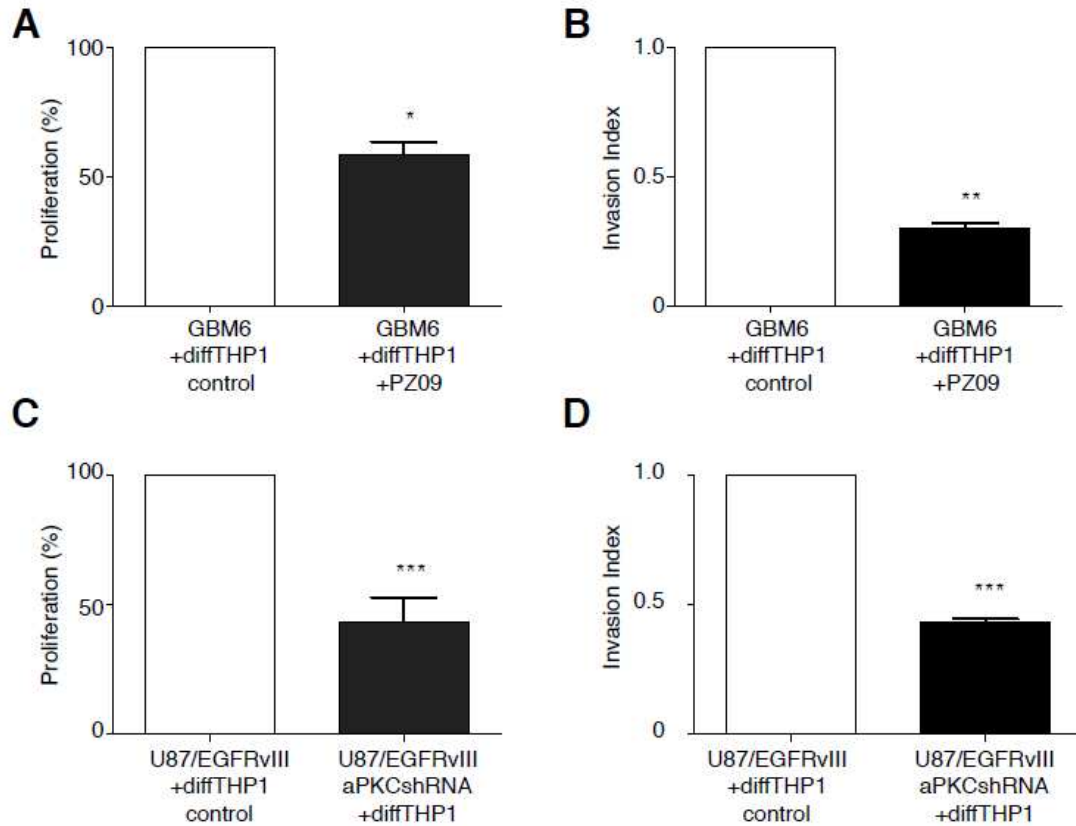


Figure 3.S11. Myeloid cell-induction of GBM proliferation and invasion is dependent on aPKC . (A) Proliferation (percentage) of GBM6 cells upon culture with THP1 cells in the presence or absence of 10 μ M PZ09. (B) Invasion indices of GBM6 cells upon culture with THP1 cells in the presence or absence of 10 μ M PZ09. (C) Proliferation (percentage) of U87/EGFRvIII cells or U87/EGFRvIII-aPKCshRNA cells upon culture with differentiated THP1 cells. (D) Invasion indices of U87/EGFRvIII cells or U87/EGFRvIII-aPKCshRNA cells upon culture with differentiated THP1 cells. Data are presented as mean \pm SEM of at least 3 independent experiments. * $p < 0.05$, ** $p < 0.01$, *** $p < 0.001$.

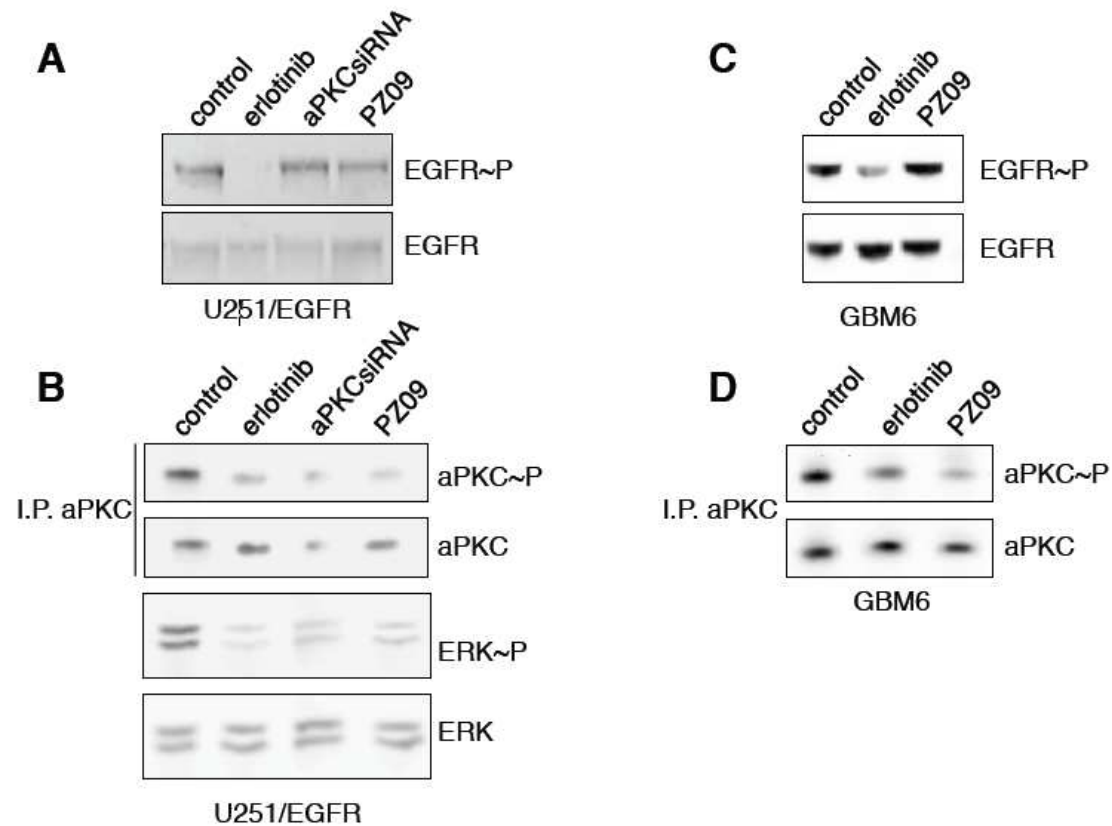


Figure 3.S12. Erlotinib, but not aPKC inhibition, suppresses EGFR phosphorylation. (A) Immunoblots of EGFR phosphorylation in U251/EGFR cells alone (control), upon incubation with 10 μ M concentration of erlotinib, in U251/EGFR cells in which aPKC expression has been silenced (aPKCsiRNA) or upon incubation with 10 μ M of PZ09. Total EGFR was used as a loading control. (B) Immunoblots of aPKC phosphorylation and total aPKC after immunoprecipitation (I.P.) in U251/EGFR cells treated as in A (top panels). Immunoblots of ERK phosphorylation and total ERK in U251/EGFR cells treated as in A (bottom panels). (C) Immunoblots of EGFR phosphorylation in GBM6 cells alone (control), upon incubation with 10 μ M of erlotinib or 10 μ M of PZ09. Total EGFR was used as a loading control. (D) Immunoblots of aPKC phosphorylation and total aPKC after immunoprecipitation (I.P.) in GBM6 cells treated as in C. Data are presented as representative blots of at least 3 independent experiments.

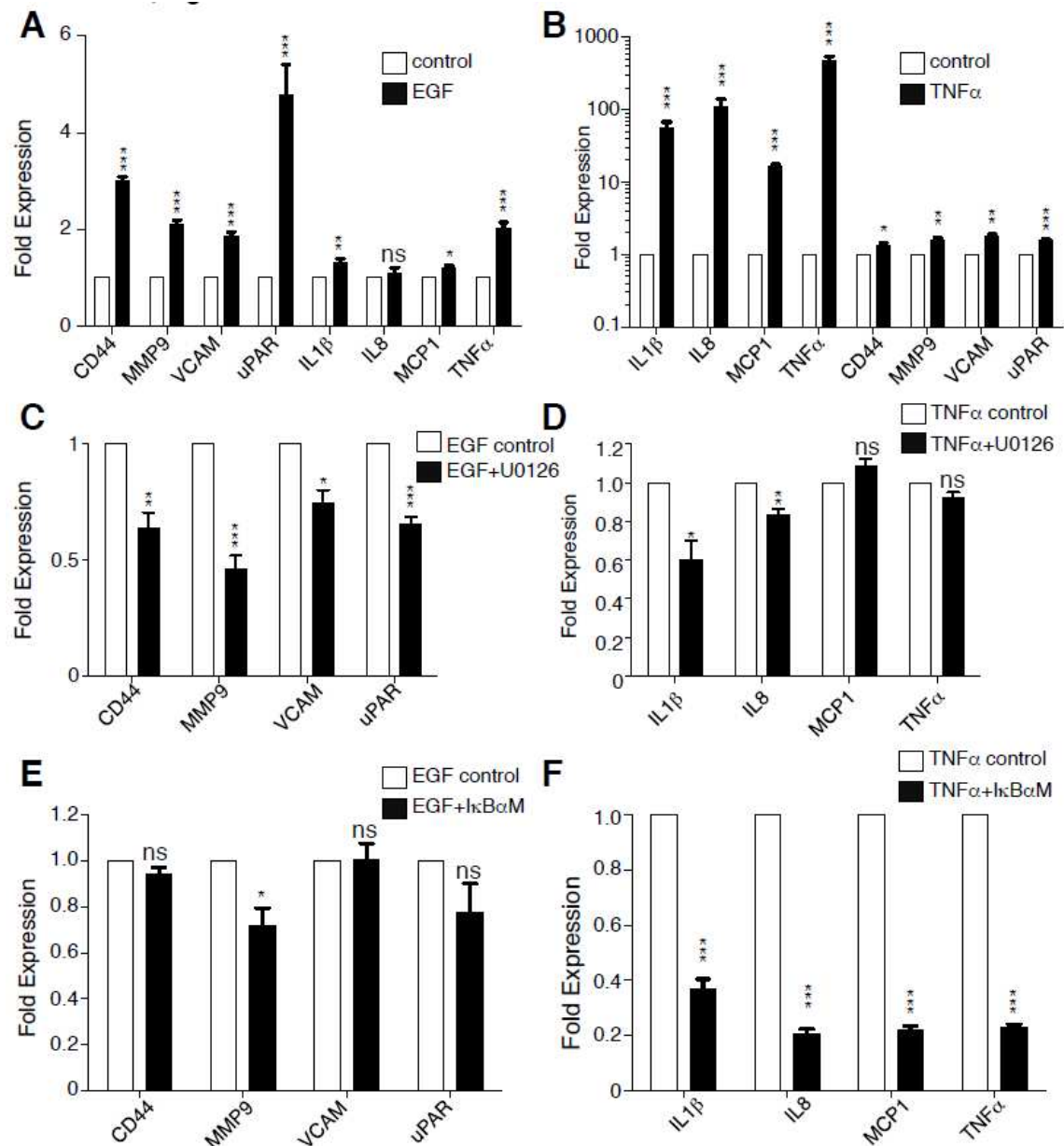


Figure 3.S13. Induction of distinct sets of genes by EGF and TNF α signaling in GBM cells. (A) Expression of indicated genes in U251/EGFR cells treated with 100 ng/mL EGF for 6 h or (B) 10 ng/mL TNF α for 1 h, as detected by RT-qPCR. (C) Expression of indicated genes in U251/EGFR cells treated with 100 ng/mL EGF for 6 h or (D) 10 ng/mL TNF α for 1 h with or without 10 μ M U0126, as detected by RT-qPCR. (E) Expression of indicated genes in U251/EGFR cells transduced with Ikb α M virus and treated with 100 ng/mL EGF for 6 h or (F) 10 ng/mL TNF α for 1 h. Data are presented as mean \pm SEM of at least 3 independent experiments. *p < 0.05, **p < 0.01, ***p < 0.001, ns is non-significant.

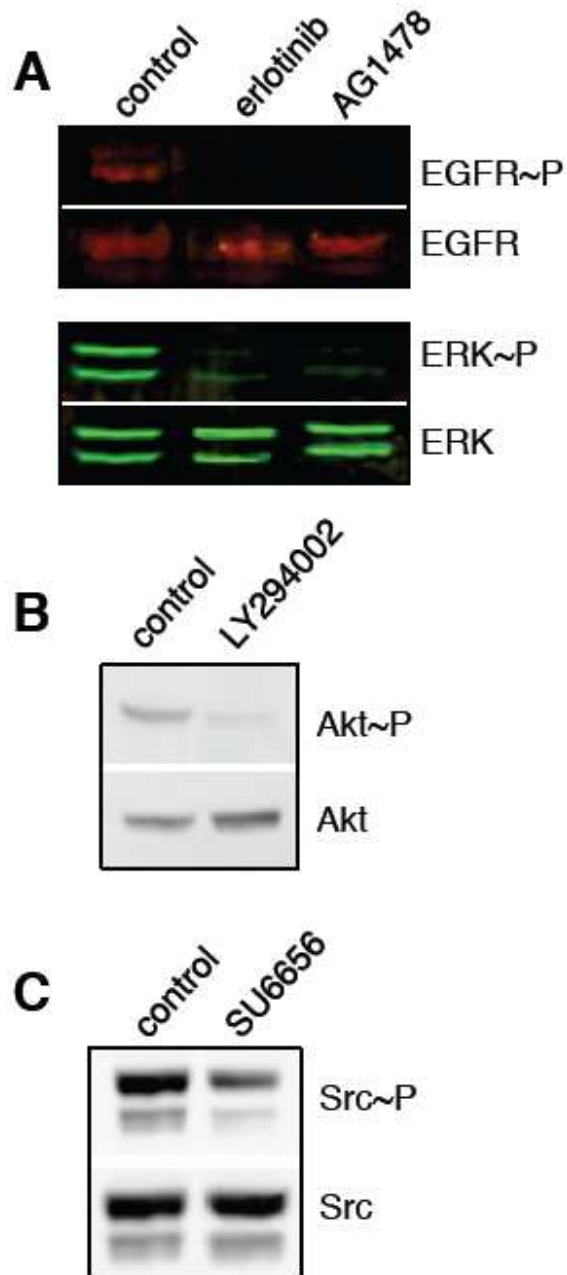


Figure 3.S14. Validation of EGFR, AKT and Src inhibition in U87/EGFRvIII. (A) Immunoblots of phospho-EGFR, total EGFR, phospho-ERK and total ERK in cell lysates from U87/EGFRvIII control or after incubation with 10 μ M of erlotinib or 10 μ M of AG1478 for 30 min. (B) Immunoblots of phospho-AKT and total AKT in cell lysates from U87/EGFRvIII control or after incubation with 20 μ M of LY294002 for 30 min. (C) Immunoblots of phospho-Src and total Src in cell lysates from U87/EGFRvIII control or after incubation with 10 μ M of SU6656 for 30 min. Data are presented as representative blots of at least 3 independent experiments.

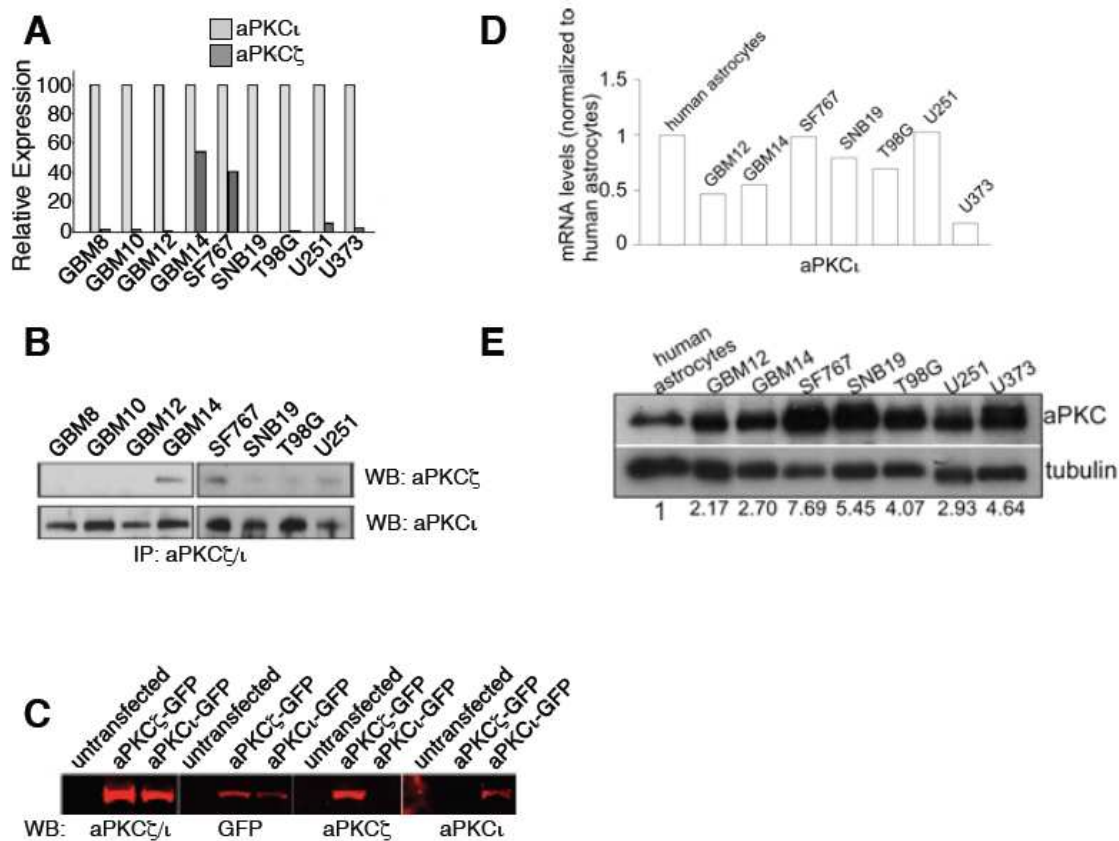


Figure 3.S15. *PRKCI* is the predominant GBM-associated isoform of aPKC. (A) Relative expression of aPKC ι (*PRKCI*) and aPKC ζ (*PRKCZ*) in patient-derived xenografts (GBM8, GBM10, GBM12, GBM14) and GBM cell lines (SF767, SNB19, T98G, U251, U373) as detected by RT-qPCR using isoform specific primers. Relative expression levels of the isoforms normalized to *PRKCI* are shown. (B) Expression of aPKC ι and aPKC ζ as detected by immunoblotting using isoform specific antibodies. Total aPKC was immunoprecipitated and probed with isoform specific antibodies. (C) Validation of isoform specific antibodies on HEK293 cells expressing aPKC-GFP fusion protein as detected by western blotting using total aPKC antibody and isoform specific aPKC antibodies. (D) Relative expression of aPKC ι in the indicated cells as detected by RT-qPCR using isoform-specific primers and normalized to human astrocytes. (E) Expression of total aPKC as detected by immunoblotting in the indicated cells. Tubulin is shown as loading control. The numbers below each lane indicate the relative expression of aPKC in the respective cell type normalized to its expression in human astrocytes.

ACKNOWLEDGEMENTS

NIH R01 CA149258, NIH P30CA023074 subaward and ABRC 8-101 to SG, NIH R01 AI089824 to CVR and SG, NIH R01 NS082745 and NIH R01 CA175391 to NS, NIH T32CA009213 to EKM, CONICET Postdoctoral Fellowship to AEE and an Achievement Rewards for College Scientists Foundation Scholar Award (YK). Zhimin Lu, Vinay Tergaonkar and Tony Hunter for reagents, Joseph Georges, Zaman Mirzadeh, Gillian Paine-Murieta and Bethany Skovan for technical assistance and advice.

CHAPTER 4

DISCUSSION AND IMPLICATIONS

mTOR Signaling in GBM

Signaling pathways rarely operate in isolation. Although Chapter 2 and Chapter 3 describe seemingly separate signaling pathways, evidence in the literature exists of the shared association and cross-talk between the signaling components. For example, mTOR signaling in GBM has been well characterized, given that mTOR is a downstream component of the highly mutated PI3K/AKT pathway (Akhavan, Cloughesy, & Mischel, 2010; Q.-W. Fan et al., 2009; Hu et al., 2005). Fan et al (2009) showed that mTOR phosphorylation and activation was directly correlated with EGFR abundance in PTEN wild-type GBMs and that phosphorylated mTOR could be used as a marker of EGFR inhibition (Q.-W. Fan et al., 2009). Another study showed that mTOR was required for the survival of GBM cells as inhibition of mTOR led to their apoptosis (Hu et al., 2005). Furthermore, several in-vivo mouse studies have showed the efficacy of mTOR inhibition for GBM with various mTOR inhibitors (Eshleman et al., 2002; Prasad et al., 2011). After showing successful inhibition of the PI3K/mTOR signaling pathway in GBM cells in-vitro, Prasad et al (2011) treated a mouse model of GBM with XL765, a dual mTOR and PI3K inhibitor. While control mice succumbed to the tumor by day 55, on average, mice treated with XL765 survived on average 13 days longer ($p=0.05$). Furthermore, although TMZ alone effectively increased the survival of these mice ($p=0.001$), the additive effect of combining XL765 with TMZ in these mice was also significant ($p<0.001$). Using rapamycin, Eshleman et al (2002) found a reduction of GBM cell proliferation in-vivo as well as increased efficacy to radiation therapy with rapamycin treatment in mice with GBM flank xenografts (Eshleman et al., 2002). Interestingly, in GBM stem-like cells (described below), Sunayama et al (2010) found that treatment with rapamycin led to a reduction in sphere formation and the decreased transcription of stem-like markers, indicating a change of cellular identity with rapamycin treatment (Sunayama et al., 2010). Furthermore, treatment of these cells with NVP-BEZ235, a dual rapamycin and a PI3K

inhibitor, led to the increased expression of differentiation markers, as well as a significant reduction in the tumorigenicity of the cells (Sunayama et al., 2010). Given the potent tumorigenic properties of these stem-like cells in GBM and the hypothesis that they are capable of populating new tumors (see below), finding an effective therapeutic which targets their signaling cascades directly may prove to be efficacious to human patients.

A recent study published in the journal *Science* examined the differences in genetic mutations between initial low-grade glioma samples and recurrent glioma arising in the same patient (B. E. Johnson et al., 2014). As described in the Introduction to Chapter 3, low-grade gliomas can recur with the same pathological grade, or can acquire new mutations and recur as a high-grade glioma (Westphal & Lamszus, 2011). Over half of the TMZ-treated initial low-grade glioma patients whose tumor recurred as high-grade experienced new oncogenic mutations in the mTOR pathway (B. E. Johnson et al., 2014). Specifically, the authors identified a TMZ-associated mutation in PIK3CA in which glutamic acid is substituted by lysine at residue 542 was found to hyperactivate AKT and lead to mTOR activation and oncogenesis (B. E. Johnson et al., 2014). Tumors which recurred as a grade IV GBM recurred with a heterozygous loss or a loss of function mutation in PTEN, while those recurring as grade II or III did not (B. E. Johnson et al., 2014). Another low-grade glioma treated with TMZ recurred with a mutation in the MTOR gene itself. This mutation was a phenylalanine substitution for a serine at 2215 (MTOR S2215F) and resulted in constitutive activation of mTOR. Sections of the tumor which immunostained strongly for mTORC1 showed increased Ki-67 staining, a proliferative marker described in the Introduction to Chapter 2. Importantly, the authors note that none of the low-grade recurrences displayed new mutations in the mTOR pathway, thus indicating the importance of this pathway as a possible driver of malignancy.

Rapamycin, among other mTOR inhibitors, have not only been used in animal models and in-vitro on GBM cells, they have additionally been used in clinical studies to treat GBM patients (Cloughesy et al., 2008; Doherty et al., 2006; Galanis et al., 2005; Kreisl et al., 2009;

Prasad et al., 2011; Sami & Karsy, 2013). However, it should be noted that conflicting data exists in these studies. For instance, in 2005, a phase II study was conducted on 65 GBM patients who were treated with temsirolimus (CCI-779), a small molecule inhibitor of mTOR (Galanis et al., 2005). 36% of treated patients showed radiographic improvement and experienced a longer time to progression than non-treated patients (Galanis et al., 2005). The authors conclude that patients whose tumors express a high level of phosphorylated p70s6 kinase, a downstream effector of mTOR, are more likely to benefit from mTOR inhibition, and this may account for the lack of response in other non-treated GBM patients from this study (Galanis et al., 2005). Furthermore, patients were treated only weekly with rapamycin, and although the authors noted mTOR inhibition was successful, other clinical studies have since used daily rapamycin treatment. Enrolling only patients with a mutation in PTEN leading to reduced expression, a phase I neoadjuvant trial of daily rapamycin treatment was conducted in 2008 (Cloughesy et al., 2008). This study showed that mTOR inhibition in the tumor cells was variable, although 50% of the patients showed a significant reduction in intratumoral Ki67 staining after 1 week of rapamycin treatment (Cloughesy et al., 2008). Given that rapamycin is an mTORC1 specific inhibitor, it is not surprising that 50% of rapamycin treated patients in this study experienced AKT activation which resulted in a reduced time to progression (Cloughesy et al., 2008). This effect is likely due to the loss of negative feedback as mTORC1 negatively regulates the AKT pathway through phosphorylation of insulin receptor substrate 1 (IRS1) via S6K. PRAS40 is a direct target of AKT phosphorylation and can be used as a marker of AKT activation. Patients who experienced a reduced time to progression had significantly increased levels of phosphor-PRAS40 (threonine 246), indicating that in deed AKT activation correlated with lack of rapamycin efficacy (Cloughesy et al., 2008). While these studies reported rapamycin efficacy in GBM patients, others have failed to find such an effect. Another Phase II clinical study which administered weekly doses of CCI-779 to 43 GBM patients found no evidence of efficacy (Chang et al., 2005). Of 28 GBM patients treated with both an EGFR inhibitor and an mTOR inhibitor, 19% of patients showed a partial

response and 50% had stable disease, or a lack of tumor progression (Doherty et al., 2006). In another study of 22 patients treated with both an EGFR inhibitor and an mTOR inhibitor, while 14% showed a partial response to treatment, the responses were not stable and the tumor eventually progressed so that only 1 patient remained progression free at 6 months (Kreisl et al., 2009). However, it is important to note that these studies are difficult to truly assess as most had small sample sizes and many other factors were not controlled, such as pretreatment with other modalities and genetic status of the tumors.

In-vitro, metformin has proved promising for the treatment of GBM (Ferla, Haspinger, & Surmacz, 2012; Sato et al., 2012; Ucbek, Özunal, Uzun, & Gepdlremen, 2014). Treating the GBM cell line, T98G with metformin resulted in increased apoptosis and reduced viability (Ucbek et al., 2014) and metformin treatment of LN18 and LN229 resulted in reduced inhibition of migration (Ferla et al., 2012). Furthermore, mice with intracranial xenografts that were pre-treated with metformin *in-vitro* survived significantly longer than mice treated with vehicle alone, as tumor formation was significantly delayed in the pre-treated metformin mice (Sato et al., 2012). *In-vivo*, mice with intracranial xenografts that were treated systemically with metformin for 5 days only 1 day after GBM implantation survived on average 12 days longer than mice treated with vehicle only (Sato et al., 2012). Furthermore, mice treated for 10 days with metformin following this experimental paradigm survived an additional 12 days, on average, indicating the overall improved survival with systemic metformin treatment was approximately 25 days (Sato et al., 2012). Although currently no published data is available on the use of metformin in clinical trials, a phase I clinical trial is currently actively recruiting patients to assess the efficacy of neoadjuvant metformin therapy on progression free survival in GBM patients. Given the promising *in-vitro* and animal model studies, an increase in progression free survival is hypothesized. However, given the complicated signaling mechanisms, it will be important to evaluate the genetic status of the tumors to account for other downstream signaling possibilities.

Given the complexity of GBM, studies continue to investigate other inhibitors with the hopes of increasing the survival for GBM patients. Current therapies are simply not effective enough and it may be that our strategies for treatment need to change. Similar to our findings presented in Chapter 3, a study by Huang *et al* (P. H. Huang et al., 2007) found that the use of an EGFR kinase inhibitor coupled with the use of a c-MET kinase inhibitor was significantly more effective in stopping glioma progression than the use of an EGFR inhibitor alone. Given that prior studies using monotherapies have failed to prolong survival in patients with GBM (Sathornsumetee et al., 2007), targeting multiple signaling pathways by using combinatorial therapies may provide better therapeutic efficacy (Bello et al., 2004; Doherty et al., 2006; Sathornsumetee et al., 2007; Thaker & Pollack, 2009). Indeed, the future of GBM therapies may lie in combinatorial targeting, especially considering the complexity of genetic mutations and aberrant signaling pathways in GBM.

aPKC and mTOR Signaling in Neural Stem Cell Proliferation and Differentiation

Signaling pathways do not occur in isolation, as evidenced by GBM, where aberrant mutations lead to abnormal signaling resulting in oncogenesis. Oncogenesis can be considered development gone awry; many of the same pathways that contribute to cancer are relevant for embryonic neural development and neurogenesis. Multiple signaling pathways contribute to the appropriate patterning of the CNS. While mTOR signaling has been shown to play a role in this process (Chapter 2); aPKC signaling (Chapter 3) has also been implicated in neurogenesis. Furthermore, aPKC signaling is known to associate within the mTOR signaling pathway in NSCs as it has been shown to be activated upon metformin treatment (J. Wang et al., 2012).

Using shRNA against aPKC ζ and aPKC ι , in separate experiments, Wang et al. (2012) described the role of aPKC in neural stem cell proliferation and differentiation. Given that *in-vivo* aPKC is localized apically along the ventricles in embryonic neural precursors, the author's electroporated the shRNAs into the cortices of E13/14 mice and found differential effects of aPKC ζ versus aPKC ι knockdown (J. Wang et al., 2012). While there was no effect on cell

survival, aPKC ζ knockdown led to a decrease in cells in the cortical plate and an increase in cells which were in the intermediate zone (J. Wang et al., 2012). This was explained by a decrease in neurogenesis and an increase in radial precursors. The authors concluded that aPKC ζ is essential for neurogenesis *in-vitro* and *in-vivo* as it promotes differentiation of neural precursors into neurons.

Interestingly, however, knockdown of aPKC ι did not have the same effect in the cortical precursors. Instead, knockdown of aPKC ι led to an alteration in the population of precursor cells (J. Wang et al., 2012). The number of Pax6 $^{+}$ and Sox2 $^{+}$ radial precursors was significantly decreased, while the number of Tbr2 $^{+}$ basal progenitors was increased (J. Wang et al., 2012). Therefore, while aPKC ζ functions to increase neurogenesis (as knockdown of aPKC ζ led to a reduction of newborns neurons *in-vitro* and *in-vivo*), aPKC ι functions to maintain radial precursors in their stem-like undifferentiated state.

In-vitro treatment with metformin of cortical precursors resulted in a significant increase in neurons and a decrease in Pax6 $^{+}$ and Sox2 $^{+}$ precursors (J. Wang et al., 2012). In addition, metformin treatment in these cells led to an increase in aPKC phosphorylation. When aPKC was knocked down in the neural precursors and they were treated with metformin, there was an inhibition of the metformin-induced increase in neurogenesis (J. Wang et al., 2012). Furthermore, the authors found metformin treatment *in-vitro* resulted in an increase in GFAP $^{+}$ astrocytes, as well as A2B5 $^{+}$ oligodendrocyte precursors (J. Wang et al., 2012). Thus, metformin signals through aPKC to affect both neuro and gliogenesis.

Downstream of aPKC ζ , the authors discovered a role for the CREB binding protein (CBP), a histone acetyltransferase that has been shown to cause Rubinstein-Taybi syndrome (RTS), a genetic disorder that results in cognitive dysfunction. Knockdown of CBP *in-vitro* and *in-vivo* results in reduced neurogenesis and gliogenesis and aPKC ζ phosphorylation of CBP was found to be an essential event in its appropriate functioning (J. Wang et al., 2010). When aPKC ζ

was knocked down, the authors noted a loss of CBP phosphorylation, as well as a decrease in neurons and glia and an increase in Pax6⁺ radial precursors (J. Wang et al., 2010). Furthermore, CBP overexpression resulted in increased gliogenesis, and knockdown of aPKC ζ , but not aPKC ι , resulted in normal gliogenesis (J. Wang et al., 2010). Therefore, an mTOR/aPKC/CBP signaling pathway plays an important role in embryonic gliogenesis and neurogenesis.

SVZ Niche, Polarity and Neural Stem Cell Proliferation and Differentiation

It should be noted that the role of aPKC in neurogenesis has not completely been elucidated. While these studies point to aPKC playing an important role downstream of mTOR signaling, another study found no effect of aPKC knockout on neurogenesis in an mouse (Imai et al., 2006). In this study, control brains expressed BrdU⁺ neuroepithelial cells in the middle layer of the ventricular zone, while aPKC $\iota^{-/-}$;Nestin-Cre⁺ brains had BrdU⁺ neuroepithelial cells dispersed throughout the ventricular zone, indicating that interkinetic nuclear migration of neuroepithelial cells was altered by the loss of aPKC ι . Interestingly, the authors found that the apical cellular process of these cells was detached from the ventricular surface, while basal processes remained attached (Imai et al., 2006). Given the importance of polarity signaling in proper neural development (discussed below) and given the importance of aPKC in mTOR-mediated regulation of neurogenesis (discussed above), the conclusion of the authors that regulation of neurogenesis is independent of aPKC ι and/or adherens junctions warrants further study (Imai et al., 2006). However, there are several factors which may account for their lack of response. For instance, the conditional nestin-cre mouse used in this study is expressed at E15; which may be too late to affect the appropriate progenitor type which relies on aPKC signaling and polarity signaling for proper differentiation. It has been shown that outer radial glia cells (oRG; nestin⁺, Sox2⁺, Pax6⁺, Tbr2⁻), shown to be present at E14.5 do not make contact with the ventricle, only contain a basal process, and do not undergo interkinetic nuclear migration during division (X. Wang, Tsai, LaMonica, & Kriegstein, 2011). Radial glial cells, however, as well as

intermediate progenitor cells, have been shown to make apical contact with the ventricle (Mirzadeh, Merkle, Soriano-Navarro, Garcia-Verdugo, & Alvarez-Buylla, 2008). Furthermore, it has been shown that Tbr2⁺ intermediate progenitors in the E14.5 cortex do not express nestin (Englund et al., 2005); thus, it is possible that the use of a different conditional cre to target other neural progenitor cells may have a significant effect despite these results. In addition, there may be significant compensatory mechanisms activated in the aPKC^Δ;Nestin-Cre⁺ mice, and this was not investigated.

One important finding from this report which was not emphasized was a loss of the ependymal layer by p3 in the aPKC^Δ;Nestin-Cre⁺ mice and the eventual development of hydrocephalus leading to brain malformations and death (Imai et al., 2006). While the authors state the presence of a well maintained neuronal structure in the knockout mice, they do note the absence of an ependymal layer. The ependymal layer has been shown to be an important regulator of neurogenesis through its robust expression of Noggin, a strong antagonist of BMPs, which are expressed by neural stem cells (Lim et al., 2000). Ectopic expression of Noggin promoted neuronal differentiation of neural stem cells and the authors conclude that Noggin protein derived from the ependymal cells in vivo aids in creating a neurogenic environment in the adult SVZ (Lim et al., 2000). Therefore, the results of this study showing that aPKC^Δ;Nestin-Cre⁺ mice did not have an effect on the proliferation or differentiation in the embryonic brain are surprising as many factors of the SVZ micro-environment, including the cytoarchitecture of the cells and the existence of ependymal cells has shown to be essential in appropriate embryonic development as well as adult neurogenesis.

In the adult, the SVZ has been classified as a neurogenic niche due to its structure and microenvironment which contains signals to regulate stem cell behavior (Alvarez-Buylla & Lim, 2004). The stem cell niche is made up of membrane bound molecules, such as adhesion junction proteins, extracellular matrix, and diffusible factors. These factors have been shown to be

instrumental in regulating the stemness of the cells, as transplantation studies have shown that the cells require this specialized niche in order to proliferate and differentiate normally (Gage, 2002). In addition to this micro-environmental niche displaying polarity, the type-B cells themselves, like neuroepithelial cells, have a polarized cell body, with a contact maintained at the basal lamina and a process extending to the ventricular surface (Chapter 2). Adult type-B cells have been shown to contain an apical process allowing direct contact to the ventricle, through the ependymal layer (Mirzadeh et al., 2008). In addition, the cells were shown to extend a basal process which extends on to vasculature (Mirzadeh et al., 2008). Furthermore, earlier work showed that some B cells residing in the subventricular zone (SVZ) have part of their membrane contacting the ventricle and that upon stimulation of proliferation, the number of apical contacts at the ventricle increases (Fiona Doetsch, Caille, Lim, García-Verdugo, & Alvarez-Buylla, 1999). Studies have shown this organization to be instructive to the fate of B cells, as this polarity allows for the regulation of the tightly controlled process of interkinetic nuclear migration. For example, Shen, et al (2008) showed that infusion of GoH3, an $\alpha 6$ integrin-blocking antibody into the lateral ventricle of adult mice, which results in loss of B-cell adhesion to the blood vessels, led to a 33.6% increase in proliferation of SVZ lineage cells (Shen et al., 2008).

This microenvironmental polar structure of the SVZ interestingly mirrors the polarity of the embryonic stem cells, for which the role of polarity in neural stem cell proliferation and differentiation has been better examined. Data has shown the importance of apical-basal polarity and aPKC/Par proteins for proliferation and differentiation in *Caenorhabditis elegans* and *Drosophila melanogaster*. The evolutionarily conserved polarity genes were first discovered in studies of *C. elegans* and *D. melanogaster*. Work on early embryonic patterning in *C. elegans* identified the genes as responsible for the development of the anterior-posterior polarity axis. Genetic manipulation of these genes in the 1-cell embryo led to dramatic polarity defects and loss of the polarity axis (Bowerman & Shelton, 1999; Kemphues & Strome, 1997; Tabuse et al., 1998). *C. elegans* embryos which lack aPKC are embryonic lethal due to the effect on polarity (Tabuse

et al., 1998), which leads to defects in embryonic cell division. Similar phenotypes resulted from experiments with Par-3 (Tabuse et al., 1998) and with Par-6 (Hung & Kemphues, 1999; Watts et al., 1996; Watts, Morton, Bestman, & Kemphues, 2000).

It has previously been shown that the aPKC/Par3/Par6 complex is present during E12-E14 stage at the apical surface of the mouse ventricular zone, and its expression is reduced in E16 (Costa, Wen, Lepier, Schroeder, & Götz, 2008). Along with the reduction of the polarity protein expression by E16, there is similarly a reduction in the pool of progenitors. Using shRNA, Costa et al. (2008) knocked-down expression of Par3 by in-utero injection at E12-E14 and found a lack of cell proliferation and an early progenitor cell cycle exit. This mirrors what is seen post-E16, when Par3 expression is reduced and there is a considerable reduction in cell proliferation. Bultje, et al. (2009) provided evidence that Par-3 plays an important role for radial glia differentiation and proliferation during embryonic development (Bultje et al., 2009). In radial glial progenitors, Par-3 was found to be localized at the lateral membrane, specifically at the ventricular endfeet during interphase, but was delocalized as the cell cycle progressed. To disrupt the polarity of the glial progenitors, the authors used both removal of Par-3 and ectopic expression, which similarly led to a decrease in asymmetric divisions. Removal of Par-3, led to an increase in production of neurons; while the ectopic expression of Par-3, led to an increase in the production of radial glia progenitors (Bultje et al., 2009). More recently, Kim et al. (2010) found that disruption of the apical complex via Pals1, an evolutionarily conserved scaffold protein which can bind to the ternary complex, led to premature cell cycle exit and excessive neuron production (S. Kim et al., 2010). Similarly, Loulier, et al. (2009) examined the role of the NSC adhesion complex at the apical surface by disrupting the attachment of the apical process from the ventricular surface, using a B1 integrin antibody during important embryonic neurogenic periods (E12-E15) (Loulier et al., 2009). Interestingly, they found an increase in NSC proliferation and alteration in the cleavage planes, indicating an increase in asymmetric division (Loulier et al., 2009). In the developing chick embryo, Ghosh, et al. (2008) found aPKC to localize at the apical

membrane of proliferating neural stem cells, but not postmitotic cells. In addition, expression of myr-aPKC, a constitutive active construct, led to increased proliferation of the cells (Ghosh et al., 2008b). Also in chick embryos, Das & Storey (2014) found aPKC localization to be restricted to an apical particle of Tuj1⁺ newborn neurons (Das & Storey, 2014). The cell retracts this apical process, losing its polarity to mediate membrane detachment from the ventricular surface. This process was also found to occur in Tuj1+ cells of the mouse spinal cord. Cells which maintain their apical contact were found to express early neuronal markers, but not late neuronal markers or post-mitotic cell markers, indicating that cells with an aPKC containing apical protrusion are not post-mitotic, or have not exited the cell cycle (Das & Storey, 2014). In addition, it has been previously shown that inheritance of polarity proteins determines asymmetric vs. symmetric division in neuroepithelial cells of E10-E12.5 mouse. In neuroepithelial cells that divided and inherited unequal distribution of the apical membrane, the daughter cell which inherited the apical membrane maintained its' stem cell fate, while the daughter cell who did not receive the apical membrane became a neuron (Kosodo et al., 2004). Therefore, this overwhelming evidence points to the microenvironmental polar niche being instructive for the proliferation and differentiation of NSC in embryonic and adult SVZ.

TNF- α and EGFR Signaling in Neural Stem Cell Proliferation and Differentiation

Interestingly, microglia-derived-TNF- α and/or exogenous TNF- α has been shown to have an effect on NSC proliferation, although the evidence is contradictory (Cacci, Ajmone-Cat, Anelli, Biagioni, & Minghetti, 2008; Iosif et al., 2006; Monje, Toda, & Palmer, 2003; Rubio-Araiz et al., 2008; Widera, Mikenberg, Elvers, Kaltschmidt, & Kaltschmidt, 2006). For instance, incubation of NSCs in conditioned media from acute activated microglia, which expressed increased TNF- α , among other cytokines such as IL-6, IL-1 β and IL-1 α , resulted in reduction of NSC survival, increased glial differentiation and prevention of neuronal differentiation (Cacci et al., 2008). In addition, another study found that mice which lack TNFR1 or TNFR2 had increased proliferation

in the SGZ, indicating that signaling through TNFR negatively regulates NSC proliferation (Iosif et al., 2006). However, through upregulation of cyclin D1, TNF- α treated NSCs displayed a significant increase in NSC proliferation as evidenced by BrdU incorporation and increased neurosphere volume (Widera, Mikenberg, Elvers, et al., 2006). Furthermore, this effect was attenuated by disrupting NF- κ B activity through IKK- β knockdown and by use of the NF- κ B super-repressor I κ B α (Widera, Mikenberg, Elvers, et al., 2006; Widera, Mikenberg, Kaltschmidt, & Kaltschmidt, 2006). The role of NF- κ B in neural stem cell proliferation and differentiation remains to be elucidated, however, studies in human embryonic stem cells showing NF- κ B activation in undifferentiated cells and down-regulation in differentiated cells points to a potential role for NF- κ B in stem-like maintenance (Armstrong et al., 2006; Dreesen & Brivanlou, 2007).

Studies also suggest EGFR signaling is an important determinant in NSC proliferation and differentiation (Ferron et al., 2010; Y. Sun, Goderie, & Temple, 2005). For instance, infusion of EGF into the lateral ventricles results in a highly significant expansion of proliferation of NSC in the SVZ (Craig et al., 1996). As the cells divide asymmetrically, unequal inheritance of EGFR leads to a differential ability to proliferate and differentiate, as neural stem cells with higher EGFR levels form 2-fold more neurospheres than those with low EGFR levels (Ferron et al., 2010; Y. Sun et al., 2005). In addition, it has been shown that both wtEGFR over-expression and EGFRvIII expression in postnatal NSCs leads to unrestricted proliferation and increased survival (Ayuso-Sacido et al., 2010). EGFR is frequently over-expressed in GBM and EGFRvIII is a common mutation which results in a truncated extracellular domain, creating a ligand-independent constitutively active EGFR kinase. Complimentary to an increase in proliferation, postnatal NSCs with wtEGFR and EGFRvIII expression in subjected to differentiation conditions, fail to differentiate, as none of the cells express Tuj1 7 days post-differentiation, compared to 25% of control cells (Ayuso-Sacido et al., 2010). Therefore, EGFR is an important determinant in the

proliferation and differentiation of neural stem cells in addition to its role in oncogenic signaling presented in Chapter 3.

EGFR Signaling and NF- κ B

It is important to note that although our studies in GBM (Chapter 3) examined 2 distinct signaling pathways both activating aPKC, recent studies have provided evidence of cross-talk between the intracellular EGFR signaling pathway and activation of NF- κ B signaling in GBM (Pianetti, Arsura, Romieu-Mourez, Coffey, & Sonenshein, 2001; Tanaka et al., 2011; Wu, Abe, Inoue, Fujiki, & Kobayashi, 2004). For instance, in 2012, Bonavia *et al* (R. Bonavia et al., 2012) found that glioma cells expressing the constitutive active mutant EGFRVIII displayed increased angiogenesis and oncogenicity through activation of NF- κ B, signaling through the PI3K/AKT pathway. Similarly, Wu *et al* (Wu et al., 2004) found that EGFRVIII expressing glioma cells were less oncogenic when NF- κ B activity was blocked using I κ B α M, the NF- κ B super-repressor. Interestingly, a report by Tanaka *et al* found that mTORC2 was stimulated downstream of EGFRVIII in glioma cells and that this led to NF- κ B activation (Tanaka et al., 2011). Furthermore, they found that this mTORC2/NF- κ B signaling pathway was responsible for glioma cell chemotherapy resistance (Tanaka et al., 2011).

As described in Chapter 3, an analysis of human GBM samples led to the discovery of a frequent deletion of *NFKBIA*, the negative inhibitor of NF- κ B (M. Bredel et al., 2011). Interestingly, this deletion is mutually exclusive with *EGFR* amplification as 52.5% of tumors had either amplification of *EGFR* or a deletion of *NFKBIA*, while only 5% had both. The reexpression of *NFKBIA* in *NFKBIA*-deleted-GBM led to reduced proliferation, migration, colony formation, as well as increased sensitivity to TMZ treatment, indicative of the tumor-suppressor activity of *NFKBIA*, as it acts to inhibit NF- κ B activity. In GBM cells with amplification of *EGFR*, expression of *NFKBIA* reduced cell viability and decreased oncogenesis. However, in cells with a normal dose of *EGFR*, this effect was not apparent (M. Bredel et al., 2011).

Although not in glioma cells, Sun & Carpenter (1998) showed that EGF activates NF- κ B in A-431 carcinoma cells. Like GBM cells, these cells over-express EGFR. They found treatment with EGF led to a degradation of I κ B α , allowing NF- κ B to enter the nucleus (L. Sun & Carpenter, 1998). In prostate cancer cells which express EGFR, Le Page et al. (2005) showed EGF induced phosphorylation of I κ B α on serine 32/36, leading to I κ B α degradation and NF- κ B activation (Le Page, Koumakpayi, Lessard, Mes-Masson, & Saad, 2005). Furthermore, the expression of a dominant negative I κ B α Serine32/36 was able to block NF- κ B activation downstream of EGFR, showing the direct association of EGFR and NF- κ B activation.

Similar to our work presented in Chapter 3, a recent study found EGF treatment of GBM cells to lead to up-regulation of vascular cell adhesion molecule-1 (VCAM-1) (Zheng, Yang, Aldape, He, & Lu, 2013). However, the authors found this to be via a different signaling mechanism than we proposed. Their results showed VCAM-1 was up-regulated after EGF treatment in a PKC ϵ and NF- κ B dependent manner (Zheng et al., 2013). Furthermore, the levels of EGFR activation in GBM samples was correlated with macrophage infiltration and EGF stimulation led to increased macrophage binding to GBM cells (Zheng et al., 2013). This increased binding was inhibited when the cells were incubated in an EGFR inhibitor. In addition, EGF-induced VCAM-1 up-regulation was inhibited in the presence of an NF- κ B inhibitor or PKC ϵ shRNA (Zheng et al., 2013), indicating that EGF is signaling through PKC ϵ to activate NF- κ B transcription of VCAM-1 in GBM cells. VCAM-1 expression was found to be crucial for macrophage to GBM cell binding. Similar to our results in chapter 3, this increased binding led to an increase in GBM cell invasion and VCAM-1 shRNA was able to block the increase in invasion (Zheng et al., 2013). While this study elucidated one potential mechanism for EGF induced NF- κ B activation, other studies have discovered alternative signaling mechanisms as well.

For instance, one study hypothesized the mechanism of EGFR induced NF- κ B activation to be similar to TNFR induced NF- κ B activation (Habib et al., 2001). Upon TNFR activation, an

adaptor protein, TRADD, associates with the receptor, which then recruits RIP and TRAF2. Co-transfection of EGFR with TRADD or Fas-associated death domain protein (FADD; an adaptor protein which also associates with TNFR upon activation) failed to show any association in 293 human embryonic kidney cells (HEK; these cells are used for their ease of transfection) (Habib et al., 2001). However, co-transfection of EGFR with RIP resulted in a physical association; and a kinase-inactive mutant of EGFR was unable to bind RIP. This association was seen in both HEK cells as well as MDA-MB-468 breast cancer cells (Habib et al., 2001). Therefore, EGFR is thought to recruit RIP in order to activate NF- κ B. In addition, EGFR was shown to associate with NF- κ B inducing kinase (NIK) (Habib et al., 2001), a kinase which integrates signals downstream of TNFR and upstream of NF- κ B. In this study, the use of a PI3K inhibitor showed no effect on EGF-induced NF- κ B activation although it blocked EGF induced AKT phosphorylation (Habib et al., 2001); indicating that this signaling pathway does not signal through AKT.

However, other reports have shown that TNF- α signaling can activate AKT and lead to NF- κ B activation. For instance, in EGFR+ breast cancer cells, the use of an EGFR antibody blocked NF- κ B activation, as well as a PI3K inhibitor, and Go6976, an NF- κ B inhibitor, as evidenced by an NF- κ B DNA binding assay (Biswas, Cruz, Gansberger, & Pardee, 2000). In GBM cells following EGF stimulation in-vitro, an increased association between Grb2-associated binder 1 (Gab1) and SHP-2 (a tyrosine phosphatase with 2 SH2 domains) was identified (Kapoor, Zhan, Johnson, & O'Rourke, 2004). This Gab1/SHP-2 complex was shown to regulate AKT activation as transfection of these proteins in GBM cells led to a threefold increase in AKT activity. Furthermore, treatment with EGF resulted in a change in NF- κ B electromobility shift assay (EMSA), indicating NF- κ B activation via DNA binding. Active AKT transfection led to increased NF- κ B activation via an NF- κ B luciferase assay while mutant-inactive AKT transfection resulted in no change (Kapoor et al., 2004). Co-transfection of the Gab1/SHP-2 complex led to a significant

increase in NF- κ B activation and an EMSA showed an increase in NF- κ B DNA binding (Kapoor et al., 2004). Thus, EGFR may directly lead to NF- κ B activation, through various mechanisms.

While these reports may contradict the results presented in Chapter 3, it does not preclude them. Multiple signaling pathways cooperate to promote oncogenesis. Furthermore, we found that EGF treatment in GBM cells led to an increase in TNF- α ligand transcription and TNF- α treatment led to an increase in EGF ligand transcription. Thus, there may be a feedback loop which is leading to coincidental activation of multiple signaling pathways within minutes of stimulation and receptor activation. While we did not investigate the activation of PKC ϵ , it is also possible that other PKC family members may be associated with these signaling cascades as various other PKCs have been implicated in GBM pathogenesis (do Carmo et al., 2013).

The glioma stem cell hypothesis

Discovering the molecular mechanisms underlying neural stem cell proliferation (as in Chapter 2) and differentiation may provide insight into novel therapeutics for the treatment of GBM. GBM tumors are extremely heterogeneous and contain many different cell types making them difficult to treat. Recently, the discovery of glioma stem cells (GSCs) has shifted the GBM research field into studying mechanisms which control GSC proliferation (Ignatova et al., 2002; Singh et al., 2004). Like neural stem cells, GSCs are also capable of proliferative self-renewal and multipotent differentiation into neurons, astrocytes and oligodendrocytes in vitro (Ignatova et al., 2002). While it requires 1 million glioma cells to initiate a tumor in mice, it was found that only 100-1,000 glioma stem cells were required to form a tumor, providing evidence regarding their strong proliferation capacity in vivo (Ignatova et al., 2002; J. Lee et al., 2006). In addition, GSCs are resistant to radiation and chemotherapy, which has led to the hypothesis that GSCs remain undetected in the brain during treatment, and later return to establish a new tumor (Bao et al., 2006; Jian Chen et al., 2012; X. Gao et al., 2013; G. Liu et al., 2006; J. Wang et al., 2012). A recent study elegantly described the resistant nature of GSCs by the use of transgenic mice

which expressed GFP in adult SVZ NSCs and GSCs. After using a chemotherapy agent to arrest the initial growth of a GBM model in these transgenic mice, Chen *et al.* (Jian Chen et al., 2012) found that the tumor regrowth began with GFP+ stem cells. Furthermore, upon ablation of these GFP+ stem cells, the authors were able to show significantly reduced tumor growth, thus providing evidence for the virulent nature of these GSCs.

What are the signaling cascades which signal to the GSC to begin proliferation? Multiple signals have been identified as important regulators in this process. For instance, the platelet-derived growth factor receptor (PDGFR) signaling pathway has also been implicated in GSC function. Interestingly, Kim *et al.* (Y. Kim et al., 2012) found that while PDGFR α is expressed on a subset of GBM cases, PDGFR β is preferentially expressed by GSCs. The blockade of the PDGFR β signaling cascade in GSCs led to reduced proliferation, oncogenicity and invasion of GBM mouse models in addition to increased survival. Downstream of PDGFR β , the authors found that signaling was dependent upon the transcription factor STAT3 as constitutively active STAT3 rescued the inhibited PDGFR β phenotype (Y. Kim et al., 2012).

Given the importance of polarity signaling in stem cell regulation (described above & Chapter 2), the possibility exists that a loss of polarity may be one of the defining characteristics of neural stem cell oncogenic proliferation. Quiñones-Hinojosa & Chaichana (2007) described the similarities between NSCs and GSCs, in that they both undergo self-renewal and multiply (Quiñones-Hinojosa & Chaichana, 2007). Therefore, it can be hypothesized that the polarity complex may regulate the proliferation and differentiation of GSCs. Aberrant function of the polarity signaling pathway may directly contribute to transformation of neural stem cell into glioma initiating cells. However, currently no data exists on this subject although it has been hypothesized that the regulation of asymmetric cell division may lead to GBM (Berger, Gay, Pelletier, Tropel, & Wion, 2004), indicating a potential important role for cellular polarity.

In line with this hypothesis, Lathia et al. (2011) found asymmetric distribution of CD133 in GSCs (Lathia et al., 2011). CD133 (also known as prominin-1) has been used for the last decade as a GSC marker despite little evidence of its signaling function (Yan, Yang, & Rich, 2013). Using CD133⁺ GSCs isolated from GBM patients, Lathia et al. (2011) found that the majority of GSCs underwent symmetric division in order to expand the stem cell population. However, upon growth factor starvation, the cells switched to asymmetric division, indicating that growth factor signaling may be responsible for the expansion and survival of GSCs within the tumor (Lathia et al., 2011). CD133 was unequally distributed in GSCs and CD133 expression leads to increased survival. Therefore, cells which inherit CD133 through symmetrical divisions maintain the stem population and experience better survival and proliferation. However, asymmetric divisions may lead to an increase in differentiated cell types, increasing the cellular heterogeneity of the tumor. Recently Wei *et al.* (Wei et al., 2013) showed that CD133 signals through the PI3K/AKT signaling pathway in GSCs. Furthermore, they showed that silencing of CD133 inhibited the PI3K/AKT pathway and resulted in reduced GSC proliferation and oncogenicity (Wei et al., 2013). Currently a phase I clinical trial is underway to evaluate the efficacy of ICT-121, a vaccine which targets CD133 (Yan et al., 2013).

The Eph RTKs have also been described as regulators of GSC tumor propagation (Day et al., 2013). While GBM tumors are made of extremely heterogeneous cell types, cells which display high EphA2 RTK expression correlated with tumor propagation capacity. The silencing of EphA2 in these cells led to reduced GSC proliferation and oncogenicity. Similar results were obtained by another group studying EphA3, however, it was found to signal through the mitogen-activated protein kinase (MAPK) cascade, a strong regulator of cell growth and proliferation (Day et al., 2013).

The discovery of signaling pathways responsible for the regulation of GSC oncogenicity may lead to promising new therapeutic targeting. GBM patient prognosis remains abysmal and new therapies are desperately needed. If researchers can identify the signaling pathway which

may directly contribute to the transformation of NSCs into GSCs, we may be able to increase the current prognosis for this disease.

Inhibitors in GBM Clinical Trials

New developments are on the horizon in the treatment of GBM. The search for inhibitors in GBM on the NIH Clinical Trials website reveals over 300 studies. In addition to the aforementioned clinical trials underway, including CD133 inhibitor, EGFR and c-MET co-inhibition, as well as the clinical trials investigating mTOR inhibition for GBM, there are other inhibitors of signaling molecules being tested. For instance, a phase I clinical trial investigating MK-1775, an inhibitor of wee1, a tyrosine kinase is currently recruiting subjects with GBM. Wee1 is a tyrosine kinase that has been shown to impair the G2 DNA damage checkpoint, which may result in increased efficacy of TMZ or other chemotherapeutic agents. Expression of wee1 in GBM tumors was negatively correlated with survival and treatment of GBM cells in-vitro with a wee1 inhibitor resulted in increased sensitivity to TMZ (Mir et al., 2010). In-vivo, mice with GBM intracranial xenografts which were treated with radiation showed no increase in survival. However, mice whose xenografted GBM cells were knocked out for wee1 showed a significant increase in survival and those with wee1 knock out GBM cells and radiation treatment showed a very significant increase in survival. Similar results were obtained using a wee1 inhibitor (Mir et al., 2010). The inhibition of the kinase wee1 in GBM patients may hopefully provide better response to chemotherapy and radiation, resulting in increased prognoses and survival.

A phase II clinical trial is currently underway investigating RO4929097, a gamma-secretase/notch signaling inhibitor. Notch signaling has been shown to maintain the stem-like cells of the tumor, and promote chemoresistance (Capaccione & Pine, 2013). Using a gamma-secretase/notch inhibitor, Chen et al (2010) treated GBM-derived neurospheres in-vitro and found a significant reduction in cell growth and proliferation (Jie Chen et al., 2010). In another study, induced expression of active notch in GSCs led to increased tumor growth, while the use of gamma secretase/notch inhibitors reduced GSC neurosphere growth (X. Fan et al., 2010).

Furthermore, implantation of GSCs pre-treated with inhibitor failed to form tumors (X. Fan et al., 2010). The authors found this effect to be mediated via AKT signaling, as AKT phosphorylation was decreased in inhibitor treated cells (X. Fan et al., 2010).

Another phase II study is investigating the efficacy of Dovitinib (also known as receptor tyrosine kinase inhibitor TKI258), an inhibitor of FGFR3, which has been shown effective in other solid tumors (André et al., 2013; Huynh et al., 2012). This inhibitor may also inhibit other RTKs such as VEGFR, FGFR1, PDGFRA (Angevin et al., 2013), and thus may result in a significant blockade in oncogenic signaling. Furthermore, given the strong reliance on RTK signaling pathways in GBM, a general RTK inhibitor may prove more effective than singular RTK targeting.

In patients with PTEN^{-/-} GBM tumors, a phase I clinical trial is investigating the use of Buparlisib (BKM120), a PI3K pathway inhibitor, and INC280, a c-MET receptor tyrosine kinase inhibitor. The use of a PI3K inhibitor in patients without PTEN should yield better clinical outcome than the treatment with an EGFR inhibitor, as PTEN loss downstream of EGFR results in active PI3K despite EGFR inhibition. c-MET signaling has been implicated in the propagation and survival of GSCs specifically (Joo et al., 2012; Y. Li et al., 2011; Rath et al., 2013), and inhibition of c-MET has been shown to disrupt GBM pathogenesis in-vitro and in-vivo (Joo et al., 2012). Therefore, targeting c-MET may allow for direct targeting of GSCs, and targeting PI3K may target both GSCs and differentiated astrocytic GBM cells, leading to significantly reduced oncogenesis and increased survival.

In patients with EGFR amplification or EGFRVIII mutation, a phase II study is assessing the efficacy of dacomitinib, an irreversible pan-EGFR inhibitor. This inhibitor is effective in preventing the transautophosphorylation, and thus activation, of EGFR, HER2, and HER4, resulting in abrogated downstream signaling. Recently tested in those with non-small cell lung cancer (NSCLC), the results were unfortunately disappointing as the inhibitor failed to show any improvement in survival when compared to erlotinib, the EGFR inhibitor. In patients with NSCLC who received no benefit from chemotherapy or erlotinib treatment, dacomitinib also provided no

benefit. In-vitro data was recently published with dacomitinib on primary GBM cells and while the inhibitor did decrease phosphorylation of EGFR, it failed to have an effect on cell viability. However, the use of a PI3K/mTOR inhibitor in addition to dacomitinib inhibited cell proliferation in GBM cells with both EGFR amplification and PI3K activation through PI3K mutation or PTEN loss (Zhu & Shah, 2014). This study emphasizes the importance of targeting the appropriate patients with the appropriate treatments.

Multiple studies are underway targeting multiple signaling pathways in GBM including many others not discussed here. By identifying the type of mutations a patient has, we can directly target the signaling pathways leading to oncogenic progression. For example, if a patient does not have an EGFR amplified tumor, treatment with an EGFR inhibitor may not be effective. However, if the same patient has an activating mutation in PI3K, the use of a PI3K inhibitor may provide efficacious results. In addition, the identification of the GBM classification (pro-neural, neural, mesenchymal, classical) would be advantageous as the identification of multiple aberrant signaling pathways associated with each classification has been discovered. The future of GBM treatment, therefore, lies in personalized medicine.

REFERENCES

- Aggarwal, B. B., Schwarz, L., Hogan, M. E., & Rando, R. F. (1996). Triple helix-forming oligodeoxyribonucleotides targeted to the human tumor necrosis factor (TNF) gene inhibit TNF production and block the TNF-dependent growth of human glioblastoma tumor cells. *Cancer research*, 56(22), 5156-5164.
- Agnihotri, S., Burrell, K. E., Wolf, A., Jalali, S., Hawkins, C., Rutka, J. T., Zadeh, G. . (2013). Glioblastoma, a Brief Review of History, Molecular Genetics, Animal Models & Novel Therapeutic Strategies. *Arch. Immunol. Ther. Exp.*, 61, 25-41.
- Ahmed, S., Reynolds, B. A., & Weiss, S. (1995). BDNF enhances the differentiation but not the survival of CNS stem cell-derived neuronal precursors. *J Neurosci*, 15(8), 5765-5778.
- Akhavan, D., Cloughesy, T. F., & Mischel, P. S. (2010). mTOR signaling in glioblastoma: lessons learned from bench to bedside. *Neuro-oncology*, 12(8), 882-889.
- Akimoto, K., Takahashi, R., Moriya, S., Nishioka, N., Takayanagi, J., Kimura, K., . . . Ohno, S. (1996). EGF or PDGF receptors activate atypical PKC λ through phosphatidylinositol 3-kinase. *The EMBO journal*, 15(4), 788-798.
- Alcedo, J., & Kenyon, C. (2004). Regulation of *C. elegans* Longevity by Specific Gustatory and Olfactory Neurons. *Neuron*, 41(1), 45-55.
- Alvarez-Buylla, A., & Lim, D. A. (2004). For the long run: maintaining germinal niches in the adult brain. *Neuron*, 41(5), 683-686.
- Alvers, A. L., Wood, M. S., Hu, D., Kaywell, A. C., Dunn, W. A., Jr., & Aris, J. P. (2009). Autophagy is required for extension of yeast chronological life span by rapamycin. *Autophagy*, 5(6), 847-849.
- Andaloussi, A. E., Han, Y., & Lesniak, M. S. (2006). Prolongation of survival following depletion of CD4⁺ CD25⁺ regulatory T cells in mice with experimental brain tumors. *Journal of neurosurgery*, 105(3), 430-437.
- André, F., Bachelot, T., Campone, M., Dalenc, F., Perez-Garcia, J. M., Hurvitz, S. A., . . . Deudon, S. (2013). Targeting FGFR with dovitinib (TKI258): preclinical and clinical data in breast cancer. *Clinical Cancer Research*, 19(13), 3693-3702.
- Angevin, E., Lopez-Martin, J. A., Lin, C.-C., Gschwend, J. E., Harzstark, A., Castellano, D., . . . Shi, M. (2013). Phase I study of dovitinib (TKI258), an oral FGFR, VEGFR, and PDGFR inhibitor, in advanced or metastatic renal cell carcinoma. *Clinical Cancer Research*, 19(5), 1257-1268.
- Anisimov, V. N., Berstein, L. M., Egormin, P. A., Piskunova, T. S., Popovich, I. G., Zabezhinski, M. A., . . . Poroshina, T. E. (2008). Metformin slows down aging and extends life span of female SHR mice. *Cell Cycle*, 7(17), 2769-2773.

- Anisimov, V. N., Berstein, L. M., Popovich, I. G., Zabezhinski, M. A., Egormin, P. A., Piskunova, T. S., . . . Poroshina, T. E. (2011). If started early in life, metformin treatment increases life span and postpones tumors in female SHR mice. *Aging*, 3(2), 148-157.
- Apfeld, J., O'Connor, G., McDonagh, T., DiStefano, P. S., & Curtis, R. (2004). The AMP-activated protein kinase AAK-2 links energy levels and insulin-like signals to lifespan in *C. elegans*. *Genes & development*, 18(24), 3004-3009.
- Araki, K., Turner, A. P., Shaffer, V. O., Gangappa, S., Keller, S. A., Bachmann, M. F., . . . Ahmed, R. (2009). mTOR regulates memory CD8 T-cell differentiation. *Nature*, 460(7251), 108-112.
- Aranda, V., Haire, T., Nolan, M. E., Calarco, J. P., Rosenberg, A. Z., Fawcett, J. P., . . . Muthuswamy, S. K. (2006). Par6-aPKC uncouples ErbB2 induced disruption of polarized epithelial organization from proliferation control. *Nat Cell Biol*, 8(11), 1235-1245.
- Aranda, V., Haire, T., Nolan, M. E., Calarco, J. P., Rosenberg, A. Z., Fawcett, J. P., . . . Muthuswamy, S. K. (2006). Par6-aPKC uncouples ErbB2 induced disruption of polarized epithelial organization from proliferation control. *Nature cell biology*, 8(11), 1235-1245.
- Armstrong, L., Hughes, O., Yung, S., Hyslop, L., Stewart, R., Wappler, I., . . . Evans, J. (2006). The role of PI3K/AKT, MAPK/ERK and NF κ B signalling in the maintenance of human embryonic stem cell pluripotency and viability highlighted by transcriptional profiling and functional analysis. *Hum Mol Genet*, 15(11), 1894-1913.
- Atkinson, G. P., Nozell, S. E., & Benveniste, E. T. (2010). NF-kappaB and STAT3 signaling in glioma: targets for future therapies. *Expert Rev Neurother*, 10(4), 575-586.
- Auerbach, B. D., Osterweil, E. K., & Bear, M. F. (2011). Mutations causing syndromic autism define an axis of synaptic pathophysiology. *Nature*, 480(7375), 63-68.
- Ayuso-Sacido, A., Moliterno, J. A., Kratovac, S., Kapoor, G. S., O'Rourke, D. M., Holland, E. C., . . . Boockvar, J. A. (2010). Activated EGFR signaling increases proliferation, survival, and migration and blocks neuronal differentiation in post-natal neural stem cells. *Journal of neuro-oncology*, 97(3), 323-337.
- Badie, B., & Scharfner, J. M. (2000). Flow cytometric characterization of tumor-associated macrophages in experimental gliomas. *Neurosurgery*, 46(4), 957-961; discussion 961-952.
- Bailey, P., Cushing H. (1926). A classification of the tumors of the Glioma group on histogenetic basis with correlated study of prognosis. *Lippincott, Philadelphia*, 175.
- Balkwill, F. (2002). Tumor necrosis factor or tumor promoting factor? *Cytokine & growth factor reviews*, 13(2), 135-141.
- Balkwill, F. R., & Mantovani, A. (2012). Cancer-related inflammation: common themes and therapeutic opportunities. *Semin Cancer Biol*, 22(1), 33-40.

- Bao, S., Wu, Q., McLendon, R. E., Hao, Y., Shi, Q., Hjelmeland, A. B., . . . Rich, J. N. (2006). Glioma stem cells promote radioresistance by preferential activation of the DNA damage response. *Nature*, 444(7120), 756-760.
- Bello, L., Lucini, V., Costa, F., Pluderi, M., Giussani, C., Acerbi, F., . . . Bikfalvi, A. (2004). Combinatorial administration of molecules that simultaneously inhibit angiogenesis and invasion leads to increased therapeutic efficacy in mouse models of malignant glioma. *Clinical cancer research : an official journal of the American Association for Cancer Research*, 10(13), 4527-4537.
- Belluzzi, O., Benedusi, M., Ackman, J., & LoTurco, J. J. (2003). Electrophysiological differentiation of new neurons in the olfactory bulb. *J Neurosci*, 23(32), 10411-10418.
- Ben-Ari, Y. (2002). Excitatory actions of gaba during development: the nature of the nurture. *Nat Rev Neurosci*, 3(9), 728-739.
- Ben-Neriah, Y., & Karin, M. (2011). Inflammation meets cancer, with NF-kappaB as the matchmaker. *Nat Immunol*, 12(8), 715-723.
- Berger, F., Gay, E., Pelletier, L., Tropel, P., & Wion, D. (2004). Development of gliomas: potential role of asymmetrical cell division of neural stem cells. *The lancet oncology*, 5(8), 511-514.
- Berra, E., Diaz-Meco, M. T., Dominguez, I., Municio, M. M., Sanz, L., Lozano, J., . . . Moscat, J. (1993). Protein kinase C ζ isoform is critical for mitogenic signal transduction. *Cell*, 74(3), 555-563.
- Berstein, L. M. (2012). Metformin in obesity, cancer and aging: addressing controversies. *Aging*, 4(5), 320-329.
- Bettinger, I., Thanos, S., & Paulus, W. (2002). Microglia promote glioma migration. *Acta Neuropathol*, 103(4), 351-355.
- Bez, A., Corsini, E., Curti, D., Biggiogera, M., Colombo, A., Nicosia, R. F., . . . Parati, E. A. (2003). Neurosphere and neurosphere-forming cells: morphological and ultrastructural characterization. *Brain research*, 993(1), 18-29.
- Bhat, K. P., Balasubramanian, V., Vaillant, B., Ezhilarasan, R., Hummelink, K., Hollingsworth, F., . . . Aldape, K. (2013). Mesenchymal Differentiation Mediated by NF-kappaB Promotes Radiation Resistance in Glioblastoma. *Cancer Cell*, 24(3), 331-346.
- Bissell, M. J., & Hines, W. C. (2011). Why don't we get more cancer? A proposed role of the microenvironment in restraining cancer progression. *Nat Med*, 17(3), 320-329.
- Bissell, M. J., & Hines, W. C. (2011). Why don't we get more cancer? A proposed role of the microenvironment in restraining cancer progression. *Nature medicine*, 17(3), 320-329.
- Bissell, M. J., & Labarge, M. A. (2005). Context, tissue plasticity, and cancer: are tumor stem cells also regulated by the microenvironment? *Cancer Cell*, 7(1), 17-23.

- Biswas, D. K., Cruz, A. P., Gansberger, E., & Pardee, A. B. (2000). Epidermal growth factor-induced nuclear factor κ B activation: A major pathway of cell-cycle progression in estrogen-receptor negative breast cancer cells. *Proceedings of the National Academy of Sciences*, 97(15), 8542-8547.
- Bivona, T. G., Hieronymus, H., Parker, J., Chang, K., Taron, M., Rosell, R., . . . Sawyers, C. L. (2011). FAS and NF-kappaB signalling modulate dependence of lung cancers on mutant EGFR. *Nature*, 471(7339), 523-526.
- Blackwood, D. H., Fordyce, A., Walker, M. T., St Clair, D. M., Porteous, D. J., & Muir, W. J. (2001). Schizophrenia and affective disorders--cosegregation with a translocation at chromosome 1q42 that directly disrupts brain-expressed genes: clinical and P300 findings in a family. *Am J Hum Genet*, 69(2), 428-433.
- Boccaccio, C., & Comoglio, P. M. (2006). Invasive growth: a MET-driven genetic programme for cancer and stem cells. *Nature reviews cancer*, 6(8), 637-645.
- Bonavia, R., Cavenee, W. K., & Furnari, F. B. (2011). Heterogeneity maintenance in glioblastoma: a social network. *Cancer research*, 71(12), 4055-4060.
- Bonavia, R., Inda, M. M., Cavenee, W. K., & Furnari, F. B. (2011). Heterogeneity maintenance in glioblastoma: a social network. *Cancer Res*, 71(12), 4055-4060.
- Bonavia, R., Inda, M. M., Vandenberg, S., Cheng, S. Y., Nagane, M., Hadwiger, P., . . . Furnari, F. B. (2012). EGFRvIII promotes glioma angiogenesis and growth through the NF-kappaB, interleukin-8 pathway. *Oncogene*, 31(36), 4054-4066.
- Bowerman, B., & Shelton, C. A. (1999). Cell polarity in the early *Caenorhabditis elegans* embryo. *Current opinion in genetics & development*, 9(4), 390-395.
- Bracko, O., Singer, T., Aigner, S., Knobloch, M., Winner, B., Ray, J., . . . Jessberger, S. (2012). Gene expression profiling of neural stem cells and their neuronal progeny reveals IGF2 as a regulator of adult hippocampal neurogenesis. *J Neurosci*, 32(10), 3376-3387.
- Brandes, A. A., Franceschi, E., Tosoni, A., Blatt, V., Pession, A., Tallini, G., . . . Ermani, M. (2008). MGMT promoter methylation status can predict the incidence and outcome of pseudoprogression after concomitant radiochemotherapy in newly diagnosed glioblastoma patients. *Journal of clinical oncology : official journal of the American Society of Clinical Oncology*, 26(13), 2192-2197.
- Bredel, M., Scholtens, D. M., Yadav, A. K., Alvarez, A. A., Renfrow, J. J., Chandler, J. P., . . . Harsh, G. R. t. (2011). NFKBIA deletion in glioblastomas. *N Engl J Med*, 364(7), 627-637.
- Bredel, M., Scholtens, D. M., Yadav, A. K., Alvarez, A. A., Renfrow, J. J., Chandler, J. P., . . . Tagge, M. J. (2011). NFKBIA deletion in glioblastomas. *New England Journal of Medicine*, 364(7), 627-637.
- Brennan, C. W., Verhaak, R. G., McKenna, A., Campos, B., Nounshmehr, H., Salama, S. R., . . . Chin, L. (2013). The somatic genomic landscape of glioblastoma. *Cell*, 155(2), 462-477.

- Breton-Provencher, V., Lemasson, M., Peralta, M. R., 3rd, & Saghatelian, A. (2009). Interneurons produced in adulthood are required for the normal functioning of the olfactory bulb network and for the execution of selected olfactory behaviors. *J Neurosci*, 29(48), 15245-15257.
- Briers, T. W., Desmaretz, C., & Vanmechelen, E. (1994). Generation and characterization of mouse microglial cell lines. *Journal of neuroimmunology*, 52(2), 153-164.
- Brown, C. E., Vishwanath, R. P., Aguilar, B., Starr, R., Najbauer, J., Aboody, K. S., & Jensen, M. C. (2007). Tumor-derived chemokine MCP-1/CCL2 is sufficient for mediating tumor tropism of adoptively transferred T cells. *The Journal of Immunology*, 179(5), 3332-3341.
- Brown, J., Cooper-Kuhn, C. M., Kempermann, G., Van Praag, H., Winkler, J., Gage, F. H., & Kuhn, H. G. (2003). Enriched environment and physical activity stimulate hippocampal but not olfactory bulb neurogenesis. *Eur J Neurosci*, 17(10), 2042-2046.
- Bultje, R. S., Castaneda-Castellanos, D. R., Jan, L. Y., Jan, Y.-N., Kriegstein, A. R., & Shi, S.-H. (2009). Mammalian Par3 regulates progenitor cell asymmetric division via notch signaling in the developing neocortex. *Neuron*, 63(2), 189-202.
- Cacci, E., Ajmone-Cat, M. A., Anelli, T., Biagioni, S., & Minghetti, L. (2008). In vitro neuronal and glial differentiation from embryonic or adult neural precursor cells are differently affected by chronic or acute activation of microglia. *Glia*, 56(4), 412-425.
- Capaccione, K. M., & Pine, S. R. (2013). The Notch signaling pathway as a mediator of tumor survival. *Carcinogenesis*, 34(7), 1420-1430.
- Carlen, M., Cassidy, R. M., Brismar, H., Smith, G. A., Enquist, L. W., & Frisen, J. (2002). Functional integration of adult-born neurons. *Curr Biol*, 12(7), 606-608.
- Carleton, A., Petreanu, L. T., Lansford, R., Alvarez-Buylla, A., & Lledo, P. M. (2003). Becoming a new neuron in the adult olfactory bulb. *Nat Neurosci*, 6(5), 507-518.
- Chang, S. M., Wen, P., Cloughesy, T., Greenberg, H., Schiff, D., Conrad, C., . . . Raizer, J. (2005). Phase II study of CCI-779 in patients with recurrent glioblastoma multiforme. *Investigational new drugs*, 23(4), 357-361.
- Charles, N. A., Holland, E. C., Gilbertson, R., Glass, R., & Kettenmann, H. (2011). The brain tumor microenvironment. *Glia*, 59(8), 1169-1180.
- Charles, N. A., Holland, E. C., Gilbertson, R., Glass, R., & Kettenmann, H. (2011). The brain tumor microenvironment. *Glia*, 59(8), 1169-1180.
- Chaturvedi, M. M., Sung, B., Yadav, V. R., Kannappan, R., & Aggarwal, B. B. (2011a). NF-kappaB addiction and its role in cancer: 'one size does not fit all'. *Oncogene*, 30(14), 1615-1630.
- Chaturvedi, M. M., Sung, B., Yadav, V. R., Kannappan, R., & Aggarwal, B. B. (2011b). NF-kB addiction and its role in cancer: 'one size does not fit all'. *Oncogene*, 30(14), 1615-1630.

- Chen, J., Kesari, S., Rooney, C., Strack, P. R., Chen, J., Shen, H., . . . Griffin, J. D. (2010). Inhibition of notch signaling blocks growth of glioblastoma cell lines and tumor neurospheres. *Genes & cancer*, 1(8), 822-835.
- Chen, J., Li, Y., Yu, T.-S., McKay, R. M., Burns, D. K., Kernie, S. G., & Parada, L. F. (2012). A restricted cell population propagates glioblastoma growth after chemotherapy. *Nature*, 488(7412), 522-526.
- Chen, Z. Y., Bath, K., McEwen, B., Hempstead, B., & Lee, F. (2008). Impact of genetic variant BDNF (Val66Met) on brain structure and function. *Novartis Found Symp*, 289, 180-188; discussion 188-195.
- Cho, J., Pastorino, S., Zeng, Q., Xu, X., Johnson, W., Vandenberg, S., . . . Dutt, A. (2011). Glioblastoma-derived epidermal growth factor receptor carboxyl-terminal deletion mutants are transforming and are sensitive to EGFR-directed therapies. *Cancer research*, 71(24), 7587-7596.
- Cloughesy, T. F., Yoshimoto, K., Nghiemphu, P., Brown, K., Dang, J., Zhu, S., . . . Youngkin, D. (2008). Antitumor activity of rapamycin in a Phase I trial for patients with recurrent PTEN-deficient glioblastoma. *PLoS medicine*, 5(1), e8.
- Cohen, E. E., Lingen, M. W., Zhu, B., Zhu, H., Straza, M. W., Pierce, C., . . . Rosner, M. R. (2006). Protein kinase C zeta mediates epidermal growth factor-induced growth of head and neck tumor cells by regulating mitogen-activated protein kinase. *Cancer research*, 66(12), 6296-6303.
- Coniglio, S. J., Eugenin, E., Dobrenis, K., Stanley, E. R., West, B. L., Symons, M. H., & Segall, J. E. (2012). Microglial stimulation of glioblastoma invasion involves epidermal growth factor receptor (EGFR) and colony stimulating factor 1 receptor (CSF-1R) signaling. *Mol Med*, 18, 519-527. doi: 10.2119/molmed.2011.00217
- Coons, S. W., & JOHNSON, P. C. (1993). Regional heterogeneity in the proliferative activity of human gliomas as measured by the Ki-67 labeling index. *Journal of Neuropathology & Experimental Neurology*, 52(6), 609-618.
- Cornu, M., Albert, V., & Hall, M. N. (2013). mTOR in aging, metabolism, and cancer. *Current opinion in genetics & development*, 23(1), 53-62.
- Costa, M. R., Wen, G., Lepier, A., Schroeder, T., & Götz, M. (2008). Par-complex proteins promote proliferative progenitor divisions in the developing mouse cerebral cortex. *Development*, 135(1), 11-22.
- Coussens, L. M., & Werb, Z. (2002). Inflammation and cancer. *Nature*, 420(6917), 860-867.
- Coussens, L. M., Zitvogel, L., & Palucka, A. K. (2013). Neutralizing tumor-promoting chronic inflammation: a magic bullet? *Science*, 339(6117), 286-291.
- Craig, C. G., Tropepe, V., Morshead, C. M., Reynolds, B. A., Weiss, S., & Van der Kooy, D. (1996). In vivo growth factor expansion of endogenous subependymal neural precursor

- cell populations in the adult mouse brain. *The Journal of Neuroscience*, 16(8), 2649-2658.
- Dandy, W. (1928). Removal of right cerebral hemisphere for certain tumors with hemiplegia: preliminary report. *JAMA*, 90(3), 101.
- Das, R. M., & Storey, K. G. (2014). Apical Abscission Alters Cell Polarity and Dismantles the Primary Cilium During Neurogenesis. *Science*, 343(6167), 200-204.
- David, D. J., Samuels, B. A., Rainer, Q., Wang, J.-W., Marsteller, D., Mendez, I., . . . Guilloux, J.-P. (2009). Neurogenesis-dependent and-independent effects of fluoxetine in an animal model of anxiety/depression. *Neuron*, 62(4), 479-493.
- Davis, E., Foster, T., & Thomas, W. (1994). Cellular forms and functions of brain microglia. *Brain research bulletin*, 34(1), 73-78.
- Day, B. W., Stringer, B. W., Al-Ejeh, F., Ting, M. J., Wilson, J., Ensbey, K. S., . . . Offenhäuser, C. (2013). EphA3 maintains tumorigenicity and is a therapeutic target in glioblastoma multiforme. *Cancer Cell*, 23(2), 238-248.
- Dayer, A. G., Ford, A. A., Cleaver, K. M., Yassaee, M., & Cameron, H. A. (2003). Short-term and long-term survival of new neurons in the rat dentate gyrus. *J Comp Neurol*, 460(4), 563-572.
- De Palma, M., Venneri, M. A., Galli, R., Sergi, L. S., Politi, L. S., Sampaolesi, M., & Naldini, L. (2005). Tie2 identifies a hematopoietic lineage of proangiogenic monocytes required for tumor vessel formation and a mesenchymal population of pericyte progenitors. *Cancer Cell*, 8(3), 211-226.
- Deng, W., Aimone, J. B., & Gage, F. H. (2010). New neurons and new memories: how does adult hippocampal neurogenesis affect learning and memory? *Nature Reviews Neuroscience*, 11(5), 339-350.
- Diaz-Meco, M. T., Dominguez, I., Sanz, L., Dent, P., Lozano, J., Municio, M. M., . . . Moscat, J. (1994). zeta PKC induces phosphorylation and inactivation of I kappa B-alpha in vitro. *Embo J*, 13(12), 2842-2848.
- Diaz-Meco, M. T., & Moscat, J. (2001). MEK5, a new target of the atypical protein kinase C isoforms in mitogenic signaling. *Molecular and cellular biology*, 21(4), 1218-1227.
- do Carmo, A., Balca-Silva, J., Matias, D., & Lopes, M. C. (2013). PKC signaling in glioblastoma. *Cancer Biol Ther*, 14(4), 287-294.
- Doetsch, F., Caille, I., Lim, D. A., García-Verdugo, J. M., & Alvarez-Buylla, A. (1999). Subventricular zone astrocytes are neural stem cells in the adult mammalian brain. *Cell*, 97(6), 703-716.
- Doetsch, F., Petreanu, L., Caille, I., Garcia-Verdugo, J. M., & Alvarez-Buylla, A. (2002). EGF converts transit-amplifying neurogenic precursors in the adult brain into multipotent stem cells. *Neuron*, 36(6), 1021-1034.

- Doherty, L., Gigas, D. C., Kesari, S., Drappatz, J., Kim, R., Zimmerman, J., . . . Wen, P. Y. (2006). Pilot study of the combination of EGFR and mTOR inhibitors in recurrent malignant gliomas. *Neurology*, 67(1), 156-158.
- Dorsky, R. I., Chang, W. S., Rapaport, D. H., & Harris, W. A. (1997). Regulation of neuronal diversity in the Xenopus retina by Delta signalling. *Nature*, 385, 67-70.
- Drappatz, J., Norden, A. D., & Wen, P. Y. (2009). Therapeutic strategies for inhibiting invasion in glioblastoma. *Expert Review of Neurotherapeutics*, 9(4): 519-534.
- Dreesen, O., & Brivanlou, A. H. (2007). Signaling pathways in cancer and embryonic stem cells. *Stem cell reviews*, 3(1), 7-17.
- Dudkin, L., Dilling, M. B., Cheshire, P. J., Harwood, F. C., Hollingshead, M., Arbuck, S. G., . . . Houghton, P. J. (2001). Biochemical correlates of mTOR inhibition by the rapamycin ester CCI-779 and tumor growth inhibition. *Clinical cancer research : an official journal of the American Association for Cancer Research*, 7(6), 1758-1764.
- Duran, A., Diaz-Meco, M. T., & Moscat, J. (2003). Essential role of RelA Ser311 phosphorylation by zetaPKC in NF-kappaB transcriptional activation. *Embo J*, 22(15), 3910-3918.
- Easton, R. M., Cho, H., Roovers, K., Shineman, D. W., Mizrahi, M., Forman, M. S., . . . Oltersdorf, T. (2005). Role for Akt3/protein kinase B in attainment of normal brain size. *Molecular and cellular biology*, 25(5), 1869-1878.
- El Andaloussi, A., & Lesniak, M. S. (2006). An increase in CD4+ CD25+ FOXP3+ regulatory T cells in tumor-infiltrating lymphocytes of human glioblastoma multiforme. *Neuro-oncology*, 8(3), 234-243.
- El Andaloussi, A., & Lesniak, M. S. (2007). CD4+ CD25+ FoxP3+ T-cell infiltration and heme oxygenase-1 expression correlate with tumor grade in human gliomas. *Journal of neuro-oncology*, 83(2), 145-152.
- Englund, C., Fink, A., Lau, C., Pham, D., Daza, R. A., Bulfone, A., . . . Hevner, R. F. (2005). Pax6, Tbr2, and Tbr1 are expressed sequentially by radial glia, intermediate progenitor cells, and postmitotic neurons in developing neocortex. *The Journal of Neuroscience*, 25(1), 247-251.
- Enwere, E., Shingo, T., Gregg, C., Fujikawa, H., Ohta, S., & Weiss, S. (2004). Aging results in reduced epidermal growth factor receptor signaling, diminished olfactory neurogenesis, and deficits in fine olfactory discrimination. *J Neurosci*, 24(38), 8354-8365.
- Eshleman, J. S., Carlson, B. L., Mladek, A. C., Kastner, B. D., Shide, K. L., & Sarkaria, J. N. (2002). Inhibition of the Mammalian Target of Rapamycin Sensitizes U87 Xenografts to Fractionated Radiation Therapy. *Cancer research*, 62(24), 7291-7297.
- Fan, Q.-W., Cheng, C., Knight, Z. A., Haas-Kogan, D., Stokoe, D., James, C. D., . . . Weiss, W. A. (2009). EGFR signals to mTOR through PKC and independently of Akt in glioma. *Science signaling*, 2(55), ra4.

- Fan, Q. W., Cheng, C. K., Gustafson, W. C., Charron, E., Zipper, P., Wong, R. A., . . . Weiss, W. A. (2013). EGFR phosphorylates tumor-derived EGFRvIII driving STAT3/5 and progression in glioblastoma. *Cancer Cell*, 24(4), 438-449.
- Fan, X., Khaki, L., Zhu, T. S., Soules, M. E., Talsma, C. E., Gul, N., . . . Maciaczyk, J. (2010). NOTCH Pathway Blockade Depletes CD133-Positive Glioblastoma Cells and Inhibits Growth of Tumor Neurospheres and Xenografts. *Stem cells*, 28(1), 5-16.
- Farmer, J.-P., Antel, J. P., Freedman, M., Cashman, N. R., Rode, H., & Villemure, J.-G. (1989). Characterization of lymphoid cells isolated from human gliomas. *Journal of neurosurgery*, 71(4), 528-533.
- Ferla, R., Haspinger, E., & Surmacz, E. (2012). Metformin inhibits leptin-induced growth and migration of glioblastoma cells. *Oncology letters*, 4(5), 1077-1081.
- Ferrara, N., & Henzel, W. J. (1989). Pituitary follicular cells secrete a novel heparin-binding growth factor specific for vascular endothelial cells. *Biochemical and biophysical research communications*, 161(2), 851-858.
- Ferron, S. R., Pozo, N., Laguna, A., Aranda, S., Porlan, E., Moreno, M., . . . Arbonés, M. L. (2010). Regulated segregation of kinase Dyrk1A during asymmetric neural stem cell division is critical for EGFR-mediated biased signaling. *Cell stem cell*, 7(3), 367-379.
- Fingar, D. C., & Blenis, J. (2004). Target of rapamycin (TOR): an integrator of nutrient and growth factor signals and coordinator of cell growth and cell cycle progression. *Oncogene*, 23(18), 3151-3171.
- Fishwick, K. J., Li, R. A., Halley, P., Deng, P., & Storey, K. G. (2010). Initiation of neuronal differentiation requires PI3-kinase/TOR signalling in the vertebrate neural tube. *Developmental biology*, 338(2), 215-225.
- Forstreuter, F., Lucius, R., & Mentlein, R. (2002). Vascular endothelial growth factor induces chemotaxis and proliferation of microglial cells. *Journal of neuroimmunology*, 132(1), 93-98.
- Franz, D. N., Leonard, J., Tudor, C., Chuck, G., Care, M., Sethuraman, G., . . . Crone, K. R. (2006). Rapamycin causes regression of astrocytomas in tuberous sclerosis complex. *Annals of neurology*, 59(3), 490-498.
- Furnari, F. B., Fenton, T., Bachoo, R. M., Mukasa, A., Stommel, J. M., Stegh, A., . . . Cavenee, W. K. (2007). Malignant astrocytic glioma: genetics, biology, and paths to treatment. *Genes & development*, 21(21), 2683-2710.
- Gage, F. H. (2002). Neurogenesis in the adult brain. *The Journal of Neuroscience*, 22(3), 612-613.
- Gaiano, N., & Fishell, G. (2002). The role of notch in promoting glial and neural stem cell fates. *Annual Review of Neuroscience*, 25(1), 471-490.

- Gaiano, N., Nye, J. S., & Fishell, G. (2000). Radial glial identity is promoted by Notch1 signaling in the murine forebrain. *Neuron*, 26(2), 395-404.
- Galanis, E., Buckner, J. C., Maurer, M. J., Kreisberg, J. I., Ballman, K., Boni, J., . . . Walsh, D. J. (2005). Phase II Trial of Temsirolimus (CCI-779) in Recurrent Glioblastoma Multiforme: A North Central Cancer Treatment Group Study. *Journal of Clinical Oncology*, 23(23), 5294-5304.
- Galarneau, H., Villeneuve, J., Gowing, G., Julien, J. P., & Vallieres, L. (2007). Increased glioma growth in mice depleted of macrophages. *Cancer Res*, 67(18), 8874-8881.
- Gao, N., Flynn, D. C., Zhang, Z., Zhong, X. S., Walker, V., Liu, K. J., . . . Jiang, B. H. (2004). G1 cell cycle progression and the expression of G1 cyclins are regulated by PI3K/AKT/mTOR/p70S6K1 signaling in human ovarian cancer cells. *American journal of physiology. Cell physiology*, 287(2), C281-291.
- Gao, N., Zhang, Z., Jiang, B.-H., & Shi, X. (2003). Role of PI3K/AKT/mTOR signaling in the cell cycle progression of human prostate cancer. *Biochemical and biophysical research communications*, 310(4), 1124-1132.
- Gao, X., McDonald, J. T., Hlatky, L., & Enderling, H. (2013). Acute and fractionated irradiation differentially modulate glioma stem cell division kinetics. *Cancer research*, 73(5), 1481-1490.
- Gheusi, G., Cremer, H., McLean, H., Chazal, G., Vincent, J. D., & Lledo, P. M. (2000). Importance of newly generated neurons in the adult olfactory bulb for odor discrimination. *Proc Natl Acad Sci U S A*, 97(4), 1823-1828.
- Ghosh, S., Marquardt, T., Thaler, J. P., Carter, N., Andrews, S. E., Pfaff, S. L., & Hunter, T. (2008a). Instructive role of aPKCzeta subcellular localization in the assembly of adherens junctions in neural progenitors. *Proc Natl Acad Sci U S A*, 105(1), 335-340.
- Ghosh, S., Tergaonkar, V., Rothlin, C. V., Correa, R. G., Bottero, V., Bist, P., . . . Hunter, T. (2006). Essential role of tuberous sclerosis genes TSC1 and TSC2 in NF-kappaB activation and cell survival. *Cancer Cell*, 10(3), 215-226.
- Giannini, C., Sarkaria, J. N., Saito, A., Uhm, J. H., Galanis, E., Carlson, B. L., . . . James, C. D. (2005b). Patient tumor EGFR and PDGFRA gene amplifications retained in an invasive intracranial xenograft model of glioblastoma multiforme. *Neuro-oncology*, 7(2), 164-176.
- Gilbert, M. R. (2011). Recurrent glioblastoma: a fresh look at current therapies and emerging novel approaches. *Semin Oncol*, 38 Suppl 4, S21-33. doi: 10.1053/j.seminoncol.2011.09.008
- Goswami, S., Gupta, A., & Sharma, S. K. (1998). Interleukin-6-mediated autocrine growth promotion in human glioblastoma multiforme cell line U87MG. *J Neurochem*, 71(5), 1837-1845.
- Grivennikov, S. I., & Karin, M. (2010). Inflammation and oncogenesis: a vicious connection. *Curr Opin Genet Dev*, 20(1), 65-71.

- Grivennikov, S. I., & Karin, M. (2011). Inflammatory cytokines in cancer: tumour necrosis factor and interleukin 6 take the stage. *Ann Rheum Dis*, 70 Suppl 1, i104-108.
- Guertin, D. A., & Sabatini, D. M. (2009). The pharmacology of mTOR inhibition. *Science signaling*, 2(67), pe24.
- Habib, A. A., Chatterjee, S., Park, S.-K., Ratan, R. R., Lefebvre, S., & Vartanian, T. (2001). The Epidermal Growth Factor Receptor Engages Receptor Interacting Protein and Nuclear Factor- κ B (NF- κ B)-inducing Kinase to Activate NF- κ B: IDENTIFICATION OF A NOVEL RECEPTOR-TYROSINE KINASE SIGNALOSOME. *Journal of Biological Chemistry*, 276(12), 8865-8874.
- Halloran, J., Hussong, S. A., Burbank, R., Podlutsкая, N., Fischer, K. E., Sloane, L. B., . . . Hart, M. J. (2012). Chronic inhibition of mammalian target of rapamycin by rapamycin modulates cognitive and non-cognitive components of behavior throughout lifespan in mice. *Neuroscience*, 223, 102-113.
- Han, J., Wang, B., Xiao, Z., Gao, Y., Zhao, Y., Zhang, J., . . . Dai, J. (2008). Mammalian target of rapamycin (mTOR) is involved in the neuronal differentiation of neural progenitors induced by insulin. *Molecular and Cellular Neuroscience*, 39(1), 118-124.
- Hanahan, D., & Weinberg, R. A. (2011). Hallmarks of cancer: the next generation. *Cell*, 144(5), 646-674.
- Harrison, D. E., Strong, R., Sharp, Z. D., Nelson, J. F., Astle, C. M., Flurkey, K., . . . Carter, C. S. (2009). Rapamycin fed late in life extends lifespan in genetically heterogeneous mice. *Nature*, 460(7253), 392-395.
- Hars, E. S., Qi, H., Ryazanov, A. G., Jin, S., Cai, L., Hu, C., & Liu, L. F. (2007). Autophagy regulates ageing in *C. elegans*. *Autophagy*, 3(2), 93.
- Hayden, M. S., & Ghosh, S. (2008). Shared principles in NF- κ B signaling. *Cell*, 132(3), 344-362.
- Hegi, M. E., Diserens, A.-C., Gorlia, T., Hamou, M.-F., de Tribolet, N., Weller, M., . . . Mariani, L. (2005). MGMT gene silencing and benefit from temozolomide in glioblastoma. *New England Journal of Medicine*, 352(10), 997-1003.
- Hennessy, B. T., Smith, D. L., Ram, P. T., Lu, Y., & Mills, G. B. (2005). Exploiting the PI3K/AKT pathway for cancer drug discovery. *Nature Reviews Drug Discovery*, 4(12), 988-1004.
- Herrera-Velit, P., Knutson, K. L., & Reiner, N. E. (1997). Phosphatidylinositol 3-kinase-dependent activation of protein kinase C-zeta in bacterial lipopolysaccharide-treated human monocytes. *The Journal of biological chemistry*, 272(26), 16445-16452.
- Hirai, T., & Chida, K. (2003). Protein kinase Czeta (PKCzeta): activation mechanisms and cellular functions. *Journal of Biochemistry*, 133(1), 1-7.
- Hirano, Y., Yoshinaga, S., Ogura, K., Yokochi, M., Noda, Y., Sumimoto, H., & Inagaki, F. (2004). Solution structure of atypical protein kinase C PB1 domain and its mode of interaction with ZIP/p62 and MEK5. *J Biol Chem*, 279(30), 31883-31890.

- Hoelzinger, D. B., Demuth, T., & Berens, M. E. (2007). Autocrine factors that sustain glioma invasion and paracrine biology in the brain microenvironment. *Journal of the National Cancer Institute*, 99(21), 1583-1593.
- Hsu, P. P., Kang, S. A., Rameseder, J., Zhang, Y., Ottina, K. A., Lim, D., . . . Sabatini, D. M. (2011). The mTOR-regulated phosphoproteome reveals a mechanism of mTORC1-mediated inhibition of growth factor signaling. *Science (New York, N.Y.)*, 332(6035), 1317-1322.
- Hu, X., Pandolfi, P. P., Li, Y., Koutcher, J. A., Rosenblum, M., & Holland, E. C. (2005). mTOR promotes survival and astrocytic characteristics induced by Pten/AKT signaling in glioblastoma. *Neoplasia (New York, NY)*, 7(4), 356.
- Huang, J., & Manning, B. D. (2009). A complex interplay between Akt, TSC2 and the two mTOR complexes. *Biochemical Society transactions*, 37(Pt 1), 217-222.
- Huang, P. H., Mukasa, A., Bonavia, R., Flynn, R. A., Brewer, Z. E., Cavenee, W. K., . . . White, F. M. (2007). Quantitative analysis of EGFRvIII cellular signaling networks reveals a combinatorial therapeutic strategy for glioblastoma. *Proceedings of the National Academy of Sciences of the United States of America*, 104(31), 12867-12872.
- Huang, S., Bjornsti, M.-A., & Houghton, P. J. (2003). Mechanism of Action and Cellular Resistance. *Cancer biology & therapy*, 2(3), 222-232.
- Huettner, C., Czub, S., Kerkau, S., Roggendorf, W., & Tonn, J. (1996). Interleukin 10 is expressed in human gliomas in vivo and increases glioma cell proliferation and motility in vitro. *Anticancer Res*, 17(5A), 3217-3224.
- Hung, T.-J., & Kemphues, K. J. (1999). PAR-6 is a conserved PDZ domain-containing protein that colocalizes with PAR-3 in *Caenorhabditis elegans* embryos. *Development*, 126(1), 127-135.
- Huse, J. T., Holland, E., & DeAngelis, L. M. (2013). Glioblastoma: molecular analysis and clinical implications. *Annual Review of Medicine*, 64, 59-70.
- Huse, J. T., & Holland, E. C. (2010). Targeting brain cancer: advances in the molecular pathology of malignant glioma and medulloblastoma. *Nature reviews cancer*, 10(5), 319-331.
- Hussain, S. F., Yang, D., Suki, D., Aldape, K., Grimm, E., & Heimberger, A. B. (2006). The role of human glioma-infiltrating microglia/macrophages in mediating antitumor immune responses. *Neuro Oncol*, 8(3), 261-279.
- Huynh, H., Chow, P. K. H., Tai, W. M., Choo, S. P., Chung, A. Y. F., Ong, H. S., . . . Shi, M. M. (2012). Dovitinib demonstrates antitumor and antimetastatic activities in xenograft models of hepatocellular carcinoma. *Journal of hepatology*, 56(3), 595-601.
- Ignatova, T. N., Kukekov, V. G., Laywell, E. D., Suslov, O. N., Vrionis, F. D., & Steindler, D. A. (2002). Human cortical glial tumors contain neural stem-like cells expressing astroglial and neuronal markers in vitro. *Glia*, 39(3), 193-206.

- Imai, F., Hirai, S.-i., Akimoto, K., Koyama, H., Miyata, T., Ogawa, M., . . . Ohno, S. (2006). Inactivation of aPKC λ results in the loss of adherens junctions in neuroepithelial cells without affecting neurogenesis in mouse neocortex. *Development*, 133(9), 1735-1744.
- Inda, M. M., Bonavia, R., Mukasa, A., Narita, Y., Sah, D. W., Vandenberg, S., . . . Furnari, F. (2010). Tumor heterogeneity is an active process maintained by a mutant EGFR-induced cytokine circuit in glioblastoma. *Genes Dev*, 24(16), 1731-1745.
- Ingram, D. K., Zhu, M., Mamczarz, J., Zou, S., Lane, M. A., Roth, G. S., & DeCabo, R. (2006). Calorie restriction mimetics: an emerging research field. *Aging cell*, 5(2), 97-108.
- Inoki, K., Corradetti, M. N., & Guan, K.-L. (2005). Dysregulation of the TSC-mTOR pathway in human disease. *Nature genetics*, 37(1), 19-24.
- Iosif, R. E., Ekdahl, C. T., Ahlenius, H., Pronk, C. J., Bonde, S., Kokaia, Z., . . . Lindvall, O. (2006). Tumor necrosis factor receptor 1 is a negative regulator of progenitor proliferation in adult hippocampal neurogenesis. *The Journal of neuroscience : the official journal of the Society for Neuroscience*, 26(38), 9703-9712.
- Iso, T., Kedes, L., & Hamamori, Y. (2003). HES and HERP families: multiple effectors of the Notch signaling pathway. *Journal of cellular physiology*, 194(3), 237-255.
- Jacinto, E., & Hall, M. N. (2003). Tor signalling in bugs, brain and brawn. *Nature reviews Molecular cell biology*, 4(2), 117-126.
- Johnson, B. E., Mazor, T., Hong, C., Barnes, M., Aihara, K., McLean, C. Y., . . . Tatsuno, K. (2014). Mutational analysis reveals the origin and therapy-driven evolution of recurrent glioma. *Science*, 343(6167), 189-193.
- Johnson, S. C., Rabinovitch, P. S., & Kaeberlein, M. (2013). mTOR is a key modulator of ageing and age-related disease. *Nature*, 493(7432), 338-345.
- Joo, K. M., Jin, J., Kim, E., Ho Kim, K., Kim, Y., Gu Kang, B., . . . Nam, D. H. (2012). MET signaling regulates glioblastoma stem cells. *Cancer Res*, 72(15), 3828-3838.
- Jun, H. J., Acquaviva, J., Chi, D., Lessard, J., Zhu, H., Woolfenden, S., . . . Charest, A. (2011). Acquired MET expression confers resistance to EGFR inhibition in a mouse model of glioblastoma multiforme. *Oncogene*.
- Kapoor, G. S., Zhan, Y., Johnson, G. R., & O'Rourke, D. M. (2004). Distinct domains in the SHP-2 phosphatase differentially regulate epidermal growth factor receptor/NF-kappaB activation through Gab1 in glioblastoma cells. *Mol Cell Biol*, 24(2), 823-836.
- Kappeler, L., De Magalhaes Filho, C., Dupont, J., Leneuve, P., Cervera, P., Périn, L., . . . Epelbaum, J. (2008). Brain IGF-1 receptors control mammalian growth and lifespan through a neuroendocrine mechanism. *PLoS biology*, 6(10), e254.
- Karin, M. (2009). NF-kappaB as a critical link between inflammation and cancer. *Cold Spring Harb Perspect Biol*, 1(5), a000141.

- Katoh-Semba, R., Asano, T., Ueda, H., Morishita, R., Takeuchi, I. K., Inaguma, Y., & Kato, K. (2002). Riluzole enhances expression of brain-derived neurotrophic factor with consequent proliferation of granule precursor cells in the rat hippocampus. *FASEB J*, 16(10), 1328-1330.
- Kee, N., Sivalingam, S., Boonstra, R., & Wojtowicz, J. M. (2002). The utility of Ki-67 and BrdU as proliferative markers of adult neurogenesis. *Journal of neuroscience methods*, 115(1), 97-105.
- Kempermann, G., Gast, D., Kronenberg, G., Yamaguchi, M., & Gage, F. H. (2003). Early determination and long-term persistence of adult-generated new neurons in the hippocampus of mice. *Development*, 130(2), 391-399.
- Kemphues, K. J., & Strome, S. (1997). 13 Fertilization and Establishment of Polarity in the Embryo. *Cold Spring Harbor Monograph Archive*, 33, 335-359.
- Kenerson, H., Dundon, T. A., & Yeung, R. S. (2005). Effects of rapamycin in the Eker rat model of tuberous sclerosis complex. *Pediatric research*, 57(1), 67-75.
- Kenerson, H. L., Aicher, L. D., True, L. D., & Yeung, R. S. (2002). Activated mammalian target of rapamycin pathway in the pathogenesis of tuberous sclerosis complex renal tumors. *Cancer research*, 62(20), 5645-5650.
- Kesari, S. (2011). Understanding glioblastoma tumor biology: the potential to improve current diagnosis and treatments. *Semin Oncol*, 38 Suppl 4, S2-10.
- Kessenbrock, K., Plaks, V., & Werb, Z. (2010). Matrix metalloproteinases: regulators of the tumor microenvironment. *Cell*, 141(1), 52-67.
- Kim, J. Y., Duan, X., Liu, C. Y., Jang, M.-H., Guo, J. U., Pow-anpongkul, N., . . . Ming, G.-I. (2009). DISC1 regulates new neuron development in the adult brain via modulation of AKT-mTOR signaling through KIAA1212. *Neuron*, 63(6), 761-773.
- Kim, S., Lehtinen, M. K., Sessa, A., Zappaterra, M. W., Cho, S.-H., Gonzalez, D., . . . Gambello, M. J. (2010). The apical complex couples cell fate and cell survival to cerebral cortical development. *Neuron*, 66(1), 69-84.
- Kim, Y., Kim, E., Wu, Q., Guryanova, O., Hitomi, M., Lathia, J. D., . . . Rich, J. N. (2012). Platelet-derived growth factor receptors differentially inform intertumoral and intratumoral heterogeneity. *Genes & development*, 26(11), 1247-1262. doi: 10.1101/gad.193565.112; 10.1101/gad.193565.112
- Kimberly Christian, H. s. a. G.-I. M. (2010). Adult neurogenesis as a cellular model to study schizophrenia. *Cell Cycle*, 9(4), 636-637.
- Kirschenbaum, B., & Goldman, S. A. (1995). Brain-derived neurotrophic factor promotes the survival of neurons arising from the adult rat forebrain subependymal zone. *Proc Natl Acad Sci U S A*, 92(1), 210-214.

- Kleihues, P. C. W. (2000). World Health Organization classification of tumors: pathology and genetic: tumors of the nervous system. . *IARC Press, Lyon*.
- Kosodo, Y., Röper, K., Haubensak, W., Marzesco, A. M., Corbeil, D., & Huttner, W. B. (2004). Asymmetric distribution of the apical plasma membrane during neurogenic divisions of mammalian neuroepithelial cells. *The EMBO journal*, 23(11), 2314-2324.
- Kreisl, T. N., Lassman, A. B., Mischel, P. S., Rosen, N., Scher, H. I., Teruya-Feldstein, J., . . . Abrey, L. E. (2009). A pilot study of everolimus and gefitinib in the treatment of recurrent glioblastoma (GBM). *Journal of neuro-oncology*, 92(1), 99-105.
- Kriegstein, A., & Alvarez-Buylla, A. (2009). The glial nature of embryonic and adult neural stem cells. *Annual Review of Neuroscience*, 32, 149-184.
- Krueger, D. A., Care, M. M., Holland, K., Agricola, K., Tudor, C., Mangeskar, P., . . . Franz, D. N. (2010). Everolimus for subependymal giant-cell astrocytomas in tuberous sclerosis. *New England Journal of Medicine*, 363(19), 1801-1811.
- Kuhn, H. G., Dickinson-Anson, H., & Gage, F. H. (1996). Neurogenesis in the dentate gyrus of the adult rat: age-related decrease of neuronal progenitor proliferation. *The Journal of neuroscience : the official journal of the Society for Neuroscience*, 16(6), 2027-2033.
- Kuhn, H. G., Winkler, J., Kempermann, G., Thal, L. J., & Gage, F. H. (1997). Epidermal growth factor and fibroblast growth factor-2 have different effects on neural progenitors in the adult rat brain. *J Neurosci*, 17(15), 5820-5829.
- Kumar, V., Zhang, M.-X., Swank, M. W., Kunz, J., & Wu, G.-Y. (2005). Regulation of dendritic morphogenesis by Ras-PI3K-Akt-mTOR and Ras-MAPK signaling pathways. *The Journal of Neuroscience*, 25(49), 11288-11299.
- Kwon, C.-H., Zhu, X., Zhang, J., & Baker, S. J. (2003). mTor is required for hypertrophy of Pten-deficient neuronal soma in vivo. *Proceedings of the National Academy of Sciences*, 100(22), 12923-12928.
- Lakka, S. S., Gondi, C. S., Yanamandra, N., Olivero, W. C., Dinh, D. H., Gujrati, M., & Rao, J. S. (2004). Inhibition of cathepsin B and MMP-9 gene expression in glioblastoma cell line via RNA interference reduces tumor cell invasion, tumor growth and angiogenesis. *Oncogene*, 23(27), 4681-4689.
- Lamming, D. W., Ye, L., Katajisto, P., Goncalves, M. D., Saitoh, M., Stevens, D. M., . . . Baur, J. A. (2012). Rapamycin-induced insulin resistance is mediated by mTORC2 loss and uncoupled from longevity. *Science (New York, N.Y.)*, 335(6076), 1638-1643.
- Lamming, D. W., Ye, L., Sabatini, D. M., & Baur, J. A. (2013). Rapalogs and mTOR inhibitors as anti-aging therapeutics. *J.Clin.Invest*, 123(3), 980-989.
- Lange, C., Huttner, W. B., & Calegari, F. (2009). Cdk4/cyclinD1 overexpression in neural stem cells shortens G1, delays neurogenesis, and promotes the generation and expansion of basal progenitors. *Cell stem cell*, 5(3), 320-331.

- Laplane, M., & Sabatini, D. M. (2012). mTOR signaling in growth control and disease. *Cell*, 149(2), 274-293.
- Lathia, J., Hitomi, M., Gallagher, J., Gadani, S., Adkins, J., Vasanji, A., . . . Wu, Q. (2011). Distribution of CD133 reveals glioma stem cells self-renew through symmetric and asymmetric cell divisions. *Cell death & disease*, 2(9), e200.
- Laver, T., Nozell, S., & Benveniste, E. N. (2009). The NF- κ B Signaling Pathway in GBMs: Implications for Apoptotic and Inflammatory Responses and Exploitation for Therapy. *CNS Cancer Models, Markers, prognostic Factors, Targets, and Therapeutic Approaches, Chapter 42*, 1011-1036.
- Lazarov, O., Mattson, M. P., Peterson, D. A., Pimplikar, S. W., & van Praag, H. (2010). When neurogenesis encounters aging and disease. *Trends in neurosciences*, 33(12), 569-579.
- Le, D. M., Besson, A., Fogg, D. K., Choi, K.-S., Waisman, D. M., Goodyer, C. G., . . . Yong, V. W. (2003). Exploitation of astrocytes by glioma cells to facilitate invasiveness: a mechanism involving matrix metalloproteinase-2 and the urokinase-type plasminogen activator-plasmin cascade. *The Journal of Neuroscience*, 23(10), 4034-4043.
- Le Good, J. A., Ziegler, W. H., Parekh, D. B., Alessi, D. R., Cohen, P., & Parker, P. J. (1998). Protein kinase C isotypes controlled by phosphoinositide 3-kinase through the protein kinase PDK1. *Science (New York, N.Y.)*, 281(5385), 2042-2045.
- Le Page, C., Koumakpayi, I. H., Lessard, L., Mes-Masson, A. M., & Saad, F. (2005). EGFR and Her-2 regulate the constitutive activation of NF- κ B in PC-3 prostate cancer cells. *The Prostate*, 65(2), 130-140.
- Lee, J., Kotliarova, S., Kotliarov, Y., Li, A., Su, Q., Donin, N. M., . . . Zhang, W. (2006). Tumor stem cells derived from glioblastomas cultured in bFGF and EGF more closely mirror the phenotype and genotype of primary tumors than do serum-cultured cell lines. *Cancer Cell*, 9(5), 391-403.
- Lee, J. H., Silhavy, J. L., Kim, S., Dixon-Salazar, T., Heiberg, A., Scott, E., . . . Funari, V. (2012). De novo somatic mutations in components of the PI3K-AKT3-mTOR pathway cause hemimegalencephaly. *Nature genetics*, 44(8), 941-945.
- Lee, L., Sudentas, P., Donohue, B., Asrican, K., Worku, A., Walker, V., . . . El-Hashemite, N. (2005). Efficacy of a rapamycin analog (CCI-779) and IFN- γ in tuberous sclerosis mouse models. *Genes, Chromosomes and Cancer*, 42(3), 213-227.
- Lehtinen, M. K., Zappaterra, M. W., Chen, X., Yang, Y. J., Hill, A. D., Lun, M., . . . Ye, P. (2011). The cerebrospinal fluid provides a proliferative niche for neural progenitor cells. *Neuron*, 69(5), 893-905.
- Leitges, M., Sanz, L., Martin, P., Duran, A., Braun, U., Garcia, J. F., . . . Moscat, J. (2001). Targeted disruption of the zetaPKC gene results in the impairment of the NF- κ B pathway. *Mol Cell*, 8(4), 771-780.

- Leuner, B., Mendolia-Loffredo, S., Kozorovitskiy, Y., Samburg, D., Gould, E., & Shors, T. J. (2004). Learning enhances the survival of new neurons beyond the time when the hippocampus is required for memory. *J Neurosci*, 24(34), 7477-7481.
- Levenson, C. W., & Rich, N. J. (2007). Eat less, live longer? New insights into the role of caloric restriction in the brain. *Nutrition reviews*, 65(9), 412-415.
- Li, L., Xu, B., Zhu, Y., Chen, L., Sokabe, M., & Chen, L. (2010). DHEA prevents A β _{25–35}-impaired survival of newborn neurons in the dentate gyrus through a modulation of PI₃-K-Akt-mTOR signaling. *Neuropharmacology*, 59(4), 323-333.
- Li, N., Lee, B., Liu, R.-J., Banasr, M., Dwyer, J. M., Iwata, M., . . . Duman, R. S. (2010). mTOR-dependent synapse formation underlies the rapid antidepressant effects of NMDA antagonists. *Science*, 329(5994), 959-964.
- Li, V. C., Ballabeni, A., & Kirschner, M. W. (2012). Gap 1 phase length and mouse embryonic stem cell self-renewal. *Proceedings of the National Academy of Sciences of the United States of America*, 109(31), 12550-12555.
- Li, Y., Li, A., Glas, M., Lal, B., Ying, M., Sang, Y., . . . Laterra, J. (2011). c-Met signaling induces a reprogramming network and supports the glioblastoma stem-like phenotype. *Proc Natl Acad Sci U S A*, 108(24), 9951-9956.
- Li, Y., Luikart, B. W., Birnbaum, S., Chen, J., Kwon, C.-H., Kerner, S. G., . . . Parada, L. F. (2008). TrkB regulates hippocampal neurogenesis and governs sensitivity to antidepressive treatment. *Neuron*, 59(3), 399-412.
- Li, Y., Mu, Y., & Gage, F. H. (2009). Development of neural circuits in the adult hippocampus. *Current topics in developmental biology*, 87, 149-174.
- Lim, D. A., Tramontin, A. D., Trevejo, J. M., Herrera, D. G., García-Verdugo, J. M., & Alvarez-Buylla, A. (2000). Noggin antagonizes BMP signaling to create a niche for adult neurogenesis. *Neuron*, 28(3), 713-726.
- Lionaki, E., Markaki, M., & Tavernarakis, N. (2013). Autophagy and ageing: Insights from invertebrate model organisms. *Ageing research reviews*, 12(1), 413-428.
- Liotta, L. A., & Kohn, E. C. (2001). The microenvironment of the tumour-host interface. *Nature*, 411(6835), 375-379.
- Liu, G., Yuan, X., Zeng, Z., Tunici, P., Ng, H., Abdulkadir, I. R., . . . John, S. Y. (2006). Analysis of gene expression and chemoresistance of CD133 cancer stem cells in glioblastoma. *Molecular cancer*, 5(1), 67.
- Liu, W., Ye, P., O'Kusky, J. R., & D'Ercole, A. J. (2009). Type 1 insulin-like growth factor receptor signaling is essential for the development of the hippocampal formation and dentate gyrus. *Journal of neuroscience research*, 87(13), 2821-2832.

- Lledo, P. M., Alonso, M., & Grubb, M. S. (2006). Adult neurogenesis and functional plasticity in neuronal circuits. *Nat Rev Neurosci*, 7(3), 179-193.
- Loulier, K., Lathia, J. D., Marthiens, V., Relucio, J., Mughal, M. R., Tang, S.-C., . . . Patton, B. (2009). $\beta 1$ integrin maintains integrity of the embryonic neocortical stem cell niche. *PLoS biology*, 7(8), e1000176.
- Lukashev, M. E., & Werb, Z. (1998). ECM signalling: orchestrating cell behaviour and misbehaviour. *Trends Cell Biol*, 8(11), 437-441.
- Magri, L., Cambiaghi, M., Cominelli, M., Alfaro-Cervello, C., Corsi, M., Pala, M., . . . Minicucci, F. (2011). Sustained activation of mTOR pathway in embryonic neural stem cells leads to development of tuberous sclerosis complex-associated lesions. *Cell stem cell*, 9(5), 447-462.
- Mair, W., Morante, I., Rodrigues, A. P. C., Manning, G., Montminy, M., Shaw, R. J., & Dillin, A. (2011). Lifespan extension induced by AMPK and calcineurin is mediated by CRTC-1 and CREB. *Nature*, 470(7334), 404-408.
- Malberg, J. E., Eisch, A. J., Nestler, E. J., & Duman, R. S. (2000). Chronic antidepressant treatment increases neurogenesis in adult rat hippocampus. *The Journal of neuroscience : the official journal of the Society for Neuroscience*, 20(24), 9104-9110.
- Mantovani, A., Allavena, P., Sica, A., & Balkwill, F. (2008). Cancer-related inflammation. *Nature*, 454(7203), 436-444.
- Mantovani, A., & Sica, A. (2010). Macrophages, innate immunity and cancer: balance, tolerance, and diversity. *Curr Opin Immunol*, 22(2), 231-237.
- Markovic, D. S., Glass, R., Synowitz, M., Rooijen, N., & Kettenmann, H. (2005). Microglia stimulate the invasiveness of glioma cells by increasing the activity of metalloprotease-2. *J Neuropathol Exp Neurol*, 64(9), 754-762.
- Markovic, D. S., Vinnakota, K., Chirasani, S., Synowitz, M., Raguet, H., Stock, K., . . . Kettenmann, H. (2009). Gliomas induce and exploit microglial MT1-MMP expression for tumor expansion. *Proc Natl Acad Sci U S A*, 106(30), 12530-12535.
- McLendon, R., Friedman, A., Bigner, D., Van Meir, E. G., Brat, D. J., Mastrogiannis, G. M., . . . Aldape, K. (2008). Comprehensive genomic characterization defines human glioblastoma genes and core pathways. *Nature*, 455(7216), 1061-1068.
- McNeill, H., Craig, G. M., & Bateman, J. M. (2008). Regulation of neurogenesis and epidermal growth factor receptor signaling by the insulin receptor/target of rapamycin pathway in *Drosophila*. *Genetics*, 179(2), 843-853.
- Meikle, L., Pollizzi, K., Egnor, A., Kramvis, I., Lane, H., Sahin, M., & Kwiatkowski, D. J. (2008). Response of a neuronal model of tuberous sclerosis to mammalian target of rapamycin (mTOR) inhibitors: effects on mTORC1 and Akt signaling lead to improved survival and function. *The Journal of Neuroscience*, 28(21), 5422-5432.

- Melemedjian, O. K., Asiedu, M. N., Tillu, D. V., Sanoja, R., Yan, J., Lark, A., . . . Lepow, T. (2011). Targeting adenosine monophosphate-activated protein kinase (AMPK) in preclinical models reveals a potential mechanism for the treatment of neuropathic pain. *Mol Pain*, 7(1), 70.
- Mellinghoff, I. K., Schultz, N., Mischel, P. S., & Cloughesy, T. F. (2011). Will Kinase Inhibitors Make it as Glioblastoma Drugs? *Curr Top Microbiol Immunol*.
- Mellinghoff, I. K., Schultz, N., Mischel, P. S., & Cloughesy, T. F. (2012). Will kinase inhibitors make it as glioblastoma drugs? *Therapeutic Kinase Inhibitors* (pp. 135-169): Springer.
- Mellinghoff, I. K., Wang, M. Y., Vivanco, I., Haas-Kogan, D. A., Zhu, S., Dia, E. Q., . . . Mischel, P. S. (2005). Molecular determinants of the response of glioblastomas to EGFR kinase inhibitors. *N Engl J Med*, 353(19), 2012-2024.
- Merlo, S., Calafiore, M., Vancheri, C., Luigi Canonico, P., Copani, A., & Sortino, M.-A. (2007). Astrocyte-like cells as a main target for estrogen action during neuronal differentiation. *Molecular and Cellular Neuroscience*, 34(4), 562-570.
- Mihaylova, M. M., & Shaw, R. J. (2011). The AMPK signalling pathway coordinates cell growth, autophagy and metabolism. *Nature cell biology*, 13(9), 1016-1023.
- Millar, J. K., Wilson-Annan, J. C., Anderson, S., Christie, S., Taylor, M. S., Semple, C. A., . . . Porteous, D. J. (2000). Disruption of two novel genes by a translocation co-segregating with schizophrenia. *Hum Mol Genet*, 9(9), 1415-1423.
- Miller, R. A., Harrison, D. E., Astle, C. M., Baur, J. A., Boyd, A. R., de Cabo, R., . . . Strong, R. (2011). Rapamycin, but not resveratrol or simvastatin, extends life span of genetically heterogeneous mice. *The journals of gerontology. Series A, Biological sciences and medical sciences*, 66(2), 191-201.
- Ming, G.-I., & Song, H. (2011). Adult neurogenesis in the mammalian brain: significant answers and significant questions. *Neuron*, 70(4), 687-702.
- Mir, S. E., De Witt Hamer, P. C., Krawczyk, P. M., Balaj, L., Claes, A., Niers, J. M., . . . Kaspers, G. J. (2010). In silico analysis of kinase expression identifies WEE1 as a gatekeeper against mitotic catastrophe in glioblastoma. *Cancer Cell*, 18(3), 244-257.
- Mirzadeh, Z., Merkle, F. T., Soriano-Navarro, M., Garcia-Verdugo, J. M., & Alvarez-Buylla, A. (2008). Neural stem cells confer unique pinwheel architecture to the ventricular surface in neurogenic regions of the adult brain. *Cell stem cell*, 3(3), 265-278.
- Monje, M. L., Toda, H., & Palmer, T. D. (2003). Inflammatory blockade restores adult hippocampal neurogenesis. *Science (New York, N.Y.)*, 302(5651), 1760-1765.
- Moscat, J., Diaz-Meco, M. T., & Wooten, M. W. (2007). Signal integration and diversification through the p62 scaffold protein. *Trends in biochemical sciences*, 32(2), 95-100.

- Moscat, J., Diaz-Meco, M. T., & Wooten, M. W. (2009). Of the atypical PKCs, Par-4 and p62: recent understandings of the biology and pathology of a PB1-dominated complex. *Cell Death & Differentiation*, 16(11), 1426-1437.
- Mueller, M. M., Herold-Mende, C. C., Riede, D., Lange, M., Steiner, H.-H., & Fusenig, N. E. (1999). Autocrine growth regulation by granulocyte colony-stimulating factor and granulocyte macrophage colony-stimulating factor in human gliomas with tumor progression. *Am J Pathol*, 155(5), 1557-1567.
- Naganuma, H., Sasaki, A., Satoh, E., Nagasaka, M., Nakano, S., Isoe, S., & Nukui, H. (1996). Modulation of transforming growth factor-beta secretion from malignant glioma cells by interleukin-1 beta. *Neurologia medico-chirurgica*, 36(3), 145-150.
- Naugler, W. E., & Karin, M. (2008). NF-kappaB and cancer-identifying targets and mechanisms. *Curr Opin Genet Dev*, 18(1), 19-26.
- Nishikawa, R., Sugiyama, T., Narita, Y., Furnari, F., Cavenee, W. K., & Matsutani, M. (2004). Immunohistochemical analysis of the mutant epidermal growth factor, deltaEGFR, in glioblastoma. *Brain Tumor Pathol*, 21(2), 53-56.
- Noda, Y., Kohjima, M., Izaki, T., Ota, K., Yoshinaga, S., Inagaki, F., . . . Sumimoto, H. (2003). Molecular recognition in dimerization between PB1 domains. *J Biol Chem*, 278(44), 43516-43524.
- Nolte, C., Kirchhoff, F., & Kettenmann, H. (1997). Epidermal growth factor is a motility factor for microglial cells in vitro: evidence for EGF receptor expression. *European Journal of Neuroscience*, 9(8), 1690-1698.
- Ohanna, M., Sobering, A. K., Lapointe, T., Lorenzo, L., Praud, C., Petroulakis, E., . . . Pende, M. (2005). Atrophy of S6K1^{-/-} skeletal muscle cells reveals distinct mTOR effectors for cell cycle and size control. *Nature cell biology*, 7(3), 286-294.
- Ohgaki, H., & Kleihues, P. (2007). Genetic pathways to primary and secondary glioblastoma. *Am J Pathol*, 170(5), 1445-1453.
- Overstreet Wadiche, L., Bromberg, D. A., Bensen, A. L., & Westbrook, G. L. (2005). GABAergic signaling to newborn neurons in dentate gyrus. *J Neurophysiol*, 94(6), 4528-4532.
- Palazuelos, J., Ortega, Z., Diaz-Alonso, J., Guzman, M., & Galve-Roperh, I. (2012). CB2 cannabinoid receptors promote neural progenitor cell proliferation via mTORC1 signaling. *The Journal of biological chemistry*, 287(2), 1198-1209.
- Paliouras, G. N., Hamilton, L. K., Aumont, A., Joppe, S. E., Barnabe-Heider, F., & Fernandes, K. J. (2012). Mammalian target of rapamycin signaling is a key regulator of the transit-amplifying progenitor pool in the adult and aging forebrain. *The Journal of neuroscience : the official journal of the Society for Neuroscience*, 32(43), 15012-15026.
- Pandita, A., Aldape, K. D., Zadeh, G., Guha, A., & James, C. D. (2004). Contrasting in vivo and in vitro fates of glioblastoma cell subpopulations with amplified EGFR. *Genes Chromosomes Cancer*, 39(1), 29-36.

- Pandita, A., Aldape, K. D., Zadeh, G., Guha, A., & James, C. D. (2004). Contrasting in vivo and in vitro fates of glioblastoma cell subpopulations with amplified EGFR. *Genes, Chromosomes and Cancer*, 39(1), 29-36.
- Panzanelli, P., Bardy, C., Nissant, A., Pallotto, M., Sassoe-Pognetto, M., Lledo, P. M., & Fritschy, J. M. (2009). Early synapse formation in developing interneurons of the adult olfactory bulb. *J Neurosci*, 29(48), 15039-15052.
- Parker, S. S., Mandell, E. K., Hapak, S. M., Maskaykina, I. Y., Kusne, Y., Kim, J. Y., . . . Ghosh, S. (2013a). Competing molecular interactions of aPKC isoforms regulate neuronal polarity. *Proc Natl Acad Sci U S A*, 110(35), 14450-14455.
- Parney, I. F., Waldron, J. S., & Parsa, A. T. (2009). Flow cytometry and in vitro analysis of human glioma-associated macrophages. Laboratory investigation. *J Neurosurg*, 110(3), 572-582.
- Pelloski, C. E., Mahajan, A., Maor, M., Chang, E. L., Woo, S., Gilbert, M., . . . Blair, H. (2005). YKL-40 expression is associated with poorer response to radiation and shorter overall survival in glioblastoma. *Clinical Cancer Research*, 11(9), 3326-3334.
- Pennica, D., Nedwin, G. E., Hayflick, J. S., Seeburg, P. H., Derynck, R., Palladino, M. A., . . . Goeddel, D. V. (1984). Human tumour necrosis factor: precursor structure, expression and homology to lymphotoxin. *Nature*, 312(5996), 724-729.
- Petreanu, L., & Alvarez-Buylla, A. (2002). Maturation and death of adult-born olfactory bulb granule neurons: role of olfaction. *J Neurosci*, 22(14), 6106-6113.
- Phillips, H. S., Kharbanda, S., Chen, R., Forrest, W. F., Soriano, R. H., Wu, T. D., . . . Soroceanu, L. (2006). Molecular subclasses of high-grade glioma predict prognosis, delineate a pattern of disease progression, and resemble stages in neurogenesis. *Cancer Cell*, 9(3), 157-173.
- Pianetti, S., Arsura, M., Romieu-Mourez, R., Coffey, R. J., & Sonenshein, G. E. (2001). Her-2/neu overexpression induces NF- κ B via a PI3-kinase/Akt pathway involving calpain-mediated degradation of I κ B- α that can be inhibited by the tumor suppressor PTEN. *Oncogene*, 20(11).
- Pistollato, F., Persano, L., Puppa, A. D., Rampazzo, E., & Basso, G. (2011). Isolation and expansion of regionally defined human glioblastoma cells in vitro. *Current protocols in stem cell biology*, 3.4. 1-3.4. 10.
- Platten, M., Kretz, A., Naumann, U., Aulwurm, S., Egashira, K., Isenmann, S., & Weller, M. (2003). Monocyte chemoattractant protein-1 increases microglial infiltration and aggressiveness of gliomas. *Annals of neurology*, 54(3), 388-392.
- Prasad, G., Sottero, T., Yang, X., Mueller, S., James, C. D., Weiss, W. A., . . . Aftab, D. T. (2011). Inhibition of PI3K/mTOR pathways in glioblastoma and implications for combination therapy with temozolomide. *Neuro-oncology*, 13(4), 384-392.

- Pyonteck, S. M., Akkari, L., Schuhmacher, A. J., Bowman, R. L., Sevenich, L., Quail, D. F., . . . Joyce, J. A. (2013). CSF-1R inhibition alters macrophage polarization and blocks glioma progression. *Nat Med*, 19(10), 1264-1272.
- Quiñones-Hinojosa, A., & Chaichana, K. (2007). The human subventricular zone: a source of new cells and a potential source of brain tumors. *Experimental neurology*, 205(2), 313-324.
- Raman, L., Kong, X., Gilley, J. A., & Kernie, S. G. (2011). Chronic hypoxia impairs murine hippocampal development and depletes the postnatal progenitor pool by attenuating mammalian target of rapamycin signaling. *Pediatric research*, 70(2), 159-165.
- Raman, L., Kong, X., & Kernie, S. G. (2013). Pharmacological inhibition of the mTOR pathway impairs hippocampal development in mice. *Neuroscience letters*, 541, 9-14.
- Ramirez-Amaya, V., Marrone, D. F., Gage, F. H., Worley, P. F., & Barnes, C. A. (2006). Integration of new neurons into functional neural networks. *The Journal of neuroscience : the official journal of the Society for Neuroscience*, 26(47), 12237-12241.
- Rath, P., Lal, B., Ajala, O., Li, Y., Xia, S., Kim, J., & Laterra, J. (2013). In Vivo c-Met Pathway Inhibition Depletes Human Glioma Xenografts of Tumor-Propagating Stem-Like Cells. *Transl Oncol*, 6(2), 104-111.
- Reardon, D. A., Desjardins, A., Vredenburgh, J. J., Gururangan, S., Friedman, A. H., Herndon li, J. E., . . . Sampson, J. H. (2010). Phase 2 trial of erlotinib plus sirolimus in adults with recurrent glioblastoma. *Journal of neuro-oncology*, 96(2), 219-230.
- RIDLEY, A., & Cavanagh, J. (1971). Lymphocytic infiltration in gliomas: evidence of possible host resistance. *Brain*, 94(1), 117-124.
- Roggendorf, W., Strupp, S., & Paulus, W. (1996). Distribution and characterization of microglia/macrophages in human brain tumors. *Acta Neuropathologica*, 92(3), 288-293.
- Rubio-Araiz, A., Arévalo-Martín, Á., Gómez-Torres, O., Navarro-Galve, B., García-Ovejero, D., Suetterlin, P., . . . Molina-Holgado, F. (2008). The endocannabinoid system modulates a transient TNF pathway that induces neural stem cell proliferation. *Molecular and Cellular Neuroscience*, 38(3), 374-380.
- Ruffell, B., Affara, N. I., & Coussens, L. M. (2012). Differential macrophage programming in the tumor microenvironment. *Trends Immunol*, 33(3), 119-126.
- Sami, A., & Karsy, M. (2013). Targeting the PI3K/AKT/mTOR signaling pathway in glioblastoma: novel therapeutic agents and advances in understanding. *Tumor Biology*, 34(4), 1991-2002.
- Santarelli, L., Saxe, M., Gross, C., Surget, A., Battaglia, F., Dulawa, S., . . . Arancio, O. (2003). Requirement of hippocampal neurogenesis for the behavioral effects of antidepressants. *Science*, 301(5634), 805-809.

- Sarbassov, D. D., Ali, S. M., Sengupta, S., Sheen, J.-H., Hsu, P. P., Bagley, A. F., . . . Sabatini, D. M. (2006). Prolonged rapamycin treatment inhibits mTORC2 assembly and Akt/PKB. *Molecular cell*, 22(2), 159-168.
- Sarkaria, J. N., Yang, L., Grogan, P. T., Kitange, G. J., Carlson, B. L., Schroeder, M. A., . . . James, C. D. (2007). Identification of molecular characteristics correlated with glioblastoma sensitivity to EGFR kinase inhibition through use of an intracranial xenograft test panel. *Mol Cancer Ther*, 6(3), 1167-1174.
- Sarnat, H., Flores-Sarnat, L., Crino, P., Hader, W., & Bello-Espinosa, L. (2012). Hemimegalencephaly: foetal tauopathy with mTOR hyperactivation and neuronal lipidosis. *Folia Neuropathol*, 50(4), 330-345.
- Sathornsumetee, S., Reardon, D. A., Desjardins, A., Quinn, J. A., Vredenburgh, J. J., & Rich, J. N. (2007). Molecularly targeted therapy for malignant glioma. *Cancer*, 110(1), 13-24.
- Sato, A., Sunayama, J., Okada, M., Watanabe, E., Seino, S., Shibuya, K., . . . Kayama, T. (2012). Glioma-initiating cell elimination by metformin activation of FOXO3 via AMPK. *MEDICINE*, 1, 000-000.
- Sauer, F. C. (1935). Mitosis in the neural tube. *Journal of Comparative Neurology*, 62(2), 377-405.
- Scharfman, H., Goodman, J., Macleod, A., Phani, S., Antonelli, C., & Croll, S. (2005). Increased neurogenesis and the ectopic granule cells after intrahippocampal BDNF infusion in adult rats. *Experimental neurology*, 192(2), 348-356.
- Scherer, H. (1940). Cerebral astrocytomas and their derivatives. *American Journal of Cancer*, 40, 159-198.
- Schlessinger, J. (2000). Cell signaling by receptor tyrosine kinases. *Cell*, 103(2), 211-225.
- Schmidt-Hieber, C., Jonas, P., & Bischofberger, J. (2004). Enhanced synaptic plasticity in newly generated granule cells of the adult hippocampus. *Nature*, 429(6988), 184-187. doi: 10.1038/nature02553
- Schratt, G. M., Nigh, E. A., Chen, W. G., Hu, L., & Greenberg, M. E. (2004). BDNF regulates the translation of a select group of mRNAs by a mammalian target of rapamycin-phosphatidylinositol 3-kinase-dependent pathway during neuronal development. *The Journal of Neuroscience*, 24(33), 7366-7377.
- Sehgal, S. N. (1998). Rapamune®(RAPA, rapamycin, sirolimus): mechanism of action immunosuppressive effect results from blockade of signal transduction and inhibition of cell cycle progression. *Clinical biochemistry*, 31(5), 335-340.
- Shapiro, J. R., Yung, W. K., & Shapiro, W. R. (1981). Isolation, karyotype, and clonal growth of heterogeneous subpopulations of human malignant gliomas. *Cancer Res*, 41(6), 2349-2359.

- Shaw, R. J., Lamia, K. A., Vasquez, D., Koo, S. H., Bardeesy, N., Depinho, R. A., . . . Cantley, L. C. (2005). The kinase LKB1 mediates glucose homeostasis in liver and therapeutic effects of metformin. *Science (New York, N.Y.)*, 310(5754), 1642-1646.
- Shen, Q., Wang, Y., Kokovay, E., Lin, G., Chuang, S.-M., Goderie, S. K., . . . Temple, S. (2008). Adult SVZ stem cells lie in a vascular niche: a quantitative analysis of niche cell-cell interactions. *Cell stem cell*, 3(3), 289-300.
- Shiao, S. L., Ganesan, A. P., Rugo, H. S., & Coussens, L. M. (2011). Immune microenvironments in solid tumors: new targets for therapy. *Genes Dev*, 25(24), 2559-2572.
- Shiota, C., Woo, J.-T., Lindner, J., Shelton, K. D., & Magnuson, M. A. (2006). Multiallelic Disruption of the *rictor* Gene in Mice Reveals that mTOR Complex 2 Is Essential for Fetal Growth and Viability. *Developmental cell*, 11(4), 583-589.
- Shirayama, Y., Chen, A. C.-H., Nakagawa, S., Russell, D. S., & Duman, R. S. (2002). Brain-derived neurotrophic factor produces antidepressant effects in behavioral models of depression. *The Journal of Neuroscience*, 22(8), 3251-3261.
- Singh, S. K., Hawkins, C., Clarke, I. D., Squire, J. A., Bayani, J., Hide, T., . . . Dirks, P. B. (2004). Identification of human brain tumour initiating cells. *Nature*, 432(7015), 396-401.
- Slipczuk, L., Bekinschtein, P., Katche, C., Cammarota, M., Izquierdo, I., & Medina, J. H. (2009). BDNF activates mTOR to regulate GluR1 expression required for memory formation. *PLoS One*, 4(6), e6007.
- Song, H., & Moon, A. (2006). Glial cell-derived neurotrophic factor (GDNF) promotes low-grade Hs683 glioma cell migration through JNK, ERK-1/2 and p38 MAPK signaling pathways. *Neuroscience Research*, 56(1), 29-38.
- Sottoriva, A., Spiteri, I., Piccirillo, S. G. M., Touloumis, A., Collins, V. P., Marioni, J. C., . . . Tavaré, S. (2013). Intratumor heterogeneity in human glioblastoma reflects cancer evolutionary dynamics. *Proceedings of the National Academy of Sciences*, 110(10), 4009-4014.
- Standaert, M. L., Bandyopadhyay, G., Kanoh, Y., Sajan, M. P., & Farese, R. V. (2001). Insulin and PIP3 activate PKC- ζ by mechanisms that are both dependent and independent of phosphorylation of activation loop (T410) and autophosphorylation (T560) sites. *Biochemistry*, 40(1), 249-255.
- Standaert, M. L., Galloway, L., Karnam, P., Bandyopadhyay, G., Moscat, J., & Farese, R. V. (1997). Protein kinase C-zeta as a downstream effector of phosphatidylinositol 3-kinase during insulin stimulation in rat adipocytes. Potential role in glucose transport. *The Journal of biological chemistry*, 272(48), 30075-30082.
- Staudt, L. M. (2010). Oncogenic activation of NF-kappaB. *Cold Spring Harb Perspect Biol*, 2(6), a000109.

- Stommel, J. M., Kimmelman, A. C., Ying, H., Nabioullin, R., Ponugoti, A. H., Wiedemeyer, R., . . . DePinho, R. A. (2007). Coactivation of receptor tyrosine kinases affects the response of tumor cells to targeted therapies. *Science*, 318(5848), 287-290.
- Streit, F., Armstrong, V. W., & Oellerich, M. (2002). Rapid liquid chromatography-tandem mass spectrometry routine method for simultaneous determination of sirolimus, everolimus, tacrolimus, and cyclosporin A in whole blood. *Clinical chemistry*, 48(6 Pt 1), 955-958.
- Sun, L., & Carpenter, G. (1998). Epidermal growth factor activation of NF- κ B is mediated through I κ B α degradation and intracellular free calcium. *Oncogene*, 16(16).
- Sun, Y., Goderie, S. K., & Temple, S. (2005). Asymmetric distribution of EGFR receptor during mitosis generates diverse CNS progenitor cells. *Neuron*, 45(6), 873-886.
- Sunayama, J., Sato, A., Matsuda, K.-i., Tachibana, K., Suzuki, K., Narita, Y., . . . Tomiyama, A. (2010). Dual blocking of mTor and PI3K elicits a prodifferentiation effect on glioblastoma stem-like cells. *Neuro-oncology*, 12(12), 1205-1219.
- Szerlip, N. J., Pedraza, A., Chakravarty, D., Azim, M., McGuire, J., Fang, Y., . . . Brennan, C. W. (2012). Intratumoral heterogeneity of receptor tyrosine kinases EGFR and PDGFRA amplification in glioblastoma defines subpopulations with distinct growth factor response. *Proceedings of the National Academy of Sciences*, 109(8), 3041-3046.
- Tabuse, Y., Izumi, Y., Piano, F., Kemphues, K. J., Miwa, J., & Ohno, S. (1998). Atypical protein kinase C cooperates with PAR-3 to establish embryonic polarity in *Caenorhabditis elegans*. *Development*, 125(18), 3607-3614.
- Takei, N., Inamura, N., Kawamura, M., Namba, H., Hara, K., Yonezawa, K., & Nawa, H. (2004). Brain-derived neurotrophic factor induces mammalian target of rapamycin-dependent local activation of translation machinery and protein synthesis in neuronal dendrites. *The Journal of Neuroscience*, 24(44), 9760-9769.
- Tanaka, K., Babic, I., Nathanson, D., Akhavan, D., Guo, D., Gini, B., . . . Mischel, P. S. (2011). Oncogenic EGFR signaling activates an mTORC2-NF- κ B pathway that promotes chemotherapy resistance. *Cancer discovery*, 1(6), 524-538.
- Tashiro, A., Sandler, V. M., Toni, N., Zhao, C., & Gage, F. H. (2006). NMDA-receptor-mediated, cell-specific integration of new neurons in adult dentate gyrus. *Nature*, 442(7105), 929-933.
- Terzic, J., Grivennikov, S., Karin, E., & Karin, M. (2010). Inflammation and colon cancer. *Gastroenterology*, 138(6), 2101-2114 e2105.
- Thaker, N. G., & Pollack, I. F. (2009). Molecularly targeted therapies for malignant glioma: rationale for combinatorial strategies. *Expert review of neurotherapeutics*, 9(12), 1815-1836.
- Tiscornia, G., Singer, O., & Verma, I. M. (2006). Production and purification of lentiviral vectors. *Nat Protoc*, 1(1), 241-245.

- Toni, N., Laplagne, D. A., Zhao, C., Lombardi, G., Ribak, C. E., Gage, F. H., & Schinder, A. F. (2008). Neurons born in the adult dentate gyrus form functional synapses with target cells. *Nat Neurosci*, 11(8), 901-907.
- Trujillo, J. I., Kiefer, J. R., Huang, W., Thorarensen, A., Xing, L., Caspers, N. L., . . . Li, X. (2009). 2-(6-Phenyl-1H-indazol-3-yl)-1H-benzo[d]imidazoles: design and synthesis of a potent and isoform selective PKC-zeta inhibitor. *Bioorg Med Chem Lett*, 19(3), 908-911.
- Tso, C.-L., Freije, W. A., Day, A., Chen, Z., Merriman, B., Perlina, A., . . . Mischel, P. S. (2006). Distinct transcription profiles of primary and secondary glioblastoma subgroups. *Cancer research*, 66(1), 159-167.
- Tsuchiya, S., Kobayashi, Y., Goto, Y., Okumura, H., Nakae, S., Konno, T., & Tada, K. (1982). Induction of maturation in cultured human monocytic leukemia cells by a phorbol diester. *Cancer Res*, 42(4), 1530-1536.
- Ucbek, A., Özünal, Z. G., Uzun, Ö., & Gepdİremen, A. (2014). Effect of metformin on the human T98G glioblastoma multiforme cell line. *Experimental and Therapeutic Medicine*, 7(5), 1285-1290.
- Uhm, J. H., Ballman, K. V., Wu, W., Giannini, C., Krauss, J. C., Buckner, J. C., . . . Flynn, P. J. (2011). Phase II evaluation of gefitinib in patients with newly diagnosed Grade 4 astrocytoma: Mayo/North Central Cancer Treatment Group Study N0074. *International Journal of Radiation Oncology* Biology* Physics*, 80(2), 347-353.
- Urbanska, M., Gozdz, A., Swiech, L. J., & Jaworski, J. (2012). Mammalian target of rapamycin complex 1 (mTORC1) and 2 (mTORC2) control the dendritic arbor morphology of hippocampal neurons. *The Journal of biological chemistry*, 287(36), 30240-30256.
- Valster, A., Tran, N. L., Nakada, M., Berens, M. E., Chan, A. Y., & Symons, M. (2005). Cell migration and invasion assays. *Methods*, 37(2), 208-215.
- Verhaak, R. G. W., Hoadley, K. A., Purdom, E., Wang, V., Qi, Y., Wilkerson, M. D., . . . Hayes, D. N. (2010). Integrated Genomic Analysis Identifies Clinically Relevant Subtypes of Glioblastoma Characterized by Abnormalities in PDGFRA, IDH1, EGFR, and NF1. *Cancer Cell*, 17(1), 98-110.
- Virchow, R. (1863). Die Krankhaften Geschwulste. H. *Hirschwald, Berlin*.
- Wang, H., Zhang, W., Huang, H. J., Liao, W. S., & Fuller, G. N. (2004). Analysis of the activation status of Akt, NFkappaB, and Stat3 in human diffuse gliomas. *Lab Invest*, 84(8), 941-951.
- Wang, J., Gallagher, D., DeVito, L. M., Cancino, G. I., Tsui, D., He, L., . . . Miller, F. D. (2012). Metformin activates an atypical PKC-CBP pathway to promote neurogenesis and enhance spatial memory formation. *Cell stem cell*, 11(1), 23-35.
- Wang, J., Weaver, I. C., Gauthier-Fisher, A., Wang, H., He, L., Yeomans, J., . . . Miller, F. D. (2010). CBP histone acetyltransferase activity regulates embryonic neural differentiation in the normal and Rubinstein-Taybi syndrome brain. *Developmental cell*, 18(1), 114-125.

- Wang, X., Tsai, J.-W., LaMonica, B., & Kriegstein, A. R. (2011). A new subtype of progenitor cell in the mouse embryonic neocortex. *Nature neuroscience*, 14(5), 555-561.
- Watters, J. J., Schartner, J. M., & Badie, B. (2005). Microglia function in brain tumors. *Journal of neuroscience research*, 81(3), 447-455.
- Watts, J. L., Etemad-Moghadam, B., Guo, S., Boyd, L., Draper, B. W., Mello, C. C., . . . Kemphues, K. J. (1996). par-6, a gene involved in the establishment of asymmetry in early *C. elegans* embryos, mediates the asymmetric localization of PAR-3. *Development*, 122(10), 3133-3140.
- Watts, J. L., Morton, D. G., Bestman, J., & Kemphues, K. J. (2000). The *C. elegans* par-4 gene encodes a putative serine-threonine kinase required for establishing embryonic asymmetry. *Development*, 127(7), 1467-1475.
- Wei, Y., Jiang, Y., Zou, F., Liu, Y., Wang, S., Xu, N., . . . Jiang, J. (2013). Activation of PI3K/Akt pathway by CD133-p85 interaction promotes tumorigenic capacity of glioma stem cells. *Proceedings of the National Academy of Sciences of the United States of America*, 110(17), 6829-6834.
- Wen, P. Y., Lee, E. Q., Reardon, D. A., Ligon, K. L., & Alfred Yung, W. K. (2012). Current clinical development of PI3K pathway inhibitors in glioblastoma. *Neuro-oncology*, 14(7), 819-829.
- Westphal, M., & Lamszus, K. (2011). The neurobiology of gliomas: from cell biology to the development of therapeutic approaches. *Nature Reviews Neuroscience*, 12(9), 495-508.
- Widera, D., Mikenberg, I., Elvers, M., Kaltschmidt, C., & Kaltschmidt, B. (2006). Tumor necrosis factor α triggers proliferation of adult neural stem cells via IKK/NF- κ B signaling. *BMC neuroscience*, 7(1), 1-18.
- Widera, D., Mikenberg, I., Kaltschmidt, B., & Kaltschmidt, C. (2006). Potential role of NF- κ B in adult neural stem cells: the underrated steersman? *International journal of developmental neuroscience*, 24(2), 91-102.
- Wiesenhofer, B., Stockhammer, G., Kostron, H., Maier, H., Hinterhuber, H., & Humpel, C. (2000). Glial cell line-derived neurotrophic factor (GDNF) and its receptor (GFR- α 1) are strongly expressed in human gliomas. *Acta Neuropathol*, 99(2), 131-137.
- Wikstrand, C. J., Bigner, S. H., & Bigner, D. D. (1983). Demonstration of complex antigenic heterogeneity in a human glioma cell line and eight derived clones by specific monoclonal antibodies. *Cancer Res*, 43(7), 3327-3334.
- Wilkinson, J. E., Burmeister, L., Brooks, S. V., Chan, C. C., Friedline, S., Harrison, D. E., . . . Wood, L. K. (2012). Rapamycin slows aging in mice. *Aging cell*, 11(4), 675-682.
- Wilson, M. I., Gill, D. J., Perisic, O., Quinn, M. T., & Williams, R. L. (2003). PB1 domain-mediated heterodimerization in NADPH oxidase and signaling complexes of atypical protein kinase C with Par6 and p62. *Mol Cell*, 12(1), 39-50.

- Wong, K.-K., Engelman, J. A., & Cantley, L. C. (2010). Targeting the PI3K signaling pathway in cancer. *Current opinion in genetics & development*, 20(1), 87-90.
- Wu, J. L., Abe, T., Inoue, R., Fujiki, M., & Kobayashi, H. (2004). Ikb α M suppresses angiogenesis and tumorigenesis promoted by a constitutively active mutant EGFR in human glioma cells. *Neurological research*, 26(7), 785-791.
- Wynn, T. A., Chawla, A., & Pollard, J. W. (2013). Macrophage biology in development, homeostasis and disease. *Nature*, 496(7446), 445-455. doi: 10.1038/nature12034
- Yamagishi, J. M., & H. Takebe, N. (1997). Enhanced radiosensitivity by inhibition of nuclear factor kappaB activation in human malignant glioma cells. *International journal of radiation biology*, 72(2), 157-162.
- Yan, K., Yang, K., & Rich, J. N. (2013). The evolving landscape of glioblastoma stem cells. *Current opinion in neurology*, 26(6), 701-707.
- Yang, C., Hu, Y.-M., Zhou, Z.-Q., Zhang, G.-F., & Yang, J.-J. (2013). Acute administration of ketamine in rats increases hippocampal BDNF and mTOR levels during forced swimming test. *Uppsala journal of medical sciences*, 118(1), 3-8.
- Zakikhani, M., Blouin, M.-J., Piura, E., & Pollak, M. N. (2010). Metformin and rapamycin have distinct effects on the AKT pathway and proliferation in breast cancer cells. *Breast cancer research and treatment*, 123(1), 271-279.
- Zanotto-Filho, A., Braganhol, E., Schröder, R., de Souza, L. H. T., Dalmolin, R. J. S., Pasquali, M. A. B., . . . Moreira, J. C. F. (2011). NF κ B inhibitors induce cell death in glioblastomas. *Biochemical pharmacology*, 81(3), 412-424.
- Zeng, L. H., Rensing, N. R., & Wong, M. (2009). The mammalian target of rapamycin signaling pathway mediates epileptogenesis in a model of temporal lobe epilepsy. *The Journal of neuroscience : the official journal of the Society for Neuroscience*, 29(21), 6964-6972.
- Zhai, H., Heppner, F. L., & Tsirka, S. E. (2011). Microglia/macrophages promote glioma progression. *Glia*, 59(3), 472-485.
- Zhang, L., Alizadeh, D., Van Handel, M., Kortylewski, M., Yu, H., & Badie, B. (2009). Stat3 inhibition activates tumor macrophages and abrogates glioma growth in mice. *Glia*, 57(13), 1458-1467.
- Zhao, C., Deng, W., & Gage, F. H. (2008). Mechanisms and functional implications of adult neurogenesis. *Cell*, 132(4), 645-660.
- Zheng, Y., Yang, W., Aldape, K., He, J., & Lu, Z. (2013). Epidermal Growth Factor (EGF)-enhanced Vascular Cell Adhesion Molecule-1 (VCAM-1) Expression Promotes Macrophage and Glioblastoma Cell Interaction and Tumor Cell Invasion. *Journal of Biological Chemistry*, 288(44), 31488-31495.
- Zhou, J., Blundell, J., Ogawa, S., Kwon, C. H., Zhang, W., Sinton, C., . . . Parada, L. F. (2009). Pharmacological inhibition of mTORC1 suppresses anatomical, cellular, and behavioral

- abnormalities in neural-specific Pten knock-out mice. *The Journal of neuroscience : the official journal of the Society for Neuroscience*, 29(6), 1773-1783.
- Zhu, Y., & Shah, K. (2014). Multiple lesions in receptor tyrosine kinase pathway determine glioblastoma response to pan-ERBB inhibitor PF-00299804 and PI3K/mTOR dual inhibitor PF-05212384. *Cancer biology & therapy*, 15(6), 0--1.
- Zigova, T., Pencea, V., Wiegand, S. J., & Luskin, M. B. (1998). Intraventricular administration of BDNF increases the number of newly generated neurons in the adult olfactory bulb. *Mol Cell Neurosci*, 11(4), 234-245.
- Zoncu, R., Efeyan, A., & Sabatini, D. M. (2011). mTOR: from growth signal integration to cancer, diabetes and ageing. *Nature reviews Molecular cell biology*, 12(1), 21-35.

APPENDIX A
CURRICULUM VITAE

CURRICULUM VITAE

Yael Kusne, PhD.

1117 E. Palm Lane

Phoenix, AZ 85006

602-509-5283

yael.kusne@asu.edu

Education:

2014-2018	Medical Student, Class of 2018 University of Arizona College of Medicine-Phoenix
2008-2014	PhD Candidate Interdisciplinary Neuroscience PhD Program Arizona State University with Barrow Neurological Institute
2002-2007	Bachelor of Arts, Arizona State University Major Program: Psychology

Awards:

2008-2009	ASU-BNI Interdisciplinary Neuroscience Fellowship
2013-2014	ARCS Foundation Scholarship

Positions and Employment:

2014-2018	Medical Student
2008-2014	Graduate Student
2006-2008	Laboratory Researcher, Barrow Neurological Institute, Phoenix
2003-2007	Accounts Manager, Gianfranco Ristorante, Scottsdale
Fall 2006	PGS499, Research Assistant for Dr. Nagoshi, Professor of Psychology, Arizona State University, Tempe
Spring 2006	PGS399, Research Assistant for Dr. Nagoshi, Professor of Psychology, Arizona State University, Tempe
2003-2006	Accounts Manager, North Desert Management, Scottsdale

Peer Reviewed Articles:

Valla J, Yaari R, Wolf AB, **Kusne Y**, Beach TG, Roher AE, et al (2010). Reduced Posterior Cingulate Mitochondrial Activity in Expired Young Adult Carriers of the APOE ϵ 4 Allele, the Major Late-Onset Alzheimer's Susceptibility Gene. *Journal of Alzheimer's Disease*, 22(1):307-13.

Nicholson R, **Kusne Y**, Nowak LA, LaFerla FM, Reiman EM, Valla J (2010). Regional cerebral glucose uptake in the 3xTG model of Alzheimer's disease highlights common regional vulnerability across AD mouse models. *Brain Research*, 1347:179-185.

Wolf AB, Braden BB, Bimonte-Nelson H, **Kusne Y**, Young N, Engler-Chiurazzi E, et al (2012). Broad-based nutritional supplementation in 3xTG mice corrects mitochondrial function and indicates sex-specificity in response to Alzheimer's disease intervention. *Journal of Alzheimer's disease*, 32(1):217-232.

Parker S, Mandell E, Hapak S, Maskaykina I, **Kusne, Y**, et al (2013). Competing molecular interactions of aPKC isoforms regulate neuronal polarity. *PNAS*, 110(35):14450-14455.

- Mirzadeh, Z, Bina, R, **Kusne, Y**, Coons, SW, Spetzler, RF, Sanai, N (2014). Predictors of functional recovery in adults with posterior fossa ependymomas. *Journal of Neurosurgery*, 1-6.
- Kusne Y**, Goldberg E, Parker SS, Maskaykina I, Price TJ, Ghosh S (2014). Contrasting effects of chronic, systemic treatment with mTOR inhibitors rapamycin and metformin on adult neural progenitors in mice. *Age*, 36: 199-212.
- Kusne Y**, Perry AS, Rushing EJ, Jabbour ME, Mandell EK, Mirzadeh Z, et al (2014). Tumor intrinsic EGFR and macrophage induced TNF- α signaling cooperate to promote GBM progression through aPKC. *Science Signaling*, in revision.

Volunteer Experiences:

May 14-16, 2013 Judge ISEF

January 2012 – September 2012 Medical Animals in Need Volunteer

January 2012 – current Rockstar Rescue volunteer foster